Generalized Ising measures for one-dimensional lattice gases and their applications

Ngo Phuoc Nguyen Ngoc

THESIS PRESENTED
TO
INSTITUTE OF MATHEMATICS AND STATISTICS
OF
UNIVERSITY OF SÃO PAULO
TO
OBTAIN THE TITLE
OF
DOCTORATE IN SCIENCE

Program: Statistics
Supervisors: Dr. Vladimir Belitsky,
                    Dr. Gunter Markus Schütz

São Paulo, May of 2022

Generalized Ising Measures for one–dimensional lattice gases and their applications

Esta versão da dissertação/tese contém as correções e alterações sugeridas pela Comissão Julgadora durante a defesa da versão original do trabalho, realizada em 9/5/2022. Uma cópia da versão original está disponível no Instituto de Matemática e Estatística da Universidade de São Paulo.

Comissão Julgadora:

- Prof. Dr. Vladimir Belitsky (Presidente) – IME-USP
- Prof. Dr. Anatoli Iambartsev – IME – USP
- Prof. Dr. José Ricardo Gonçalves de Mendonça – EACH–USP
- Prof. Dr. Paulo Afonso Faria de Veiga – ICMC-USP
- Prof. Dr. Manuel Alejandro González-Navarrete – University Bio-Bio

Abstract

Ngoc, N.P.N. **Generalized Ising measures for one-dimensional lattice gases and their applications**. 2022. Thesis (PhD) – Instituto de Matemática e Estatística, Universidade de São Paulo, São Paulo, 2022.

The processes studied are Interacting Particle Systems in which particles move on sites of a lattice with periodic boundary conditions. The particle interaction rule is the exclusion rule. Among the two classes of processes studied here, the first class is a generalization of the Exclusion Process. The generalization amounts to an extension of the dependence upon neighboring particles of a particle transition rate. In the other class of the processes studied, we substituted particles with rods that occupy several contiguous sites, defined that each rod may be in one of two possible states, and defined the rules for state switch. The transition rules for rod motion are similar to the rules for particles in our generalizations of the Exclusion Process. For each process constructed, we studied the conditions that ensure that its time-invariant distribution is an Ising type measure. The results relate the rates of motion and their ranges to the range and the interactions expressed in the potential function of Ising measure. We also studied the behavior of the process when they evolve in their respective invariant states. The study revealed novel phenomena in the behavior of particle flux as a function of particle density. One of the phenomena is non-monotonicity which has not been observed in the Classical Exclusion Process. For the interacting rod system, we revealed and explained the effect of cooperative pushing that had been observed previously in the RNA transcription process executed by RNA polymerase enzymes. Our results apply to understanding this biological process and to the traffic of cars that are traditionally modeled by the Exclusion Process.

Keywords: RNA polymerase, Transcription elongation, Markov models, Exclusion process, Cooperativity, Gibbs measure, Ising measure, Kramers–Wannier matrices, Canonical ensemble, Grand-canonical ensemble.

Resumo

Ngoc, N.P.N. **Medidas de Ising generalizadas para os gases em redes unidimensionais e suas aplicações**. 2022. Tese (Doutorado) - Instituto de Matemática e Estatística, Universidade de São Paulo, São Paulo, 2022.

Os processes estudados na tese são sistemas de partículas que se movimentam pelos sítios de uma rede unidimensional com a condição periódica de fronteira. As partículas interagem pela lei de exclusão. Os processos estudados, nos quais cada partícula pode ocupar um só sítio da rede, são generalizações do Processo de Exclusão; a essência da generalização é a extensão do alcance de dependência de parâmetros de movimentos de partícula da posição e da presença de outras partículas. No outro tipo dos processos estudados substituímos partículas por bastões que ocupam mais que um sítio e definimos que cada bastão pode estar num de dois possíveis estados. As regras de interação entre os bostões são parecidas com as regras aplicadas na generalização do processo de Exclusão. Para cada processo construído estudamos as condições necessárias e suficientes para que a distribuição invariante de processo esteja do tipo da medida de Ising. Os resultados mostram as relações entre os parâmetros de interação entre partículas (ou bastões) e a forma da função-potencial nas correspondentes medidas de Ising. Na tese, analisamos também o comportamento dos processos construídos quando eles evoluem de acordo com suas distribuições invariantes. Os resultados de análise revelam diversos fenómenos novos que ocorrem no fluxo de partículas e de bostões. Observamos e explicamos o comportamento não monótono de fluxo em relação da densidade de partículas que estaria ausente caso as partículas se movimentassem no Processo clássico de Exclusão. Também, observamos e explicamos o efeito de cooperação de bastões que aumenta a velocidade de cada bastão ("empurrão coletivo"). Os resultados aplicam-se aos estudos do processo de transcição de RNA produzido por RNA polimerase a partir da informação contida em DNA, e também aos estudos de trânsito de veículos.

Palavras-chave: RNA polimerase, alongamento de transcrição de RNA, modelos de Markov, processo de exclusão, cooperatividade, medida de Gibbs, medida de Ising, matrizes de Kramers–Wannier, conjunto canônico, conjunto grand canônico.

Acknowledgement

Contents

Abbreviation

RNAP	RNA polymerase
TEC	Transcription elongation complex
NTP	Nucelotriphospate
bp	Base pair
PP_i	Pyrophosphate
ASEP	Asymmetric simple exclusion process
TASEP	Totally asymmetric simple exclusion process
EP	Exclusion process

Frequently Used Notation

$\mathbb{N}$ The set of natural numbers

$\mathbb{Z}$ The set of integer numbers

L Number of sites of a lattice

N Number of particles or rods

$\mathbb{T}_L$ One dimensional ring with L sites

$\boldsymbol{\eta}, \boldsymbol{\zeta}$ Allowed configurations

δ Kronecker symbol

$|\cdot\rangle$ Ket–vector

$\langle\cdot|$ Bra–vector

$\langle\cdot|\cdot\rangle$ Inner product

$\langle\cdot\rangle$ Expectation

$\otimes$ Kronecker product

Tr Trace of a matrix

$\mathbb{1}$ Identity matrix

ρ Average density of particles or rods

$\mathbb{P}$ Probability measure

δ^L Kronecker symbol with arguments understood modulo L due to periodic boundary conditions

Part I

A brief introduction to the models proposed and studied in the thesis and the background information related to their constructions

Chapter 1

A brief introduction to the models and the main results of our study of the models

Section 1.1 of this chapter will present a general view at six novel interacting particle models/systems[1] that we have constructed and studied in the thesis (we note here that to each of the models, there will be devoted a separate chapter; those are the Chapters 3–8 of the thesis).

In order to justify the structure of the contents of Chapter 1 posterior to the Section 1.1, we note that all our models may be separated in two groups. The first group comprises the models that we have created for the elongation step of the biological process called RNA transcription (see [2, 4, 32] with the references therein, and/or the description that we shall provide in Section 2.3). The second group comprises diverse extensions of the classical Exclusion Process (see [18, 19, 26] and/or the description that we shall provide in Section 2.2). Certainly, the groups are related intrinsically. However, the relation will be revealed in the next chapters. As for the current chapter, it will speak separately about the groups in its Sections 1.2 and 1.3.

1.1 A general view

1.1.1 The construction and the approach to the study of our models

By employing the classical and commonly accepted terminology, we may say that the models proposed and studied in the thesis are one-dimensional lattice gases with periodic boundary conditions, whereas

---

[1] The term Interacting Particle System is more traditional in the field of Stochastic Processes but the term Interaction Particle Model allows for an easy, obvious and handy abbreviation "model".

♣ the rates at which the gas' particles translocate along the lattice and change their states are configuration dependent, and

♡ any gas' particles cannot overlap with any other particles and cannot jump over any other particle when translocates.

The first step of our study of each one of our models is to find its time-invariant measure. Since the number of model's parameters is large (e.g. the simplest models in the first group (Chapter 3) and in the second group (Chapter 7) need 18 and 6 parameters, respectively), this task is solved in the following way:

♠ we impose that the invariant measure must be an Ising–like measure and then, we find the relation between the measure's parameters and the model's parameters that ensure the desired relation between the model and the measure.

At the second step of our study,

◇ we calculate diverse characteristics of the models when they evolve in their respective invariant distribution.

For example, we calculate space correlations and we provide the functional dependence of the particles' flux and velocity on the particles' density.

We close the present subsection with the note that the items ♣, ♡, ♠, ◇ mark the steps that will be present in our treatment of each one of the six models.

1.1.2 The construction motivation and application

The models' construction and the study directions were motivated by the ongoing research of the elongation step of the biological process known under the name "RNA transcription" (already cited in the text above Section 1.1).

In the elongation step of the RNA transcription, specific enzymes called "RNA polymerises" (abbreviated to RNAP henceforth) walk along a DNA strand, read the information contained in the strand and concatenate nucleotides forming thus a RNA. From Biology, we know that various RNAPs walk simultaneously along the same strand and all their walks drift in the same direction. It is obvious that the walking RNAPs cannot overlap nor can any one of them overtake any other one. Thus, they naturally interact: when one RNAP temporarily stops to walk it will then block the motion of other RNAPs that follow it. But aside of this obvious interaction, it has been conjectured in biological literature that an RNAP may also push and pull its neighbors, and that, in general, an RNAP's walk speed may depend upon the positions of its neighbors in some finite but extended neighborhood.

Our primary aim was to infer–through statistical modeling and analysis–whether the above formulated conjecture is realistic or not, and, if possible, reveal the range of the

RNAPs interaction and its magnitudes. For the needs of the inference, it was necessary for us to understand what characteristics of the process may be measured in practice. One of those that turns out to be very handy is related to the release of pyrophosphate by an RNAP that occurs when a RNAP concatenates a nucleotide to the nucleotide sequence that will be a RNA at the end of the transcription process. Thus, in order to model this release in our model, we postulate that

‡ every model's particle is always in one of two possible states and can flip from a state to another state;

One of the states corresponds to the situation when a pyrophosphate is attached to a RNAP and the other state corresponds to a RNAP without a pyrophosphate. The actual rules of the state flip are specific for every model and, thus, will be specified when appropriate.

By now, we have exposed what motivated us to create and study the Stochastic Processes that have been characterized in Section 1.1 by the features ♣ and ♡. Following the motivation, these processes will be called in the thesis by **interacting RNAP models** or, simply, **RNAP models**. We draw our reader's attention to the fact that our exposition of the motivations explains our study aims that we have already formulated in ◇ and it also clarifies why the process' particles must transit between two different states, as has been mentioned in ♣ and explicitly stated in ‡.

In the course of our work on RNAP models, it turned out, however, that when we postulate that the particles of a RNAP model are all in one unique state all the time, then the modified RNAP model becomes an extension of the Exclusion Process. This is the process of a long history; it was suggested in 1974, and since then has been intensively studied. In particular, the contemporary study of the Exclusion Process is aligned with our modified RNAP models. Accordingly, the sole-state RNAP models have been included in the thesis. They will be referred to as **extensions and modifications of the Exclusion Process** or, simply, as **Exclusion Process**.

1.1.3   The relation between our models and previous studies

Certainly, our models are not totally novel. As for our RNAP models, their direct ancestor is the process that has been suggested and studied by Belistky and Schütz (see [4, 5]). Belitsky and Schütz, in turn, had been inspired by the Exclusion Process and its diverse application (see [26] as the first appearance of the Exclusion Process and see [18], [19] for a contemporary exposition). By this reason, the flow of our exposition will now be interrupted by a brief description of the Exclusion Process. We give it in the next paragraph. A detailed exposition of this process will be given in Section 2.2.

The Exclusion Process is the name for a group of identical volumeless particles that move on the sites of a lattice according to the following rules: each particle attempts to

execute the simple random walk on the sites (exactly, a continuous time discrete space random walk with the jumps to the nearest neighbor sites on the lattice), and it is actually allowed to execute the walk jumps unless the jump target site is currently occupied by another particle (the so-called "exclusion rule" that excludes the possibility for more than one particle to occupy simultaneously the same site). The lattice is usually taken to be of one of the following types: (1) $\mathbb{Z}$, i.e., each site corresponds to an integer, or (2) an "interval" of length L in $\mathbb{Z}$, i.e., the site set $\{1, \ldots, L\}$, $L \in \mathbb{N}$. In the second case, which is also the case of our study, it is necessary to decide what particles may do when they are at the boundary sites 1 and L. In our case, we declare that 1 is the right neighbor site of L, i.e., our lattice is a ring in $\mathbb{Z}$ of size L.

With a reference to the Exclusion Process just depicted, we may say that our models are its extensions. The extension directions are the following ones: *(a)* there are two states between which any particle may switch (flip the state is the term we shall use); in other words, in our models, any particle may either jump–as if it is an Exclusion Process' particle–, or flip without jumping, or jump and flip; and *(b)* particle's rates (of the jump, of the flip and of jump-and-flip) may depend on the presence, the positions and the states of other particles in its neighborhood.

The differences between our models and the Exclusion Process determine the division of our models into two groups.

The first group contains the two-state models. As explained above, they are models for the biological process called RNA transcription. The difference among these models is in the form according to which the flip and the jump rates depend on neighboring particles. Also to each model there is attributed its specific Ising-like measure which is tested as the model's time-invariant distribution. The basics of the construction and the results for the first group models are resumed in Section 1.2 of the present chapter. A thorough treatment of the models, the proofs and the applications are presented in Chapters 3, 4 and 5.

The studies of the models of the first group suggested the patterns of the rates' dependence that may be interesting even for one-state models. In other words, our study of the first group motivated the study of specific extensions of the classical Exclusion Process. One of them turns out to be a generalization of an already investigated modification of the Exclusion Process called Katz-Lebowitz-Spohn model. The three models derived by us in the just depicted manner will be thoroughly presented in Chapters 6, 7, 8 of the thesis while the Section 1.3 of the present chapter will speak about them in a resumed manner.

1.2   An extended summary of our RNAP models and their basic properties

1.2.1   The common feature of our three RNAP models

Our three RNAP models that will appear in Chapters from 3 to 5 have certain similarities. We speak about them now. The exposition helps our reader to capture the basic features of our approach to modeling RNAPs interactions.

1.2.1.1   Lattice

Our lattice sites/nodes model the DNA monomer nucleotides while the lattice bonds/edges organize these monomers in a sequence modeling by this a DNA strand along which RNAPs move.

The formal construction of the model lattice is as follows. For an arbitrary but fixed beforehand integer L, we take the integer points $\{1, 2, \ldots, L\}$ of $\mathbb{R}$, call them **sites** or **nodes** and declare that for each $i = 1, 2, \ldots, L - 1$, the sites i and $i + 1$ are **neighbors** and also that the sites 1 and L are neighbors. The graph thus constructed (certainly, we have constructed a graph: its **vertices** are our sites and its **edges** or **bonds** are naturally determined by the neighboring relation) will be called **lattice** of the **size** L. In mathematical literature this lattice is also named as **torus of size** L **in** $\mathbb{Z}$; and its formal definition is $\mathbb{Z}/L\mathbb{Z}$ (for our work, this definition is irrelevant). We shall usually denote our lattice as $\mathbb{T}_L$.

As we already have mentioned above, each site of our lattice models a nucleotide of a strand of DNA along which RNAPs move, while the lattice neighboring relation models the ways that a RNAP may take when it jumps/moves along a strand. We assume in our model that RNAPs read the information contained in DNA when they move from the lattice site 1 to the lattice site L. This assumption determines the directions on our lattice: a move from the site i to the site $i + 1$ will be called a step **forward** or a step **rightwards**, while a move from i to $i - 1$ will be called a step **backward** or **leftwards**; the terms forward and backward will be sometimes substituted by **clockwise** and **anticlockwise** that makes sense since we imagine our lattice as a ring (see Figure 1.1).

Our lattice has one essential difference from the DNA strand that it models, the difference is that in the real world, the link between the sites 1 and L does not exist. In a more realistic model, the lattice site 1 would be the entrance of rods into the lattice and the site L would be the exit (the term "rod" used here refers to the model counterpart of an RNAP; it will be defined properly in Section 1.2.1.2). Nevertheless, we expect that certain useful statistical properties of the stationary distribution of an ensemble of rods on this lattice may be revealed through analysis of the invariant distribution of rods on our circular lattice.Since we posses handy mathematical tools for analysis of the circular lattice, it has been accepted by us to model the rout of RNAPs.

1.2.1.2   Rods on lattice

An initial idea within the framework of RNAP interaction modeling was to model each RNAP by a particle that jumps on the lattice sites, whereas those sites model the DNA nucleotides. However, in the real world, a real RNAP is larger in the volume than a single nucleotide, and thus an RNAP covers simultaneously more than one DNA nucleotide. Accordingly, a RNAP will be modelled by a **rod** that occupies simultaneously a certain number of contiguous lattice sites. This number is one of the model parameters; it will be denoted by ℓ.

The rods in our model obey the **exclusion rule**: no two rods may occupy simultaneously the same lattice site. This requirement reflects the fact that RNAPs do not overlap in the real world.

We shall now present the nomenclature related to rods. When a rod covers the lattice sites $k, k+1, \ldots, k+\ell-1$, for some $k \in \{1, 2, \ldots, L\}$, then k (respectively, $k+\ell-1$) is called the rod's **left** or **trailing** (respectively, **right** or **leading**) site **position**. The **position of a rod** is defined as the position of the rod's trailing site. We note that the adjectives "trailing" and "leading" are intuitively clear because we have defined the walk direction on the lattice.

Each rod may in one of two states (the dynamics of the process will allow rods to switch states). We code the states as 1 and 2. The state 2 corresponds to the situation when the pyrophosphate is attached to RNAP, while the state 1 corresponds to an RNAP that has released the pyrophosphate. Because of the interpretation attached/detached, in our pictures, we shall paint black the RNAPs that are in the state 1 and we shall paint white those that are in the state 2.

In order to have a notation that is handy for the future needs, we suggest now the following numbering of rods. We start from the site 1, go along the lattice bonds towards the site L and number consecutively the encountered rods' trailing sites. In respect to this procedure, we now note that it is not ambiguous because–as a consequence of the exclusion rule– any two rods cannot occupy the same lattice sites. Then, we postulate that a rod acquires the number i, if i is the number that has been given to its trailing site; see Figure 1.1 for an illustration. With this numbering procedure at hand, we introduce the following notation: x_i means the position of the i-th rod (recall, the rod's position is the lattice site number occupied by the rod's trailing site), and s_i means the state of the i-th rod (recall, a rod state may be either 1 or 2).

Since our research substrate is the process which state space is the set of the allowed configuration of rods on lattice, then will now define this concept and introduce the related notations (Fig. 1.1 illustrate the definitions to be introduced). A configuration of rods on lattice is called **allowed** is–no matter what the rods' states are–no two rods occupy a common lattice site. Since we consider only allowed configurations, then we

shall abbreviate their name to just **configurations**. The generic symbol for a configuration will be $\boldsymbol{\eta}$. We recall x_i and s_i denote, respectively, the position and the state of i-th rod. Thus, a configuration of N rods may be also presented by pair $(\mathbf{x}, \mathbf{s})$ where $\mathbf{x} = (x_1, ..., x_N)$ is the **coordinate vector** and $\mathbf{s} = (s_1, ..., s_N)$ is the **state vector.**
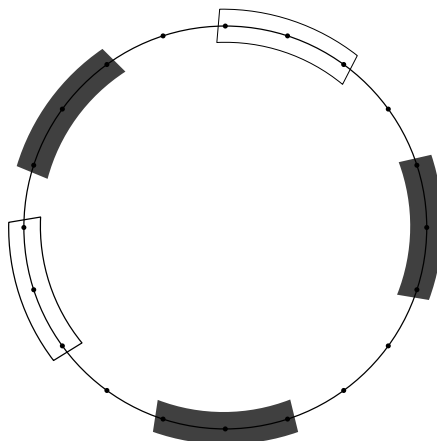
Figure 1.1: *An allowed configuration on the model lattice of length $L = 20$. The lattice is shown as a ring since its sites 1 and L are linked by a bond. In this picture the site at the twelve o'clock position has number 1. There are $N = 5$ rods in this picture. Each rod occupied three lattice sites; accordingly, the parameter ℓ of the model 3. Black rods are in state 1 and blank rods are in state 2. When we execute the numbering procedure described in the text, the number 1 is attributed to the rod that covers the site at the twelve o'clock position, the number 2 is attributed to the rod that covers the sites $5, 6, 7$.*

1.2.1.3   General features of rods' dynamics on lattice

In each one of our models, rods "walk" over a "circular" lattice. The walks are random, but the parameters of the randomness may change in time because–due to the construction–the value of any parameter of the walk of any rod at any time t depends upon the positions and the states of other rods (typically, of the rods that are in a specific finite neighborhood of the rod that walks). By this reason, the system as a whole may be called "Markov Processes with Local Interaction". Besides of this meaningful name, there exists an alternative name: "Interacting Particle System". The mathematical construction of such a system is thoroughly shown by Liggett in [18], [19]. In Liggett's framework, our rod is seen as just a particle in the sense that it may occupy only one lattice site at every single instance. Nevertheless, the framework applies to rods without a necessity of any serious adaptation. This framework notions and notations will be used now in order to speak about general features of rods' dynamics.

In accordance to the mathematical theory mentioned in the above paragraph, in order to specify a system it is sufficient to describe the rods' change rates. What is common across our models is the essence of what rod's quality may change. First of all, a rod may instantly translocate by one lattice site to the right or to the left. This may be formalized as follows: for each i, the i-th rod that occupied at time t^- the sites $x_i, x_i+1, ..., x_i+\ell-1$, turns to occupy the sites $x_i + 1, ..., x_i + \ell - 1, x_i + \ell$ at time t–this is called a jump, or a

translocation, to the right. The jump, or translocation, to the left is defined in a similar manner.

Also, any rod may change its state. To define this change rigorously, we define that each rod may be in one of two possible states; we call them 1 and 2. We then postulate that any rod may flip its state instantly (at a rate that depends upon the configuration of other rods; this dependence will be specific for each model).

Next, there arises the question as whether a rod may translocate and change its state simultaneously. In our models it is possible since we believe that this reflects the reality. Summarizing, we get the following list of possible changes:

(a)   a rod translocates one lattice site to the right and changes its state from 1 to 2;
(b)   a rod translocates one lattice site to the left and changes its state from 2 to 1;
(c)   a rod stays at its position and changes its state from 1 to 2;
(d)   a rod stays at its position and changes its state from 2 to 1.

Our reader will see that not all the possibilities (a)–(d) will be represented in each one our models. The reduction of the possibilities is dictated by the need to diminish the number of model's parameters and by the real process observation that have showed that certain changes do not occur or do occur with a negligible probability.

1.2.1.4   Ising–like measures for rods distribution on lattice

We recall that the final aim of our study is to find models' macroscopic characteristics when the model evolves in its invariant distribution. In order to facilitate the calculation of such a distribution, we impose apriori that it is of specific type. The details are given below.

The invariant distributions of the processes considered in this section are the generalized Ising measures which have the following general form

$$\hat{\pi}(\boldsymbol{\eta}) = \frac{1}{Z_L} \exp\left[-\frac{1}{k_B T}(U(\mathbf{x}) + \lambda B(\mathbf{s})) \right] \tag{1.1}$$

where $B(\mathbf{s}) = \sum_{i=1}^{N}(3 - 2s_i)$ and

$$U(\mathbf{x}) = \sum_{i=1}^{L} \left(J_1 \delta_{x_{i+1}, x_i + \ell} + J_2 \delta_{x_{i+1}, x_i + \ell + 1} + \dots + J_d \delta_{x_{i+1}, x_i + \ell + d - 1} \right). \tag{1.2}$$

here, d is an integer-valued parameter that is called "the interaction range", and δ is Kronecker symbol defined by

$$\delta_{\alpha, \beta} = \begin{cases} 1 & \text{if } \alpha = \beta, \\ 0 & \text{otherwise} \end{cases} \tag{1.3}$$

for α, β from any set.

Apart from the measure (1.1), we shall also consider its grand-canonical counterpart. This consideration is motivated by the fact that the grand-canonical measure is more convenient for the calculation of diverse model's proprties, like for example, the rods' average flux and velocity.

We note here that a generalized Ising measure (1.1) may be treated by the Transfer Matrix Techniques for small values of d, like $1, 2$. For more details about the use of this techniques, see [5, 15, 16, 25].

1.2.2 The RNAP model studied in Chapter 3

The relation to other models of the thesis. The model proposed in this subsection is a generalization of the RNAP model introduced by Belistky and Schütz [4, 5] in the sense that in our model we allow the rods to execute a transition that was prohibited in the original model. This is the transition which rate is to be denoted below by ϕ and τ. Exactly to state, if we set $\phi^\star = \tau^\star = 0$ in the rates (1.5) and (1.7) below, then we reduce our model to the model considered in [4, 5].

In comparison to our other RNAP models, we may say that the current model realizes the most complete set of rod transitions, but those transitions have the shortest interaction range among the ranges of all our RNAP models.

Dynamics and result. Transition rates of the ith rod at position x_i which are of the following form

$$\omega_i(\boldsymbol{\eta}) = \omega^\star \delta_{s_i,1}(1 + d^{1\star}\delta_{x_{i-1}+\ell,x_i} + d^{\star 01}\delta_{x_i+\ell+1,x_{i+1}})(1 - \delta_{x_i+\ell,x_{i+1}}), \tag{1.4}$$

$$\phi_i(\boldsymbol{\eta}) = \phi^\star \delta_{s_i,2}(1 + e^{10\star}\delta_{x_{i-1}+\ell+1,x_i} + e^{\star 1}\delta_{x_i+\ell,x_{i+1}})(1 - \delta_{x_{i-1}+\ell,x_i}), \tag{1.5}$$

$$\kappa_i(\boldsymbol{\eta}) = \kappa^\star \delta_{s_i,2}(1 + f^{1\star}\delta_{x_{i-1}+\ell,x_i} + f^{\star 1}\delta_{x_i+\ell,x_{i+1}} + f^{1\star 1}\delta_{x_{i-1}+\ell,x_i}\delta_{x_i+\ell,x_{i+1}}$$
$$+ f^{10\star}(1 - \delta_{x_{i-1}+\ell,x_i})\delta_{x_{i-1}+\ell+1,x_i} + f^{\star 01}(1 - \delta_{x_i+\ell,x_{i+1}})\delta_{x_i+\ell+1,x_{i+1}}), \tag{1.6}$$

$$\tau_i(\boldsymbol{\eta}) = \tau^\star \delta_{s_i,1}(1 + g^{1\star}\delta_{x_{i-1}+\ell,x_i} + g^{\star 1}\delta_{x_i+\ell,x_{i+1}} + g^{1\star 1}\delta_{x_{i-1}+\ell,x_i}\delta_{x_i+\ell,x_{i+1}}$$
$$+ g^{10\star}(1 - \delta_{x_{i-1}+\ell,x_i})\delta_{x_{i-1}+\ell+1,x_i} + g^{\star 01}(1 - \delta_{x_i+\ell,x_{i+1}})\delta_{x_i+\ell+1,x_{i+1}}). \tag{1.7}$$

where δ is Kronecker symbol defined as in (1.3). The phenomenological dimensionless parameters $d^{1\star}, d^{\star 01}, e^{10\star}, e^{\star 1}$, and $f^{1\star}, f^{\star 1}, f^{1\star 1}, f^{10\star}, f^{\star 01}$, and $g^{1\star}, g^{\star 1}, g^{1\star 1}, g^{10\star}, g^{\star 01}$ describe the interaction between neighboring rods. These parameters must be greater than -1 and their actual values must assure that the rates are non-negative. Namely, the parameter range is $d^{1\star} + d^{\star 01} \geq -1, e^{10\star} + e^{\star 1} \geq -1, f^{1\star} + f^{\star 1} \geq -1, f^{1\star} + f^{\star 01} \geq -1, f^{10\star} + f^{\star 1} \geq -1, f^{10\star} + f^{\star 01} \geq -1, f^{1\star 1} \geq -1, g^{10\star} + g^{\star 1} \geq -1, g^{10\star} + g^{\star 01} \geq -1, g^{1\star 1} \geq -1$.

Let us now provide a verbal description of the construction of the rates (1.4)–(1.7) and of

the rates' effects on rods' transitions. First of all, we observe that the function $\delta_{s_i,\alpha}, \alpha \in \{1,2\}$ is used in the rate expression in order to indicate the state of the rod to which the rate applies. Then, the overall factor $(1 - \delta_{x_i+\ell,x_{i+1}})$ specifies that $\omega_i(\boldsymbol{\eta})$ applies solely in the case when there is at least one empty site to the right of ith rod. Notice that superscript $\star$ indicates the position of the whole rod i. In this manner, parameter $d^{1\star}$ should be read as the contribution to rate $\omega_i(\boldsymbol{\eta})$ in the case when the rod $i-1$ abuts on the rod i. This is taken into account by the multiplier $\delta_{x_{i-1}+\ell,x_i}$ which is 1, if only if the abutting holds true. Meanwhile parameter $d^{\star 01}$ contributes to the rate only when the site $x_i + \ell + 1$ is occupied by the leading rod meaning that the rod $i+1$ is at position $x_i + \ell + 1$. In the same fashion, one can explain the contributions of $(1 - \delta_{x_{i-1}+\ell,x_i})$, $e^{\star 1}$ and $e^{10\star}$ to the backward jump rate $\phi_i(\boldsymbol{\eta})$. As for the flip rate $\kappa_i(\boldsymbol{\eta})$, the values $f^{10\star}$, $f^{1\star}$ contribute to the rate when the front site of the rod $i-1$ is at position $x_i - 2, x_i - 1$, respectively. Similarly, the values $f^{\star 1}$, $f^{\star 01}$ are added to the rate when the position of the rod $i+1$ is at $x_i + \ell$ and $x_i + \ell + 1$, respectively. Especially, only when the rods $i-1$ and $i+1$ are neighbors of the rod i, the value $f^{1\star 1}$ contributes to the rate. The roles of the values $g^{1\star}, g^{10\star}, g^{1\star 1}, g^{\star 1}$ and $g^{\star 01}$ in the formation of the rate $\tau_i(\boldsymbol{\eta})$ are similar to the roles of $f^{1\star}, f^{10\star}, f^{1\star 1}, f^{\star 1}$ and $f^{\star 01}$ in the formation of the rate $\kappa_i(\boldsymbol{\eta})$. In Fig. 1.2 we present examples of the translocation rate $\omega_i(\boldsymbol{\eta})$, and in Fig. 1.3 we give examples of the rates $\kappa_i(\boldsymbol{\eta})$ and $\tau_i(\boldsymbol{\eta})$.

(a) $\omega_i(\boldsymbol{\eta}) = \omega^\star$

(b) $\omega_i(\boldsymbol{\eta}) = \omega^\star(1 + d^{1\star})$

(c) $\omega_i(\boldsymbol{\eta}) = \omega^\star(1 + d^{1\star} + d^{\star 01})$

(d) $\omega_i(\boldsymbol{\eta}) = 0$
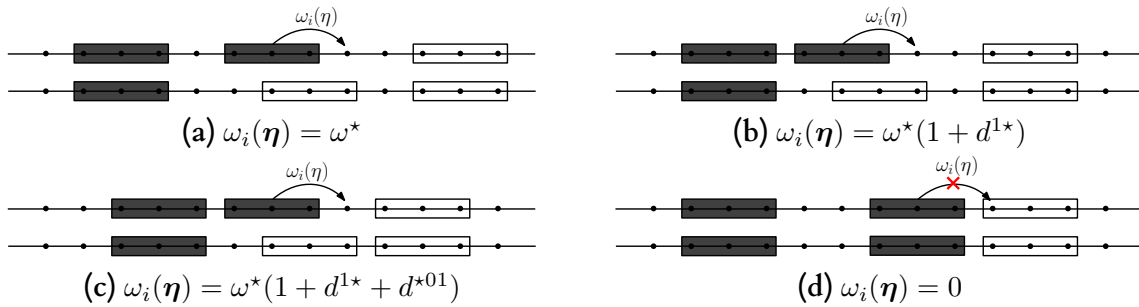
Figure 1.2: *Here, we show the dynamics of a rod in state 1 when its transition is rules by the rate $\omega_i(\boldsymbol{\eta})$. In this picture, black rods are in state 1 and blank rods are in state 2.*

(a) $\kappa_i(\boldsymbol{\eta}) = \kappa^\star(1 + f^{1\star})$

(b) $\tau_i(\boldsymbol{\eta}) = \tau^\star(1 + g^{1\star})$

(c) $\kappa_i(\boldsymbol{\eta}) = \kappa^\star(1 + f^{10\star} + f^{\star 01})$

(d) $\tau_i(\boldsymbol{\eta}) = \tau^\star(1 + g^{10\star} + g^{\star 01})$
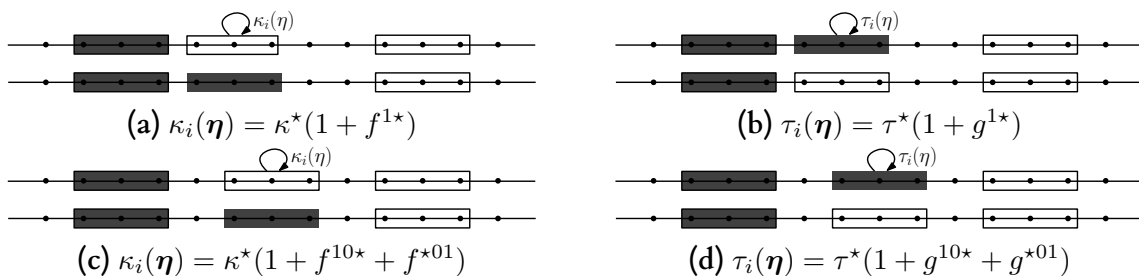
Figure 1.3: *This picture exemplifies the transitions of rods when they evolve due to the rates $\kappa_i(\boldsymbol{\eta})$ and $\tau_i(\boldsymbol{\eta})$. In this picture, black rods are in state 1 and blank rods are in state 2.*

The model defined above will be studied in Chapter 3. There, we shall find its invariant distribution and calculate its macroscopic properties when it evolves in accordance to this distribution. Here, we find it useful to describe the invariant distribution because

this description is the log of the study, and also because it will make it more easy to compare the currently treated model with other RNAP models.

Theorem 1.1. *The conditions* $(1.8) - (1.13)$ *upon the transition rates of the process defined in this section are sufficient for this process to have its stationary distribution in the form* (1.1):

$$\frac{1 + d^{1\star}}{1 + d^{\star 01}} = \frac{1 + e^{\star 1}}{1 + e^{10\star}} \tag{1.8}$$

$$x\kappa^\star f^{1\star} - \tau^\star g^{1\star} = \frac{1}{1+x}(-\omega^\star + x\phi^\star) - \frac{x}{1+x}(-\omega^\star d^{1\star} + x\phi^\star e^{\star 1}) \tag{1.9}$$

$$x\kappa^\star f^{\star 1} - \tau^\star g^{\star 1} = \frac{x}{1+x}(-\omega^\star + x\phi^\star) - \frac{1}{1+x}(-\omega^\star d^{1\star} + x\phi^\star e^{\star 1}) \tag{1.10}$$

$$x\kappa^\star f^{1\star 1} - \tau^\star g^{1\star 1} = -\omega^\star d^{1\star} + x\phi^\star e^{\star 1} \tag{1.11}$$

$$x\kappa^\star f^{10\star} - \tau^\star g^{10\star} = -\frac{1}{1+x}(-\omega^\star d^{\star 01} + x\phi^\star e^{10\star}) \tag{1.12}$$

$$x\kappa^\star f^{\star 01} - \tau^\star g^{\star 01} = -\frac{x}{1+x}(-\omega^\star d^{\star 01} + x\phi^\star e^{10\star}). \tag{1.13}$$

where $x = \dfrac{\omega^\star + \tau^\star}{\phi^\star + \kappa^\star}$. *The actual form of the stationary distribution is then as follows:*

$$\hat{\pi}(\boldsymbol{\eta}) = \frac{1}{Z_L} \left(\frac{\omega^\star + \tau^\star}{\phi^\star + \kappa^\star}\right)^{\sum_{i=1}^{N} -3/2 + s_i} \left(\frac{1 + d^{1\star}}{1 + d^{\star 01}}\right)^{-\sum_{i=1}^{N} \delta_{x_{i+1}, x_{i+\ell}}} \tag{1.14}$$

where Z_L *is the partition function.*

1.2.3 The RNAP model studied in Chapter 4

We start our exposition noting that the invariant distribution of the model studied in Chapter 3 has a "short interacting energy", namely, when measure $\hat{\pi}$ that has been expressed in (1.14) is written in the generic form (1.1) then the function $U(\mathbf{x})$ acquires the form $J_1 \sum_{i=1}^{L} \delta_{x_{i+1}, x_{i+\ell}}$, and this form says that U will depend upon x_i only if it is concatenated by x_{i+1} from its right or by x_{i-1} from its left. This fact suggests naturally the question: "If the function U is extended so that its interaction becomes longer, can the corresponding measure be an invariant distribution of a RNAP-like model?" This question is answered by the study presented in our Chapter 4.

Let us now pose the above question in a more concrete form and let us then explain how we solve it. Our first step is to add one more term to the interaction energy $U(\mathbf{x})$. it is a so-called next-nearest-interaction energy term. Thus, the interaction energy acquires the following form:

$$U(\mathbf{x}) = J_1 \sum_{i=1}^{N} \delta_{x_{i+1}, x_{i+\ell}} + J_2 \sum_{i=1}^{N} \delta_{x_{i+1}, x_{i+\ell+1}}. \tag{1.15}$$

At our second step of the argument, we pose the question in the exact terms: "Can one modify the dynamics of the RNAP model studied in Chapter 3 in the way so that its invariant distribution corresponds to (1.15)?" The core of the question is whether the range of dependence of the transition rates of the model in the question should be compatible with the interaction energy range. Accordingly, when searching for an answer, we are not obliged to extend the range of all the rates of the model from Chapter 3. This fact explains why the construction presented below is actually an answer to the posed question.

Dynamics: The dynamics of our process is constructed on the basis of the dynamics that we analyse in Chapter 3. There are however, certain deep structural changes. Namely, we preserve the rates $\omega_i(\boldsymbol{\eta}), \kappa_i(\boldsymbol{\eta})$ but nullify the rates $\phi_i(\boldsymbol{\eta}), \tau_i(\boldsymbol{\eta})$. This means that a rod in state 2 is not allowed to jump backward and a rod in state 1 is not allowed to change its state into 2 without jumping. As for the preserved rates, we extend their ranges in the manner exposed below; the reason for this extension has been explained above. The translocation rate $\omega_i(\boldsymbol{\eta})$ is now of the form

$$\omega_i(\boldsymbol{\eta}) = \delta_{s_i,1}(w_i^1(\boldsymbol{\eta}) + w_i^2(\boldsymbol{\eta})) \tag{1.16}$$

where

- $w_i^1(\boldsymbol{\eta}) := \omega_1^\star(1 + d^{1\star}\delta_{x_i,x_{i-1}+\ell} + d^{10\star}\delta_{x_i,x_{i-1}+\ell+1})(1 - \delta_{x_{i+1},x_i+\ell})\delta_{x_{i+1},x_i+\ell+1};$

- $w_i^2(\boldsymbol{\eta}) := \omega_2^\star(1 + e^{1\star}\delta_{x_i,x_{i-1}+\ell} + e^{10\star}\delta_{x_i,x_{i-1}+\ell+1})(1 - \delta_{x_{i+1},x_i+\ell})(1 - \delta_{x_{i+1},x_i+\ell+1}).$

and the transition rate $\kappa_i(\boldsymbol{\eta})$ is now of the form

$$\kappa_i(\boldsymbol{\eta}) = \delta_{s_i,2}(\kappa_i^0(\boldsymbol{\eta}) + \kappa_i^1(\boldsymbol{\eta}) + \kappa_i^2(\boldsymbol{\eta})), \tag{1.17}$$

where

- $\kappa_i^0(\boldsymbol{\eta}) := \kappa^\star(1 + f_0^{10\star}\delta_{x_i,x_{i-1}+\ell+1} + f_0^{1\star}\delta_{x_i,x_{i-1}+\ell} + f_0^{\star 1}\delta_{x_{i+1},x_i+\ell})\delta_{x_{i+1},x_i+\ell};$

- $\kappa_i^1(\boldsymbol{\eta}) := \kappa^\star(1+f_1^{10\star}\delta_{x_i,x_{i-1}+\ell+1}+f_1^{1\star}\delta_{x_i,x_{i-1}+\ell}+f_1^{\star 01}\delta_{x_{i+1},x_i+\ell+1})(1-\delta_{x_{i+1},x_i+\ell})\delta_{x_{i+1},x_i+\ell+1};$

- $\kappa_i^2(\boldsymbol{\eta}) := \kappa^\star(1 + f_2^{10\star}\delta_{x_i,x_{i-1}+\ell+1} + f_2^{1\star}\delta_{x_i,x_{i-1}+\ell})(1 - \delta_{x_{i+1},x_i+\ell})(1 - \delta_{x_{i+1},x_i+\ell+1}).$

In words, if a rod i at position x_i is in state 1, it can hop forward one site provided site $x_i + \ell$ is vacant. However, the rate may depend on occupancy of site $x_i + \ell + 1$. Namely, if site $x_i + \ell + 1$ is occupied, the jump rate takes place with $\omega_i^1(\boldsymbol{\eta})$, if not it takes place with $\omega_i^2(\boldsymbol{\eta})$. See Fig. 1.4 for some examples of translocation rate $\omega_i(\boldsymbol{\eta})$. As for transition rate $\kappa_i(\boldsymbol{\eta})$ of a rod at position x_i provided it is in state 2, the rate takes place with $\kappa_i^0(\boldsymbol{\eta}), \kappa_i^1(\boldsymbol{\eta})$, or $\kappa_i^2(\boldsymbol{\eta})$ depending on the position of its rightmost rod at $x_i + \ell, x_i + \ell + 1$, or $x_i + \ell + k$ for $k \geq 2$. See Fig. 1.5 for some examples of transition rate $\kappa_i(\boldsymbol{\eta})$.

Figure 1.4: *Some examples of translocation rate $\omega_i(\boldsymbol{\eta})$ of a rod in state 1. Black rods are in state 1 and blank rods are in state 2.*
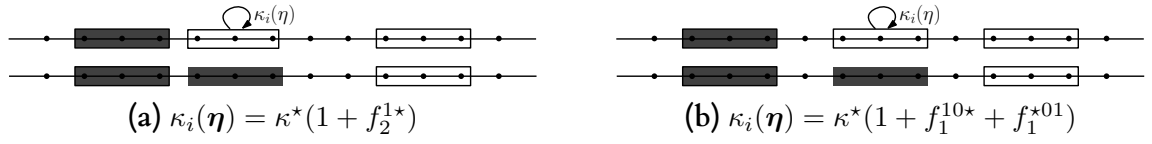
Figure 1.5: *Some examples of transition rate $\kappa_i(\boldsymbol{\eta})$. Black rods are in state 1 and blank rods are in state 2.*

Notice that the parameter must be chosen to ensure positivity of all the rates. Namely, the following inequalities must hold true: $\omega_1^\star, \omega_2^\star, \kappa^\star > 0$; $e^{1\star}, e^{10\star}, d^{1\star}, d^{10\star} \geq -1$; $f_0^{1\star} + f_0^{\star 1}, f_0^{10\star} + f_0^{\star 1} \geq -1$; $f_1^{1\star} + f_1^{\star 01}, f_1^{10\star} + f_1^{\star 01} \geq -1$; and $f_2^{1\star}, f_2^{\star 01} \geq -1$.

Our answer to the central question posed in the beginning of the present section is the essence of the following theorem.

Theorem 1.2. *The conditions* (1.18) − (1.27) *formulated below are sufficient for the the process with the corresponding dynamics to posses the stationary distribution of the form* (1.1).

$$d^{1\star} = \frac{\omega_2^\star}{\omega_1^\star}(e^{1\star} - e^{10\star}) \tag{1.18}$$

$$d^{10\star} = e^{10\star} \tag{1.19}$$

$$f_0^{\star 1} = \frac{1}{1+x}e^{1\star} - \frac{x}{1+x}, \tag{1.20}$$

$$f_0^{10\star} = -\frac{1}{1+x}e^{10\star} + \frac{\omega_1^\star}{\omega_2^\star}\frac{1}{1+x} - \frac{1}{1+x}, \tag{1.21}$$

$$f_0^{1\star} = -\frac{1}{1+x}e^{1\star} - \frac{1}{1+x}, \tag{1.22}$$

$$f_1^{\star 01} = \frac{1}{1+x}e^{10\star} + \frac{\omega_1^\star}{\omega_2^\star}\frac{x}{1+x} - \frac{x}{1+x}, \tag{1.23}$$

$$f_1^{10\star} = \left(\frac{\omega_1^\star}{\omega_2^\star} - \frac{1}{1+x}\right)e^{10\star} + \frac{\omega_1^\star}{\omega_2^\star}\frac{1}{1+x} - \frac{1}{1+x}, \tag{1.24}$$

$$f_1^{1\star} = \frac{x}{1+x}e^{1\star} - e^{10\star} - \frac{1}{1+x}, \tag{1.25}$$

$$f_2^{10\star} = \frac{x}{1+x}e^{10\star} + \frac{\omega_1^\star}{\omega_2^\star}\frac{1}{1+x} - \frac{1}{1+x}, \tag{1.26}$$

$$f_2^{1\star} = \frac{x}{1+x}e^{1\star} - \frac{1}{1+x}. \tag{1.27}$$

where $x = \dfrac{\omega_2^\star}{\kappa^\star}$. Moreover, when those conditions are satisfied, the stationary distribution acquires the following form:

$$\hat{\pi}(\boldsymbol{\eta}) = \frac{1}{Z_L}\left(\frac{\omega_2^\star}{\kappa^\star}\right)^{\sum_{i=1}^{N}-3/2+s_i}\left(\frac{\omega_2^\star}{\omega_1^\star}(1+e^{1\star})(1+e^{10\star})\right)^{-\sum_{i=1}^{N}\delta_{x_{i+1},x_i+\ell}^L}$$
$$\times(1+e^{10\star})^{-\sum_{i=1}^{N}\delta_{x_{i+1},x_i+\ell+1}} \tag{1.28}$$

where Z_L is the partition function.

1.2.4   The RNAP models studied in Chapter 5

In this subsection, we will propose kinetic assumptions for rods' dynamics in which interaction range among rod neighbors is wider than that of the RNAP models described in Subsections 1.2.2 and 1.2.3. Our main aim is to investigate relation between interaction range of the dynamics and the interaction energy (1.2) expressed by parameter d. In order to facilitate our investigation and to provide a clear view at the results, we will propose and study two different models; they are **Model 1** and **Model 2** to be defined below. At the moment, we just underline the main differences. In **Model 1**, the translocation rate (1.29) of a rod depends only on the occupancy of the lattice neighboring site on the left; as for the dependence of the configuration on its right, the rate depends on the position of the rightmost rod neighbor. It is interesting to notice that in this model, if the rate of a rod depends on the occupancy of the left neighbor lattice site, then d must be equal to 1. This means that the rate depends only the occupancy of the next and next–nearest lattice sites on the right. As for **Model 2**, it is a generalization of the model introduced in section 1.2.3. Notice the difference of its dynamics in comparison to that of **Model 1**: the dynamics (1.43) of a rod in **Model 2** depends both on the positions of its leftmost and rightmost rod neighbors.

<u>**Model 1:**</u> Similarly to how it has already been done in Section 1.2.3, we nullify certain rates and preserve only the rates $\omega_i(\boldsymbol{\eta})$ and $\kappa_i(\boldsymbol{\eta})$; the actual form of those rates depends now on a parameter $d = 1, 2, \ldots$ and have the following form:

$$w_i(\boldsymbol{\eta}) = \omega^\star\delta_{s_i,1}(1+e^{1\star}\delta_{x_i,x_{i-1}+\ell} + \sum_{k=1}^{d}e^{\star\bar{k}1}\delta_{x_{i+1},x_i+\ell+k})(1-\delta_{x_{i+1},x_i+\ell}), \tag{1.29}$$

$$\kappa_i(\boldsymbol{\eta}) = \kappa^\star\delta_{s_i,2}(1+\sum_{k=0}^{d}f^{1\bar{k}\star}\delta_{x_i,x_{i-1}+\ell+k} + \sum_{k=0}^{d}f^{\star\bar{k}1}\delta_{x_{i+1},x_i+\ell+k}). \tag{1.30}$$

The parameters must be chosen so that the rates are positive. Namely, the parameters must satisfy the following constraints: $\omega^\star, \kappa^\star > 0$, $e^{1\star} \geq -1$, $e^{\star\bar{k}1} \geq -1$, $e^{1\star} + e^{\star\bar{k}1} \geq -1$, for $k = 1, ..., d$, and $f^{1\bar{k}\star} + f^{\star\bar{l}1} \geq -1$, for $k, l = 0, ..., d$. Here we use the notation $\bar{k}$, for $k \in \{0, .., d\}$, to indicate that there are k vacant sites between the rod i^{th} and its rightmost or leftmost neighbor. One notices that the translocation rate $\omega_i(\boldsymbol{\eta})$ of a rod at position x_i depends on occupancy of site $x_i - 1$ on the left, meanwhile, on the right, it depends on the position of the rightmost neighbor. As for the transition rate $\kappa_i(\boldsymbol{\eta})$, we note here that although its interaction range is longer than the ranges of the models of subsections 1.2.2 and 1.2.3, still we did not include the parameter $f^{1\star1}$ into the rate expression. It will turn out that parameters $f^{1\bar{0}\star}$ and $f^{\star\bar{0}1}$ play the role of $f^{1\star1}$. Finally, we note that Fig. 1.6 pictures some examples of translocation rate $\omega_i(\boldsymbol{\eta})$ and Fig. 1.7 pictures some examples of transition rate $\kappa_i(\boldsymbol{\eta})$.

(a) $\omega_i(\boldsymbol{\eta}) = \omega^\star(1 + e^{\star\bar{1}1})$ **(b)** $\omega_i(\boldsymbol{\eta}) = \omega^\star(1 + e^{\star\bar{2}1})$

(c) $\omega_i(\boldsymbol{\eta}) = \omega^\star(1 + e^{\star\bar{3}1})$ **(d)** $\omega_i(\boldsymbol{\eta}) = 0$
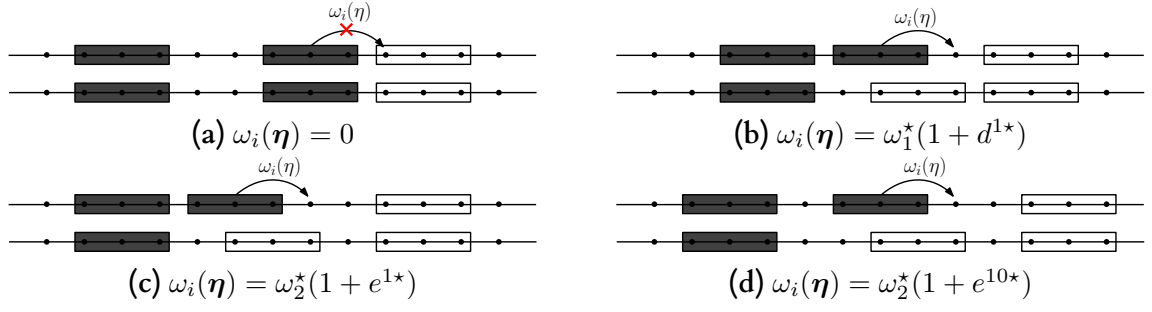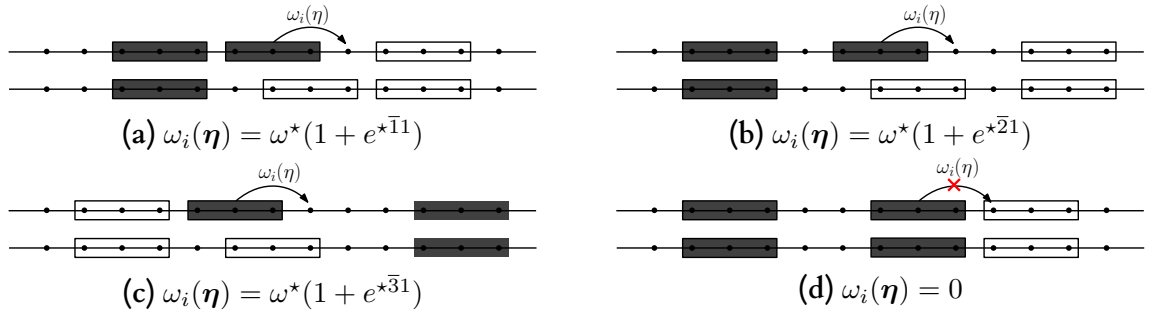
Figure 1.6: *Some examples of translocation rate $\omega_i(\boldsymbol{\eta})$ of a rod in state 1. Black rods are in state 1 and blank rods are in state 2.*

**(a)** $\kappa_i(\boldsymbol{\eta}) = \kappa^\star(1 + f^{1\bar{0}\star} + f^{\star\bar{2}1})$ **(b)** $\kappa_i(\boldsymbol{\eta}) = \kappa^\star(1 + f^{1\bar{1}\star} + f^{\star\bar{1}1})$
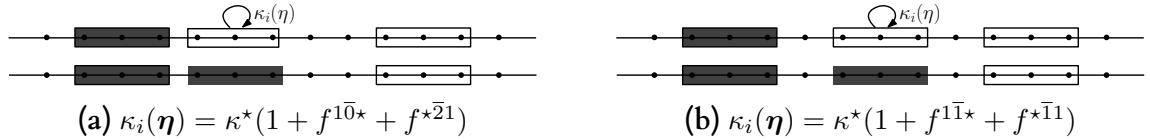
Figure 1.7: *Some examples of transition rate $\kappa_i(\boldsymbol{\eta})$. Black rods are in state 1 and blank rods are in state 2.*

As we shall show in Chapter 5, in order to ensure that the process stationary distribution acquires the desired form, it is necessary that the parameters appearing in the rates (1.29)–(1.30) satisfy the following constraints

$$
\begin{cases}
e^{1\star}e^{\star\bar{k}1} & = 0, \text{ for } k \geq 2, \\
f^{1\bar{0}\star} & = \dfrac{x}{1+x}e^{1\star} - \dfrac{1}{1+x}, \\
f^{\star\bar{0}1} & = \dfrac{1}{1+x}e^{1\star} - \dfrac{x}{1+x}, \\
f^{\star\bar{k}1} & = \dfrac{1}{1+x}e^{\star\bar{k}1}, \text{ for } k = 1, ..., d, \\
f^{\star\bar{k}1} & = \dfrac{x}{1+x}e^{\star\bar{k}1}, \text{ for } k = 1, ..., d,
\end{cases}
\tag{1.31}
$$

where $x = \dfrac{\omega^\star}{\kappa^\star}$. The first of the constraints splits the further considerations into two cases: in Case a, we accept $e^{1\star} = 0$, while in Case b, we accept $e^{1\star} \neq 0$.

Case a: If $e^{1\star} \neq 0$, as we accept in this case, then $e^{\star\overline{k}1} = 0$, for $k \geq 2$, and consequently, the rates are:

$$w_i(\boldsymbol{\eta}) = \omega^\star \delta_{s_i,1}(1 + e^{1\star}\delta_{x_i,x_{i-1}+\ell} + e^{\star\overline{1}1}\delta_{x_{i+1},x_i+\ell+1})(1 - \delta_{x_{i+1},x_i+\ell}), \tag{1.32}$$

$$\kappa_i(\boldsymbol{\eta}) = \kappa^\star \delta_{s_i,2}(1 + f^{1\overline{0}\star}\delta_{x_i,x_{i-1}+\ell} + f^{1\overline{1}\star}\delta_{x_i,x_{i-1}+\ell+1} + f^{\star\overline{0}1}\delta_{x_{i+1},x_i+\ell} + f^{\star\overline{1}1}\delta_{x_{i+1},x_i+\ell+1}). \tag{1.33}$$

The rate form deduced for Case a yields the following result that is identical to the main result of the manuscript [4].

Theorem 1.3. *For the process defined in* **Case a** *above, the conditions* (1.32) – (1.33) *upon its dynamics rates acquire the following form:*

$$\begin{cases} f^{1\overline{0}\star} &= \dfrac{x}{1+x}e^{1\star} - \dfrac{1}{1+x}, \\ f^{\star\overline{0}1} &= \dfrac{1}{1+x}e^{1\star} - \dfrac{x}{1+x}, \\ f^{\star\overline{1}1} &= \dfrac{1}{1+x}e^{\star\overline{1}1} \\ f^{\star\overline{1}1} &= \dfrac{x}{1+x}e^{\star\overline{1}1}. \end{cases} \tag{1.34}$$

These conditions are sufficient for the process' stationary distribution be of the form (1.1)*. In this case, the stationary distribution acquires the following expression*

$$\hat{\pi}_1(\boldsymbol{\eta}) = \dfrac{1}{Z_{1,L}}\left(\dfrac{\omega^\star}{\kappa^\star}\right)^{\sum_{i=1}^{N} -3/2+s_i}\left(\dfrac{1+e^{1\star}}{1+e^{\star\overline{1}1}}\right)^{-\sum_{i=1}^{N}\delta^L_{x_{i+1},x_i+\ell}} \tag{1.35}$$

where $Z_{1,L}$ is the partition function.

Case b: This is the case in which the first of the constrains (1.31) is satisfied because, due to our imposition, $e^{1\star} = 0$. With this equality being true, the other rates acquire the following form (below, $d \geq 1$):

$$w_i(\boldsymbol{\eta}) = \omega^\star \delta_{s_i,1}\left(1 + \sum_{k=1}^{d} e^{\star\overline{k}1}\delta_{x_{i+1},x_i+\ell+k}\right)(1 - \delta_{x_{i+1},x_i+\ell}), \tag{1.36}$$

$$\kappa_i(\boldsymbol{\eta}) = \kappa^\star \delta_{s_i,2}\left(1 + \sum_{k=0}^{d} f^{1\overline{k}\star}\delta_{x_i,x_{i-1}+\ell+k} + \sum_{k=0}^{d} f^{\star\overline{k}1}\delta_{x_{i+1},x_i+\ell+k}\right), \tag{1.37}$$

The model of Case b obeys the following property:

Theorem 1.4. *For the process defined in **Case b** above, the conditions* (1.36)–(1.37) *upon its dynamics rates acquire the following form:*

$$
\begin{cases}
f^{1\bar{0}\star} &= \dfrac{x}{1+x}e^{1\star} - \dfrac{1}{1+x}, \\[2mm]
f^{\star\bar{0}1} &= \dfrac{1}{1+x}e^{1\star} - \dfrac{x}{1+x}, \\[2mm]
f^{\star\bar{k}1} &= \dfrac{1}{1+x}e^{\star\bar{k}1}, \text{ for } k = 1, ..., d, \\[2mm]
f^{\star\bar{k}1} &= \dfrac{x}{1+x}e^{\star\bar{k}1}, \text{ for } k = 1, ..., d,
\end{cases}
\tag{1.38}
$$

These conditions are sufficient for the process' stationary distribution be of the form (1.1). *Namely, when the conditions hold, the stationary distribution acquires the following expression*

$$
\hat{\pi}_d(\boldsymbol{\eta}) = \frac{1}{Z_{d,L}} \left(\frac{\omega^\star}{\kappa^\star}\right)^{\sum_{i=1}^{N} -3/2 + s_i} \prod_{k=1}^{d} \left(\prod_{j=1}^{d-k+1} \frac{1}{1+e^{\star\overline{d-j+1}1}}\right)^{-\sum_{i=1}^{N} \delta_{x_{i+1}, x_i + \ell + k - 1}}
\tag{1.39}
$$

where $Z_{d,L}$ is the partition function.

Model 2: This model is an generalization of the model in Section 1.2.3. The "upgrade" is that the configuration-dependent translocation rate $\omega_i(\boldsymbol{\eta})$ acquires now the form

$$
w_i(\boldsymbol{\eta}) = \delta_{s_i,1}(\omega_i^1(\boldsymbol{\eta}) + ... + \omega_i^d(\boldsymbol{\eta}))
\tag{1.40}
$$

where

$$
\omega_i^k(\boldsymbol{\eta}) = \omega_k^\star \left(1 + \sum_{j=0}^{d-1} e_k^{1\bar{j}\star} \delta_{x_i, x_{i-1}+\ell+j}\right)(1 - \delta_{x_i, x_{i-1}+\ell})(1 - \delta_{x_i, x_{i-1}+\ell+1}) \cdots (1 - \delta_{x_i, x_{i-1}+\ell+k-1})
$$
$$
\times \, \delta_{x_i, x_{i-1}+\ell+k}, \text{ for } 1 \leq k \leq d-1,
\tag{1.41}
$$
$$
\omega_i^d(\boldsymbol{\eta}) = \omega_d^\star \left(1 + \sum_{j=0}^{d-1} e_d^{1\bar{j}\star} \delta_{x_i, x_{i-1}+\ell+j}\right)(1 - \delta_{x_i, x_{i-1}+\ell})(1 - \delta_{x_i, x_{i-1}+\ell+1}) \cdots (1 - \delta_{x_i, x_{i-1}+\ell+d-1})
$$
$$
\times \, (1 - \delta_{x_i, x_{i-1}+\ell+d})
\tag{1.42}
$$

while the transition rate $\kappa_i(\boldsymbol{\eta})$ acquires now the form

$$
\kappa_i(\boldsymbol{\eta}) = \delta_{s_i,2}(\kappa_i^1(\boldsymbol{\eta}) + ... + \kappa_i^d(\boldsymbol{\eta}))
\tag{1.43}
$$

where

$$
\kappa_i^k(\boldsymbol{\eta}) = \kappa^\star \left(1 + \sum_{j=0}^{d-1} f_k^{1\bar{j}\star} \delta_{x_i, x_{i-1}+\ell+j} + f_k^{\star\bar{k}1} \delta_{x_{i+1}, x_i+\ell+k}\right)(1 - \delta_{x_{i+1}, x_i+\ell})
$$

$$\times (1 - \delta_{x_{i+1},x_i+\ell+1}) \cdots (1 - \delta_{x_{i+1},x_i+\ell+k-1})\delta_{x_{i+1},x_i+\ell+k}, \text{ for } 0 \leq k \leq d-1,$$
$$(1.44)$$

$$\kappa_i^d(\boldsymbol{\eta}) = \kappa^\star \left(1 + \sum_{j=0}^{d-1} f_d^{1\bar{j}\star}\delta_{x_i,x_{i-1}+\ell+j} \right) (1 - \delta_{x_{i+1},x_i+\ell})(1 - \delta_{x_{i+1},x_i+\ell+1}) \cdots (1 - \delta_{x_{i+1},x_i+\ell+d-1})$$
$$\times (1 - \delta_{x_{i+1},x_i+\ell+d}). \tag{1.45}$$

The parameters of the model must satisfy the following constraints: $\kappa^\star > 0, \omega_k^\star > 0$ for $k = 1, ..., d$, $e_k^{1\bar{j}\star} \geq -1$ for $k = 1, ..., d; j = 0, ..., d-1$, $f_k^{1\bar{j}\star} + f_k^{\star\bar{k}1} \geq -1$, for $k, j = 0, ..., d-1$, and $f_d^{1\bar{j}} \geq -1$. These constraints ensure that all jump rates are positive. We illustrate the behaviour of the model in Figs. 1.4 and 1.5; they apply to the case when $d = 2$.

As mentioned above, the dynamics of this model is different from the dynamics in **Case b** of **Model 1**. The latter depends only on the position of the rightmost neighboring rod, while the former depends also on the leftmost neighboring rod.

In respect to the model constructed above, we have the following result:

Theorem 1.5. *If the rates* (1.40) *and* (1.43) *of **Model 2** satisfy the constraint*

$$\begin{cases} e_k^{1\bar{0}\star} & = \dfrac{\omega_d^\star}{\omega_k^\star}(e_d^{1\bar{0}\star} - e_d^{1\bar{k}\star}), \text{ for } k = 1, 2, ..., d-1, \\[2ex] e_k^{1\bar{j}\star} & = \dfrac{\omega_j^\star}{\omega_k^\star}\dfrac{1 + e_d^{1\bar{k}\star}}{1 + e_d^{1\bar{j-1}\star}}(1 + e_{k+1}^{1\bar{j-1}\star}) - \dfrac{\omega_d^\star}{\omega_k^\star}(e_d^{1\bar{j}\star} - e_d^{1\bar{k}\star}) - \dfrac{\omega_j^\star}{\omega_k^\star}, \end{cases} \tag{1.46}$$

(where in the last equation the indices k, j run from 1 to $d-1$) and the constraint

$$\begin{cases} f_d^{1\bar{k}\star} & = \dfrac{x}{1+x}e_d^{1\bar{k}\star} + \dfrac{\omega_k^\star}{\omega_d^\star}\dfrac{1}{1+x} - \dfrac{1}{1+x}, \text{ for } k = 0, ..., d-1, \\[2ex] f_k^{\star\bar{k}1} & = \dfrac{1}{1+x}e_d^{1\bar{k}\star} + \dfrac{\omega_k^\star}{\omega_d^\star}\dfrac{x}{1+x} - \dfrac{x}{1+x}, \text{ for } k = 0, ..., d-1, \\[2ex] f_k^{\star\bar{j}1} & = -\dfrac{1}{1+x}e_d^{1\bar{j}\star} + \dfrac{\omega_k^\star}{\omega_d^\star}e_k^{1\bar{j}1} + \dfrac{\omega_k^\star}{\omega_d^\star}\dfrac{1}{1+x} - \dfrac{1}{1+x}, \text{ for } k, j = 0, ..., d-1. \end{cases} \tag{1.47}$$

*(where $x = \dfrac{\omega_d^\star}{\kappa^\star}$) then the stationary distribution of **Model 2** is of the form* (1.1). *Specifically, the constraints yield the following expressions for the parameters of the distribution* (1.1):

$$\hat{\pi}(\boldsymbol{\eta}) = \dfrac{1}{Z_{d,L}} \left(\dfrac{\omega_d^\star}{\kappa^\star} \right)^{\sum_{i=1}^{N} -3/2+s_i} \prod_{k=1}^{d} \left(\prod_{j=k}^{d} \dfrac{\omega_d^\star}{\omega_j^\star} \left(1 + e_d^{1\bar{j-1}\star} \right) \right)^{-\sum_{i=1}^{N} \delta_{x_{i+1},x_i+\ell+k-1}^L}, \tag{1.48}$$

where $Z_{d,L}$ is the partition function.

1.3   Exclusion processes with many speeds

We have already mentioned above that one of the bases of our RNA construction is the exclusion principle. This principle was used in '70 to construct the process called Exclusion Process. Thus, the study of that and its extensions that we present in this thesis is a natural part of the main thesis' theme that is the RNA transcription models and their properties. This section resumes all that we will show in Chapters 6, 7 and 8 related to the Exclusion Process.

From the formal standpoint, we may say that the "passage" from RNAP models back to the Exclusion Process consists of focusing the study attention solely at the translocation dynamics of rods whereas the length of rods is taken to be comparable to the interaction range, i.e., it is 1. There is, however, a more deep reason that makes it possible to transit freely between the RNAP models and the Exclusion Process within the framework of our study. The reason roots in the factorization of the generalized Ising measure (1.1) we are interested in. Namely, this measure factorizes into the distance part and the part that takes into account the fact that the RNAP rods may be in two different states. Since in the Exclusion Process the rods are of the same type, then one could guess their invariant distribution should be of the form (1.50) which is a family of generalized Ising measures. In this way, we pass to investigate the relation between the Ising measures and the particle distribution in the Exclusion Process. Those result enhance our understanding of the behaviour of our RNAP models.

We stress that instead of finding the transition rates in parameterized forms, as we do for the RNAP models, in Chapters 3, 4, and 5, an alternative approach will be taken in Chapter 6. There, we shall find, the most general form of particles' translocation rates that ensures that the measure (1.50) is the invariant distributions for the Exclusion Process. It turns out that the result of Chapter 6 is an extension of one of the results from [1]. Speaking about Chapters 7 and 8, the results they present complement the results from Chapters 3 and 4 in the sense that they provide direct proofs for the theorems and investigate the average currents of particles. We stress that the models considered in 7 and 8 are generalizations of Katz-Lebowitz-Spohn model for a one-dimensional lattice gas.

1.3.1   A family of generalized Ising measures as invariant distributions for exclusion processes with many speeds – Chapter 6

In Chapter 6, we construct one-dimensional totally asymmetric exclusion process on the ring $\mathbb{T}_L$ which particle jumps to the right at distance 1, but the jumping rate depends on the distance between the hopping particle and its right-most neighboring particle. Namely, the jump rate of a particle is r_k, if the distance between it and its rightmost particle neighbor is $k + 1$ which means the number of vacant sites between them is k. Thus, r_0 is the jump rate of a particle when its rightmost nearest site is occupied by

another particle. It thus holds that r_0 is always 0 (since we want the exclusion rule to hold true), r_1 is the jump rate of a particle when the its rightmost neighboring site is free but the next site is occupied by another particle, and so forth for $r_2, r_3, \ldots$. See Fig. 1.8 for an example.
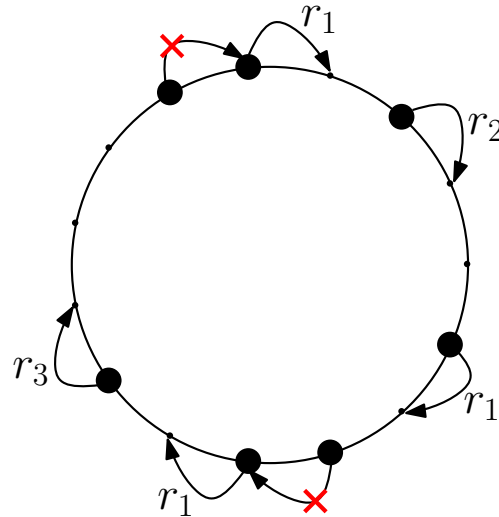
Figure 1.8: *A configuration on ring $\mathbb{T}_{15}$ with 7 particles.*

We represent the possible configurations of the considered process by arrays of occupation numbers $\boldsymbol{\eta} = (\eta_1, \ldots, \eta_L)$ where $\eta_k \in \{0, 1\}$. Because of periodic boundary conditions, one has $\eta_{i+mL} := \eta_i$ for $i \in \{1, \ldots, L\}$ and any integer $m \in \mathbb{Z}$.

Our aim is to check whether the invariant distribution of the constructed process may be a member of the family of Ising measures $\hat{\pi}_d$ where $d \in \{1, 2, \ldots, L-1\}$ on the ring $\mathbb{T}_L$ with L sites. Denote by π_d the unnormalized measure corresponding to $\hat{\pi}_d$ which is of the following form

$$\pi_d(\boldsymbol{\eta}) = \exp\left\{-\beta \sum_{i=1}^{L} \left\{ \sum_{n=1}^{d} J_n \eta_i (1 - \eta_{i+1})(1 - \eta_{i+2}) \cdots (1 - \eta_{i+n-1}) \eta_{i+n} + h \eta_i \right\} \right\},$$
(1.49)

where $J_1, \ldots, J_d$ are real numbers. The constants β, h play the roles of inverse temperature and of a chemical potential, respectively. Denote by $Z_{d,L}$ the partition function of the measure $\hat{\pi}_d$. One has

$$Z_{d,L} = \sum_{\boldsymbol{\eta}} \pi_d(\boldsymbol{\eta}) \quad \text{and} \quad \hat{\pi}_d(\boldsymbol{\eta}) = \frac{1}{Z_{d,L}} \pi_d(\boldsymbol{\eta}).$$
(1.50)

With the notation introduced above, the answer to our main question is provided by the following result that we shall prove in Chapter 6.

Theorem 1.6. *With convention that $J_k = 0$ for $k > d$, invariant distribution of the process*

is $\hat{\pi}_d$ if only if the hopping rates are of the following form

$$r_k = r \exp\{J'_k - J'_{k+1}\}, \quad \text{for } k \geq 1 \tag{1.51}$$

where r is a free parameter and $J'_k = -\beta J_k$ for all k.

1.3.2   A generalization of one-dimensional Katz-Lebowitz-Spohn model – Chapter 7

In Chapter 7, we construct Exclusion Process on the ring $\mathbb{T}_L$ with N particles. The process' dynamics is identical to the translocation part of process described in Section 1.2.2. Our current modification of the Exclusion Process may be described as follows. With the notation $\mathbf{x} = (x_1, x_2, ..., x_N)$ for the positions of the particles in an allowed configuration $\boldsymbol{\eta}$, the jump rates acquire the following form (below, x_i means the position of the particle that will jump):

$$\omega_i(\boldsymbol{\eta}) = \omega^\star(1 + d^{1\star}\delta_{x_{i-1}+1,x_i} + d^{\star 01}\delta_{x_{i+2},x_{i+1}})(1 - \delta_{x_i+1,x_{i+1}}), \tag{1.52}$$

$$\phi_i(\boldsymbol{\eta}) = \phi^\star(1 + e^{10\star}\delta_{x_{i-1}+2,x_i} + e^{\star 1}\delta_{x_i+1,x_{i+1}})(1 - \delta_{x_{i-1}+1,x_i}). \tag{1.53}$$

In words, the microscopic dynamics is as follows. We associate with each particle two random Poissonian clocks, say 1 and 2, with the rates $\omega_i(\boldsymbol{\eta})$ and $\phi_i(\boldsymbol{\eta})$ respectively. If one of the two clocks on i^{th} particle at position x_i rings, we have two possibilities. If the clock is 1 or 2, the particle hops to site $x_i + 1$ or $x_i - 1$ provided the target site is vacant respectively. For pictorial representations, see Figs. 1.9 and 1.10 for some examples of the rates.

(a) $\omega_i(\boldsymbol{\eta}) = \omega^\star(1 + d^{1\star} + d^{\star 01})$ **(b)** $\omega_i(\boldsymbol{\eta}) = \omega^\star(1 + d^{1\star})$

(c) $\omega_i(\boldsymbol{\eta}) = \omega^\star(1 + d^{\star 01})$ **(d)** $\omega_i(\boldsymbol{\eta}) = \omega^\star$
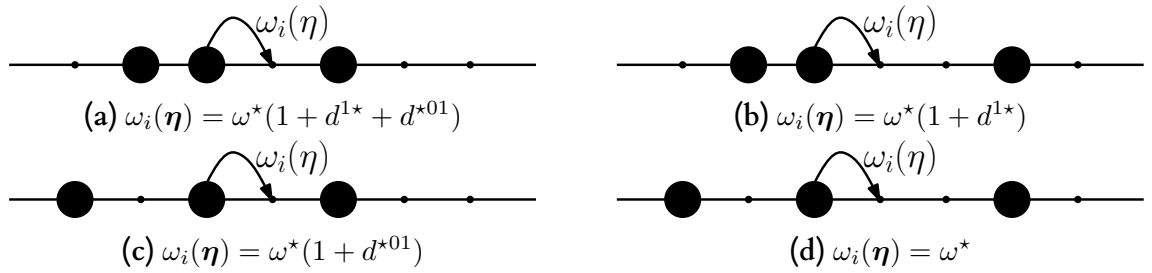
Figure 1.9: *Some examples of the jump rates to the right.*

(a) $\phi_i(\boldsymbol{\eta}) = \phi^\star(1 + e^{\star 1})$ **(b)** $\phi_i(\boldsymbol{\eta}) = \phi^\star(1 + e^{\star 1} + e^{10\star})$

(c) $\phi_i(\boldsymbol{\eta}) = \phi^\star(1 + e^{10\star})$ **(d)** $\phi_i(\boldsymbol{\eta}) = \phi^\star$
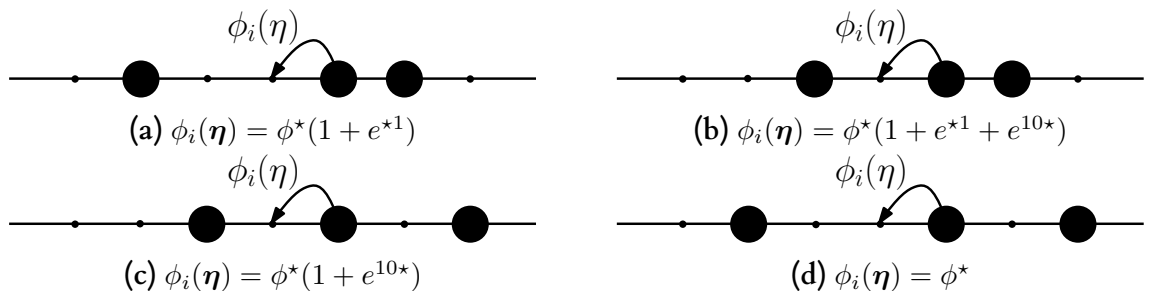
Figure 1.10: *Some examples of the jump rates to the left.*

The aim of the study is to find conditions that ensure that the process' invariant measure is an Ising type measure. This question is answered by us as follows:

Theorem 1.7. *If the parameters $d^{1\star}, d^{\star 01}, e^{\star 1}$ and $d^{\star 10}$ in the translocation rates* (1.52) *and* (1.53) *satisfy the following constraint*

$$\frac{1 + d^{1\star}}{1 + d^{\star 01}} = \frac{1 + e^{\star 1}}{1 + e^{10\star}}, \tag{1.54}$$

then the invariant distribution of the process is the following

$$\hat{\pi}(\boldsymbol{\eta}) = \frac{1}{Z_L} \left(\frac{1 + d^{1\star}}{1 + d^{\star 01}} \right)^{-\sum_{i=1}^{L} \eta_i \eta_{i+1}} \tag{1.55}$$

where Z_L is the partition function.

Remark 1.1. *We note here that the process considered in Chapter 7 is a generalization the Katz-Lebowitz-Spohn (KLS) model in the dimension 1. To make this statement more specific, we recall that the dynamics of KLS process is as follows:*

$$0\widehat{10}0 \xrightarrow{r(1+\delta)} 0010, \ 1\widehat{10}0 \xrightarrow{r(1+\epsilon)} 1010, \ 0\widehat{10}1 \xrightarrow{r(1-\epsilon)} 0011, \ 1\widehat{10}1 \xrightarrow{r(1-\delta)} 1011$$

$$0\widehat{01}0 \xrightarrow{\ell(1+\delta)} 0100, \ 1\widehat{01}0 \xrightarrow{\ell(1-\epsilon)} 1100, \ 0\widehat{01}1 \xrightarrow{\ell(1+\epsilon)} 0101, \ 1\widehat{01}1 \xrightarrow{\ell(1-\delta)} 1101$$

We thus turn our process into the KLS model, if its parameters (cf. Eqs. (1.52)–(1.53)*) are chose so that the identities below hold true*

$$\begin{cases} \omega^\star &= r(1+\delta) \\ d^{1\star} &= \dfrac{1+\epsilon}{1+\delta} - 1 \\ d^{\star 01} &= \dfrac{1-\epsilon}{1+\delta} - 1 \\ \phi^\star &= \ell(1+\delta) \\ e^{\star 1} &= \dfrac{1+\epsilon}{1+\delta} - 1 \\ e^{10\star} &= \dfrac{1-\epsilon}{1+\delta} - 1 \end{cases} \tag{1.56}$$

1.3.3 Generalized Ising measure with nearest and next–nearest neighbors interaction for an one-dimensional lattice gas – Chapter 8

In Chapter 8, we consider exclusion process on the ring $\mathbb{T}_L$ with N particles. The process' dynamics is identical to the translocation part of process described in Section 1.2.3. Our current modification of the Exclusion Process may be described as follows. With the notation $\mathbf{x} = (x_1, x_2, ..., x_N)$ for the positions of the particles in an allowed configuration $\boldsymbol{\eta}$, the jump rates acquire the following form (below, x_i means the position of

the particle that will jump):

$$\omega_i(\boldsymbol{\eta}) = w_i^1(\boldsymbol{\eta}) + w_i^2(\boldsymbol{\eta}) \tag{1.57}$$

where

- $w_i^1(\boldsymbol{\eta}) := \omega_1^\star(1 + d^{1\star}\delta_{x_i,x_{i-1}+1} + d^{10\star}\delta_{x_i,x_{i-1}+2})(1 - \delta_{x_{i+1},x_i+1})\delta_{x_{i+1},x_i+2}$;

- $w_i^2(\boldsymbol{\eta}) := \omega_2^\star(1 + e^{1\star}\delta_{x_i,x_{i-1}+1} + e^{10\star}\delta_{x_i,x_{i-1}+2})(1 - \delta_{x_{i+1},x_i+1})(1 - \delta_{x_{i+1},x_i+2})$.

In words, the microscopic dynamics is as follows. We associate with each particle a random Poissonian clock with a rate depending on occupancy of its nearest and next-nearest neighbor sites on both sides (left and right). When the ith clock on the particle at position x_i rings, the particle hops to the site $x_i + 1$ provided the target site is vacant. For pictorial representations of the rate, see Fig. 1.11.
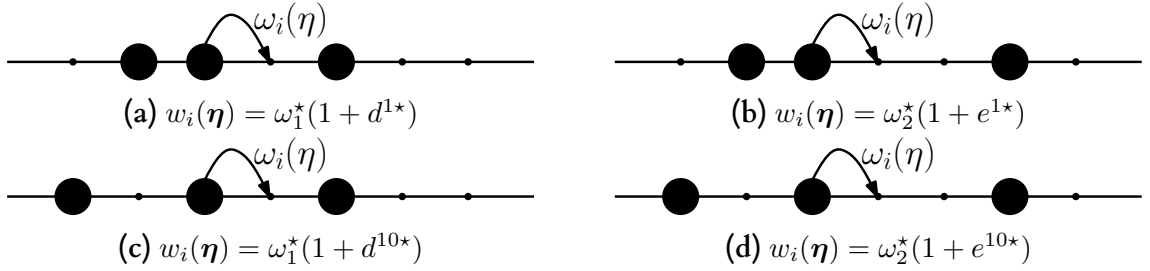
Figure 1.11: *Some examples of the jump rates.*

The aim of the study is to find conditions that ensure that the process' invariant measure is an Ising type measure. This question is answered by us as follows:

Theorem 1.8. *If parameters $d^{1\star}, d^{\star 01}, e^{1\star}$ and $e^{10\star}$ in the rate* (1.57) *satisfy the following constraints*

$$d^{1\star} = \frac{\omega_2^\star}{\omega_1^\star}(e^{1\star} - e^{10\star}), \tag{1.58}$$

$$d^{10\star} = e^{10\star}, \tag{1.59}$$

then the process has invariant distribution which is of the following form

$$\hat{\pi}(\boldsymbol{\eta}) = \frac{1}{Z_L}\left(\frac{\omega_2^\star}{\omega_1^\star}(1 + e^{1\star})(1 + e^{10\star})\right)^{-\sum_{i=1}^{L}\eta_i\eta_{i+1}}(1 + e^{10\star})^{-\sum_{i=1}^{L}\eta_i(1-\eta_{i+1})\eta_{i+2}} \tag{1.60}$$

where Z_L is the partition function.

Chapter 2

Background information

2.1 Mathematical aspects of the construction of our models

We shall present here the mathematical basis for our models. The aim is to explain the procedure we shall follow when we define our models (see Section 2.1.1) and to introduce several tools that will be employed when we look for the model's time–invariant distribution (see Section 2.1.3).

2.1.1 The construction via specifying the transition rates

In technical terms, our RNAP models are continuous time Markov Processes which trajectories are continuous from the right and have finite limits from the left at every time instance. What is specific in our models is that a model moves from one state to another one by an instantaneous "jump" of one of model's rod; here, "jump" means either a move from one lattice position to another one, or the change of the rod's state, or both. The question addressed in the present section is whether the definition in terms of rod jumps may be pursued forward to achieve a correct and unique stochastic process. The answer is "yes". This answer is provided by the theory of stochastic processes that are called Interacting Particle Systems ([18], [19]), or, alternatively, Interacting Markov Processes, or Markov Processes with Local Interactions. All our models fit absolutely well with this theory. In fact, our models are simpler than most of the Interacting Particle Systems because unlike it happens in the most general and most difficult case, our model's state space is finite; it is a subspace of $\{0, 1, 2\}^L$, where L is some finite integer (that typically represents the number of sites in the lattice mentioned above). However, we can use the general theory in order to ensure that the description via jump rates (see below) is enough to guarantee that there exists a unique continuous–time Markov process that fits this description. Here is how it is executed for the most general case of our RNAP model.

The transition rates definition: As we have stated above, each rod of our process may instantaneously move, or change its state, or both. It is a tradition to call a move by "jump", and to call a state change by "flip". Since our rods may either jump or flip or both, we need a general term, and it will be "transition". This gives rise to the term "transition rate" that we use below for the definition of the rules that govern transitions. The definition itself is called "microscopic dynamics definition" and it is as follows. On the periodic domain $\mathbb{T}_L$, we associate with each rod four random Poissonian clocks, say 1,2,3 and 4, with the configuration-dependent rates $\omega_i(\boldsymbol{\eta}), \tau_i(\boldsymbol{\eta}), \phi_i(\boldsymbol{\eta})$ and $\kappa_i(\boldsymbol{\eta})$ respectively. When one of the four clocks on the rod i (at position x_i) rings, there are the following possibilities.

- Rod i in state 1: If the clock is 3 or 4, nothing happens. If the clock is 1, the rod i hops forward one site provided the target site $x_i + \ell$ is vacant, i.e., the coordinate of ith rod now is $x_i + 1$, and changes its state into 2 instantaneously. If the clock is 2, the rod stays unmoved however its state changes to 2.

- Rod i in sate 2: If the clock is 1 or 2, nothing happens. If the clock is 3, the rod i hops backward one site provided the target site $x_i - 1$ is vacant, i.e., the coordinate of rod i^{th} now is $x_i - 1$, and changes its state into 1 instantaneously. If the clock is 4, the rod stays unmoved however its state changes to 1.

The rates of the Poisson clocks used in the above definition are called rods' transition rates.

2.1.2   The construction via the Master Equation

In discrete-time description of Markov chain $\boldsymbol{\eta}_t$ with time steps Δt, by the law of total probability, one has that

$$\mathbb{P}_{\boldsymbol{\eta}}(t + \Delta t) = \sum_{\boldsymbol{\eta}' \in X} p_{\boldsymbol{\eta}' \to \boldsymbol{\eta}} \mathbb{P}_{\boldsymbol{\eta}'}(t). \tag{2.1}$$

where $p_{\boldsymbol{\eta}' \to \boldsymbol{\eta}}$ is the transition probability from state $\boldsymbol{\eta}'$ at time t to state $\boldsymbol{\eta}$ at time $t + \Delta t$. One can rewrite (2.1) as follows

$$\mathbb{P}_{\boldsymbol{\eta}}(t + \Delta t) - \mathbb{P}_{\boldsymbol{\eta}}(t) = \sum_{\boldsymbol{\eta}' \in \Omega \setminus \boldsymbol{\eta}} p_{\boldsymbol{\eta}' \to \boldsymbol{\eta}} \mathbb{P}_{\boldsymbol{\eta}'}(t) - (1 - p_{\boldsymbol{\eta} \to \boldsymbol{\eta}}) \mathbb{P}_{\boldsymbol{\eta}}(t). \tag{2.2}$$

Here, one has $1 - p_{\boldsymbol{\eta} \to \boldsymbol{\eta}} = \sum_{\boldsymbol{\eta}' \neq \boldsymbol{\eta}} p_{\boldsymbol{\eta} \to \boldsymbol{\eta}'}$ which is the probability of finding the system not in state $\boldsymbol{\eta}$ at time $t + \Delta t$.

In continuous-time description, the dynamics of the Markov chain can be characterized by *transition rates* $\omega(\boldsymbol{\eta}' \to \boldsymbol{\eta})$ (see e.g. [18] or [19]) defined by

$$w(\boldsymbol{\eta}' \to \boldsymbol{\eta}) := \lim_{\Delta t \to 0} \frac{p_{\boldsymbol{\eta}' \to \boldsymbol{\eta}}}{\Delta t}, \text{ for } \boldsymbol{\eta} \neq \boldsymbol{\eta}' \tag{2.3}$$

which satisfy $0 \leq w(\boldsymbol{\eta} \to \boldsymbol{\eta}') < \infty$. Dividing both sides of (2.2) by Δt and in the limit of infinitesimal time steps $\Delta t \to 0$, one gets the following equation

$$\frac{d}{dt}\mathbb{P}_{\boldsymbol{\eta}}(t) = \sum_{\boldsymbol{\eta}' \neq \boldsymbol{\eta}} [w(\boldsymbol{\eta}' \to \boldsymbol{\eta})\mathbb{P}_{\boldsymbol{\eta}'}(t) - w(\boldsymbol{\eta} \to \boldsymbol{\eta}')\mathbb{P}_{\boldsymbol{\eta}}(t)] \qquad (2.4)$$

which is called *master equation* of the process. For more details, we refer a reader to [22, 24].

2.1.3   The condition for the stationary distribution

Suppose that measure $\hat{\pi}$ on state space Ω is an invariant distribution of process $\boldsymbol{\eta}_t$. Thus, the time evolution of the process does not alter $\hat{\pi}_t$, distribution of the process at time t, given at time $t = 0$, $\boldsymbol{\eta}_0$ is distributed by $\hat{\pi}$. This means that under this initial condition, $\hat{\pi}$ is a invariant measure if only if $\frac{d}{dt}\hat{\pi}_{\boldsymbol{\eta}}(t) = 0$. In other words, $\hat{\pi}$ is the invariant of the process if only if the following equation holds for all configurations

$$\sum_{\substack{\boldsymbol{\eta}' \neq \boldsymbol{\eta} \\ \boldsymbol{\eta}' \in \Omega}} [w(\boldsymbol{\eta}' \to \boldsymbol{\eta})\hat{\pi}(\boldsymbol{\eta}') - w(\boldsymbol{\eta} \to \boldsymbol{\eta}')\hat{\pi}(\boldsymbol{\eta})] = 0. \qquad (2.5)$$

Example: Consider a random walker on a ring $\mathbb{T}_L = \mathbb{Z}/(L\mathbb{Z})$ with L sites. The walker moves to the right and left with rates r and ℓ respectively. Denote by $\boldsymbol{\eta}^i$ the position on the lattice of the walker which is i. The master equation (written for the position of the walker to be at site i at time t) is the following

$$\frac{d}{dt}\mathbb{P}_{\boldsymbol{\eta}^i}(t) = w(\boldsymbol{\eta}^{i-1} \to \boldsymbol{\eta}^i)\mathbb{P}_{\boldsymbol{\eta}^{i-1}}(t) + w(\boldsymbol{\eta}^{i+1} \to \boldsymbol{\eta}^i)\mathbb{P}_{\boldsymbol{\eta}^{i+1}}(t)$$
$$- (w(\boldsymbol{\eta}^i \to \boldsymbol{\eta}^{i-1}) + w(\boldsymbol{\eta}^i \to \boldsymbol{\eta}^{i+1}))\mathbb{P}_{\boldsymbol{\eta}^i}(t)$$
$$= r\mathbb{P}_{\boldsymbol{\eta}^{i-1}}(t) + \ell\mathbb{P}_{\boldsymbol{\eta}^{i+1}}(t) - (r + \ell)\mathbb{P}_{\boldsymbol{\eta}^i}(t). \qquad (2.6)$$

Since the Markov chain is irreducible and since its state space is finite, the process has a unique invariant measure. One notices that the measure $\hat{\pi}$ with $\hat{\pi}(\boldsymbol{\eta}^i) = 1/L, \quad \forall i \in 1, ..., L$, is the invariant measure of the process since it satisfies the stationary conditions (2.5).

2.2   One-dimensional exclusion processes

2.2.1   Justification

The *Exclusion Process* (EP) is a simple particle–hopping model introduced in 1970 by Spitzer [26]. Since then EP has become an extensively studies process in nonequilibrium statistical physics as the exactly solvable model of nonequilibrium behavior, boundary-

induced phase transitions.

The EP plays a central role in our thesis. On the one hand, all our RNAP models are based upon EP: essentially, the extension that creates RNAPs from EP amounts to allowing each particle to switch between two states during the process evolution. On the other hand, our studies of the RNAPs' transition rates and of the potential function of their invariant measures suggested to us to construct and investigate certain extensions of the EP. Then, we saw that the scientific community carries research on EP in similar directions. Accordingly, the EP and its modifications turned out to be the object of the study of the present thesis.

2.2.2   Definition

The EP is a continuous time Markov process for particles that cannot occupy the same position (exclusion principle). Additionally, a particle can hop from one lattice site to one of its neighboring sites provided the target site is vacant. The local state of the process can be represented by a value belonging to set $E = \{0, 1\}$. If a site is vacant denoted by 0 and if it is occupied by a particle denoted by 1. Thus, the state space of the process on the integer lattice Λ is $\Omega_\Lambda = \{0, 1\}^\Lambda$ with a configuration denoted by $\boldsymbol{\eta} = (\eta_1, ..., \eta_L)$ where $\eta_i \in \{0, 1\}$. In one dimension, the transition rates are given by

- $w(\boldsymbol{\eta} \to \boldsymbol{\eta}') = r$ if there exists i such that $\eta_i = 1, \eta_{i+1} = 0, \eta_i' = 0, \eta_{i+1}' = 1$, and $\eta_j = \eta_j'$ for all $j \neq i, i+1$,

- $w(\boldsymbol{\eta} \to \boldsymbol{\eta}') = \ell$ if there exists i such that $\eta_i = 0, \eta_{i+1} = 1, \eta_i' = 1, \eta_{i+1}' = 0, \eta_j = \eta_j'$ for all $j \neq i, i+1$,

- Other cases, one has $w(\boldsymbol{\eta} \to \boldsymbol{\eta}') = 0$.

2.2.3   Terminology

The process is called *Asymmetric Simple Exclusion Process* (ASEP) if $r > \ell > 0$ or $0 < r < \ell$. In the case that particles allow moving only one direction which means $r = 0$ or $\ell = 0$, we call it *Totally Asymmetric Simple Exclusion Process* (TASEP). For the case, $r = \ell$, one uses the term *Symmetric Simple Exclusion Process* (SSEP or SEP).

2.2.4   Boundary conditions

We consider the process defined on a finite lattice $\Lambda = \{1, ..., L\}$. One has to specify boundary conditions.

● *Periodic boundary conditions:* The one-dimensional lattice Λ, in this case, is a ring which means that the sites 1 and L are made nearest-neighbors of each other, all the sites are treated on an equal footing. Note in this case that the dynamics conserves the total

number N of particles.

• *Open boundary conditions:* For the simple exclusion process with open boundary conditions, at the boundary sites 1 and L, we allow creating and annihilating particles with rates $\alpha, \beta, \gamma, \delta$ as indicated in Figure 2.1.
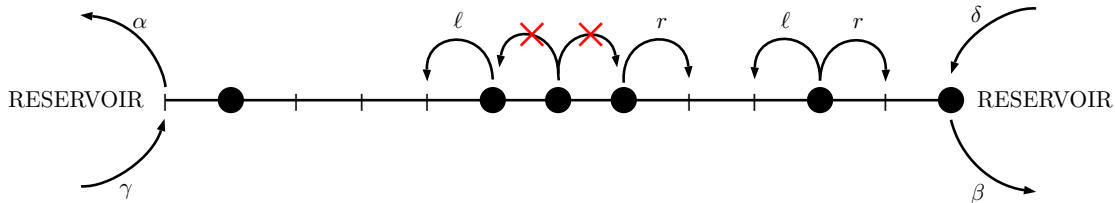
Figure 2.1: *ASEP with open boundaries. In the bulk, hoping rates to the right and left are r and ℓ respectively.*

2.2.5   Stationary current, flux, and velocity

Let us consider the system in equilibrium. *Stationary current j* is the quantity which is defined by the net number of particles that flows across a lattice bond $(i, i+1)$ per infinitesimal time interval. That is stationary expectation of the *instantaneous current $j_i(t)$* defined for the process in Fig. 2.1 in the bulk as follows

$$j_i(t) := r\eta_i(t)(1 - \eta_{i+1}(t)) - \ell(1 - \eta_i(t))\eta_{i+1}(t). \qquad (2.7)$$

Thus, the stationary current with respect to invariant measure $\hat{\pi}$ reads

$$j := r\langle \eta_i(t)(1 - \eta_{i+1}(t))\rangle_{\hat{\pi}} - \ell\langle(1 - \eta_i(t))\eta_{i+1}(t)\rangle_{\hat{\pi}}. \qquad (2.8)$$

In the example above, the stationary flux is just $j = (r - \ell)\rho(1 - \rho)$. The stationary flux j (with the same notation of stationary current) and stationary velocity ν are related by $j = \rho\nu$ where ρ is the particle density. However, almost everywhere in this thesis, we consider generalized exclusion processes which have configuration-dependent jump rates. Roughly speaking, the rates r and ℓ of a particle are random variables depending on the current state $\boldsymbol{\eta}$ denoted by $r(\boldsymbol{\eta})$ and $\ell(\boldsymbol{\eta})$, respectively. With this setting, the stationary flux is just the expectation of the rate $r(\boldsymbol{\eta})$ minus rate $\ell(\boldsymbol{\eta})$, i.e., $j = \langle r(\boldsymbol{\eta}) - \ell(\boldsymbol{\eta})\rangle_{\hat{\pi}}$ and we also have the relation $j = \rho\nu$.

2.2.6   Thermodynamic limit

Statistical mechanics often deals with many-body problems, e.g., 6.02×10^{23}-body problem. The number is finite but huge. To investigate that kind of problem, one first works with a system containing a finite number of particles N (atoms or molecules) with finite volume L and then let N and L go to infinity such that the particle density

N/L tends to a constant value. Namely,

$$N \to \infty, L \to \infty, \frac{N}{L} = \rho = \text{constant}. \tag{2.9}$$

This procedure is called the *thermodynamic limit* which is also called *macroscopic limit*.

Since real physical systems are finite but large, one should take care of results in the thermodynamic limit which describes the systems more accurately. It is worth noticing that many characteristic properties of macroscopic physical systems only appear in this limit, namely phase transitions, universality classes, and other critical phenomena. For more interesting discussions, we refer a reader to [17, 28].

Example: Consider the TASEP on the finite, periodic lattice $\mathbb{T}_L$. When the number of particles is fixed to N, since the invariant measure is unique in this case, one can see that all possible configurations have the same weight satisfying the equation (2.5), one gets

$$\hat{\pi}_{L,N}(\boldsymbol{\eta}) = 1 \Big/ \binom{L}{N} = N!(L-N)!/L!, \tag{2.10}$$

which is the invariant distribution of the process.

In this example, the stationary current between sites $(i, i+1)$ is the following

$$j_i = \langle \eta_i(1 - \eta_{i+1}) \rangle_{\hat{\pi}_{L,N}}. \tag{2.11}$$

One has the density profile and the correlation function as follows

$$\langle \eta_i \rangle_{\hat{\pi}_{L,N}} = \frac{N}{L} = \rho, \quad \langle \eta_i \eta_j \rangle_{\hat{\pi}_{L,N}} = \frac{(N-1)N}{(L-1)L} \approx \rho^2, \tag{2.12}$$

leading to the following expression for the current

$$j_i = \frac{N}{L}\frac{L-N}{L-1} = \rho(1-\rho) + O(L^{-1}). \tag{2.13}$$

In the thermodynamic limit $L \to \infty$, one has

$$j = \rho(1 - \rho). \tag{2.14}$$

As one can see, the current is a function of the density. In scientific literature, the current–density relation is often called the *fundamental diagram*. From Fig. 2.2, one sees that the current reaches maximum at density 1/2.
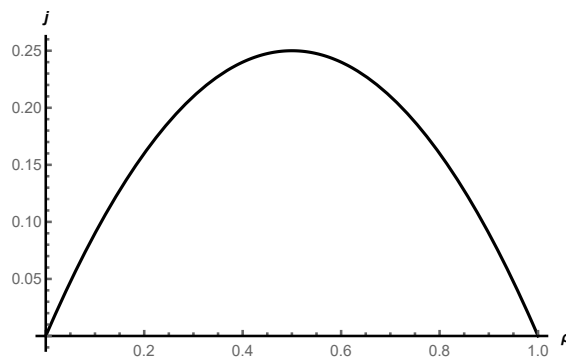
Figure 2.2: *Stationary current j as a function of the density ρ in TASEP with periodic boundary conditions.*

2.3   Brief description of the elongation step of RNA transcription

RNA polymerase (RNAP) is an enzyme that is a molecular motor that transcribes the information coded in the base pair[1] (bp) sequence of DNA into an RNA. Transcription takes place in three steps which are initiation, elongation, and termination. Namely, *initiation* is the beginning of transcription. It occurs when RNAP binds to a region which is called *promoter sequence* on the DNA. Once RNAP is at the position of the promoter sequence, it locally creates the so-called transcription bubble which causes two DNA strands to detach, and once the transcription bubble has formed, the step *elongation* can begin. Stepping along the base pairs of the DNA, the RNAP forms the transcription elongation complex (TEC) which polymerizes the monomeric subunits of the RNA by the addition of nucleotides, as determined by the corresponding sequence on the template DNA. During each elongation step, the catalytic mechanism of RNAP consists the several steps whose major steps are (1) Nucleoside triphosphate (NTP) binding, (2) NTP hydrolysis, (3) Release of pyrophosphate (PP_i), one of the products of hydrolysis, (4) Accompanying forward step of the RNAP along with the DNA template by one base pair (see [2, 32]). *Termination* is the ending of transcription which occurs when the TEC reaches the termination sequence.

The typical size of a transcription bubble is around 15 bp whereas the TEC covers a DNA segment of up to 35 bp. To highlight the effect of interactions, we do not describe the various transformations of the TEC during each elongation step. We simplify the

---

[1]In molecular biology, two nucleotides on opposite complementary DNA or RNA strands that are connected via hydrogen bonds are called a base pair (often abbreviated bp). In the canonical Watson–Crick base pairing, adenine (A) forms a base pair with thymine (T), as does guanine (G) with cytosine (C) in DNA. In RNA, thymine is replaced by uracil (U). Non–Watson-Crick base pairing with alternate hydrogen bonding patterns also occur, especially in RNA; common such patterns are Hoogsteen base pairs.

Base pairing is also the mechanism by which codons on messenger RNA molecules are recognized by anticodons on transfer RNA during protein translation. Some DNA- or RNA-binding enzymes can recognize specific base pairing patterns that identify particular regulatory regions of genes.

complicated geometry of the TEC by representing it as a rod covering ℓ lattice sites, where ℓ is a parameter of our model, and not differentiate between the TEC and the RNAP.

RNAPs on the same promoter sequence often move simultaneously, so that one cannot ignore their mutual interactions. The repulsion which is assumed in most modeling approaches to molecular motor traffic is a hardcore interaction [29, 30]. With only this steric interaction, one can successfully capture the traffic jam phenomenon which occurs when there is a pausing RNAP that prevents other RNAPs from moving forward. However, as demonstrated in [7, 8], the interaction may also be cooperative. This means a trailing RNAP can "push" the leading RNAP out of pause sites. Thus, the elongation is enhanced. Belitsky and Schütz in [4, 5] introduced a lattice gas model which predicts the conditions under which collective jamming and pushing can arise. The model is a generalization of the asymmetric simple exclusion process (ASEP) [21, 22] with an internal degree of freedom whose transition rates are configuration-dependent. We emphasize that on the microscopic level, the configuration-dependent rates describe the mutual interaction among neighboring RNAPs, while on the macroscopic level, those rates lead to cooperative jamming and pushing.

An RNAP appears in only two distinct polymerization states, namely without PP_i bound to it (state 1) or with PP_i (state 2). It is then convenient to characterize the state of TEC mathematically not in terms of the length k of the RNA transcript attached to it but to describe it in terms of the corresponding base pair so that $x = k$ marks the position of the RNAP on the template DNA. The RNAP moves forward along the DNA by one bp (a step length of $\delta = 0.34$ nm), i.e., from x to $x+1$ only after PP_i release, i.e., only the RNAP is in state 1. Meanwhile, the RNAP moves backward along the DNA by one bp, i.e., from x to $x-1$ even in the case with PP_i bound to it, i.e., only the RNAP is in state 2. Without loss of generality we define x to be the lattice position of the left end of the rod in the random walk model.

We denote the rate at which an elongation step of RNAP i occurs by $\omega_i(\boldsymbol{\eta})$. The rate of PP_i release is denoted by $\kappa_i(\boldsymbol{\eta})$. The rate of reverse transitions, which result in depolymerization of the RNA is denoted by $\phi_i(\boldsymbol{\eta})$. Finally, $\tau_i(\boldsymbol{\eta})$ is the rate of association of PP_i.

To understand clearer the transition rates, one can use Fig. 2.3 that presents the minimal reaction scheme (see [4]) sketched for a single RNAP, following the description in [32]. The ith RNAP in state 1_k can move from base pair k to $k + 1$ with a configuration-dependent rate $\omega_i(\boldsymbol{\eta})$. It can perform the forward translocation step after PP_i release with a configuration-dependent rate $\kappa_i(\boldsymbol{\eta})$ (transition from state 2_{k+1} to state 1_{k+1}). The RNAP can move from base pair $k + 1$ to k provided it is in state 2_{k+1} with the depolymerization rate of RNA denoted by $\phi_i(\boldsymbol{\eta})$ (transition from state 2_{k+1} to state 1_k). The association rate of PP_i is $\tau_{k+1}(\boldsymbol{\eta})$ (transition from state 1_{k+1} to state 2_{k+1}).
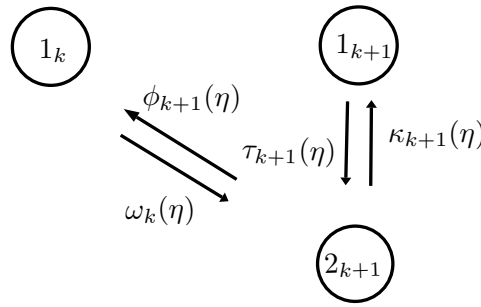
Figure 2.3: *Minimal scheme of the mechano-chemical cycle of an RNAP. The RNAP without PP$_i$ bounds to it is in state 1 and with PP$_i$ is in state 2. The integer subscript k labels the position of the RNAP on the DNA template.*

2.4   Gibbs ensembles

Gibbs measures are present in our work because we take them as candidates for time-invariant distributions of our stochastic models. This fact motivated us to include the present section whose contents may help our readers to understand the formulations and the proofs in which Gibbs measures are involved. For a detailed introduction of the Gibbs measures and their properties, we refer a reader to Chapter 1 in [10].

2.4.1   Ensemble

The term *ensemble*, often used in physics, has been introduced by J. Willard Gibbs in 1902. In probability theory, it is equivalent to *probability distribution*.

2.4.2   Boltzmann weights

Consider a physical system defined on a lattice Λ which can be any countable set. At each lattice site in Λ, the local state is a value belonging to a finite set E. Thus, a state of the system is an element of $\Omega_\Lambda := E^\Lambda$ which is often called the microstate, and set Ω_Λ of all states is called state space. A well-established empirical fact that in thermal equilibrium, the probability of finding a system in the microstate $\boldsymbol{\eta}$ with energy H is proportional to $\exp(-H/k_B T)$, where T is the temperature and k_B is the Boltzmann constant. Thus, to define the model fully at thermal equilibrium, one posits an energy function $H : \Omega_\Lambda \to \mathbb{R}$ and we introduce the *Boltzmann weight*

$$w(\boldsymbol{\eta}) := e^{-\beta H(\boldsymbol{\eta})}. \tag{2.15}$$

Here, the non-negative real parameter $\beta \in \mathbb{R}_+ := (0, \infty)$ is proportional to the inverse of experimentally measured strictly positive temperature $T \in \mathbb{R}_+$ of the system. From the Boltzmann weight (2.15) one computes the *partition function*

$$Z := \sum_{\boldsymbol{\eta} \in \Omega} w(\boldsymbol{\eta}). \tag{2.16}$$

This is a finite number for any temperature $T > 0$. Thus, in thermal equilibrium, the probability of finding the physical system in configuration $\boldsymbol{\eta}$ is given by the following

$$\pi(\boldsymbol{\eta}) := \frac{1}{Z} e^{-\beta H(\boldsymbol{\eta})} \tag{2.17}$$

which is called *Boltzmann factor*. By the construction, this is a probability measure which is a *Gibbs ensemble* (defined above).

2.4.3 Observable

Physical observable is a quantity that can be measured. Mathematically, it corresponds to a random variable $O : \Omega_\Lambda \to \mathbb{R}$. Quantities that can be observed in experiments are expectation values denoted by the angular brackets. Thus, the expectation of observable O with respect to Boltzmann factor π (2.17) is the following

$$\langle O \rangle_\pi := \sum_{\boldsymbol{\eta} \in \Omega} O(\boldsymbol{\eta}) \pi(\boldsymbol{\eta}) = \frac{1}{Z} \sum_{\boldsymbol{\eta} \in \Omega} O(\boldsymbol{\eta}) w(\boldsymbol{\eta}). \tag{2.18}$$

From a physics perspective, these expectations are equilibrium averages.

2.4.4 Canonical Gibbs ensemble

Consider a physical system with N particles located inside the finite lattice Λ that can exchange temperature with the environment. Denote by $\Omega_{\Lambda,N}$ the state space and let H be the Hamiltonian of the system. A measure π in $\mathcal{P}$ where $\mathcal{P}$ the space of probability measures on $\Omega_{\Lambda,N}$ is called Gibbs if at the fixed temperature it follows the *Maximum Entropy Principle*. Namely, it maximizes the Shannon entropy defined below under the constraint that $\langle H \rangle_\pi = U$ where $U \in \mathcal{U}$ with $\mathcal{U} := \{U = E(\boldsymbol{\eta}) : \boldsymbol{\eta} \in \Omega_{L,N}\}$.

Definition 2.1. *Let π be an element of $\mathcal{P}$. The Shannon entropy of π is defined by*

$$S(\pi) = -\sum_{\boldsymbol{\eta} \in \Omega} \pi(\boldsymbol{\eta}) \log \pi(\boldsymbol{\eta}). \tag{2.19}$$

Thus, in order to find the Gibbs ensemble, one needs to minimize $\sum_{\boldsymbol{\eta}} \pi(\boldsymbol{\eta}) \log \pi(\boldsymbol{\eta})$ under the following conditions

$$\begin{cases} \sum_{\boldsymbol{\eta} \in \Omega_{L,N}} \pi(\boldsymbol{\eta}) = 1, \\ \sum_{\boldsymbol{\eta} \in \Omega_{L,N}} \pi(\boldsymbol{\eta}) H(\boldsymbol{\eta}) = U. \end{cases} \tag{2.20}$$

By considering Lagrange function with two Lagrange multipliers λ and β as follows

$$L(\pi) = \sum_{\boldsymbol{\eta}} \pi(\boldsymbol{\eta}) \log \pi(\boldsymbol{\eta}) + \lambda \sum_{\boldsymbol{\eta} \in \Omega_{L,N}} \pi(\boldsymbol{\eta}) + \beta \sum_{\boldsymbol{\eta} \in \Omega_{L,N}} \pi(\boldsymbol{\eta}) H(\boldsymbol{\eta}) \tag{2.21}$$

gives us the solution

$$\pi(\boldsymbol{\eta}) = \frac{e^{-\beta H(\boldsymbol{\eta})}}{\sum_{\boldsymbol{\eta}' \in \Omega_{L,N}} e^{-\beta H(\boldsymbol{\eta}')}}, \tag{2.22}$$

where β is chosen such that $\langle H \rangle_\pi = U$. The measure (2.22) is called *canonical Gibbs ensemble* at parameter β on $\Omega_{\Lambda,N}$ and $Z = \sum_{\boldsymbol{\eta}' \in \Omega_{L,N}} e^{-\beta H(\boldsymbol{\eta}')}$ is called the *canonical partition function*.

2.4.5   The grand–canonical Gibbs ensemble

The canonical Gibbs ensemble above describes the system at equilibrium and at a fixed temperature with an unchanged number of particles. Now, we consider a system that can exchange not only temperature but also particles with the environment. From the thermodynamic point of view, such a system is characterized by its temperature and chemical potential.

Denote by Ω_Λ the state space of the system. One has $\Omega_\Lambda = \bigcup_{N=0}^{|\Lambda|} \Omega_{\Lambda,N}$ where $|\Lambda|$ is the the cardinality of Λ. Similarly to what was discussed above, at a fixed temperature and number of particles, one can find the canonical ensemble on $\Omega_{\Lambda,N}$. By using two Lagrange multipliers β and μ, the measure on Ω which follows the Maximum Entropy Principle is of the following form

$$\pi_{gc}(\boldsymbol{\eta}) = \frac{e^{-\beta H(\boldsymbol{\eta}) - \mu N}}{Z_{gc}}, \quad \text{if } \boldsymbol{\eta} \in \Omega_{L,N}, \tag{2.23}$$

where $Z_{gc} = \sum_{N=0}^{|L|} \sum_{\boldsymbol{\eta} \in \Omega_{L,N}} e^{-\beta H(\boldsymbol{\eta}) - \mu N}$ is the normalizing sum. The measure π_{gc} in (2.23) on Ω_Λ is called *grand–canonical Gibbs ensemble* and its normalizing sum Z_{gc} is called *grand–canonical partition function*.

2.5   Some notations of linear algebra

Next, we recall some notation of linear algebra that we will make use of in this thesis, see the appendix [24] for more details.

Bra-ket notations: Bra-ket is a way of writing vectors used in Quantum Physics. Namely, *ket-vector A* denoted by $|A\rangle$ is a column vector, whereas *bra-vector B* denoted by $\langle B|$ is a row vector. For examples,

$$|A\rangle = \begin{pmatrix} A_1 \\ A_2 \\ \vdots \\ A_m \end{pmatrix}, \quad \langle B| = (B_1, B_2, ..., B_n). \tag{2.24}$$

If $A_l = \delta_{p,l}$ and $B_l = \delta_{q,l}$ then we denote the corresponding bra and ket vectors by $|p\rangle, \langle q|$. For a matrix product of the form $C = \langle A||B\rangle$, we omit one of the two central vertical lines and write $C = \langle A|B\rangle$.

Projector: For Kronecker products of bra and ket vectors $\langle p|$ and $|q\rangle$ with components $A_p = \delta_{p,l}$ and $B_q = \delta_{q,l}$, we note that

$$|p\rangle \otimes \langle q| \equiv |p\rangle \langle q| = E^{pq}. \tag{2.25}$$

For dimensions $m = n$ the Kronecker product $|p\rangle \otimes \langle p| = E^{pp}$ is called *projector* on p. Obviously, one has the completeness property

$$\sum_{p=1}^{m} |p\rangle \langle p| = \sum_{p=1}^{m} E^{pp} = \mathbb{1} \tag{2.26}$$

for any $m \geq 1$, where $\mathbb{1}$ is the unit matrix.

Completeness of eigenvectors: Denote by $\boldsymbol{\lambda} := \{\lambda_1, ..., \lambda_n\}$ the set of all eigenvalues of a $n \times n$ square matrix A. Recall that the left and right eigenvalues are equivalent. We denote left and right eigenvectors by $\langle \lambda|$ and $|\lambda\rangle$, respectively, where $\lambda \in \boldsymbol{\lambda}$. The eigenvectors can be normalized in the way such that the completeness property

$$\sum_{\lambda \in \boldsymbol{\lambda}} |\lambda\rangle \langle \lambda| = \mathbb{1} \tag{2.27}$$

holds. We also have the biorthogonal property

$$\langle \lambda|\mu\rangle = \delta_{\lambda,\mu} \tag{2.28}$$

for the normalized eigenvector with eigenvalues λ and μ.

Trace of a matrix: The trace of a n-dimensional square matrix $A := (A_{i,j})_{n \times n}$ is the sum of all diagonal elements, i.e.,

$$\mathrm{Tr}A = \sum_{i=1}^{n} A_{ii}. \tag{2.29}$$

One has

$$\mathrm{Tr}A = \sum_{i=1}^{n} \lambda_i, \tag{2.30}$$

where λ_i, $i = 1, ..., n$, are eigenvalues of matrix A. Moreover, the trace is invariant under cyclic permutation, i.e.,

$$\mathrm{Tr}ABC = \mathrm{Tr}CAB = \mathrm{Tr}BCA. \tag{2.31}$$

We also note that

$$A_{ii} = \langle i | A | i \rangle = \text{Tr} | i \rangle \langle i | A = \text{Tr} A | i \rangle \langle i |. \tag{2.32}$$

In particular, by summing over i it follows that

$$\text{Tr} A = \sum_{i=1}^{n} \text{Tr} \langle i | A | i \rangle = \text{Tr} \mathbb{1} A = \text{Tr} A \mathbb{1}. \tag{2.33}$$

2.6 Kramers–Wannier transfer matrix for Ising model in one dimension

In this section, let us consider the one-dimensional Ising model with periodic boundary conditions with L spins. It will serve us to demonstrate the matrix technique. In this model, each spin only interacts with its neighbors on either side and with the external magnetic field h. The interaction energy of configuration $\mathbf{s} = (s_1, ..., s_L)$ where $s_i \in \{-1, 1\}$ is

$$H(\mathbf{s}) = J \sum_{i=1}^{L} s_i s_{i+1} + h \sum_{i=1}^{L} s_i. \tag{2.34}$$

Thus, at thermal equilibrium, the Boltzmann factor is defined by

$$\pi(\mathbf{s}) := \frac{1}{Z_L} e^{-\beta H(\mathbf{s})} \tag{2.35}$$

Here Z_L is the partition function computed by

$$Z_L = \sum_{s_1=-1,1} \sum_{s_2=-1,1} \cdots \sum_{s_L=-1,1} \exp \left\{ -\beta \sum_{i=1}^{L} (J s_i s_{i+1} + h s_i) \right\}. \tag{2.36}$$

Kramers and Wannier [15, 16] showed that the partition function can be expressed in terms of matrices as the following. Introduce the function $T : \{-1, 1\} \times \{-1, 1\} \to \mathbb{R}_+$

$$T(s, s') = e^{-\beta(Jss' + \frac{1}{2}h(s+s'))}. \tag{2.37}$$

This allows us to define the *transfer matrix*

$$T := \begin{pmatrix} T(-1, -1) & T(-1, 1) \\ T(1, -1) & T(1, 1) \end{pmatrix} = \begin{pmatrix} yx^{-1/2} & y^{-1} \\ y^{-1} & y^{-1}x^{1/2} \end{pmatrix} \tag{2.38}$$

where $x = e^{-\beta h}, y = e^{-\beta J}$. With the bra and ket vectors

$$\langle -1 | = (1, 0), \quad \langle 1 | = (0, 1), \quad | i \rangle = \langle i |^T \tag{2.39}$$

one gets

$$T(s, s') = \langle s | T | s' \rangle .\tag{2.40}$$

Thus, one can write the partition function in the form

$$
\begin{aligned}
Z_L &= \sum_{s_1=-1,+1} \sum_{s_2=-1,+1} \cdots \sum_{s_L=-1,+1} \langle s_1 | T | s_2 \rangle \langle s_2 | T | s_3 \rangle ... \langle s_L | T | s_1 \rangle \\
&= \sum_{s_1=-1,+1} \langle s_1 | T^L | s_1 \rangle \\
&= \mathrm{Tr} T^L \\
&= \lambda_+^L + \lambda_-^L,
\end{aligned}
\tag{2.41}
$$

where λ_+ and λ_- are the two eigenvalues of T with $\lambda_+ > \lambda_-$. The eigenvalues are the following

$$\lambda_{\pm} = \frac{x + y^2 \pm \sqrt{4x + x^2 - 2xy^2 + y^4}}{2\sqrt{xy}} .\tag{2.42}$$

As an application of the matrix technique, we calculate the Helmholtz free energy $F = -k_B T \ln Z_L$. One has

$$-\frac{F}{k_B T} = \ln Z_L = \ln\left(\lambda_+^N + \lambda_-^N\right)\tag{2.43}$$

$$= \ln\left\{ \lambda_+^L \left(1 + \left(\frac{\lambda_-}{\lambda_+}\right)^L\right) \right\}\tag{2.44}$$

and we introduce the free energy per lattice site $f = F/L$. In the thermodynamic limit $L \to \infty$, the Helmholtz free energy per spin is

$$f = \lim_{L\to\infty} \frac{F}{L} = -k_B T \ln \lambda_+ .\tag{2.45}$$

Part II

Modeling interacting RNAPs at the elongation step of RNA transcription

Chapter 3

RNAP model: Range–2 interaction rate and range–1 pair potential

Before we start, we recall the main ideas of our modeling, the construction of the model, the study approach, and the aims. All this is in the paragraph below.

Our construction consists of the following steps. We take the DNA template as a one-dimensional lattice of length L (i.e. the lattice sites are $1, \ldots, L$). We model each RNAP by a rod that occupies ℓ consecutive sites (this model the fact that an RNAP covers ℓ nucleotides). Then, we define the states at which each rod may be. Next, we define the translocation rules for each rod. The rods interact between themselves because RNAPs cannot overlap. Thus, there is an interaction that is similar to that of particles in the Simple Exclusion Process. However, we want the interaction rule to be a bit more sophisticated (as we shall show this sophistication causes phenomena that the Simple Exclusion Process cannot exhibit). The interactions are expressed through the explicit formulas for the transition rates. Then, we postulate that the stationary distribution of our model must have a specific form. Finally, we find the constraints upon the transition rates that guarantee that the desired distribution is in fact the stationary distribution for the dynamics specified by those rates. This is the Existence Theorem proved in Section 3.1.3. Then, we study properties of the model such as average excess and dwell times in Subsection 3.2.3 and especially average elongation rate in Subsection 3.2.4.

3.1 The RNAP model with short range interaction

In this chapter, we investigate the RNAP model by utilizing the transition rates outlined in Fig. 2.3, i.e., we focus on examining RNAP processes, specifically including inverse transitions that were neglected in the papers [4, 5]. For the convenience of the readers, we provide the figure here to facilitate their understanding and follow the discussion.
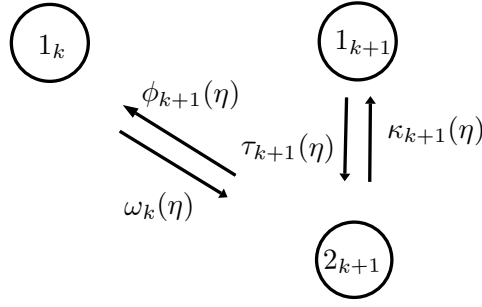
Figure 3.1: *Minimal scheme of the mechano-chemical cycle of an RNAP. The RNAP without PP_i bounds to it is in state 1 and with PP_i is in state 2.*

To understand the model's state space, please refer to Subsections 2.1.1 and 2.3. Our current emphasis is on the model's dynamics in the next subsection.

3.1.1 The dynamics

Let $\boldsymbol{\eta}$ be an allowed configuration with the coordinate vector $\mathbf{x} = \{x_1, ..., x_N\}$ and state vector $\mathbf{s} = \{s_1, ..., s_N\}$. The term allowed means that the ordering condition $x_{i+1} \geq x_i + \ell$ must be satisfied by the configuration (this is due to the fact that TECs cannot overtake each other). We say that two RNAPs i and $i+1$ are neighbors when the front of rod i and the left edge of rod $i+1$ occupy neighboring lattice sites, i.e., when $x_{i+1} = x_i + \ell$. Thus the rates are of the forms

$$\omega_i(\boldsymbol{\eta}) = \omega^\star \delta_{s_i,1}(1 + d^{1\star}\delta_{x_{i-1}+\ell,x_i} + d^{\star 01}\delta_{x_i+\ell+1,x_{i+1}})(1 - \delta_{x_i+\ell,x_{i+1}}), \tag{3.1}$$

$$\phi_i(\boldsymbol{\eta}) = \phi^\star \delta_{s_i,2}(1 + e^{10\star}\delta_{x_{i-1}+\ell+1,x_i} + e^{\star 1}\delta_{x_i+\ell,x_{i+1}})(1 - \delta_{x_{i-1}+\ell,x_i}), \tag{3.2}$$

$$\begin{aligned}\kappa_i(\boldsymbol{\eta}) = {} & \kappa^\star \delta_{s_i,2}(1 + f^{1\star}\delta_{x_{i-1}+\ell,x_i} + f^{\star 1}\delta_{x_i+\ell,x_{i+1}} + f^{1\star 1}\delta_{x_{i-1}+\ell,x_i}\delta_{x_i+\ell,x_{i+1}} \\ & + f^{10\star}(1 - \delta_{x_{i-1}+\ell,x_i})\delta_{x_{i-1}+\ell+1,x_i} + f^{\star 01}(1 - \delta_{x_i+\ell,x_{i+1}})\delta_{x_i+\ell+1,x_{i+1}}),\end{aligned} \tag{3.3}$$

$$\begin{aligned}\tau_i(\boldsymbol{\eta}) = {} & \tau^\star \delta_{s_i,1}(1 + g^{1\star}\delta_{x_{i-1}+\ell,x_i} + g^{\star 1}\delta_{x_i+\ell,x_{i+1}} + g^{1\star 1}\delta_{x_{i-1}+\ell,x_i}\delta_{x_i+\ell,x_{i+1}} \\ & + g^{10\star}(1 - \delta_{x_{i-1}+\ell,x_i})\delta_{x_{i-1}+\ell+1,x_i} + g^{\star 01}(1 - \delta_{x_i+\ell,x_{i+1}})\delta_{x_i+\ell+1,x_{i+1}}).\end{aligned} \tag{3.4}$$

where in the setting of Wang *et al.* [32], when both neighboring sites $x_i - 1$ and $x_i + \ell$ are empty, the rates $\kappa^\star, \omega^\star, \phi^\star$, and $\tau^\star$ take the values

$$\omega^\star = [\text{NTP}](\mu M)^{-1}s^{-1}, \quad \phi^\star = 0.21s^{-1}, \quad \kappa^\star = 31.4s^{-1}, \quad \tau^\star = [\text{PP}_i](\mu M)^{-1}s^{-1}. \tag{3.5}$$

Here $[\text{NTP}]$ and $[\text{PP}_i]$ are the NTP and PP_i concentrations which are parameters of our model. With this setting, the transition rates are configuration-dependent in which the parameters $d^{1\star}, d^{\star 01}, e^{10\star}, e^{\star 1}$, and $f^{1\star}, f^{\star 1}, f^{1\star 1}, f^{10\star}, f^{\star 01}$, and $g^{1\star}, g^{\star 1}, g^{1\star 1}, g^{10\star}, g^{\star 01}$ describe the interaction between neighboring RNAP. One requires these parameters are greater that -1 and must be chosen to ensure the positivity of the rates. Namely, the parameter range is $d^{1\star} + d^{\star 01} \geq -1$, $e^{10\star} + e^{\star 1} \geq -1$, $f^{1\star} + f^{\star 1} \geq -1$, $f^{1\star} + f^{\star 01} \geq -1$, $f^{10\star} + f^{\star 1} \geq -1$, $f^{10\star} + f^{\star 01} \geq -1$, $f^{1\star 1} \geq -1$. The overall factors $(1 - \delta_{x_i+\ell,x_{i+1}})$ and $(1 - \delta_{x_{i-1}+\ell,x_i})$ forbid jumps onto an occupied site.

To get a deeper insight at the rates (3.1)–(3.4), we refer a reader to Section 1.2.2. However, let us clarify here the role of the parameters and notations appearing in the rates by taking $\omega_i(\boldsymbol{\eta})$ as an example. $\omega_i(\boldsymbol{\eta})$ is the rate at which the rod at the position x_i jumps one lattice site rightwards and changes its state from 1 to 2. (We will call it "jump-and-flip" rate.) The expression for $\omega_i(\boldsymbol{\eta})$ will be given below. The expression will involve the rods which positions in $\boldsymbol{\eta}$ are x_{i-1} and x_{i+1}. The correct notations thus would be $x_{i-1}(\boldsymbol{\eta})$, $x_i(\boldsymbol{\eta})$ and $x_{i+1}(\boldsymbol{\eta})$. Nevertheless, we shall write x_{i-1}, x_i and x_{i+1} instead.

$(1 - \delta_{x_i+\ell+1,x_{i+1}})$ is nil if and only if the rod at x_i leans over the rod at x_{i+1}, that is, iff there is no vacant site to the right of the rod x_i. In this case, the rod cannot jump forward, and, accordingly, the rate $\omega_i(\boldsymbol{\eta})$ is 0. In any other case, the jump is possible, which is reflected by the fact that the multiplier $(1 - \delta_{x_i+\ell+1,x_{i+1}})$ is 1.

The factor $\delta_{s_i,1}$ says that the rate applies exclusively to the case when the rod is in the state 1.

As for the actual value of $\omega_i(\boldsymbol{\eta})$, it is composed as a product of the constant $\omega^\star$ and a variable quantity $(1 + d^{1\star}\delta_{x_{i-1}+\ell,x_i} + d^{\star 01}\delta_{x_i+\ell+1,x_{i+1}})$. Let us show how the second term contributes to the value of $\omega_i(\boldsymbol{\eta})$.

Note that $\delta_{x_{i-1}+\ell,x_i}$ is 1 iff the rods at x_{i-1} and at x_i are neighbors. Otherwise, $\delta_{x_{i-1}+\ell,x_i}$ is 0. Thus, $d^{1\star}$ will be added to the second product member iff the particles at x_{i-1} and at x_i are neighbors. Note that this condition is reflected in the notation once the superscript $1\star$ is read in the following manner: "$\star$" means the particle at x_i and the number at the left of $\star$ codes the presence/absence of a particle at its left; the number 1 means that the left neighboring site is occupied by a rod. A similar codification has been used to mark the meaning of $d^{\star 01}$: "$\star$" means the rod at x_i and the numbers at the right of $\star$ code the presence/absence of a rod at those sites. Thus, $d^{\star 01}$ means that this value will be added if and only if the rightmost site to the position x_i is empty of a rod, while the next site is occupied. This is what the notation tells us, but in order to write this rule rigorously, we write $d^{\star 01}\delta_{x_i+\ell+1,x_{i+1}}$. Note that this is an equivalent expression because x_{i+1} means the position of the nearest rod to the right of x_i and, thus, $\delta_{x_i+\ell+1,x_{i+1}} = 1$ if and only if the site to the right of the rod at x_i is empty while the next site is occupied.

3.1.2 The candidate for the stationary distribution

As mentioned above, we consider the Boltzmann factor which is of the same form as the one in papers [4, 5]. Namely, at the equilibrium, the probability of finding the rods at positions $\mathbf{x} = (x_1,...,x_N)$ with states $\mathbf{s} = (s_1,...,s_N)$ in the configuration $\boldsymbol{\eta}$ is the following

$$\hat{\pi}(\boldsymbol{\eta}) = \frac{1}{Z}\pi(\boldsymbol{\eta}) \tag{3.6}$$

where $\pi(\boldsymbol{\eta})$ is the Boltzmann weight which is of the form

$$\pi(\boldsymbol{\eta}) = \exp\left[-\frac{1}{k_B T}(U(\mathbf{x}) + \lambda B(\mathbf{s}))\right].\tag{3.7}$$

Here U is the short-range interaction energy

$$U(\mathbf{x}) = J\sum_{i=1}^{N}\delta_{x_{i+1},x_i+\ell}^{L}.\tag{3.8}$$

where δ^L denotes the Kronecker symbol with arguments understood modulo L due to periodic boundary conditions. B is the excess which is $N^1 - N^2$ where N^α the fluctuating number of RNAPs in state $\alpha \in \{1, 2\}$. Z is the partition function

$$Z = \sum_{\boldsymbol{\eta}}\pi(\boldsymbol{\eta}).\tag{3.9}$$

Positive J corresponds to repulsion. The chemical potential λ is a Lagrange multiplier that takes care of the fluctuations in the excess

$$B(\boldsymbol{s}) = \sum_{i=1}^{N}(3 - 2s_i)\tag{3.10}$$

due to the interplay of NTP hydrolysis and PP_i release.

For the convenience of computation, one introduces

$$x = e^{\frac{2\lambda}{k_B T}}, \quad y = e^{\frac{J}{k_B T}}.\tag{3.11}$$

so that $x > 1$ corresponds to an excess of RNAP in state 1 and repulsive interaction corresponds to $y > 1$. Thus, the normalized stationary distribution (3.6) for allowed configurations is then given by

$$\hat{\pi}(\boldsymbol{\eta}) = \frac{1}{Z}\prod_{i=1}^{N}x^{-3/2+s_i}y^{-\delta_{x_{i+1},x_i+\ell}^{L}}.\tag{3.12}$$

3.1.3   The conditions for the existence

The present section culminates with Theorem 3.1 that gives the conditions that must be satisfied by the transition rates in order that the dynamics of our process would be compatible with the stationary distribution set in Section 3.1.2. In respect to this, we note that that distribution has been set ad hoc and that there have been no guarantees that the model's dynamics will have that distribution as its steady state. Thus, we may say that Theorem 3.1 is the main theoretical result of the present chapter. In the next

section, we will use it to calculate our model's characteristics which values may be compared to their counterparts' values measured in experiments.

3.1.3.1   Master equation

The master equation for the probability $\mathbb{P}_t(\boldsymbol{\eta})$ of finding the rods at time t in the configuration $\boldsymbol{\eta}$

$$
\frac{d}{dt}\mathbb{P}(\boldsymbol{\eta}, t) = \sum_{i=1}^{N}\left[\omega_i(\boldsymbol{\eta}_{tlf}^i)\mathbb{P}(\boldsymbol{\eta}_{tlf}^i, t) + \phi_i(\boldsymbol{\eta}_{tlb}^i)\mathbb{P}(\boldsymbol{\eta}_{tlb}^i, t) + \kappa_i(\boldsymbol{\eta}_{rel}^i)\mathbb{P}(\boldsymbol{\eta}_{rel}^i, t)\right.
$$
$$
\left. + \tau_i(\boldsymbol{\eta}_{bin}^i)\mathbb{P}(\boldsymbol{\eta}_{bin}^i, t) - (\omega_i(\boldsymbol{\eta}) + \phi_i(\boldsymbol{\eta}) + \kappa_i(\boldsymbol{\eta}) + \tau_i(\boldsymbol{\eta}))\mathbb{P}(\boldsymbol{\eta}, t)\right] \quad (3.13)
$$

where $\boldsymbol{\eta}_{tlf}^i$ is the configuration that leads to $\boldsymbol{\eta}$ before a forward translocation of RNAP i (i.e., with coordinate $x_i^{tlf} = x_i - 1$ and state $s_i^{tlf} = 3 - s_i$), $\boldsymbol{\eta}_{tlb}^i$ is the configuration that leads to $\boldsymbol{\eta}$ before a backward translocation of RNAP i (i.e., $x_i^{tlb} = x_i + 1, s_i^{tlb} = 3 - s_i$), $\boldsymbol{\eta}_{rel}^i$ is the configuration $\boldsymbol{\eta}$ before PP_i release at RNAP i (i.e., $x_i^{rel} = x_i$ and $s_i^{rel} = 3 - s_i$), and $\boldsymbol{\eta}_{bin}^i$ is the configuration leads to $\boldsymbol{\eta}$ before PP_i binding at RNAP i (i.e., $x_i^{bin} = x_i, s_i^{bin} = 3 - s_i$). Notice here that due to periodicity, the positions x_i of the rods are counted modulo L and labels i are counted modulo N.

Dividing (3.13) by the stationary distribution (3.6), the stationary condition becomes

$$
\sum_{i=1}^{N}\left[\omega_i(\boldsymbol{\eta}_{tlf}^i)\frac{\pi(\boldsymbol{\eta}_{tlf}^i)}{\pi(\boldsymbol{\eta})} + \phi_i(\boldsymbol{\eta}_{tlb}^i)\frac{\pi(\boldsymbol{\eta}_{tlb}^i)}{\pi(\boldsymbol{\eta})} + \kappa_i(\boldsymbol{\eta}_{rel}^i)\frac{\pi(\boldsymbol{\eta}_{rel}^i)}{\pi(\boldsymbol{\eta})} + \tau_i(\boldsymbol{\eta}_{bin}^i)\frac{\pi(\boldsymbol{\eta}_{bin}^i)}{\pi(\boldsymbol{\eta})}\right.
$$
$$
\left. - (\omega_i(\boldsymbol{\eta}) + \phi(\boldsymbol{\eta}) + \kappa_i(\boldsymbol{\eta}) + \tau_i(\boldsymbol{\eta}))\right] = 0. \quad (3.14)
$$

Now we introduce the quantities

$$
D_i(\boldsymbol{\eta}) = \omega_i(\boldsymbol{\eta}_{tlf}^i)\frac{\pi(\boldsymbol{\eta}_{tlf}^i)}{\pi(\boldsymbol{\eta})} - \omega_i(\boldsymbol{\eta}), \quad (3.15)
$$

$$
E_i(\boldsymbol{\eta}) = \phi_i(\boldsymbol{\eta}_{tlb}^i)\frac{\pi(\boldsymbol{\eta}_{tlb}^i)}{\pi(\boldsymbol{\eta})} - \phi_i(\boldsymbol{\eta}), \quad (3.16)
$$

$$
F_i(\boldsymbol{\eta}) = \kappa_i(\boldsymbol{\eta}_{rel}^i)\frac{\pi(\boldsymbol{\eta}_{rel}^i)}{\pi(\boldsymbol{\eta})} - \kappa_i(\boldsymbol{\eta}), \quad (3.17)
$$

$$
G_i(\boldsymbol{\eta}) = \tau_i(\boldsymbol{\eta}_{bin}^i)\frac{\pi(\boldsymbol{\eta}_{bin}^i)}{\pi(\boldsymbol{\eta})} - \tau_i(\boldsymbol{\eta}). \quad (3.18)
$$

Taking into account periodicity, the stationary condition (3.14) is satisfied if the lattice

divergence condition

$$D_i(\boldsymbol{\eta}) + E_i(\boldsymbol{\eta}) + F_i(\boldsymbol{\eta}) + G_i(\boldsymbol{\eta}) = \Phi_i(\boldsymbol{\eta}) - \Phi_{i+1}(\boldsymbol{\eta}) \tag{3.19}$$

holds for all allowed configurations with a family of functions $\Phi_i(\boldsymbol{\eta})$ satisfying $\Phi_{N+1}(\boldsymbol{\eta}) = \Phi_1(\boldsymbol{\eta})$. The lattice divergence condition can be understood as a specific discrete form of the Noether theorem.

3.1.3.2 Mapping to the headway process

It is convenient to work with the headway process. Due to translation invariance, an allowed configuration of RNAPs can be specified by the distance vector $\mathbf{m} := (m_1, ..., m_N)$ and the state vector $\mathbf{s} = (s_1, ..., s_N)$ where the headway distance m_i is the number of empty sites between neighboring rods i^{th} and $(i+1)^{th}$. Thus, one has $m_i = x_{i+1} - (x_i + \ell) \mod L$ and the total number of vacant sites is $M = L - \ell N$. We denote by

$$\theta_i^p := \delta_{m_i,p} = \delta_{x_{i+1},x_i+\ell+p} \tag{3.20}$$

the indicator functions on a headway of length p (in units of bp) with the index i taken modulo N, i.e., $\theta_0^p \equiv \theta_N^p$. In terms of the parameters (3.11) and the new distance variables (3.20) one rewrites the stationary distribution (3.6) as follows

$$\tilde{\pi}(\boldsymbol{\zeta}) = \frac{1}{Z} \prod_{i=i}^{N} \left(x^{-3/2+s_i} y^{-\theta_i^0} \right). \tag{3.21}$$

Notice that the measure (3.21) factorizes, fact that indicates the absence of distance correlations.

Due to steric hard core repulsion, a forward translocation of ith RNAP from x_i to x_i+1 corresponding to the transition $(m_{i-1}, m_i) \to (m_{i-1}+1, m_i-1)$ takes place if $m_i > 0$. Similarly, only if $m_{i-1} > 0$ the backward translocation corresponding to the transition $(m_{i-1}, m_i) \to (m_{i-1}-1, m_i+1)$ can occurs. In terms of the new stochastic variables $\boldsymbol{\zeta} = (\mathbf{m}, \mathbf{s})$ given by the distance vector $\mathbf{m}$ and the state vector $\mathbf{s}$ the transition rates (3.1 – 3.4) become

$$\tilde{\omega}_i(\boldsymbol{\zeta}) = \omega^\star \delta_{s_i,1}(1 + d^{1\star}\theta_{i-1}^0 + d^{\star 01}\theta_i^1)(1 - \theta_i^0); \tag{3.22}$$

$$\tilde{\phi}_i(\boldsymbol{\zeta}) = \phi^\star \delta_{s_i,2}(1 + e^{10\star}\theta_{i-1}^1 + e^{\star 1}\theta_i^0)(1 - \theta_{i-1}^0); \tag{3.23}$$

$$\tilde{\kappa}_i(\boldsymbol{\zeta}) = \kappa^\star \delta_{s_i,2}(1 + f^{1\star}\theta_{i-1}^0 + f^{\star 1}\theta_i^0 + f^{1\star 1}\theta_{i-1}^0\theta_i^0 + f^{10\star}\theta_{i-1}^1 + f^{\star 01}\theta_i^1); \tag{3.24}$$

$$\tilde{\tau}_i(\boldsymbol{\zeta}) = \tau^\star \delta_{s_i,1}(1 + g^{1\star}\theta_{i-1}^0 + g^{\star 1}\theta_i^0 + g^{1\star 1}\theta_{i-1}^0\theta_i^0 + g^{10\star}\theta_{i-1}^1 + g^{\star 01}\theta_i^1). \tag{3.25}$$

Before writing the master equation for the headway process, we introduce notation for the configuration that lead to a given configuration $\boldsymbol{\zeta}$. Namely, $\boldsymbol{\zeta}^{i-1,i}, \boldsymbol{\zeta}^{i,i-1}$ correspond to forward and backward translocation and $\boldsymbol{\zeta}^{i,rel}, \boldsymbol{\zeta}^{i,bin}$ correspond to PP_i release and binding respectively. Before introducing these configurations, we denote (k, l)

by $(i-1, i)$ or $(i, i-1)$ and $\sharp$ by the superscript *rel* or *bin*. Thus, the configurations $\boldsymbol{\zeta}^{i-1,i}, \boldsymbol{\zeta}^{i,i-1}, \boldsymbol{\zeta}^{i,rel}$, and $\boldsymbol{\zeta}^{i,bin}$ are defined by

$$m_j^{k,l} := m_j + \delta_{j,l} - \delta_{j,k} \text{ and } s_j^{k,l} := s_j + (3 - 2s_j)\delta_{j,i}, \tag{3.26}$$

$$m_j^{i,\sharp} := m_j \text{ and } s_j^{i,\sharp} := s_j + (3 - 2s_j)\delta_{j,i}. \tag{3.27}$$

This yields the following master equation

$$\frac{d\mathbb{P}(\boldsymbol{\zeta}, t)}{dt} = \sum_{i=1}^{N} Q_i(\boldsymbol{\zeta}, t) \tag{3.28}$$

with

$$\begin{aligned}
Q_i(\boldsymbol{\zeta}, t) = \ & \tilde{\omega}_i(\boldsymbol{\zeta}^{i-1,i})\mathbb{P}(\boldsymbol{\zeta}^{i-1,i}, t) - \tilde{\omega}_i(\boldsymbol{\zeta})\mathbb{P}(\boldsymbol{\zeta}, t) + \tilde{\phi}_i(\boldsymbol{\zeta}^{i,i-1})\mathbb{P}(\boldsymbol{\zeta}^{i,i-1}, t) - \tilde{\phi}_i(\boldsymbol{\zeta})\mathbb{P}(\boldsymbol{\zeta}, t) \\
& + \tilde{\kappa}_i(\boldsymbol{\zeta}^{i,rel})\mathbb{P}(\boldsymbol{\zeta}^{i,rel}, t) - \tilde{\kappa}_i(\boldsymbol{\zeta})\mathbb{P}(\boldsymbol{\zeta}, t) + \tilde{\tau}_i(\boldsymbol{\zeta}^{i,bin})\mathbb{P}(\boldsymbol{\zeta}^{i,bin}, t) - \tilde{\tau}_i(\boldsymbol{\zeta})\mathbb{P}(\boldsymbol{\zeta}, t)
\end{aligned} \tag{3.29}$$

where

$$\tilde{\omega}_i(\boldsymbol{\zeta}^{i-1,i}) = \omega^\star \delta_{s_i,2}(1 + d^{1\star}\theta_{i-1}^1 + d^{\star 01}\theta_i^0)(1 - \theta_{i-1}^0), \tag{3.30}$$

$$\tilde{\phi}_i(\boldsymbol{\zeta}^{i,i-1}) = \phi^\star \delta_{s_i,1}(1 + e^{10\star}\theta_{i-1}^0 + e^{\star 1}\theta_i^1)(1 - \theta_i^0), \tag{3.31}$$

$$\tilde{\kappa}_i(\boldsymbol{\zeta}^{i,rel}) = \kappa^\star \delta_{s_i,1}(1 + f^{1\star}\theta_{i-1}^0 + f^{\star 1}\theta_i^0 + f^{1\star 1}\theta_{i-1}^0\theta_i^0 + f^{10\star}\theta_{i-1}^1 + f^{\star 01}\theta_i^1), \tag{3.32}$$

$$\tilde{\tau}_i(\boldsymbol{\zeta}^{i,bin}) = \tau^\star \delta_{s_i,2}(1 + g^{1\star}\theta_{i-1}^0 + g^{\star 1}\theta_i^0 + g^{1\star 1}\theta_{i-1}^0\theta_i^0 + g^{10\star}\theta_{i-1}^1 + g^{\star 01}\theta_i^1). \tag{3.33}$$

3.1.3.3 Stationary conditions

By using the Noether theorem, one can rephrase the stationarity condition for the headway process in a local divergence form which is equivalent to (3.19). Let us first introduce the following notations

$$\tilde{D}_i(\boldsymbol{\zeta}) = \tilde{\omega}_i(\boldsymbol{\zeta}^{i-1,i})\frac{\tilde{\pi}(\boldsymbol{\zeta}^{i-1,i})}{\tilde{\pi}(\boldsymbol{\zeta})} - \tilde{\omega}_i(\boldsymbol{\zeta}), \tag{3.34}$$

$$\tilde{E}_i(\boldsymbol{\zeta}) = \tilde{\phi}_i(\boldsymbol{\zeta}^{i,i-1})\frac{\tilde{\pi}(\boldsymbol{\zeta}^{i,i-1})}{\tilde{\pi}(\boldsymbol{\zeta})} - \tilde{\phi}_i(\boldsymbol{\zeta}), \tag{3.35}$$

$$\tilde{F}_i(\boldsymbol{\zeta}) = \tilde{\kappa}_i(\boldsymbol{\zeta}^{i,rel})\frac{\tilde{\pi}(\boldsymbol{\zeta}^{i,rel})}{\tilde{\pi}(\boldsymbol{\zeta})} - \tilde{\kappa}_i(\boldsymbol{\zeta}), \tag{3.36}$$

$$\tilde{G}_i(\boldsymbol{\zeta}) = \tilde{\tau}_i(\boldsymbol{\zeta}^{i,bin})\frac{\tilde{\pi}(\boldsymbol{\zeta}^{i,bin})}{\tilde{\pi}(\boldsymbol{\zeta})} - \tilde{\tau}_i(\boldsymbol{\zeta}). \tag{3.37}$$

Again, we will make use of (k,l) for $(i-1,i)$ or $(i,i-1)$ and $\sharp$ for the superscript *rel* or *bin*. Notice that

$$\theta_j^p(\boldsymbol{\zeta}^{k,l}) = \delta_{m_j+\delta_{j,l}-\delta_{j,k},p} = \theta_j^{p-\delta_{j,l}+\delta_{j,k}}(\boldsymbol{\zeta}) \text{ and } \delta_{s_i^{k,l},\alpha} = \delta_{s_i,3-\alpha}; \tag{3.38}$$

$$\theta_j^p(\boldsymbol{\zeta}^{i,\sharp}) = \theta_j^p(\boldsymbol{\zeta}) \text{ and } \delta_{s_i^{i,\sharp},\alpha} = \delta_{s_i,3-\alpha}, \tag{3.39}$$

one gets

$$\frac{\tilde{\pi}(\boldsymbol{\zeta}^{i,\sharp})}{\tilde{\pi}(\boldsymbol{\zeta})} = x^{3-2s_i}, \tag{3.40}$$

$$\frac{\tilde{\pi}(\boldsymbol{\zeta}^{k,l})}{\tilde{\pi}(\boldsymbol{\zeta})} = x^{-3+2s_i}y^{\theta_k^0-\theta_k^1+\theta_l^0}. \tag{3.41}$$

Hence,

$$\tilde{D}_i(\boldsymbol{\zeta}) = x^{-1}y^{\theta_{i-1}^0+\theta_i^0-\theta_{i-1}^1}\omega^\star\delta_{s_i,2}(1+d^{1\star}\theta_{i-1}^1+d^{\star01}\theta_i^0)(1-\theta_{i-1}^0)$$
$$- \omega^\star\delta_{s_i,1}(1+d^{1\star}\theta_{i-1}^0+d^{\star01}\theta_i^1)(1-\theta_i^0), \tag{3.42}$$

$$\tilde{E}_i(\boldsymbol{\zeta}) = xy^{\theta_i^0-\theta_i^1+\theta_{i-1}^1}\phi^\star\delta_{s_i,1}(1+e^{10\star}\theta_{i-1}^0+e^{\star1}\theta_i^1)(1-\theta_i^0)$$
$$- \phi^\star\delta_{s_i,2}(1+e^{10\star}\theta_{i-1}^1+e^{\star1}\theta_i^0)(1-\theta_{i-1}^0), \tag{3.43}$$

$$\tilde{F}_i(\boldsymbol{\zeta}) = (x\delta_{s_i,1}-\delta_{s_i,2})\kappa^\star(1+f^{1\star}\theta_{i-1}^0+f^{\star1}\theta_i^0+f^{1\star1}\theta_{i-1}^0\theta_i^0+f^{10\star}\theta_{i-1}^1+f^{\star01}\theta_i^1), \tag{3.44}$$

$$\tilde{G}_i(\boldsymbol{\zeta}) = (x^{-1}\delta_{s_i,2}-\delta_{s_i,1})\tau^\star(1+g^{1\star}\theta_{i-1}^0+g^{\star1}\theta_i^0+g^{1\star1}\theta_{i-1}^0\theta_i^0+g^{10\star}\theta_{i-1}^1+g^{\star01}\theta_i^1). \tag{3.45}$$

One requires
$$\tilde{D}_i + \tilde{E}_i + \tilde{F}_i + \tilde{G}_i = \tilde{\Phi}_{i-1} - \tilde{\Phi}_i, \tag{3.46}$$

where $\tilde{\Phi}_i$ is of the form $\tilde{\Phi}_i = (a+b\theta_i^0+c\theta_i^1)(\delta_{s_i,1}+\delta_{s_i,2}) = a+b\theta_i^0+c\theta_i^1$. Notice that $\tilde{\Phi}_i$ must be of that form since $\tilde{D}_i, \tilde{E}_i, \tilde{F}_i, \tilde{G}_i$ depend on the state of RNAP i and variables $\theta_{i-1}^0, \theta_{i-1}^1, \theta_i^0, \theta_i^1$ belonging to $\{0,1\}$.

By considering all possible cases of (3.46), see Appendix (C), one gets the following stationary conditions

$$x = \frac{\omega^\star + \tau^\star}{\phi^\star + \kappa^\star} \tag{3.47}$$

$$y = \frac{1+d^{1\star}}{1+d^{\star01}} = \frac{1+e^{\star1}}{1+e^{10\star}} \tag{3.48}$$

$$x\kappa^\star f^{1\star} - \tau^\star g^{1\star} = \frac{1}{1+x}(-\omega^\star+x\phi^\star) - \frac{x}{1+x}(-\omega^\star d^{1\star}+x\phi^\star e^{\star1}) \tag{3.49}$$

$$x\kappa^\star f^{\star1} - \tau^\star g^{\star1} = \frac{x}{1+x}(-\omega^\star+x\phi^\star) - \frac{1}{1+x}(-\omega^\star d^{1\star}+x\phi^\star e^{\star1}) \tag{3.50}$$

$$x\kappa^\star f^{1\star1} - \tau^\star g^{1\star1} = -\omega^\star d^{1\star}+x\phi^\star e^{\star1} \tag{3.51}$$

$$x\kappa^{\star}f^{10\star} - \tau^{\star}g^{10\star} = \frac{1}{1+x}(\omega^{\star}d^{\star 01} - x\phi^{\star}e^{10\star}) \tag{3.52}$$

$$x\kappa^{\star}f^{\star 01} - \tau^{\star}g^{\star 01} = \frac{x}{1+x}(\omega^{\star}d^{\star 01} - x\phi^{\star}e^{10\star}). \tag{3.53}$$

Remark 3.1. *If we set that $\tau^{\star} = \phi^{\star} = 0$, the stationary conditions* (3.47) – (3.53) *recover the ones in the paper* [4].

The relations (3.47) – (3.53) must be satisfied for (3.6) to be stationary. Thus, one gets the following statement which is the content of Theorem 1.1.

Theorem 3.1. *For the process defined in this chapter, the conditions* (3.47) – (3.53) *upon its dynamics rates* (3.1) – (3.4) *are sufficient for its stationary distribution be of the form* (3.6). *In this case, the stationary distribution acquires the following expression*

$$\hat{\pi}(\boldsymbol{\eta}) = \frac{1}{Z}\left(\frac{\omega^{\star} + \tau^{\star}}{\phi^{\star} + \kappa^{\star}}\right)^{\sum_{i=1}^{N} -3/2 + s_i} \left(\frac{1 + d^{1\star}}{1 + d^{\star 01}}\right)^{-\sum_{i=1}^{N} \delta_{x_{i+1},x_i+\ell}^{L}} \tag{3.54}$$

where Z is the partition function.

Remark 3.2. *Although, the form of the measure* (3.54) *dose not contain the parameters $e^{\star 1}, e^{10\star}$ indicating the hoping backward, however they still contribute their roles to the invariant distribution due to the relation* (3.48).

Remark 3.3. *As mentioned above, our model is a generalization of the model proposed by Belitsky and Schütz* [4] *by forcing $\phi^{\star} = \tau^{\star} = 0$. Thus, the relations* (3.47) – (3.53) *recover the relations in that paper as follows*

$$x = \frac{\omega^{\star}}{\kappa^{\star}} \tag{3.55}$$

$$y = \frac{1 + d^{1\star}}{1 + d^{\star 01}} \tag{3.56}$$

$$f^{1\star} = d^{1\star}\frac{x}{1+x} - \frac{1}{1+x} \tag{3.57}$$

$$f^{\star 1} = d^{1\star}\frac{1}{1+x} - \frac{x}{1+x} \tag{3.58}$$

$$f^{1\star 1} = -d^{1\star} \tag{3.59}$$

$$f^{10\star} = d^{\star 01}\frac{1}{1+x} \tag{3.60}$$

$$f^{\star 01} = d^{\star 01}\frac{x}{1+x}. \tag{3.61}$$

Thus, the stationary distribution of the process in this case becomes

$$\hat{\pi}(\boldsymbol{\eta}) = \frac{1}{Z}\left(\frac{\omega^{\star}}{\kappa^{\star}}\right)^{\sum_{i=1}^{N} -3/2 + s_i} \left(\frac{1 + d^{1\star}}{1 + d^{\star 01}}\right)^{-\sum_{i=1}^{N} \delta_{x_{i+1},x_i+\ell}^{L}} \tag{3.62}$$

where Z is the partition function.

3.2 Properties of the model

We have considered the Boltzmann factor (3.6) which is of the similar form as in papers [4, 5], so that in the stationary state, all the obtained properties bellow are similar to the ones in those papers. Since the lack of writing concrete calculations in those papers, we would like to provide them here for a reader following easier.

In this section, it is convenient to work in the grand-canonical ensemble that is the same as has been done in [5] where it has been defines the following:

$$\tilde{\pi}_{gc}(\boldsymbol{\zeta}) = \frac{1}{Z_{gc}} \prod_{i=1}^{N} (x^{-3/2+s_i} y^{-\theta_i^0} z^{m_i}), \tag{3.63}$$

where $Z_{gc} = (Z_1 Z_2)^N$ with

$$Z_1 = \frac{1+(y-1)z}{y(1-z)}, \quad Z_2 = x^{1/2} + x^{-1/2}. \tag{3.64}$$

We shall show that the grand-canonical ensemble is well-defined in the sense that one can always select a value of fugacity z for a given density of RNAP such that $Z_{gc} < \infty$ which means one should find such a value of z satisfying $0 \leq z < 1$. Let us first explain why the grand-canonical ensemble is of (3.63) form.

It is clear that one has

$$Z_{gc} = \sum_{\boldsymbol{\zeta}} \prod_{i=1}^{N} (x^{-3/2+s_i} y^{-\theta_i^0} z^{m_i}). \tag{3.65}$$

Notice that a configuration $\boldsymbol{\zeta}$ is defined by its headway and state vectors $\mathbf{m} = (m_1, ..., m_N)$ and $\mathbf{s} = (s_1, ..., s_N)$. Thus,

$$Z_{gc} = \sum_{m_i=0,1,...} \sum_{s_i=1,2} \prod_{i=1}^{N} (x^{-3/2+s_i} y^{-\theta_i^0} z^{m_i}) \tag{3.66}$$

$$= \sum_{s_i=1,2} \prod_{i=1}^{N} x^{-3/2+s_i} \sum_{m_i=0,1,...} \prod_{i=1}^{N} (y^{-\theta_i^0} z^{m_i}) \tag{3.67}$$

One has

$$\sum_{m_i=0,1,...} \prod_{i=1}^{N} (y^{-\theta_i^0} z^{m_i}) = \prod_{i=1}^{N} \sum_{m_i=0,1,...} (y^{-\theta_i^0} z^{m_i}) = (y^{-1} + z + z^2 + ...)^N \tag{3.68}$$

One notices that $y^{-1} + z + z^2 + ...$ converges to $Z_1 = \dfrac{1+(y-1)z}{y(1-z)}$ if $0 \leq z < 1$. One

also has

$$\sum_{s_i=1,2} \prod_{i=1}^{N} x^{-3/2+s_i} = (x^{-1/2} + x^{1/2})^N = Z_2^N \tag{3.69}$$

where $Z_2 = x^{-1/2} + x^{1/2}$. Hence, if $0 \leq z < 1$, the grand partition function Z_{gc} is of the form $Z_{gc} = (Z_1 Z_2)^N$.

3.2.1   Mean headway

Lemma 3.1. *The stationary mean headway of the process, $\langle m_i \rangle$, obeys the following expression*

$$\langle m_i \rangle = \frac{yz}{(1-z)(1+(y-1)z)}. \tag{3.70}$$

Proof. From grand-canonical distribution (3.63), one obtains the mean headway

$$\langle m_i \rangle = \sum_{\boldsymbol{\zeta}} m_i \tilde{\pi}_{gc}(\boldsymbol{\zeta})$$

$$= \sum_{\boldsymbol{\zeta}} m_i \frac{1}{Z_{gc}} \prod_{j=1}^{N} (x^{-3/2+s_j} y^{-\theta_i^0} z^{m_j})$$

$$= \frac{z}{Z_{gc}} \sum_{\boldsymbol{\zeta}} \prod_{j=1,j\neq i}^{N} (x^{-3/2+s_j} y^{-\theta_j^0} z^{m_j})(x^{-3/2+s_i} y^{-\theta_i^0})(m_i z^{m_i-1})$$

$$= \frac{z}{Z_{gc}} \sum_{\boldsymbol{\zeta}} \prod_{j=1,j\neq i}^{N} (x^{-3/2+s_j} y^{-\theta_j^0} z^{m_j})(x^{-3/2+s_i} y^{-\theta_i^0})(z^{m_i})'.$$

One has $\langle m_1 \rangle = \cdots = \langle m_N \rangle$ which implies

$$N \langle m_i \rangle = \frac{z}{Z_{gc}} \sum_{i=1}^{N} \sum_{\boldsymbol{\zeta}} \prod_{j=1,j\neq i}^{N} (x^{-3/2+s_j} y^{-\theta_j^0} z^{m_j})(x^{-3/2+s_i} y^{-\theta_i^0})(z^{m_i})'.$$

Notice that

$$\sum_{i=1}^{N} \sum_{\boldsymbol{\zeta}} \prod_{j=1,j\neq i}^{N} (x^{-3/2+s_j} y^{-\theta_j^0} z^{m_j})(x^{-3/2+s_i} y^{-\theta_i^0})(z^{m_i})' = (Z_{gc})_z'.$$

Therefore,

$$\langle m_i \rangle = \frac{1}{N} z \frac{\mathrm{d}}{\mathrm{d}z} \ln Z_{gc}, \tag{3.71}$$

so that

$$\langle m_i \rangle = \frac{yz}{(1-z)(1+(y-1)z)}. \tag{3.72}$$

The proof is complete. □

Proposition 3.1. *The grand-canonical measure* (3.63) *is well-defined.*

Proof. On the one hand, one has the mean headway quantity (3.70). On the other hand, this is the mean available empty space on the lattice $L - \ell N$ per rod which gives

$$\langle m_i \rangle = \frac{L - \ell N}{N} = \frac{1}{\rho} - \ell, \tag{3.73}$$

where $\rho = \dfrac{N}{L}$ is the RNAP density. Comparing (3.70) with (3.73) gives us the auxiliary variable z which is the solution of the quadratic equation

$$(y - 1)z^2 + z\left(\frac{y\rho}{1 - \ell\rho} - y + 2\right) - 1 = 0. \tag{3.74}$$

One can select one solution such that $0 \leq z < 1$. Namely,

$$z = \frac{-\left(\dfrac{\rho y}{1 - \ell\rho} - y + 2\right) + \sqrt{\left(\dfrac{\rho y}{1 - \ell\rho} - y + 2\right)^2 + 4(y - 1)}}{2(y - 1)}. \tag{3.75}$$

One has

$$
\begin{aligned}
z &= \frac{-\left(\dfrac{\rho y}{1 - \ell\rho} - y + 2\right) + \sqrt{\left(\dfrac{\rho y}{1 - \ell\rho} - y + 2\right)^2 + 4(y - 1)}}{2(y - 1)} \\
&= -\frac{y\rho - (y - 2)(1 - \ell\rho) - \sqrt{[y\rho - (y - 2)(1 - \ell\rho)]^2 + 4(y - 1)(1 - \ell\rho)^2}}{2(y - 1)(1 - \ell\rho)} \\
&= -\frac{[y\rho - (y - 2)(1 - \ell\rho)]\frac{1 - y^{-1}}{y - 1} - \sqrt{\left[(y\rho - (y - 2)(1 - \ell\rho))\frac{1 - y^{-1}}{y - 1}\right]^2 + \dfrac{4(1 - \ell\rho)^2(1 - y^{-1})^2}{y - 1}}}{2(1 - \ell\rho)(1 - y^{-1})}
\end{aligned}
$$

Notice that $\dfrac{1 - y^{-1}}{y - 1} = \dfrac{1}{y}$, thus

$$
\begin{aligned}
z &= -\frac{[\rho - (1 - 2y^{-1})(1 - \ell\rho)] - \sqrt{[\rho - (1 - 2y^{-1})(1 - \ell\rho)]^2 + \dfrac{4}{y}(1 - \ell\rho)^2(1 - y^{-1})}}{2(1 - \ell\rho)(1 - y^{-1})} \\
&= 1 - \frac{1 - (\ell - 1)\rho - \sqrt{(1 - (\ell - 1)\rho)^2 - 4\rho(1 - \ell\rho)(1 - y^{-1})}}{2(1 - \ell\rho)(1 - y^{-1})}.
\end{aligned}
$$

The final form of the solution is the following

$$z = 1 - \frac{1 - (\ell - 1)\rho - \sqrt{(1 - (\ell - 1)\rho)^2 - 4\rho(1 - \ell\rho)(1 - y^{-1})}}{2(1 - \ell\rho)(1 - y^{-1})}. \tag{3.76}$$

Notice that the density of the model is in the range $0 < \rho \leq 1/\ell$. This ensures that $0 \leq z < 1$ and therefore the partition function (3.63) is well-defined. □

3.2.2 RNAP headway distribution

Denote by $P_h(r)$ the distribution of the headway between the front of a trailing rod i and the back of a leading rod $i+1$ which means $P_h(r) = \frac{1}{\rho} \langle \delta_{x_{i+1} - x_i - \ell, r} \rangle = \langle \theta_i^r \rangle$, $r \in \mathbb{N}$ where $\mathbb{N} = \{0, 1, 2...\}$. Since the headway distance does not depend on states of RNAPs, and value y appearing in the stationary distribution may be expressed through only the parameters $d^{1\star}$ and $d^{\star 01}$ (both $d^{1\star}$ and $d^{\star 01}$ indicate forward translocation), then one can guess that the distribution $P_h(r)$ is the same as [5]. This is indeed the case, and one has the following lemma.

Lemma 3.2. *The distribution of the headway of the process is the following*

$$P_h(r) = \begin{cases} \dfrac{1 - z}{1 + (y - 1)z} & \text{for } r = 0, \\ y P_h(0) z^r & \text{for } r \geq 1. \end{cases} \tag{3.77}$$

Proof. Denote by $\boldsymbol{\zeta} = (\zeta_1, ..., \zeta_N)$ the configuration of RNAPs and let $f = Z_1 Z_2$. One gets

$$\langle \theta_i^0 \rangle = \sum_{\boldsymbol{\zeta}} \theta_i^0 \tilde{\pi}_{gc}(\boldsymbol{\zeta})$$

$$= \frac{1}{Z_{gc}} \sum_{\boldsymbol{\zeta}} \theta_i^0 \prod_{j=1}^{N} (x^{-3/2 + s_j} y^{-\theta_j^0} z^{m_j})$$

$$= \frac{1}{Z_{gc}} \sum_{\zeta_1} \cdots \sum_{\zeta_N} \theta_i^0 \prod_{j=1}^{N} (x^{-3/2 + s_j} y^{-\theta_j^0} z^{m_j})$$

$$= \frac{1}{f^N} \sum_{\zeta_1} \cdots \sum_{\zeta_N} \theta_i^0 \prod_{j=1}^{N} (x^{-3/2 + s_j} y^{-\theta_j^0} z^{m_j})$$

$$= \prod_{j=1, j \neq i}^{N} \left(\frac{1}{f} \sum_{\zeta_j} x^{-3/2 + s_j} y^{-\theta_j^0} z^{m_j} \right) \left(\frac{1}{f} \sum_{\zeta_i} \theta_i^0 x^{-3/2 + s_i} y^{-\theta_i^0} z^{m_i} \right).$$

One has here that

$$\frac{1}{f}\sum_{\zeta_j} x^{-3/2+s_j} y^{-\theta_j^0} z^{m_j} = 1, \quad \forall j = 1..N, \tag{3.78}$$

and

$$\frac{1}{f}\sum_{\zeta_i} \theta_i^0 x^{-3/2+s_i} y^{-\theta_i^0} z^{m_i} = \frac{1}{f}\left(-y\frac{\mathrm{d}}{\mathrm{d}y}\right)\sum_{\zeta_i} x^{-3/2+s_i} y^{-\theta_i^0} z^{m_i} = -y\frac{1}{f}\frac{\mathrm{d}}{\mathrm{d}y}f.$$

Hence,

$$\langle\theta_i^0\rangle = -y\frac{1}{f}\frac{\mathrm{d}}{\mathrm{d}y}f = \frac{1-z}{1+(y-1)z}. \tag{3.79}$$

Now we compute $\langle\theta_i^r\rangle$ for $r \geq 1$.

$$\begin{aligned}
\langle\theta_i^r\rangle &= \sum_{\boldsymbol{\zeta}} \theta_i^r(\boldsymbol{\zeta})\tilde{\pi}_{gc}(\boldsymbol{\zeta}) \\
&= \frac{1}{Z_{gc}}\sum_{\boldsymbol{\zeta}} \theta_i^r \prod_{j=1}^{N}(x^{-3/2+s_j} y^{-\theta_j^0} z^{m_j}) \\
&= \frac{1}{Z_{gc}}\sum_{\zeta_1}\cdots\sum_{\zeta_N} \theta_i^r \prod_{j=1}^{N}(x^{-3/2+s_j} y^{-\theta_j^0} z^{m_j}) \\
&= \frac{1}{f^N}\sum_{\zeta_1}\cdots\sum_{\zeta_N} \theta_i^r \prod_{j=1}^{N}(x^{-3/2+s_j} y^{-\theta_j^0} z^{m_j}) \\
&= \prod_{j=1,j\neq i}^{N}\left(\frac{1}{f}\sum_{\zeta_j} x^{-3/2+s_j} y^{-\theta_j^0} z^{m_j}\right)\left(\frac{1}{f}\sum_{\zeta_i} \theta_i^r x^{-3/2+s_i} y^{-\theta_i^0} z^{m_i}\right).
\end{aligned}$$

Using again identity (3.78) and noticing that $\theta_i^r = 1$ implies $\theta_i^0 = 0$ and that $z^{m_i} = z^r$, one gets

$$\begin{aligned}
\langle\theta_i^r\rangle &= \frac{1}{f}\sum_{\zeta_i} \theta_i^r x^{-3/2+s_i} y^{-\theta_i^0} z^{m_i} \\
&= \frac{1}{f}z^r \sum_{\zeta_i} x^{-3/2+s_i}. \tag{3.80}
\end{aligned}$$

Finally, one notices that

$$\sum_{\zeta_i} x^{-3/2+s_i} = x^{-1/2} + x^{1/2}. \tag{3.81}$$

Therefore,

$$\langle \theta_i^r \rangle = y z^r \frac{1-z}{1+(y-1)z} = y z^r \langle \theta_i^0 \rangle . \tag{3.82}$$

By the above computations, one gets

$$P_h(r) = \begin{cases} \dfrac{1-z}{1+(y-1)z} & \text{for } r = 0, \\ y P_h(0) z^r & \text{for } r \geq 1. \end{cases} \tag{3.83}$$

The proof is completed. □

Let us plot graphs of the headway distribution function (3.77) for some choices of parameter y.
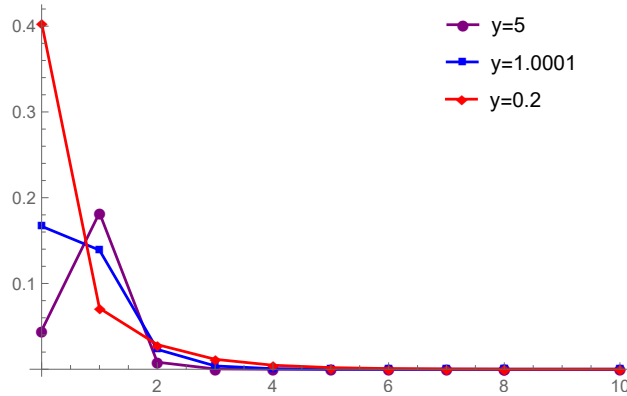
Figure 3.2: *RNAP headway distribution $P_h(r)$ (y-axis) for different interaction strengths y at average RNAP density $\rho = 0.1$. The x-axis is the integer lattice distance. The lines joining the data points are just guides to the eye.*
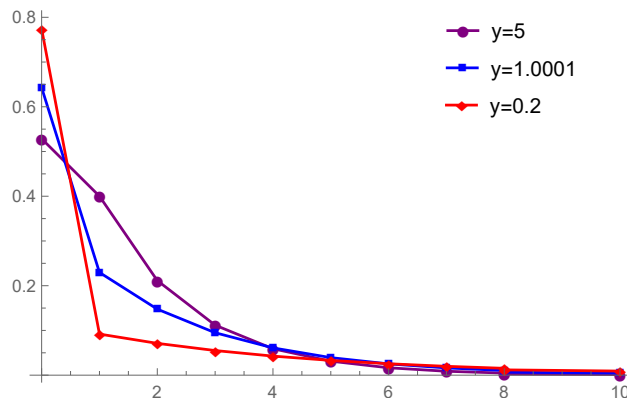
Figure 3.3: *RNAP headway distribution $P_h(r)$ (y-axis) for different interaction strengths y at average RNAP density $\rho = 0.18$. The x-axis is the integer lattice distance. The lines joining the data points are just guides to the eye.*
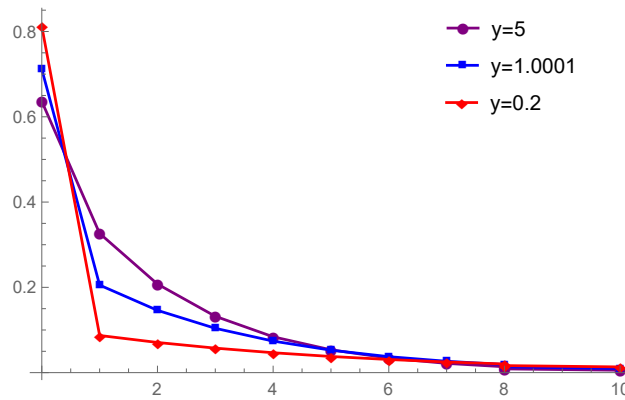
Figure 3.4: *RNAP headway distribution $P_h(r)$ (y-axis) for different interaction strengths y at average RNAP density $\rho = 0.185$. The x-axis is the integer lattice distance. The lines joining the data points are just guides to the eye.*
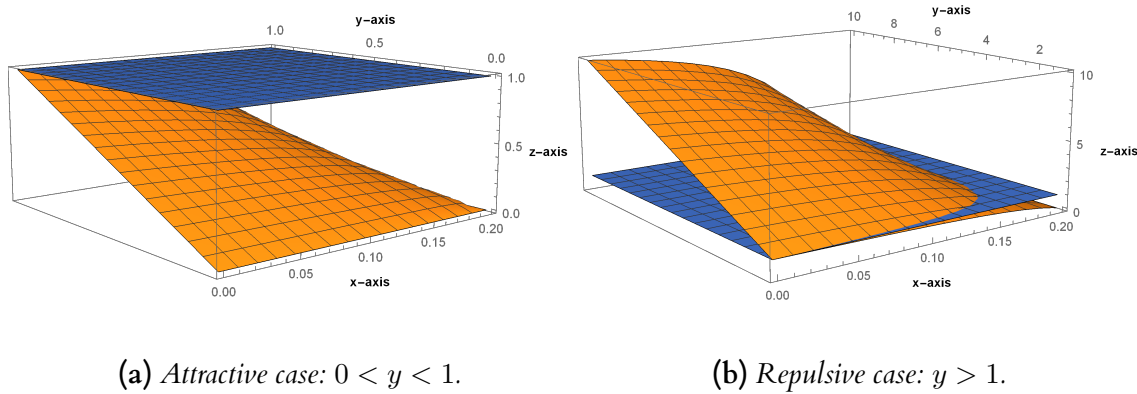
(a) *Attractive case: $0 < y < 1$.*

(b) *Repulsive case: $y > 1$.*

Figure 3.5: *Comparison yz (yellow) with 1 (blue) (z-axis). The x-axis is the density of RNAPs and y-axis is the values of y.*

Remark 3.4. *Since $z < 1$ then function $P_h(r)$ decreases, when $r \geq 1$. Consequently, in order to compare $P_h(0)$ with $P_h(1)$ (expressed in the distribution (3.77)), one only needs to compare yz with 1: if $yz > 1$, then $P_h(1) > P_h(0)$. One can see from Fig. 3.5a that $yz < 1$, thus for the attractive case $0 < y < 1$ one has $P_h(1) < P_h(0)$. Also, examining the Fig. 3.5b we see that at high density, even for very strong repulsion (y large), it holds that $yz < 1$ which implies in this case that $P_h(1) < P_h(0)$ (Figs. 3.3 and 3.4). However, Fig. 3.5b also shows that at low density occurs the following phenomenon: if y is close to 1, one has $yz < 1$ while if y is large enough, one has $yz > 1$, and hence one can compare $P_h(1)$ with $P_h(0)$ (Fig. 3.2).*

3.2.3 Average excess and dwell times

Average excess: As mentioned in [4], the simplest measure that characterizes the distribution of RNAP is the average excess density of rods not bound to PP_i over the rods that are bound to PP_i:

$$\sigma = \frac{\langle N^1 \rangle - \langle N^2 \rangle}{L}. \tag{3.84}$$

Proposition 3.2. *The average excess is computed as follows*

$$\sigma = \frac{1-x}{1+x}\rho. \tag{3.85}$$

Remark 3.5. *One recognizes that the form of the average excess that we present in* (3.85) *is the same as in* [4, 5]. *However, there is a difference: our result comes from the value of x and x depends not only on the rates $\omega^\star, \kappa^\star$, as this happens to be in* [4], *but also on the rates $\phi^\star, \tau^\star$.*

Proof of Proposition 3.2. By (3.6) and (3.7), one has

$$\sigma = \frac{\langle B(s)\rangle}{L} = \frac{\sum_{\boldsymbol{\eta}} B(s)\pi^\star(\boldsymbol{\eta})}{L}.$$

Notice that

$$\begin{aligned}
\sum_{\boldsymbol{\eta}} B(s)\pi^\star(\boldsymbol{\eta}) &= \sum_{\boldsymbol{\eta}} B(s)\frac{1}{Z}\exp\left[-\frac{1}{k_B T}(U + \lambda B)\right] \\
&= -k_B T \frac{\mathrm{d}}{\mathrm{d}\lambda}\sum_{\boldsymbol{\eta}}\frac{1}{Z}\exp\left[-\frac{1}{k_B T}(U + \lambda B)\right] \\
&= -k_B T \frac{1}{Z}\frac{\mathrm{d}}{\mathrm{d}\lambda}\sum_{\boldsymbol{\eta}}\exp\left[-\frac{1}{k_B T}(U + \lambda B)\right] \\
&= -k_B T \frac{1}{Z}\frac{\mathrm{d}}{\mathrm{d}\lambda}Z \\
&= -k_B T \frac{\mathrm{d}}{\mathrm{d}\lambda}\ln Z.
\end{aligned}$$

On the other hand, it is easy to see that

$$\frac{\mathrm{d}}{\mathrm{d}\lambda}\ln Z = \frac{\mathrm{d}}{\mathrm{d}\lambda}\ln Z_{gc}.$$

Therefore, one gets

$$\sigma = -\frac{k_B T}{L}\frac{\mathrm{d}}{\mathrm{d}\lambda}\ln Z_{gc} = \frac{1-x}{1+x}\rho. \tag{3.86}$$

The proof is complete. □

Average densities of each RNAP state: We denote by

$$\rho^\alpha := \langle \delta_{s_i,\alpha}\rangle = \frac{1}{L}\langle N^\alpha\rangle, \quad \alpha \in \{1,2\}, \tag{3.87}$$

the average densities of RNAP in state $1, 2$. Because of the fact that $\rho^1 + \rho^2 = \rho$ and (3.85), one gets

$$\rho^1 = \frac{1}{1+x}\rho, \quad \rho^2 = \frac{x}{1+x}\rho. \tag{3.88}$$

Average dwell times: We denote by ρ^α, $\alpha \in \{1, 2\}$, the average dwell time that an RNAP spends in a chemical state $1, 2$. Due to ergodicity one has $\tau^\alpha = \rho^\alpha / \rho$, thus one gets

$$\tau^1 = \frac{1}{1+x}, \quad \tau^2 = \frac{x}{1+x}. \tag{3.89}$$

and arrives at the balance equation

$$\frac{\rho^1}{\rho^2} = \frac{\tau^1}{\tau^2} = \frac{\phi^\star + \kappa^\star}{\omega^\star + \tau^\star} \tag{3.90}$$

which expresses the ensemble ratio in terms of the single-RNAP translocation rates $\omega^\star, \phi^\star$ and the single-RNAP PP_i release and binding rates $\kappa^\star, \tau^\star$.

3.2.4 Average elongation rate

3.2.4.1 Mean velocity of a single isolated RNAP

As in [4], we would like to elucidate here the effect of interactions on the average elongation rate. In order to do that, we compute, using the results of Wang et al [32], the mean velocity of a single isolated RNAP:

$$\nu^\star = \frac{\omega^\star \kappa^\star - \phi^\star \tau^\star}{\omega^\star + \phi^\star + \kappa^\star + \tau^\star}. \tag{3.91}$$

Then, by using results (3.88) from our setting, we rewrite $\nu^\star$ as follows

$$\nu^\star = \frac{\rho_1}{\rho} \omega^\star - \frac{\rho_2}{\rho} \phi^\star \tag{3.92}$$

where $\rho^1 = \dfrac{1}{1+x}\rho, \rho^2 = \dfrac{x}{1+x}\rho$.

Notice that if one discards the mutual interaction among RNAPs on the same DNA track and considers an RNAP as a simple random walk then its velocity is $\nu_0^\star = \omega^\star - \phi^\star$. One recognizes $\nu_0^\star$ is different from the expression (3.92), by the prefactors $\dfrac{\rho_1}{\rho}, \dfrac{\rho_2}{\rho}$ which are the averages of the times spent in the mobile states 1 and 2, respectively.

Remark 3.6. *If $\phi^\star = \tau^\star = 0$, one has $\nu^\star = \dfrac{\rho_1}{\rho}\omega^\star$ which is the result in [4].*

3.2.4.2 Average velocity and flux

The flux which is defined in [29] is the average number of RNAP crossing a site per unit time (second). Thus, the average flux j is the expectation of random variables $\omega_i(\boldsymbol{\eta}) - \phi_i(\boldsymbol{\eta})$ with respect to the stationary distribution (3.6) which gives the total elongation rate. Along with the average flux j, the average speed ν of an RNAP is also

a measure of the average elongation rate; it is related to j by

$$j = \rho \nu. \tag{3.93}$$

Using the factorization property of the stationary distribution, the relation (3.6) yields the following:

$$
\begin{aligned}
j &= \omega^\star \rho^1 \langle \left(1 + d^{1\star}\theta^0_{i-1} + d^{\star 01}\theta^1_i\right)\left(1 - \theta^0_i\right)\rangle - \phi^\star \rho^2 \langle(1 + e^{10\star}\theta^1_{i-1} + e^{\star 1}\theta^0_i)(1 - \theta^0_i)\rangle \\
&= \omega^\star \rho^1 (1 + d^{1\star}\langle\theta^0_{i-1}\rangle + d^{\star 01}\langle\theta^1_i\rangle)\left(1 - \langle\theta^0_i\rangle\right) - \phi^\star \rho^2(1 + e^{10\star}\langle\theta^1_{i-1}\rangle + e^{\star 1}\langle\theta^0_i\rangle)(1 - \langle\theta^0_i\rangle).
\end{aligned}
\tag{3.94}
$$

The values $\langle\theta^0_i\rangle, \langle\theta^1_i\rangle$ are computed by using Lemma 3.2. Thus, one can draw graphs of the average velocity and flux of RNAP. In all the plots (both of average velocity and of flux) shown below, the parameters are as follows: $[NTP] = 10^{-3}$, $[PP_i] = 10^{-5}$, the values of $\omega^\star, \phi^\star, \kappa^\star, \tau^\star$ are as in (3.5), and the length of RNAP $\ell = 5$.

(a) *Average velocity ν*   (b) *Average flux j*
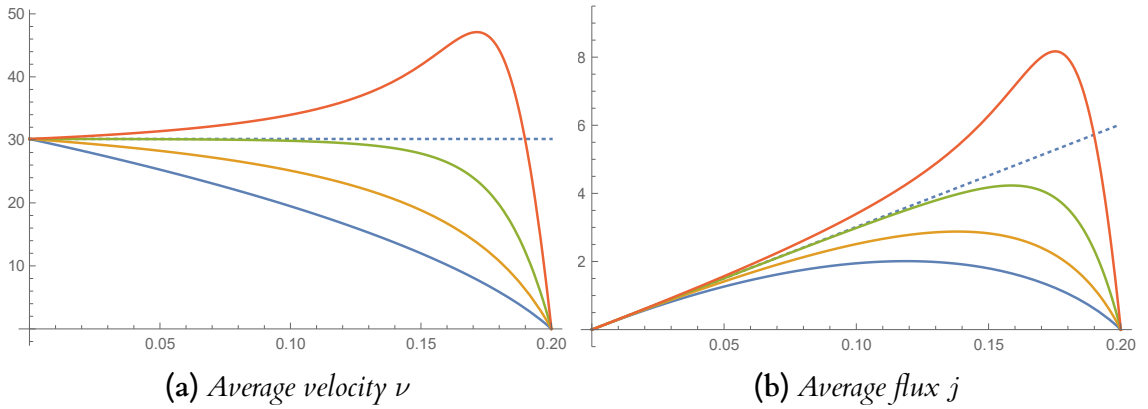
Figure 3.6: *The RNAP velocity ν and the RNAP flux j as function of RNAP density (x-axis) corresponding to $d^{\star 01} = e^{10\star} = 0$ and to different interaction strength y. Curves from top to bottom correspond to $y : 5, 2, 1.001, 0.5$. The dotted lines correspond to non-interacting RNAP.*

(a) *Average velocity ν*   (b) *Average flux j*
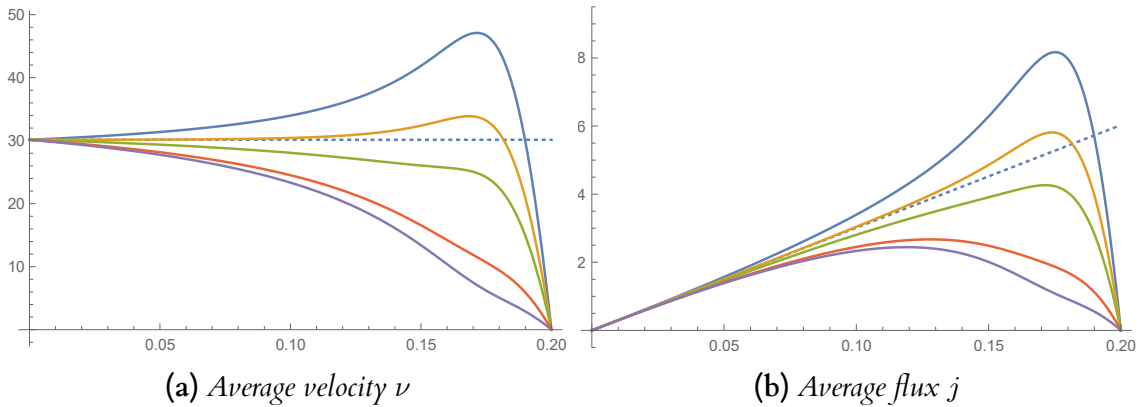
Figure 3.7: *The RNAP velocity ν and the RNAP flux j as function of RNAP density (x-axis) corresponding to the interaction strength $y = 5$ and $e^{10\star} = 0$ for different values of $d^{\star 01}$. Curves from top to bottom correspond to $d^{\star 01} : 0, -0.3, -0.5, -0.8, -0.9$. The dotted lines correspond to non-interacting RNAP.*

(a) *Average velocity ν*

(b) *Average flux j*
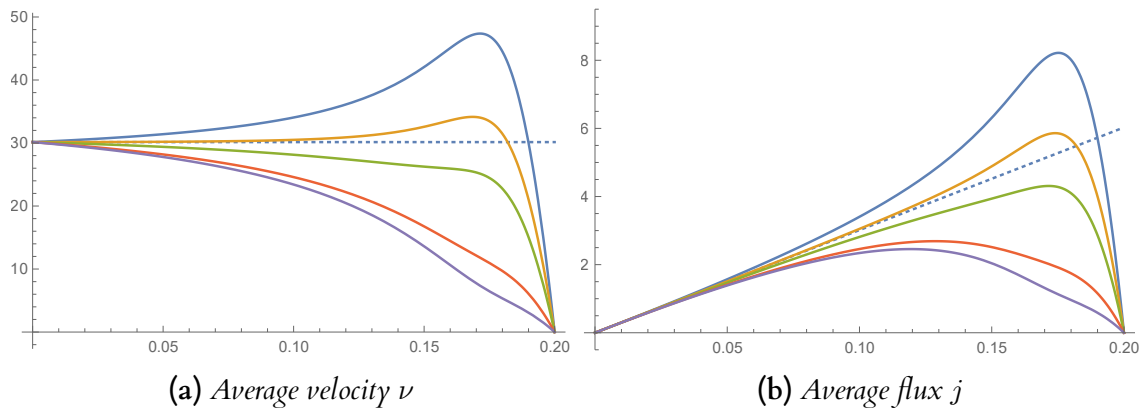
Figure 3.8: *The RNAP velocity ν and the RNAP flux j as function of RNAP density (x-axis) corresponding to interaction strength $y = 5$ and $e^{10\star} = -0.9$ for different values $d^{\star 01}$. Curves from top to bottom correspond to $d^{\star 01}$: $0, -0.3, -0.5, -0.8, -0.9$. The dotted lines correspond to non-interacting RNAP.*

(a) *Average velocity ν*

(b) *Average flux j*
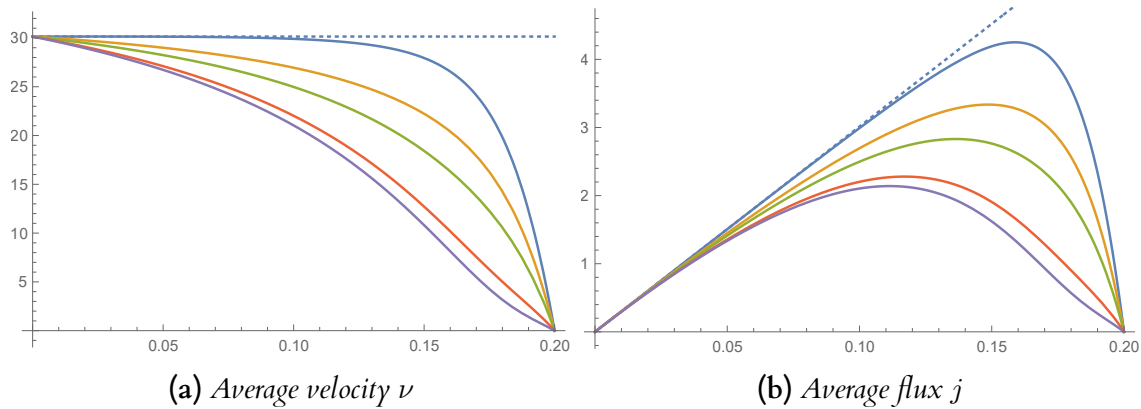
Figure 3.9: *The RNAP velocity ν and the RNAP flux j as function of RNAP density (x-axis) corresponding to interaction strength $y = 2$ and $e^{10\star} = -0.9$ for different values of $d^{\star 01}$. Curves from top to bottom correspond to $d^{\star 01}$: $0, -0.3, -0.5, -0.8, -0.9$. The dotted lines correspond to non-interacting RNAP.*

(a) *Average velocity ν*   (b) *Average flux j*
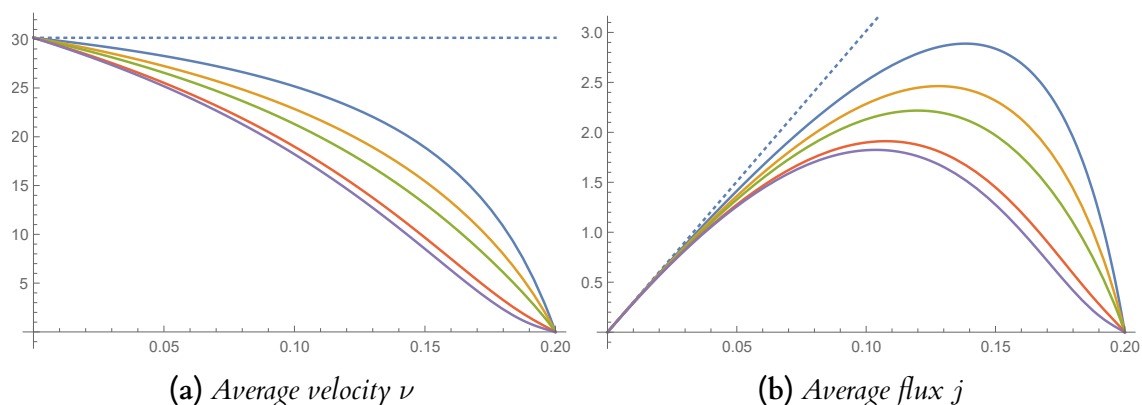
Figure 3.10: *The RNAP velocity ν and the RNAP flux j as function of RNAP density (x-axis) corresponding to interaction strength $y = 1.0001$ and $e^{10\star} = -0.9$ for different values of $d^{\star 01}$. Curves from top to bottom correspond to $d^{\star 01}$: $0, -0.3, -0.5, -0.8, -0.9$. The dotted lines correspond to non-interacting RNAP.*

(a) *Average velocity ν*   (b) *Average flux j*
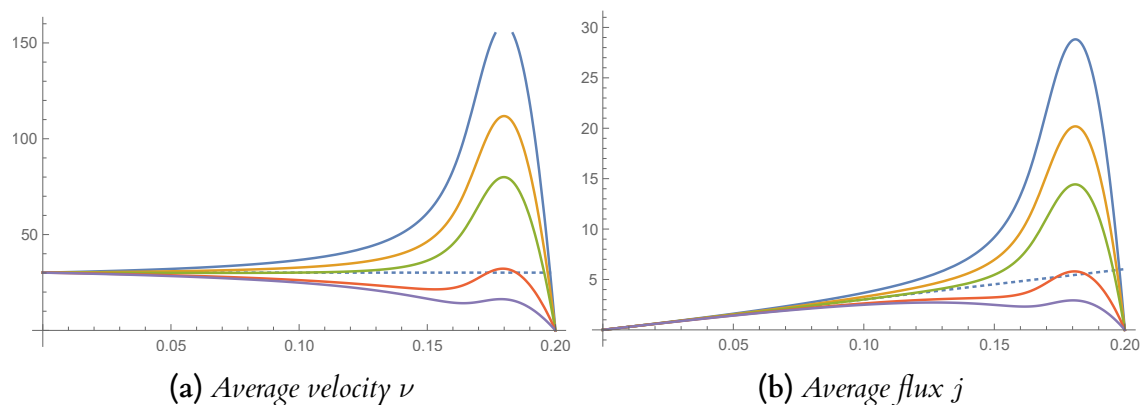
Figure 3.11: *The RNAP velocity ν and the RNAP flux j as function of RNAP density (x-axis) corresponding to interaction strength $y = 20$ and $e^{10\star} = -0.9$ for different values of $d^{\star 01}$. Curves from top to bottom correspond to $d^{\star 01}$: $0, -0.3, -0.5, -0.8, -0.9$. The dotted lines correspond to non-interacting RNAP.*

(a) *Average velocity*   (b) *Average flux*
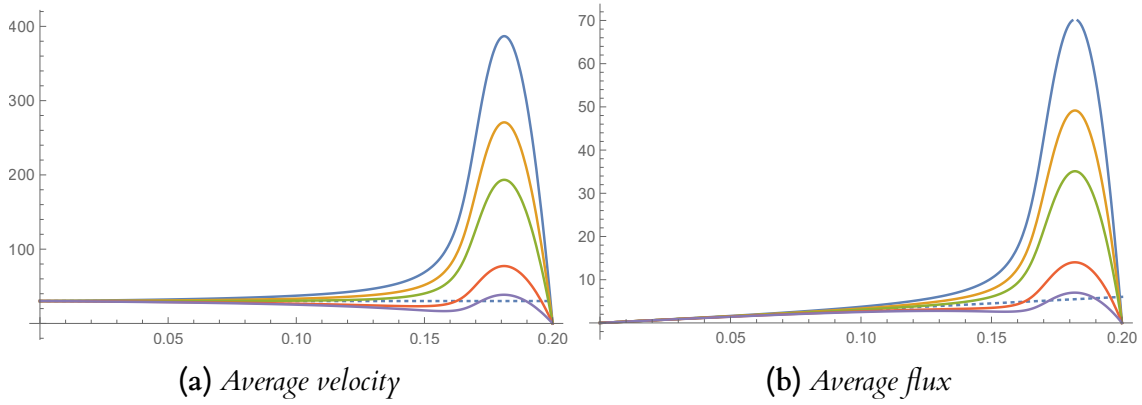
Figure 3.12: *The RNAP velocity ν and the RNAP flux j as function of RNAP density (x-axis) corresponding to interaction strength $y = 50$ and $e^{10\star} = -0.9$ for different values of $d^{\star 01}$. Curves from top to bottom correspond to $d^{\star 01}$: $0, -0.3, -0.5, -0.8, -0.9$. The dotted lines correspond to non-interacting RNAP.*

Let us zoom in the pictures of the case $y = 50, e^{1\star} = -0.9$ with $d^{\star 1} = -0.8, -0.9$, see Fig. 3.13.

(a) *Average velocity ν*   (b) *Average flux j*
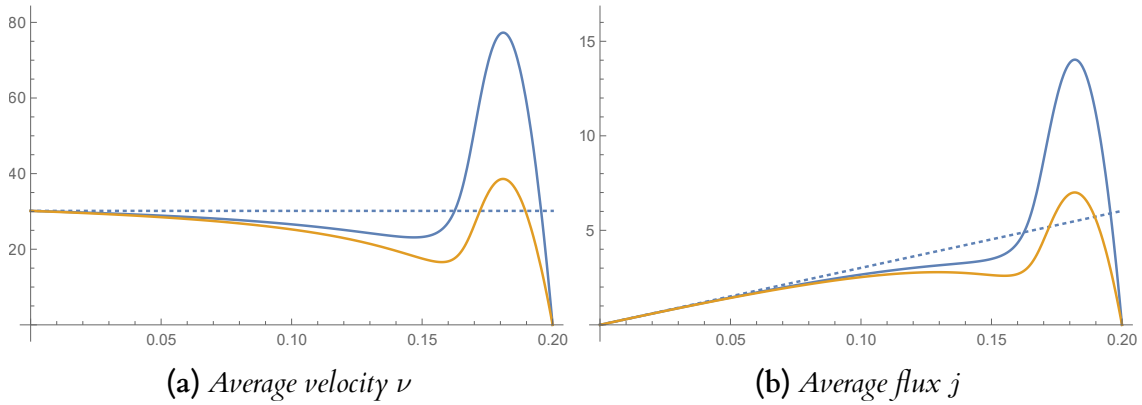
Figure 3.13: *The RNAP velocity ν and the RNAP flux j as function of RNAP density (x-axis) corresponding to interaction strength $y = 50$ and $e^{10\star} = -0.9$ for different values of $d^{\star 01}$: -0.8 (above), -0.9 (below). The dotted lines correspond to non-interacting RNAP.*

3.3 Discussion

3.3.1 Regarding the Minimal interaction range

It is interesting that if $d^{\star 01} = e^{10\star} = 0$ (that is interpreted as the minimal possible interaction range case) then, from identity (3.48), one has that $d^{1\star} = e^{\star 1}$. Thus, one obtains the average velocity as follows

$$\nu = \frac{1 - x}{1 + x} \left(1 + \frac{1 - z}{1 + (y - 1)z} d^{1\star} \right) \left(1 - \frac{1 - z}{1 + (y - 1)z} \right) \tag{3.95}$$

which is of the same form as in [4] except for the prefactor $\frac{1-x}{1+x}$. Note that z is a function of the RNAP density. By taking the derivative of (3.95) w.r.t. the density, one has that the derivative is 0 when $z = 1/(y-1)$ which implies that the velocity increases and reaches a maximum at $\rho^\star > 0$ only if $y > 2$ since $0 < z < 1$, see Fig. 3.6. This is an outcome of paper [4]. Thus, the cited paper and our results lead to the same conclusions for the explanation of the cooperative pushing effect. Hence, in the minimal interaction range case, only if the static repulsion $y > 2$, the speed increases and reaches its global maximum at $\rho^\star$ above which the velocity drops from the maximum to zero. When y is not strong enough ($y \leq 2$), the speed is less than the speed of a single RNAP (dotted line). Fig. 3.6a illustrates these features. In contrast, as Fig. 3.6b shows, the average elongation rate j increases for any interaction strength y. However, the cooperative pushing occurs only if the strength y above the critical value $y_c = 2$.

3.3.2   Regarding the extended interaction range

In all plots of Section 3.2.4, we have that $d^{\star 01}, e^{10\star} < 0$ (the extended interaction range case) which means that stochastic blocking enhancement holds at both sides of any rod. It is not surprising that the graph–shapes of average velocity and flux are not different from the ones in paper [4]. This can be explained by the fact that translocation backward rates are small. Even if backward blocking is very strong (i.e., $e^{10\star}$ is close to -1), it affects weakly the average elongation rate (see Figs. 3.7 and 3.8 for an illustration). Thus, one can predict the circumstances in which the cooperative pushing effect can occur only through static repulsion y and forward stochastic blocking ($d^{\star 01} < 0$). When the repulsive strength is not strong enough ($y \leq 2$), the speed and flux do not "feel" stochastic blocking and their values are less than the ones generated by a single RNAP (see Figs. 3.9 and 3.10 for an illustration). Fig. 3.13 shows that when the density is low and when the stochastic blocking enhancement is too strong ($d^{\star 01}$ is close to -1), then even strong stochastic pushing (y arbitrarily large) does not lead to cooperative pushing. Moreover, it also shows that when both strength y and stochastic blocking enhancement are very strong, the average elongation rate can exhibit two maxima and the cooperative pushing appears at higher densities. See also Figs. 3.11 and 3.12 that show that when densities are high and the static repulsive strength is strong, the average elongation rate exhibits a maximum which deepens with decrease of the stochastic (forward) blocking.

Chapter 4

RNAP model: range–3 interaction rate and range–2 pair potential

4.1   The model dynamics and stationary distribution

We consider the minimal reaction scheme of RNAP translocation presented in Fig. 4.1. This means that our model neglects the reverse process in the same way as this has been done in [4, 5] (the reversing here means that a RNAP returns backward and leaves the PP_i that has been bound to it). However, in this chapter, compared to [4, 5], we shall propose new kinetic assumptions that will allow us to obtain a more detailed biological description of the mechanochemical cycle of the RNAP during elongation and also of the collective incorporating of RNAPs on the same DNA track.
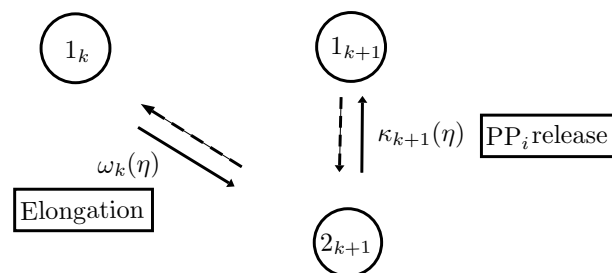
Figure 4.1: *Minimal reaction scheme of RNAP translocation. Reverse reactions (not considered in our models presented here) are indicated with dashed arrows.*

4.1.1   The model dynamics

The configuration-dependent translocation rate $\omega_i(\boldsymbol{\eta})$ and PP_i release, see Figs. 1.4 and 1.5 for pictorial representations, are the following

$$\omega_i(\boldsymbol{\eta}) = \delta_{s_i,1}(w_i^1(\boldsymbol{\eta}) + w_i^2(\boldsymbol{\eta})), \tag{4.1}$$

$$\kappa_i(\boldsymbol{\eta}) = \delta_{s_i,2}(\kappa_i^0(\boldsymbol{\eta}) + \kappa_i^1(\boldsymbol{\eta}) + \kappa_i^2(\boldsymbol{\eta})), \tag{4.2}$$

where

- $w_i^1(\boldsymbol{\eta}) := \omega_1^\star(1 + d^{1\star}\delta_{x_i,x_{i-1}+\ell} + d^{10\star}\delta_{x_i,x_{i-1}+\ell+1} + d^{100\star}\delta_{x_i,x_{i-1}+\ell+2})(1 - \delta_{x_{i+1},x_i+\ell})$
  $\times \delta_{x_{i+1},x_i+\ell+1}$;

- $w_i^2(\boldsymbol{\eta}) := \omega_2^\star(1 + e^{1\star}\delta_{x_i,x_{i-1}+\ell} + e^{10\star}\delta_{x_i,x_{i-1}+\ell+1} + e^{100\star}\delta_{x_i,x_{i-1}+\ell+2})(1 - \delta_{x_{i+1},x_i+\ell})(1 - \delta_{x_{i+1},x_i+\ell+1})$,

- $\kappa_i^0(\boldsymbol{\eta}) = \kappa^\star(1 + f_0^{10\star}\delta_{x_i,x_{i-1}+\ell+1} + f_0^{1\star}\delta_{x_i,x_{i-1}+\ell} + f_0^{\star 1}\delta_{x_{i+1},x_i+\ell})\delta_{x_{i+1},x_i+\ell}$;

- $\kappa_i^1(\boldsymbol{\eta}) = \kappa^\star(1 + f_1^{10\star}\delta_{x_i,x_{i-1}+\ell+1} + f_1^{1\star}\delta_{x_i,x_{i-1}+\ell} + f_1^{\star 01}\delta_{x_{i+1},x_i+\ell+1})(1 - \delta_{x_{i+1},x_i+\ell})\delta_{x_{i+1},x_i+\ell+1}$;

- $\kappa_i^2(\boldsymbol{\eta}) = \kappa^\star(1 + f_2^{10\star}\delta_{x_i,x_{i-1}+\ell+1} + f_2^{1\star}\delta_{x_i,x_{i-1}+\ell})(1 - \delta_{x_{i+1},x_i+\ell})(1 - \delta_{x_{i+1},x_i+\ell+1})$.

The parameters must be chosen to ensure that all the rates are positive. Namely, the parameter range is $\omega_1^\star, \omega_2^\star, \kappa^\star > 0$; $e^{1\star}, e^{10\star}, d^{1\star}, d^{10\star} \geq -1$; $f_0^{1\star} + f_0^{\star 1}, f_0^{10\star} + f_0^{\star 1} \geq -1$; $f_1^{1\star} + f_1^{\star 01}, f_1^{10\star} + f_1^{\star 01} \geq -1$; and $f_2^{1\star}, f_2^{\star 01} \geq -1$.

4.1.2   The model stationary distribution

We will search for the stationary distribution of the model, which can be expressed in the form of (4.5) below. In this form, the energy function U that governs the interactions not only includes the nearest interaction energy used in [4] and Chapter 3, but also an additional term known as the "next-nearest–interaction" energy. Thus, the interaction energy is of the form

$$U(\mathbf{x}) = J_1 \sum_{i=1}^N \delta_{x_{i+1},x_i+\ell}^L + J_2 \sum_{i=1}^N \delta_{x_{i+1},x_i+\ell+1}^L. \tag{4.3}$$

Above, as everywhere else, δ^L is the Kronecker symbol which arguments should be understood modulo L due to periodic boundary conditions. We also note that the form of U means that positive J_1 and J_2 correspond to repulsion.

As mentioned in Chapter 3, an allowed configuration can be specified by the position vector $\mathbf{x} = (x_1, ..., x_N)$ and state vector $\mathbf{s} = (s_1, ..., x_N)$. We define the excess $B(\mathbf{s}) = N^1 - N^2$ where N^α is the fluctuating number of RNAPs in state $\alpha \in \{1, 2\}$. The stationary distribution for allowed configurations thus takes the form

$$\hat{\pi}(\boldsymbol{\eta}) = \frac{1}{Z}\pi(\boldsymbol{\eta}) \tag{4.4}$$

with the Boltzmann weights

$$\pi(\boldsymbol{\eta}) = \exp\left[-\frac{1}{k_B T}(U + \lambda B)\right] \tag{4.5}$$

and the partition function

$$Z = \sum_{\boldsymbol{\eta}} \pi(\boldsymbol{\eta}). \tag{4.6}$$

Lagrange multiplier λ plays the role of chemical potential that takes care of the fluctuations in the excess

$$B(\mathbf{s}) = \sum_{i=1}^{N}(3 - 2s_i) \tag{4.7}$$

due to the interplay of NTP hydrolysis and PP_i release.

We introduce the parameters

$$x = e^{\frac{2\lambda}{k_B T}}, \quad y_1 = e^{\frac{J_1}{k_B T}}, \quad y_2 = e^{\frac{J_2}{k_B T}} \tag{4.8}$$

so that $x > 1$ corresponds to an excess of RNAP in state 1 over those in state 2, and $y_1 > 1$ and $y_2 > 1$, correspond, respectively, to repulsive nearest and next-nearest interactions. The normalized stationary distribution for allowed configurations is then given by

$$\hat{\pi}(\boldsymbol{\eta}) = \frac{1}{Z}\prod_{i=1}^{N} x^{-3/2+s_i} y_1^{-\delta^L_{x_{i+1},x_i+\ell}} y_2^{-\delta^L_{x_{i+1},x_i+\ell+1}}. \tag{4.9}$$

Let us speak about some choices for parameters J_1 and J_2 which are related to some models in aqueous solutions, which one has in a biological cell.

- **Fully repulsive case:** $J_1 > J_2 > 0$. This is a simple discretization of the Debye–Hückel theory of electrostatic interaction between ions. The interaction is repulsive and decays with distance. See Fig. 4.2a for the potential in our discretization setting.

- **Lennard Jones potential:** $J_1 > 0, J_2 < 0$ such that $|J_2| < J_1$. The potential approximates the interaction between two particles which is a repulsion at a very short range, an attraction at a moderate distance, and is nil at a long range. Our model with the choice of parameters J_1, J_2 is just a simple discretization of the Lennard Jones potential, see Fig. 4.2b.

- **DLVO theory:** $J_2 > 0$ such that $J_2 > |J_1|$. DLVO theory describes the stabilization of colloidal dispersions which used the sum of van der Waals (attractive) and electrical double layers (repulsive) forces as total potential energy to describe the interaction of two particles. The two forces increase when two particles approach closer to each other which implies that at a short distance the interaction is either

repulsion or attraction. However, van der Waals's force quickly vanishes when two particles are far away one from other. See Fig. 4.2c for the potential in our discretization setting.

Since all these potentials play an important role in the study of particles in aqueous solutions, one may assume that anyone of them may be relevant for molecular motors. Thus, all these potentials will be considered in our work.

(a) *Debye–Hückel potential.* (b) *Lennard Jones potential.*
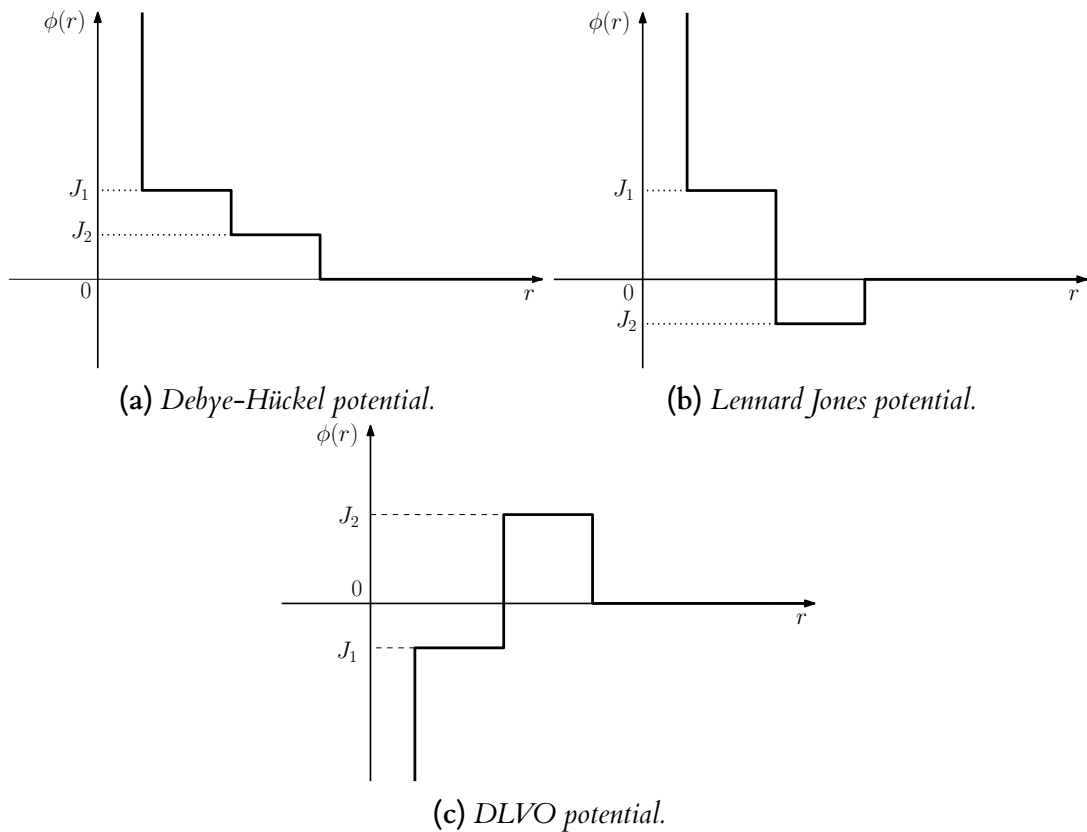
(c) *DLVO potential.*

Figure 4.2: *Debye–Hückel, Lennard Jones, and DLVO potentials $\phi(r)$ are as functions of the distance r in the discretizattion settings.*

4.2   The conditions for the existence

In this section, we shall find conditions upon the parameters appearing in the rates that make it that the measure (4.4) becomes invariant for the considered process. Our approach is based on analysis of the master equation of the process.

4.2.1 Master equation

The master equation for the probability $\mathbb{P}_t(\boldsymbol{\eta})$ of finding the rods in the configuration $\boldsymbol{\eta}$ at time t is as follows:

$$\frac{d}{dt}\mathbb{P}(\boldsymbol{\eta},t) = \sum_{i=1}^{N}[\omega_i(\boldsymbol{\eta}_{tl}^i)\mathbb{P}(\boldsymbol{\eta}_{tl}^i,t) + \kappa_i(\boldsymbol{\eta}_{rel}^i)\mathbb{P}(\boldsymbol{\eta}_{rel}^i,t) - (\omega_i(\boldsymbol{\eta}) + \kappa_i(\boldsymbol{\eta}))\mathbb{P}(\boldsymbol{\eta},t)], \quad (4.10)$$

where $\boldsymbol{\eta}_{tl}^i$ is the configuration that leads to $\boldsymbol{\eta}$ before a translocation of RNAP i (i.e., the RNAP with coordinate $x_i^{tl} = x_i - 1$ and state $s_i^{tl} = 3 - s_i$) while $\boldsymbol{\eta}_{rel}^i$ is the configuration $\boldsymbol{\eta}$ before PP$_i$ release at RNAP i (i.e., $x_i^{rel} = x_i$ and $s_i^{rel} = 3 - s_i$). Due to lattice structure (the periodicity), the positions x_i of the rods are counted modulo L and labels i are counted modulo N.

Dividing (4.10) by the stationary distribution (4.4), the stationary condition becomes

$$\sum_{i=1}^{N}\left(\omega_i(\boldsymbol{\eta}_{tl}^i)\frac{\pi(\boldsymbol{\eta}_{tl}^i)}{\pi(\boldsymbol{\eta})} - \omega_i(\boldsymbol{\eta}) + \kappa_i(\boldsymbol{\eta}_{rel}^i)\frac{\pi(\boldsymbol{\eta}_{rel}^i)}{\pi(\boldsymbol{\eta})} - \kappa_i(\boldsymbol{\eta})\right) = 0. \qquad (4.11)$$

Now we introduce the quantities

$$D_i(\boldsymbol{\eta}) = \omega_i(\boldsymbol{\eta}_{tl}^i)\frac{\pi(\boldsymbol{\eta}_{tl}^i)}{\pi(\boldsymbol{\eta})} - \omega_i(\boldsymbol{\eta}), \qquad (4.12)$$

$$F_i(\boldsymbol{\eta}) = \kappa_i(\boldsymbol{\eta}_{rel}^i)\frac{\pi(\boldsymbol{\eta}_{rel}^i)}{\pi(\boldsymbol{\eta})} - \kappa_i(\boldsymbol{\eta}). \qquad (4.13)$$

Taking into account the periodicity, we get that the stationary condition (4.11) is satisfied if the following lattice divergence condition

$$D_i(\boldsymbol{\eta}) + F_i(\boldsymbol{\eta}) = \Phi_i(\boldsymbol{\eta}) - \Phi_{i+1}(\boldsymbol{\eta}) \qquad (4.14)$$

holds for all allowed configurations and with a family of functions $\Phi_i(\boldsymbol{\eta})$ satisfying $\Phi_{N+1}(\boldsymbol{\eta}) = \Phi_1(\boldsymbol{\eta})$.

4.2.2 Mapping to the headway process

Recall that an allowed configuration of RNAPs can be specified by the distance vector $\mathbf{m} = (m_1, ..., m_N)$ and the state vector $\mathbf{s} = (s_1, ..., s_N)$. Let us rewrite the indicator functions

$$\theta_i^p = \delta_{m_i,p} = \delta_{x_{i+1},x_i+\ell+p} \qquad (4.15)$$

on a headway of length p (in units of bp) with the index i taken modulo N, i.e., $\theta_0^p \equiv \theta_N^p$.

Thus, in terms of the variables (4.8) and the distance variables (4.15), the stationary

distribution (4.4) acquires the expression

$$\tilde{\pi}(\boldsymbol{\zeta}) = \frac{1}{Z} \prod_{i=i}^{N} \left(x^{-3/2+s_i} y_1^{-\theta_i^0} y_2^{-\theta_i^1} \right) \tag{4.16}$$

which is of the factorized form, the fact that indicates the absence of distance correlations.

A translocation of RNAP i corresponds to the transition $(m_{i-1}, m_i) \rightarrow (m_{i-1}+1, m_i-1)$ with all other distances kept unchanged. Due to steric hardcore repulsion, this transition can only take place if $m_i > 0$. Thus, the transition rates (4.1) and (4.2) for an allowed configuration $\boldsymbol{\zeta} = (\mathbf{m}, \mathbf{s})$ can be written using the configuration's distance and state vectors $\mathbf{m}$ and $\mathbf{s}$; the result is as follows:

$$\begin{aligned}
\tilde{\omega}_i(\boldsymbol{\zeta}) &= \delta_{s_i,1}[\omega_1^\star(1 + d^{1\star}\theta_{i-1}^0 + d^{10\star}\theta_{i-1}^1 + d^{100\star}\theta_{i-1}^2)(1 - \theta_i^0)\theta_i^1 \\
&\quad + \omega_2^\star(1 + e^{1\star}\theta_{i-1}^0 + e^{10\star}\theta_{i-1}^1 + e^{100\star}\theta_{i-1}^2)(1 - \theta_i^0)(1 - \theta_i^1)], \tag{4.17}
\end{aligned}$$

$$\begin{aligned}
\tilde{\kappa}_i(\boldsymbol{\zeta}) &= \kappa^\star \delta_{s_i,2}[(1 + f_0^{1\star}\theta_{i-1}^0 + f_0^{10\star}\theta_{i-1}^1 + f_0^{\star 1}\theta_i^0)\theta_i^0 \\
&\quad + (1 + f_1^{1\star}\theta_{i-1}^0 + f_1^{10\star}\theta_{i-1}^1 + f_1^{\star 01}\theta_i^0)(1 - \theta_i^0)\theta_i^1 \\
&\quad + (1 + f_2^{1\star}\theta_{i-1}^0 + f_2^{10\star}\theta_{i-1}^1)(1 - \theta_i^0)(1 - \theta_i^1)]. \tag{4.18}
\end{aligned}$$

Before writing the master equation for the headway process, we introduce notation for the configurations that lead to a given configuration $\boldsymbol{\zeta}$. Namely, $\boldsymbol{\zeta}^{i-1,i}$ corresponds to forward translocation and $\boldsymbol{\zeta}^i$ corresponds to PP$_i$ release. For a fixed $\boldsymbol{\zeta}$, these configurations are defined by

$$s_j^{i-1,i} = s_j + (3 - 2s_j)\delta_{j,i}, \quad m_j^{i-1,i} = m_j + \delta_{j,i} - \delta_{j,i-1}, \tag{4.19}$$

$$s_j^i = s_j + (3 - 2s_j)\delta_{j,i}, \quad m_j^i = m_j. \tag{4.20}$$

This yields the master equation

$$\frac{d\mathbb{P}(\boldsymbol{\zeta}, t)}{dt} = \sum_{i=1}^{N} Q_i(\boldsymbol{\zeta}, t) \tag{4.21}$$

with

$$Q_i(\boldsymbol{\zeta}, t) = \tilde{\omega}_i(\boldsymbol{\zeta}^{i-1,i})\mathbb{P}(\boldsymbol{\zeta}^{i-1,i}, t) - \tilde{\omega}_i(\boldsymbol{\zeta})\mathbb{P}(\boldsymbol{\zeta}, t) + \tilde{\kappa}_i(\boldsymbol{\zeta}^i)\mathbb{P}(\boldsymbol{\zeta}^i, t) - \tilde{\kappa}_i(\boldsymbol{\zeta})\mathbb{P}(\boldsymbol{\zeta}, t) \tag{4.22}$$

where the transition rates $\tilde{\omega}_i(\boldsymbol{\zeta}^{i-1,i}), \tilde{\kappa}_i(\boldsymbol{\zeta}^i)$ are of the forms

$$\begin{aligned}
\tilde{\omega}_i(\boldsymbol{\zeta}^{i-1,i}) &= \delta_{s_i,2}[\omega_1^\star(1 + d^{1\star}\theta_{i-1}^1 + d^{10\star}\theta_{i-1}^2)(1 - \theta_{i-1}^0)\theta_i^0 \\
&\quad + \omega_2^\star(1 + e^{1\star}\theta_{i-1}^1 + e^{10\star}\theta_{i-1}^2)(1 - \theta_{i-1}^0)(1 - \theta_i^0)], \tag{4.23}
\end{aligned}$$

$$\tilde{\kappa}_i(\boldsymbol{\zeta}^i) = \kappa^\star \delta_{s_i,1}[(1 + f_0^{1\star}\theta_{i-1}^0 + f^{10\star}\theta_{i-1}^1 + f_0^{\star 1}\theta_i^0)\theta_i^0$$

$$+ (1 + f_1^{1\star}\theta_{i-1}^0 + f_1^{10\star}\theta_{i-1}^1 + f_1^{\star 01}\theta_i^0)(1 - \theta_i^0)\theta_i^1$$
$$+ (1 + f_2^{1\star}\theta_{i-1}^0 + f_2^{10\star}\theta_{i-1}^1)(1 - \theta_i^0)(1 - \theta_i^1)]. \tag{4.24}$$

4.2.3 Stationary conditions

By the discrete version of the Noether theorem, one can rephrase the master equation (4.21) for the headway process when the process is in its stationary state; the rephrasing is in a local divergence form which is equivalent to (4.14). Before doing that let us first introduce the following notations

$$\tilde{D}_i(\boldsymbol{\zeta}) = \tilde{\omega}_i(\boldsymbol{\zeta}^{i-1,i})\frac{\tilde{\pi}(\boldsymbol{\zeta}^{i-1,i})}{\tilde{\pi}(\boldsymbol{\zeta})} - \tilde{\omega}_i(\boldsymbol{\zeta}), \tag{4.25}$$

$$\tilde{F}_i(\boldsymbol{\zeta}) = \tilde{\kappa}_i(\boldsymbol{\zeta}^i)\frac{\tilde{\pi}(\boldsymbol{\zeta}^i)}{\tilde{\pi}(\boldsymbol{\zeta})} - \tilde{\kappa}_i(\boldsymbol{\zeta}), \tag{4.26}$$

and let us also notice that

$$\theta_j^p(\boldsymbol{\zeta}^{i-1,i}) = \delta_{m_j+\delta_{j,i}-\delta_{j,i-1},p} = \theta_j^{p-\delta_{j,i}+\delta_{j,i-1}}(\boldsymbol{\zeta}) \text{ and } \delta_{s_i^{i-1,i},\alpha} = \delta_{s_i,3-\alpha}; \tag{4.27}$$

$$\theta_j^p(\boldsymbol{\zeta}^i) = \theta_j^p(\boldsymbol{\zeta}) \text{ and } \delta_{s_i^i,\alpha} = \delta_{s_i,3-\alpha}. \tag{4.28}$$

One has

$$\frac{\tilde{\pi}(\boldsymbol{\zeta}^i)}{\tilde{\pi}(\boldsymbol{\zeta})} = x^{3-2s_i}, \tag{4.29}$$

and

$$\frac{\tilde{\pi}(\boldsymbol{\zeta}^{i-1,i})}{\tilde{\pi}(\boldsymbol{\zeta})} = \frac{y_1^{-\theta_{i-1}^0(\boldsymbol{\zeta}^{i-1,i})}y_2^{-\theta_{i-1}^1(\boldsymbol{\zeta}^{i-1,i})}x^{-3/2+s_{i-1}(\boldsymbol{\zeta}^{i-1,i})}}{y_1^{-\theta_{i-1}^0}y_2^{-\theta_{i-1}^1}x^{-3/2+s_{i-1}}} \cdot \frac{y_1^{-\theta_i^0(\boldsymbol{\zeta}^{i-1,i})}y_2^{-\theta_i^1(\boldsymbol{\zeta}^{i-1,i})}x^{-3/2+s_i(\boldsymbol{\zeta}^{i-1,i})}}{y_1^{-\theta_i^0}y_2^{-\theta_i^1}x^{-3/2+s_i}}$$

$$= x^{-1}y_1^{\theta_{i-1}^0+\theta_i^0-\theta_{i-1}^1}y_2^{-\theta_{i-1}^2+\theta_{i-1}^1-\theta_i^0+\theta_i^1}. \tag{4.30}$$

Hence,

$$\tilde{D}_i(\boldsymbol{\zeta}) = x^{-1}y_1^{\theta_{i-1}^0+\theta_i^0-\theta_{i-1}^1}y_2^{-\theta_{i-1}^2+\theta_{i-1}^1-\theta_i^0+\theta_i^1}\tilde{\omega}_i(\boldsymbol{\zeta}^{i-1,i}) - \tilde{\omega}_i(\boldsymbol{\zeta}), \tag{4.31}$$

$$\tilde{F}_i(\boldsymbol{\zeta}) = x^{3-2s_i}\tilde{\kappa}_i(\boldsymbol{\zeta}^i) - \tilde{\kappa}_i(\boldsymbol{\zeta}). \tag{4.32}$$

One requires

$$\tilde{D}_i + \tilde{F}_i = \tilde{\Phi}_{i-1} - \tilde{\Phi}_i, \tag{4.33}$$

where $\tilde{\Phi}_i$ is of the form $\tilde{\Phi}_i = (a_0 + a_1\theta_i^0 + a_2\theta_i^1 + a_3\theta_i^2)(\delta_{s_i,1} + \delta_{s_i,2}) = a_0 + a_1\theta_i^0 + a_2\theta_i^1 + a_3\theta_i^2$. Notice that $\tilde{\Phi}_i$ must be of that form since $\tilde{D}_i, \tilde{F}_i$ depend on the state of RNAP i and on variables $\theta_{i-1}^0, \theta_{i-1}^1, \theta_{i-1}^2, \theta_i^0, \theta_i^1, \theta_i^2$ that attain their values in $\{0, 1\}$.

We set $a_k = 0$ for $k > 3$ and suppose that $m_{i-1} = m$ and $m_i = n$. By plugging $s_i = 1, 2$ into equation (4.33), one has the system of equations (4.34)–(4.35) below.

– If $s_1 = 1$, one has

$$-\tilde{\omega}_i(\boldsymbol{\zeta}) + x\tilde{\kappa}_i(\boldsymbol{\zeta}^i) = a_{m+1} - a_{n+1}. \tag{4.34}$$

– If $s_1 = 2$, one has

$$x^{-1}y_1^{\theta_{i-1}^0+\theta_i^0-\theta_{i-1}^1}y_2^{-\theta_{i-1}^2+\theta_{i-1}^1-\theta_i^0+\theta_i^1}\tilde{\omega}_i(\boldsymbol{\zeta}^{i-1,i}) - \kappa_i(\boldsymbol{\zeta}) = a_{m+1} - a_{n+1}. \tag{4.35}$$

System of equations (4.34)–(4.35) is equivalent to the system (4.37)–(4.36) below

$$-\tilde{\omega}_i(\boldsymbol{\zeta}) + x\tilde{\kappa}_i(\boldsymbol{\zeta}^i) = a_{m+1} - a_{n+1}, \tag{4.36}$$

$$y_1^{\theta_{i-1}^0+\theta_i^0-\theta_{i-1}^1}y_2^{-\theta_{i-1}^2+\theta_{i-1}^1-\theta_i^0+\theta_i^1}\tilde{\omega}_i(\boldsymbol{\zeta}^{i-1,i}) - \tilde{\omega}_i(\boldsymbol{\zeta}) = (1+x)(a_{m+1} - a_{n+1}). \tag{4.37}$$

Let us consider equation (4.37) case by case.

– Consider the case $m = 0$:

  • If $n \geq 3$, one has $-\omega_2^\star(1 + e^{1\star}) = (1+x)a_1$. Thus,

$$a_1 = \frac{-\omega_2^\star(1 + e^{1\star})}{1 + x}. \tag{4.38}$$

  • If $n = 2$, one has $-\omega_2^\star(1 + e^{1\star}) = (1+x)(a_1 - a_3)$ which implies $a_3 = 0$.

  • If $n = 1$, one has $-\omega_1^\star(1 + d^{1\star}) = (1+x)(a_1 - a_2)$. Thus,

$$a_2 = \frac{\omega_1^\star(1 + d^{1\star}) - \omega_2^\star(1 + e^{1\star})}{1 + x}. \tag{4.39}$$

– Consider the case $m = 3$ and $n \geq 2$, one gets $\omega_2^\star(1 + e^{100\star}) - \omega_2^\star = 0$, thus $e^{100\star} = 0$.

– Consider the case $m = 2$:

  • If $n \geq 2$, one has $y_2^{-1}\omega_2^\star(1 + e^{10\star}) - \omega_2^\star = 0$, which implies $y_2 = 1 + e^{10\star}$

  • If $n = 1$, one has $\omega_2^\star(1 + e^{10\star}) - \omega_1^\star = -(1+x)a_2$, thus $d^{1\star} = \frac{\omega_2^\star}{\omega_1^\star}(e^{1\star} - e^{10\star})$.

– Consider the case $m = 1, n \geq 2$, one has $y_1^{-1}y_2\omega_2^\star(1 + e^{1\star}) - \omega_2^\star(1 + e^{10\star}) = (1+x)a_2$ which implies $y_1 = \frac{\omega_2^\star}{\omega_1^\star}(1 + e^{1\star})(1 + e^{10\star})$.

– Consider the case $m = 2, n = 0$, one has $y_1 y_2^{-2}\omega_1^\star(1 + d^{10\star}) = -(1+x)a_1$ which implies $d^{10\star} = e^{10\star}$.

– Consider the case $m = 3$ and $n = 0$ one gets $y_1 y_2^{-1}\omega_1^\star(1 + d^{100\star}) = -(1+x)a_1$, thus $d^{100\star} = 0$.

Therefore, one obtains

$$a_1 = \frac{-\omega_2^\star(1 + e^{1\star})}{1 + x},\tag{4.40}$$

$$a_2 = \frac{\omega_1^\star(1 + d^{1\star}) - \omega_2^\star(1 + e^{1\star})}{1 + x},\tag{4.41}$$

$$a_3 = 0,\tag{4.42}$$

and

$$e^{100\star} = d^{100\star} = 0,\tag{4.43}$$

$$e^{10\star} = d^{10\star},\tag{4.44}$$

$$d^{1\star} = \frac{\omega_2^\star}{\omega_1^\star}(e^{1\star} - e^{10\star}),\tag{4.45}$$

$$y_1 = \frac{\omega_2^\star}{\omega_1^\star}(1 + e^{1\star})(1 + e^{10\star}),\tag{4.46}$$

$$y_2 = (1 + e^{10\star}).\tag{4.47}$$

From here, one easily shows that equation (4.37) holds for all allowed configurations. In other words, one has the following lemma.

Lemma 4.1. *If the constraints* (4.43)–(4.47) *are satisfied, then equation* (4.37) *holds for all configurations.*

Next, we shall find parameters appearing in the release rate by considering equation (4.36).

– Consider the case $n \geq 2$:

- If $m \geq 2$, one has $-\omega_2^\star + x\kappa^\star = 0$, thus

$$x = \frac{\omega_2^\star}{\kappa^\star}.\tag{4.48}$$

- If $m = 1$, one has $-\omega_2^\star(1 + e^{10\star}) + x\kappa^\star(1 + f_2^{10\star}) = a_2$ which implies

$$f_2^{10\star} = \frac{x}{1 + x}e^{10\star} + \frac{\omega_1^\star}{\omega_2^\star}\frac{1}{1 + x} - \frac{1}{1 + x}.\tag{4.49}$$

- If $m = 0$, one has $-\omega_2^\star(1 + e^{1\star}) + x\kappa^\star(1 + f_2^{1\star}) = a_1$ which implies

$$f_2^{1\star} = \frac{x}{1 + x}e^{1\star} - \frac{1}{1 + x}.\tag{4.50}$$

– Consider the case $n = 1$:

- If $m \geq 2$, one has $-\omega_1^\star + x\kappa^\star(1 + f_1^{\star 01}) = -a_2$ which implies

$$f_1^{\star 01} = \frac{1}{1+x}e^{10\star} + \frac{\omega_1^\star}{\omega_2^\star}\frac{x}{1+x} - \frac{x}{1+x}. \tag{4.51}$$

- If $m = 1$, one has $-\omega_1^\star(1 + e^{10\star}) + x\kappa^\star(1 + f_1^{10\star} + f_1^{\star 01}) = 0$ which implies

$$f_1^{10\star} = \left(\frac{\omega_1^\star}{\omega_2^\star} - \frac{1}{1+x}\right)e^{10\star} + \frac{\omega_1^\star}{\omega_2^\star}\frac{1}{1+x} - \frac{1}{1+x}. \tag{4.52}$$

- If $m = 0$, one has $-\omega_1^\star(1 + d^{1\star}) + x\kappa^\star(1 + f_1^{1\star} + f_1^{\star 01}) = a_1 - a_2$ which implies

$$f_1^{1\star} = \frac{x}{1+x}e^{1\star} - e^{10\star} - \frac{1}{1+x}. \tag{4.53}$$

– Consider the case $n = 0$:

- If $m \geq 2$, one has $x\kappa^\star(1 + f_0^{\star 1}) = -a_1$ which implies

$$f_0^{\star 1} = \frac{1}{1+x}e^{1\star} - \frac{x}{1+x}. \tag{4.54}$$

- If $m = 1$, one has $x\kappa^\star(1 + f_0^{10\star} + f_0^{\star 1}) = a_2 - a_1$ which implies

$$f_0^{10\star} = -\frac{1}{1+x}e^{10\star} + \frac{\omega_1^\star}{\omega_2^\star}\frac{1}{1+x} - \frac{1}{1+x}. \tag{4.55}$$

- If $m = 0$, one has $x\kappa^\star(1 + f_0^{1\star} + f_0^{\star 1}) = 0$ which implies

$$f_0^{1\star} = -\frac{1}{1+x}e^{1\star} - \frac{1}{1+x}. \tag{4.56}$$

Therefore, one obtains

$$x = \frac{\omega_2^\star}{\kappa^\star}, \tag{4.57}$$

$$f_0^{\star 1} = \frac{1}{1+x}e^{1\star} - \frac{x}{1+x}, \tag{4.58}$$

$$f_0^{10\star} = -\frac{1}{1+x}e^{10\star} + \frac{\omega_1^\star}{\omega_2^\star}\frac{1}{1+x} - \frac{1}{1+x}, \tag{4.59}$$

$$f_0^{1\star} = -\frac{1}{1+x}e^{1\star} - \frac{1}{1+x}, \tag{4.60}$$

$$f_1^{\star 01} = \frac{1}{1+x}e^{10\star} + \frac{\omega_1^\star}{\omega_2^\star}\frac{x}{1+x} - \frac{x}{1+x}, \tag{4.61}$$

$$f_1^{10\star} = \left(\frac{\omega_1^\star}{\omega_2^\star} - \frac{1}{1+x}\right)e^{10\star} + \frac{\omega_1^\star}{\omega_2^\star}\frac{1}{1+x} - \frac{1}{1+x}, \tag{4.62}$$

$$f_1^{1\star} = \frac{x}{1+x}e^{1\star} - e^{10\star} - \frac{1}{1+x}, \tag{4.63}$$

$$f_2^{10\star} = \frac{x}{1+x}e^{10\star} + \frac{\omega_1^\star}{\omega_2^\star}\frac{1}{1+x} - \frac{1}{1+x}, \tag{4.64}$$

$$f_2^{1\star} = \frac{x}{1+x}e^{1\star} - \frac{1}{1+x}. \tag{4.65}$$

By now, we have considered all possible cases of values m and n that may appear when one looks for the parameters of the release rate that guarantee that (4.36) holds for all allowed configurations. Thus, we may summarize in the following lemma.

Lemma 4.2. *If the constraints* (4.43)–(4.47) *and* (4.57)–(4.65) *are satisfied, then equation* (4.36) *holds for all configurations.*

Remark 4.1. *One has $d^{100\star} = e^{100\star} = 0$, so that the interaction range is not larger than 2.*

Remark 4.2. *From the fact that $d^{10\star} = e^{10\star}$ one concludes that the influence on RNAP i executed by its leftmost neighbor with the front site at position $x_i - 2$ does not depend on whether the RNAP has a neighbor at the position $x_i + 1$.*

Since one requires that $d^{100\star} = e^{100\star}$ holds in order to ensure the stationarity, we shall rewrite here the translocation rate in the form that is shorter than that of (4.1). This will facilitate the forthcoming analysis. Note, however, that the release rate (4.2) is the kept unchanged. The translocation rate $\omega_i(\boldsymbol{\eta})$ is of the form

$$\omega_i(\boldsymbol{\eta}) = \delta_{s_i,1}(w_i^1(\boldsymbol{\eta}) + w_i^2(\boldsymbol{\eta})) \tag{4.66}$$

where

- $w_i^1(\boldsymbol{\eta}) = \omega_1^\star(1 + d^{1\star}\delta_{x_i,x_{i-1}+\ell} + d^{10\star}\delta_{x_i,x_{i-1}+\ell+1})(1 - \delta_{x_{i+1},x_i+\ell})\delta_{x_{i+1},x_i+\ell+1}$;
- $w_i^2(\boldsymbol{\eta}) = \omega_2^\star(1 + e^{1\star}\delta_{x_i,x_{i-1}+\ell} + e^{10\star}\delta_{x_i,x_{i-1}+\ell+1})(1 - \delta_{x_{i+1},x_i+\ell})(1 - \delta_{x_{i+1},x_i+\ell+1})$.

Notice that the constraints (4.43)–(4.47) and (4.57)–(4.65) must be satisfied in order to ensure the stationarity. Taking this fact into account and using Lemmas 4.1 and 4.2 we obtain Theorem 1.2. It is reformulated below:

Theorem 4.1. *For the process defined in this chapter, the following conditions*

$$d^{10\star} = e^{10\star}, \tag{4.67}$$

$$d^{1\star} = \frac{\omega_2^\star}{\omega_1^\star}(e^{1\star} - e^{10\star}), \tag{4.68}$$

together with conditions (4.58)–(4.65) *upon its dynamics rates* (4.66) *and* (4.2) *are sufficient for its stationary distribution to be of the form* (4.4). *In this case, the stationary distribution acquires the following expression*

$$\hat{\pi}(\boldsymbol{\eta}) = \frac{1}{Z_L}\left(\frac{\omega_2^\star}{\kappa^\star}\right)^{\sum_{i=1}^{N} -3/2+s_i}\left(\frac{\omega_2^\star}{\omega_1^\star}(1+e^{1\star})(1+e^{10\star})\right)^{-\sum_{i=1}^{N}\delta_{x_{i+1},x_i+\ell}^L}$$

$$\times (1 + e^{10\star})^{-\sum_{i=1}^{N} \delta^L_{x_{i+1}, x_i + \ell + 1}}, \tag{4.69}$$

where Z_L is the partition function.

4.3   Properties of RNAP model

In this section, we shall work with the grand-canonical ensemble of the headway process defined by (4.70) below; this is sensible because the sum of headways $\sum_{i=1}^{N} m_i$ is conserved.

$$\tilde{\pi}_{gc}(\boldsymbol{\zeta}) = \frac{1}{Z_{gc}} \prod_{i=i}^{N} \left(x^{-3/2 + s_i} y_1^{-\theta_i^0} y_2^{-\theta_i^1} z^{m_i} \right) \tag{4.70}$$

where $Z_{gc} = (Z_1 Z_2)^N$ with

$$Z_1 = \frac{(y_2 + y_1 z)(1 - z) + y_1 y_2 z^2}{y_1 y_2 z}, \quad Z_2 = x^{1/2} + x^{-1/2}. \tag{4.71}$$

We shall show that the grand-canonical ensemble is well-defined in the sense that one can always select a value of fugacity z for a given density of RNAP such that $Z_{gc} < \infty$ which amounts to the task of finding an appropriate value of z in the interval $[0, 1)$.

4.3.1   Mean headway

Lemma 4.3. *The stationary mean headway of the process is the following*

$$\langle m_i \rangle = \frac{y_1 z (1 - z)^2 + y_1 y_2 (2z^2 - z^3)}{(y_2 + y_1 z)(1 - z)^2 + y_1 y_2 z^2 (1 - z)}. \tag{4.72}$$

Proof. From grand-canonical distribution (4.70) one can obtains the mean headway. Namely, for $i = 1, ..., N$, one has

$$\langle m_i \rangle = \sum_{\boldsymbol{\zeta}} m_i \tilde{\pi}_{gc}(\boldsymbol{\zeta})$$

$$= \sum_{\boldsymbol{\zeta}} m_i \frac{1}{Z_{gc}} \prod_{j=1}^{N} (x^{-3/2 + s_j} y_1^{-\theta_j^0} y_2^{-\theta_j^1} z^{m_j})$$

$$= \frac{z}{Z_{gc}} \sum_{\boldsymbol{\zeta}} \prod_{j=1, j \neq i}^{N} (x^{-3/2 + s_j} y_1^{-\theta_j^0} y_2^{-\theta_j^1} z^{m_j})(x^{-3/2 + s_i} y_1^{-\theta_i^0} y_2^{-\theta_i^1})(m_i z^{m_i - 1})$$

$$= \frac{z}{Z_{gc}} \sum_{\boldsymbol{\zeta}} \prod_{j=1, j \neq i}^{N} (x^{-3/2 + s_j} y_1^{-\theta_j^0} y_2^{-\theta_j^1} z^{m_j})(x^{-3/2 + s_i} y_1^{-\theta_i^0} y_2^{-\theta_i^1})(z^{m_i})'.$$

Due to translation invariance, one has $\langle m_1 \rangle = \cdots = \langle m_N \rangle$ which implies

$$N \langle m_i \rangle = \frac{z}{Z_{gc}} \sum_{i=1}^{N} \sum_{\zeta} \prod_{j=1, j \neq i}^{N} (x^{-3/2+s_j} y_1^{-\theta_j^0} y_2^{-\theta_j^1} z^{m_j})(x^{-3/2+s_i} y_1^{-\theta_i^0} y_2^{-\theta_i^1})(z^{m_i})'.$$

Notice that

$$\sum_{i=1}^{N} \sum_{\zeta} \prod_{j=1, j \neq i}^{N} (x^{-3/2+s_j} y_1^{-\theta_j^0} y_2^{-\theta_j^1} z^{m_j})(x^{-3/2+s_i} y_1^{-\theta_i^0} y_2^{-\theta_i^1})(z^{m_i})' = (Z_{gc})'_z.$$

Therefore,

$$\langle m_i \rangle = \frac{1}{N} z \frac{\mathrm{d}}{\mathrm{d}z} \ln Z_{gc}, \tag{4.73}$$

which yields

$$\langle m_i \rangle = \frac{y_1 z(1-z)^2 + y_1 y_2 (2z^2 - z^3)}{(y_2 + y_1 z)(1-z)^2 + y_1 y_2 z^2 (1-z)}. \tag{4.74}$$

The proof is complete.   □

Lemma 4.4. *The grand canonical ensemble (4.70) is well-defined.*

Proof. On the one hand, one has (4.72) as the expression for the mean headway. On the other hand, this is the mean available empty space on the lattice $L - \ell N$ per rod which gives

$$\langle m_i \rangle = \frac{L - \ell N}{N} = \frac{1}{\rho} - \ell, \tag{4.75}$$

where $\rho = \dfrac{N}{L}$ is the RNAP density.

Comparing (4.72) and (4.75) gives us the auxiliary variable z which is the solution of the following equation

$$\frac{y_1 z(1-z)^2 + y_1 y_2 (2z^2 - z^3)}{(y_2 + y_1 z)(1-z)^2 + y_1 y_2 z^2 (1-z)} = \frac{1}{\rho} - \ell \tag{4.76}$$

We shall now prove that above equation has a solution $0 \leq z < 1$. We set that

$$f(z) = \frac{y_1 z(1-z)^2 + y_1 y_2 (2z^2 - z^3)}{(y_2 + y_1 z)(1-z)^2 + y_1 y_2 z^2 (1-z)} - \left(\frac{1}{\rho} - \ell \right). \tag{4.77}$$

Notice that the model allows for a number density in the range $0 < \rho \leq 1/\ell$ which implies that $f(0) f(1^-) < 0$. Thus, (4.76) has a solution belonging to $(0, 1)$ which implies that the grand-canonical ensemble is well-defined, when z is equal to that solution. The proof is complete.   □

Remark 4.3. *Since given RNAP density ρ, one can find the fugacity z that solves the equation*

(4.76) *then z is as a function of ρ, y_1, y_2. It is, however, difficult to find the close-form solution for z. Consequently, we shall use the numerical methods. This is how all the graphs of the present chapter will be obtained.*

4.3.2   Average excess and dwell time

Recall the average excess density

$$\sigma = \frac{\langle N^1 \rangle - \langle N^2 \rangle}{L} \tag{4.78}$$

of RNAPs without a PP_i over RNAPs with PP_i bound to them. From the grand-canonical stationary distribution (4.70) one obtains

$$\sigma = -\frac{k_B T}{L} \frac{\mathrm{d}}{\mathrm{d}\lambda} \ln Z_{gc} = \frac{1-x}{1+x}\rho. \tag{4.79}$$

One can see that the result above is the same as in (3.85). This coincidence is not surprising, since the invariant generalized Ising measure (4.4) factorizes into two factors, one being responsible for presence/absence of PP_I's, and the other one being similar to the Boltzmann factor (3.7).

For the densities of RNAPs in each of two states

$$\rho^\alpha := \langle \delta_{s_i,\alpha} \rangle = \frac{1}{L}\langle N^\alpha \rangle \tag{4.80}$$

one gets

$$\rho^1 = \frac{1}{1+x}\rho, \qquad \rho^2 = \frac{x}{1+x}\rho. \tag{4.81}$$

and one also gets dwell times $\tau^\alpha = \rho^\alpha/\rho$ that a RNAP spends in the state 1 and the state 2:

$$\tau^1 = \frac{1}{1+x}, \quad \tau^2 = \frac{x}{1+x}. \tag{4.82}$$

Next, employing the stationarity and noting that it requires that $x = \frac{\omega_2^\star}{\kappa}$ in (4.57), we arrive at the following balance equation

$$\frac{\rho^1}{\rho^2} = \frac{\tau^1}{\tau^2} = \frac{\kappa^\star}{\omega_2^\star} \tag{4.83}$$

which expresses the ensemble ratio in terms of the single-RNAP translocation rate $\omega_2^\star$ and the single-RNAP PP_i release rate $\kappa^\star$.

4.3.3 RNAP headway distribution

Denote by $P_h(r)$ the distribution of the headway between the front of a trailing rod i and the back of a leading rod $i+1$. It means $P_h(r) = \dfrac{1}{\rho} \left\langle \delta_{x_{i+1}-x_i-\ell, r} \right\rangle = \langle \theta_i^r \rangle, r \in \mathbb{N}$ where $\mathbb{N} = \{0, 1, 2...\}$ is the natural number set.

Lemma 4.5. *The distribution of the headway of the process is the following*

$$P_h(r) = \begin{cases} \dfrac{y_2(1-z)}{(y_2 + y_1 z)(1-z) + y_1 y_2 z^2} & \text{for } r = 0, \\[3mm] \dfrac{y_1 z(1-z)}{(y_2 + y_1 z)(1-z) + y_1 y_2 z^2} & \text{for } r = 1, \\[3mm] \dfrac{y_1 y_2 z^r(1-z)}{(y_2 + y_1 z)(1-z) + y_1 y_2 z^2} & \text{for } r \geq 2. \end{cases} \tag{4.84}$$

Proof. Denote by $\boldsymbol{\zeta} = (\zeta_1, ..., \zeta_N)$ the configuration of RNAPs and let $f = Z_1 Z_2$. For $r = 0, 1$, one gets

$$\langle \theta_i^r \rangle = \sum_{\boldsymbol{\zeta}} \theta_i^r \tilde{\pi}_{gc}(\boldsymbol{\zeta})$$

$$= \frac{1}{Z_{gc}} \sum_{\boldsymbol{\zeta}} \theta_i^r \prod_{j=1}^{N} (x^{-3/2+s_j} y_1^{-\theta_j^0} y_2^{-\theta_j^1} z^{m_j})$$

$$= \frac{1}{Z_{gc}} \sum_{\zeta_1} \cdots \sum_{\zeta_N} \theta_i^r \prod_{j=1}^{N} (x^{-3/2+s_j} y_1^{-\theta_j^0} y_2^{-\theta_j^1} z^{m_j})$$

$$= \frac{1}{f^N} \sum_{\zeta_1} \cdots \sum_{\zeta_N} \theta_i^r \prod_{j=1}^{N} (x^{-3/2+s_j} y_1^{-\theta_j^0} y_2^{-\theta_j^1} z^{m_j})$$

$$= \prod_{j=1, j \neq i}^{N} \left(\frac{1}{f} \sum_{\zeta_j} x^{-3/2+s_j} y_1^{-\theta_j^0} y_2^{-\theta_j^1} z^{m_j} \right) \left(\frac{1}{f} \sum_{\zeta_i} \theta_i^r x^{-3/2+s_i} y_1^{-\theta_i^0} y_2^{-\theta_i^1} z^{m_i} \right).$$

One has here that

$$\frac{1}{f} \sum_{\zeta_j} x^{-3/2+s_j} y_1^{-\theta_j^0} y_2^{-\theta_j^1} z^{m_j} = 1, \text{ for all } j. \tag{4.85}$$

and

$$\frac{1}{f} \sum_{\zeta_i} \theta_i^r x^{-3/2+s_i} y_1^{-\theta_i^0} y_2^{-\theta_i^1} z^{m_i} = \frac{1}{f} \left(-y_{r+1} \frac{d}{dy_{r+1}} \right) \sum_{\zeta_i} x^{-3/2+s_i} y_1^{-\theta_i^0} y_2^{-\theta_i^1} z^{m_i}$$

$$= -y_{r+1} \frac{1}{f} \frac{d}{dy_{r+1}} f.$$

Hence,

$$\langle \theta_i^0 \rangle = \frac{y_2(1-z)}{(y_2 + y_1 z)(1-z) + y_1 y_2 z^2} \tag{4.86}$$

$$\langle \theta_i^1 \rangle = \frac{y_1 z(1-z)}{(y_2 + y_1 z)(1-z) + y_1 y_2 z^2}. \tag{4.87}$$

Next, we compute $\langle \theta_i^r \rangle$ for $r \geq 2$.

$$\langle \theta_i^r \rangle = \sum_{\zeta} \theta_i^r(\zeta)\tilde{\pi}_{gc}(\zeta)$$

$$= \frac{1}{Z_{gc}} \sum_{\zeta} \theta_i^r \prod_{j=1}^{N} (x^{-3/2+s_j} y_1^{-\theta_j^0} y_2^{-\theta_j^1} z^{m_j})$$

$$= \frac{1}{Z_{gc}} \sum_{\zeta_1} \cdots \sum_{\zeta_N} \theta_i^r \prod_{j=1}^{N} (x^{-3/2+s_j} y_1^{-\theta_j^0} y_2^{-\theta_j^1} z^{m_j})$$

$$= \frac{1}{f^N} \sum_{\zeta_1} \cdots \sum_{\zeta_N} \theta_i^r \prod_{j=1}^{N} (x^{-3/2+s_j} y_1^{-\theta_j^0} y_2^{-\theta_j^1} z^{m_j})$$

$$= \prod_{j=1,j\neq i}^{N} \left(\frac{1}{f} \sum_{\zeta_j} x^{-3/2+s_j} y_1^{-\theta_j^0} y_2^{-\theta_j^1} z^{m_j} \right) \left(\frac{1}{f} \sum_{\zeta_i} \theta_i^r x^{-3/2+s_i} y_1^{-\theta_i^0} y_2^{-\theta_i^1} z^{m_i} \right).$$

Using again identity (4.85) and noticing that $\theta_i^r = 1$ implies $\theta_i^k = 0$ for $k = 0, 1$ and $z^{m_i} = z^r$, we get that

$$\langle \theta_i^r \rangle = \frac{1}{f} \sum_{\zeta_i} \theta_i^r x^{-3/2+s_i} y_1^{-\theta_i^0} y_2^{-\theta_i^1} z^{m_i} \tag{4.88}$$

$$= \frac{1}{f} z^r \sum_{\zeta_i} x^{-3/2+s_i}. \tag{4.89}$$

Finally, one notices that

$$\sum_{\zeta_i} x^{-3/2+s_i} = x^{-1/2} + x^{1/2}. \tag{4.90}$$

Hence,

$$\langle \theta_i^r \rangle = \frac{y_1 y_2 z^r (1-z)}{(y_2 + y_1 z)(1-z) + y_1 y_2 z^2}. \tag{4.91}$$

By the computations above, one obtains

$$
P_h(r) = \begin{cases}
\dfrac{y_2(1-z)}{(y_2+y_1z)(1-z)+y_1y_2z^2} & \text{for } r=0, \\[2ex]
\dfrac{y_1z(1-z)}{(y_2+y_1z)(1-z)+y_1y_2z^2} & \text{for } r=1, \\[2ex]
\dfrac{y_1y_2z^r(1-z)}{(y_2+y_1z)(1-z)+y_1y_2z^2} & \text{for } r\geq 2.
\end{cases}
\tag{4.92}
$$

This completes the proof. $\qquad\qquad\qquad\qquad\qquad\qquad\qquad\qquad\qquad\qquad\qquad\qquad\square$

Let us plot the headway distribution $P_h(r)$ for $\ell = 5, \rho = 0.15$ and certain specific choices of parameters J_1, J_2.

– The fully repulsive case: $J_1 > J_2 > 0$, see Fig. (4.3).

Figure 4.3: *RNAP headway distribution $P_h(r)$ for the full repulsive case for different interaction strengths y_1, y_2 (y-axis). x-axis is the integer lattice distance. The lines joining the data points are just guides to the eye.*

– Lennard Jones potential: $J_1 > 0, J_2 < 0$ such that $|J_2| < J_1$, see Fig. (4.4).
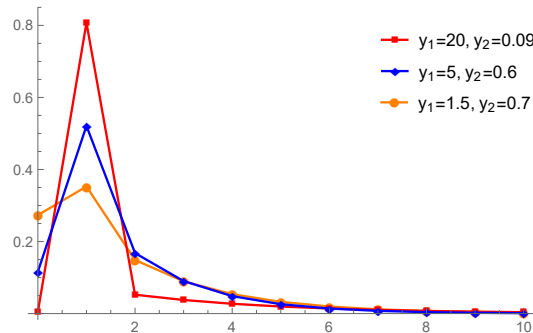
Figure 4.4: *RNAP headway distribution $P_h(r)$ for Lennard Jones potential case for different interaction strengths y_1, y_2 (y-axis). x-axis is the integer lattice distance. The lines joining the data points are just guides to the eye.*

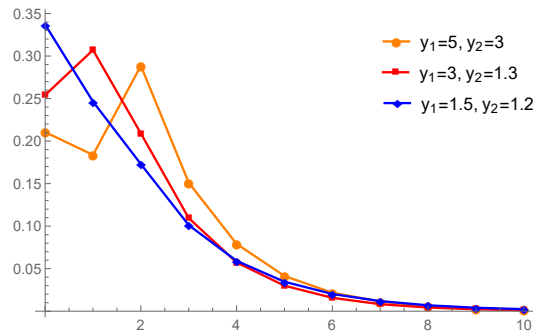**– DLVO theory:** $J_2 > 0$ such that $J_2 > |J_1|$, see Fig. (4.5).
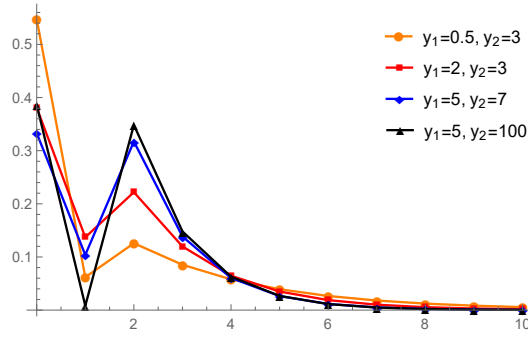
Figure 4.5: *RNAP headway distribution $P_h(r)$ for the DLVO theory case for different interaction strengths y_1, y_2 (y-axis). x-axis is the integer lattice distance. The lines joining the data points are just guides to the eye.*

Remark 4.4. *From the headway distribution (4.84), taking into account that $0 \leq z < 1$, one has that $P_h(r)$ is decreasing when $r \geq 2$. As for $P_h(0)$ and $P_h(1)$, it is clear that they depend on the value of y_1 and y_2. It is also clear from (4.84) that in the case of Lennard Jones potential one has $P_h(0) < P_h(1)$ and in the DLOV theory case one has $P_h(0) > P_h(1)$.*

4.3.4 Elongation rate

Mean velocity of a single isolated RNAP: From the work of Wang et al [32] one can compute the mean velocity of a single isolated RNAP as follows

$$\nu^\star = \frac{\omega_2^\star \kappa^\star}{\omega_2^\star + \kappa^\star} = \frac{1}{1+x}\omega_2^\star. \tag{4.93}$$

The expression (4.93) differs from the expression $\nu_0^\star = \omega_2^\star$ that is valid for a simple random walk by prefactor $\dfrac{1}{1+x}$ which is the average time spent in the mobile state 1.

Average velocity and flux: As in paper [4], the total elongation rate is the stationary RNAP flux j which is defined as the average number of RNAP translocation per second and per base-pair. Besides the average flux j, the average speed ν of an RNAP is also a measure of the average elongation rate which is related to j by

$$j = \rho\nu \tag{4.94}$$

The average flux j is the expectation of translocation rate $\omega_i(\boldsymbol{\eta})$ taken with respect to the stationary distribution (4.4). Using the factorization property of the stationary distribution, we get that

$$
\begin{aligned}
j = \rho^1 \langle \omega_1^\star (1 + \frac{\omega_2^\star}{\omega_1^\star}(e^{1\star} - e^{10\star})\theta_{i-1}^0 + e^{10\star}\theta_{i-1}^1)(1 - \theta_i^0)\theta_i^1 \\
+ \omega_2^\star(1 + e^{1\star}\theta_{i-1}^0 + e^{10\star}\theta_{i-1}^1)(1 - \theta_i^0)(1 - \theta_i^1)\rangle \\
= \frac{1}{1+x}\omega_2^\star\left(\frac{\omega_1^\star}{\omega_2^\star} - 1 - e^{10\star}\langle\theta_{i-1}^0\rangle\right)(1 - \langle\theta_i^0\rangle)\langle\theta_i^1\rangle + (1 + e^{1\star}\langle\theta_{i-1}^0\rangle + e^{10\star}\langle\theta_{i-1}^1\rangle)(1 - \langle\theta_i^0\rangle).
\end{aligned}
\tag{4.95}
$$

Since the fugacity z is a function of ρ, y_1, y_2, one obtains

$$\nu = A\left(\frac{\omega_1^\star}{\omega_2^\star}, y_1, y_2, \rho\right)\nu^\star, \tag{4.96}$$

where

$$A\left(\frac{\omega_1^\star}{\omega_2^\star}, y_1, y_2, \rho\right) = \left(\frac{\omega_1^\star}{\omega_2^\star} - 1 - e^{10\star}\langle\theta_{i-1}^0\rangle\right)(1-\langle\theta_i^0\rangle)\langle\theta_i^1\rangle + (1+e^{1\star}\langle\theta_{i-1}^0\rangle + e^{10\star}\langle\theta_{i-1}^1\rangle)(1-\langle\theta_i^0\rangle). \tag{4.97}$$

which is the average RNAP velocity amplitude. Hence, the average RNAP flux amplitude is $\rho A\left(\frac{\omega_1^\star}{\omega_2^\star}, y_1, y_2, \rho\right)$.

Below, we present some plots of average RNAP velocity and flux amplitudes.

– Fully repulsive case: $J_1 > J_2 > 0$. See Fig. 4.6, 4.7, and 4.8 for the cases when y_2 is "small", and Fig. 4.9, 4.10, and 4.11 for the cases when y_2 is "large".

(a) *RNAP velocity amplitude* (b) *RNAP flux amplitude*

Figure 4.6: *Average RNAP velocity and flux amplitudes for the interaction strengths values $y_1 = 1.5, y_2 = 1.2$. Curves from top to bottom correspond to the values $\omega_1^\star/\omega_2^\star$: 0.95, 0.7, 0.3. The dotted reference line corresponds to non-interacting RNAPs.*

(a) *RNAP velocity amplitude*   (b) *RNAP flux amplitude*

Figure 4.7: *Average RNAP velocity and flux amplitudes for the interaction strengths values $y_1 = 5, y_2 = 1.2$. Curves from top to bottom correspond to the values $\omega_1^\star/\omega_2^\star$: 0.95, 0.7, 0.3, 0.1. The dotted reference line corresponds to non-interacting RNAPs.*

(a) *RNAP velocity amplitude*   (b) *RNAP flux amplitude*

Figure 4.8: *Average RNAP velocity and flux amplitudes for the interaction strengths values $y_1 = 100, y_2 = 1.2$. Curves from top to bottom correspond to the values $\omega_1^\star/\omega_2^\star$: 0.95, 0.7, 0.3, 0.1. The dotted reference line corresponds to non-interacting RNAPs.*

(a) *Average velocity v*   (b) *Average flux j*

Figure 4.9: *Average RNAP velocity and flux amplitudes for the interaction strengths values $y_1 = 5, y_2 = 3$. Curves from top to bottom correspond to the values $\omega_1^\star/\omega_2^\star$: 0.95, 0.7, 0.3. The dotted reference line corresponds to non-interacting RNAPs.*

(a) *Average velocity* v (b) *Average flux* j

Figure 4.10: *Average RNAP velocity and flux amplitudes for the interaction strengths values* $y_1 = 20, y_2 = 3$. *Curves from top to bottom correspond to the values* $\omega_1^\star/\omega_2^\star$: *0.95, 0.7, 0.3, 0.1. The dotted reference line corresponds to non-interacting RNAPs.*

(a) *Average velocity* v (b) *Average flux* j

Figure 4.11: *Average RNAP velocity and flux amplitudes for the interaction strengths values* $y_1 = 100, y_2 = 3$. *Curves from top to bottom with correspond to the values* $\omega_1^\star/\omega_2^\star$: *0.7, 0.3, 0.1. The dotted reference line corresponds to non-interacting RNAPs.*

– Lennard Jones potential : $J_1 > 0, J_2 < 0$ such that $|J_2| < J_1$.

(a) *RNAP velocity amplitude*   (b) *RNAP flux amplitude*

Figure 4.12: *Average RNAP velocity and flux amplitudes for the interaction strengths values* $y_1 = 1.2, y_2 = 0.85$. *Curves from top to bottom correspond to the values* $\omega_1^\star/\omega_2^\star$: *5, 0.9, 0.1. The dotted reference line corresponds to non-interacting RNAPs.*

(a) *RNAP velocity amplitude*   (b) *RNAP flux amplitude*

Figure 4.13: *Average RNAP velocity and flux amplitudes for the interaction strengths values $y_1 = 100, y_2 = 0.85$. Curves from top to bottom correspond to $\omega_1^\star/\omega_2^\star$: 0.6, 0.1, 0.05, 0.01. The dotted reference line corresponds to non-interacting RNAPs.*

(a) *RNAP velocity amplitude*   (b) *RNAP flux amplitude*

Figure 4.14: *Average RNAP velocity and flux amplitudes for the interaction strengths values $y_1 = 5, y_2 = 0.2$. Curves from top to bottom correspond to the values $\omega_1^\star/\omega_2^\star$: 0.9, 0.5, 0.2. The dotted reference line corresponds to non-interacting RNAPs.*

– DLVO theory: $J_2 > 0$ such that $J_2 > |J_1|$.

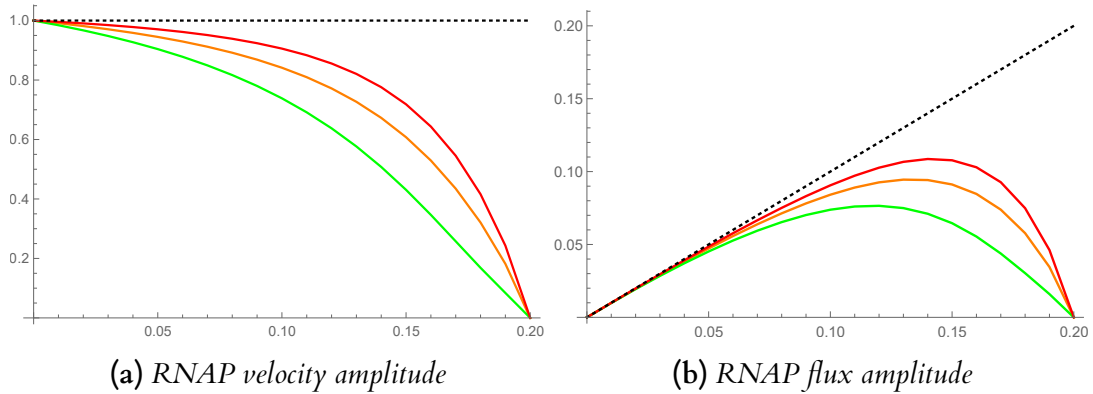(a) *RNAP velocity amplitude*   (b) *Average flux j*
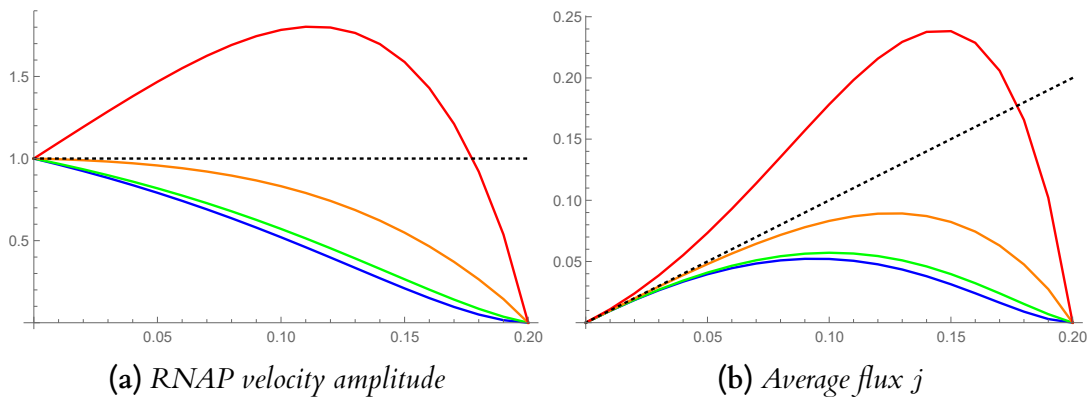
Figure 4.15: *Average RNAP velocity and flux amplitudes for the interaction strengths values $y_1 = 0.5, y_2 = 3$. Curves from top to bottom correspond to the values $\omega_1^\star/\omega_2^\star$: 20, 5, 0.9, 0.1. The dotted reference line corresponds to non-interacting RNAPs.*

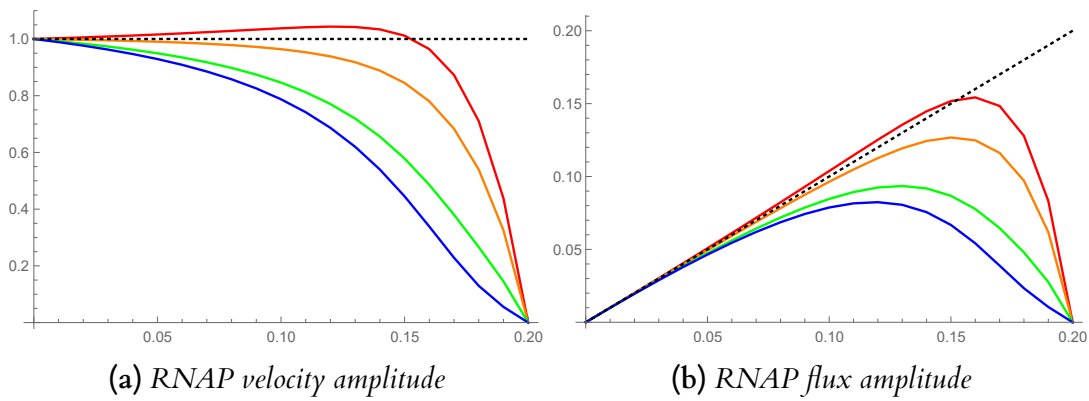(a) *RNAP velocity amplitude*   (b) *Average flux j*
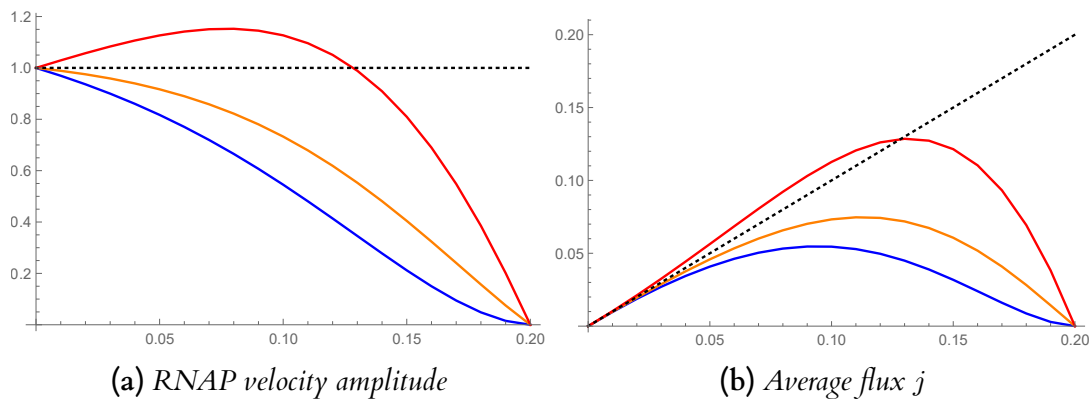
Figure 4.16: *Average RNAP velocity and flux amplitudes for the interaction strengths values* $y_1 = 0.5, y_2 = 100$. *Curves from top to bottom correspond to the values* $\omega_1^\star/\omega_2^\star$: *300, 100, 5. The dotted reference line corresponds to non–interacting RNAPs.*

(a) *RNAP velocity amplitude*   (b) *Average flux j*
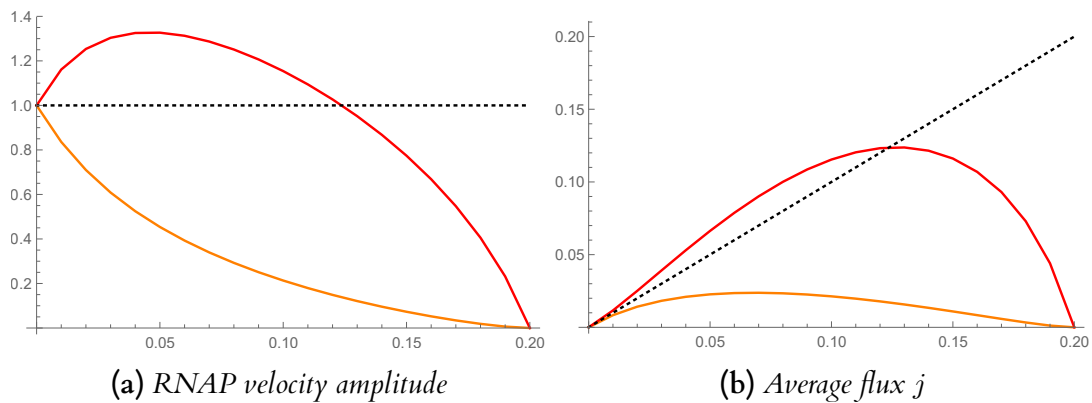
Figure 4.17: *Average RNAP velocity and flux amplitudes for the interaction strengths values* $y_1 = 0.1, y_2 = 1000$. *Curves from top to bottom correspond to the values* $\omega_1^\star/\omega_2^\star$: *20000, 5. The dotted reference line corresponds to non–interacting RNAPs.*

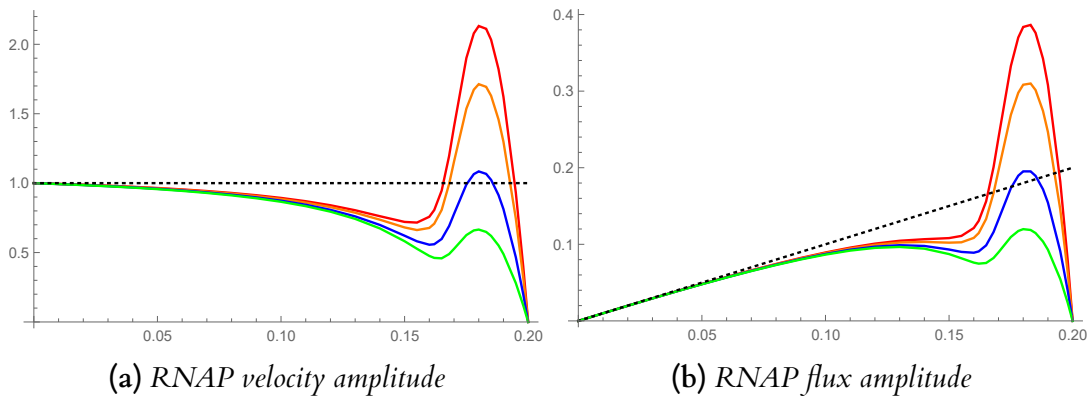(a) *RNAP velocity amplitude*   (b) *Average flux j*
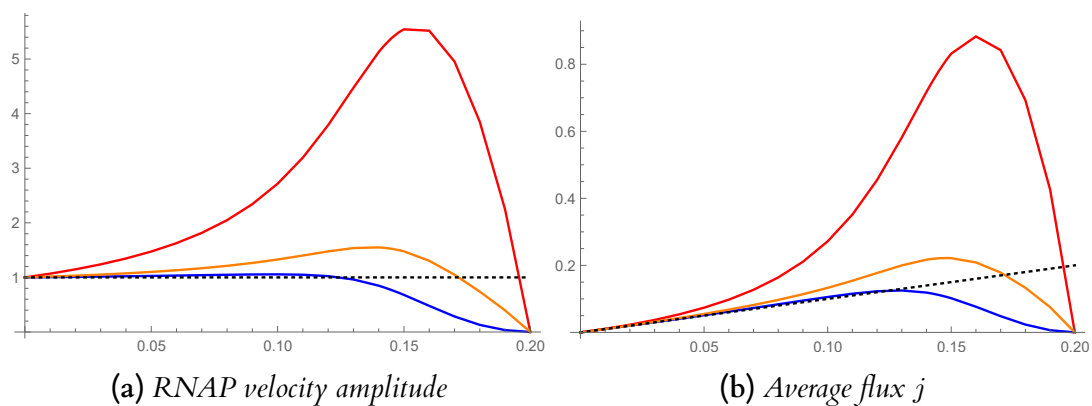
Figure 4.18: *Average RNAP velocity and flux amplitudes for the interaction strengths values* $y_1 = 5, y_2 = 10$. *Curves from top to bottom correspond to the values* $\omega_1^\star/\omega_2^\star$: *30,5,0.1. The dotted reference line corresponds to non–interacting RNAPs.*

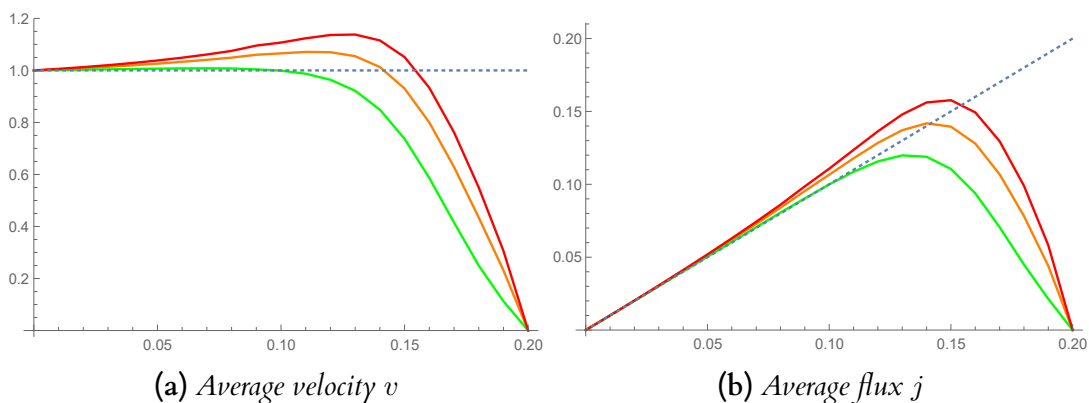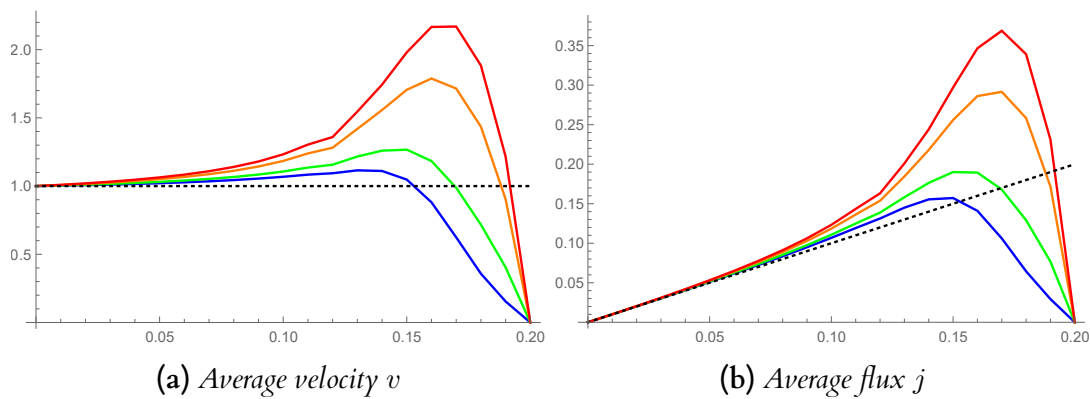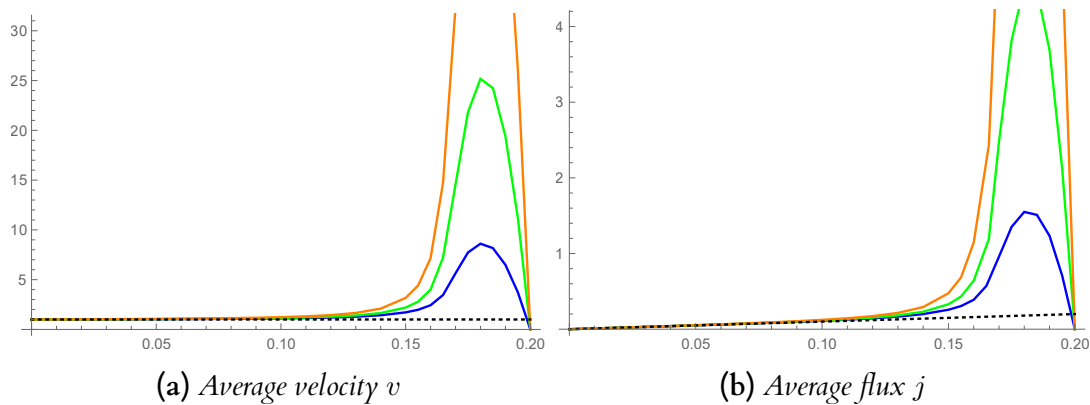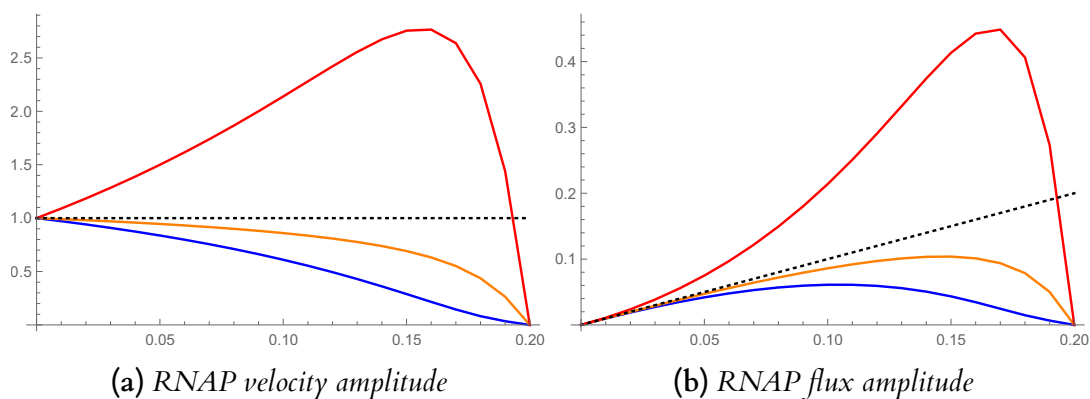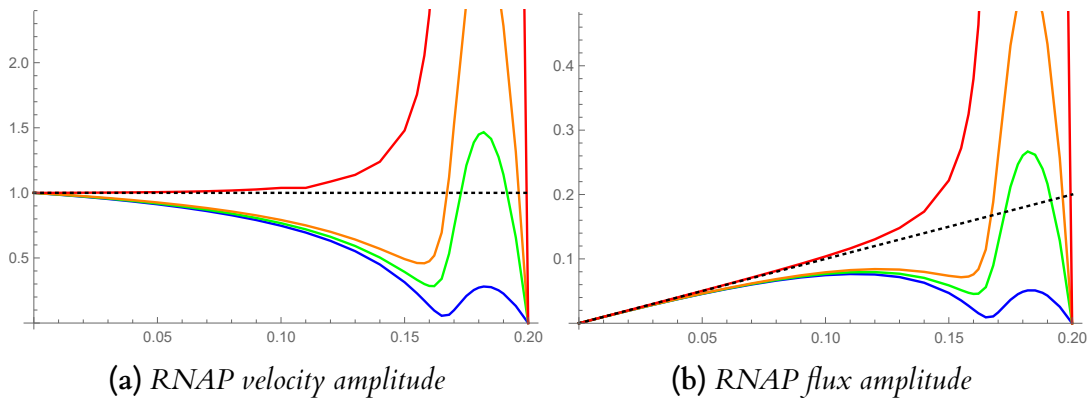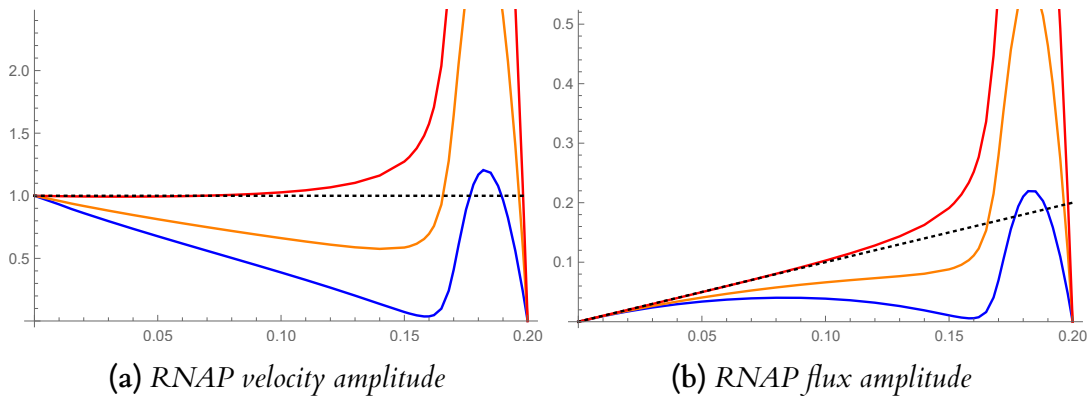(a) *RNAP velocity amplitude*   (b) *Average flux j*
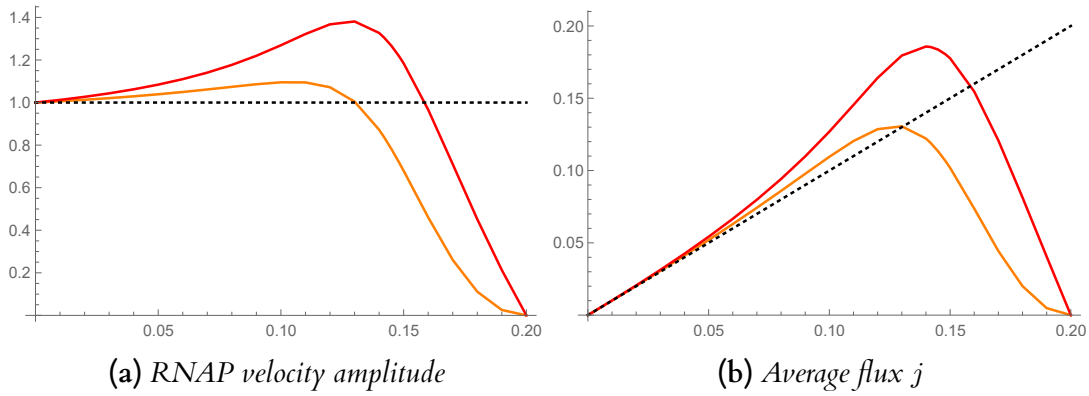
Figure 4.19: *Average RNAP velocity and flux amplitudes for the interaction strengths values $y_1 = 5, y_2 = 100$. Curves from top to bottom correspond to the values $\omega_1^\star/\omega_2^\star$: 30, 0.1. The dotted reference line corresponds to non-interacting RNAPs.*

4.4 Discussion

4.4.1 Stochastic pushing, blocking, and attraction

Let us consider three situations regarding the translocation rate $\omega_i(\boldsymbol{\eta})$ of i-th of a RNAP that is at the state 1. Depending on the position of its leading RNAP, i.e., depending on distance m_i, the translocation rate can be determined as follows. Corresponding to $m_i = 1$ or $m_i > 1$ respectively, we have that if $m_{i-1} > 2$ then $\omega_i(\boldsymbol{\eta}) = w_1^\star$ or $\omega_i(\boldsymbol{\eta}) = w_2^\star$, while if $m_{i-1} = 2$ then $\omega_i(\boldsymbol{\eta}) = w_1^\star(1 + e^{10\star}) = w_1^\star y_2$ or $\omega_i(\boldsymbol{\eta}) = w_2^\star(1 + e^{10\star}) = w_2^\star y_2$, and, finally, if $m_{i-1} = 1$ then $\omega_i(\boldsymbol{\eta}) = w_1^\star(1 + d^{1\star}) = w_1^\star(1 + y_1/y_2 - w_2^\star y_2/w_1^\star)$ or $\omega_i(\boldsymbol{\eta}) = w_2^\star(1 + e^{1\star}) = w_1^\star y_1/y_2$.

Depending on static interaction strengths y_1, y_2, the left neighbor can cause attractive or repulsive effects on the leading RNAP. This means, for example, that if the leftmost neighbor of RNAP i is at distance 1 (i.e., $m_{i-1} = 1$) then the translocation takes place with the rate $\omega_1 y_2$ or $\omega_2 y_2$. Thus, if $y_2 > 1$ then a so-called "pushing" takes place that means the RNAP i moves away from its leftmost neighbor faster than it were if there had not been this neighbor. If $y_2 < 1$ then an attraction takes place that means the RNAP i moves away from its leftmost neighbor slower compared to the speed/rate of an isolated RNAP. In the same fashion, one can explain the effects on RNAP acceleration or dis-acceleration caused by the RNAP to which it approaches.

The case

$$\begin{cases} w_1^\star(1 + d^{1\star}) > w_1^\star(1 + e^{10\star}) > \omega_1^\star, \\ w_2^\star(1 + e^{1\star}) > w_2^\star(1 + e^{10\star}) > \omega_2^\star, \end{cases} \tag{4.98}$$

which is equivalent to

$$\begin{cases} d^{1\star} > e^{10\star} > 0, \\ e^{1\star} > e^{10\star} > 0, \end{cases} \tag{4.99}$$

is referred to as *fully stochastic pushing* since (in this specific range of the interaction parameters) the rate at which an RNAP distances apart from its trailing neighbor increases when the distance between them decreases. We will refer to the case $e^{10\star} > 0$ as "next-nearest stochastic pushing" and to the case $d^{1\star} > 0, e^{1\star} > 0$ as "nearest stochastic pushing".

The case

$$\begin{cases} \omega_1^\star < \omega_2^\star, \\ w_1^\star(1 + e^{10\star}) < w_2^\star(1 + e^{10\star}), \\ w_1^\star(1 + d^{1\star}) < w_2^\star(1 + e^{1\star}), \end{cases} \tag{4.100}$$

which is equivalent to

$$\begin{cases} \omega_1^\star < \omega_2^\star, \\ w_1^\star(1 + d^{1\star}) < w_2^\star(1 + e^{1\star}), \end{cases} \tag{4.101}$$

will be referred to as *fully stochastic blocking enhancement* or simply *jamming* since in this range of the interaction parameters, the rate at which an RNAP approaches its right neighbor is reduced compared to the rate of the motion on "free road ahead". We will call the case $\omega_1^\star < \omega_2^\star$ *stochastic blocking* and call the ratio $\omega_1^\star/\omega_2^\star$ *strength of blocking*. For example, we will say that the blocking is very strong, if the ratio is close to 0. Especially, in the fully repulsive case, we will say that the blocking is weak, if the ratio is close to but less than 1.

One notices that the totally stochastic blocking only happens in the fully repulsive case (in all three cases considered here). Indeed, in this case one has that $y_1 > y_2 > 1$ (as it follows from (4.46) and (4.47)) which is equivalent to

$$\begin{cases} e^{10\star} > 0, \\ \dfrac{\omega_2^\star}{\omega_1^\star}(1 + e^{1\star}) > 1. \end{cases} \tag{4.102}$$

If stochastic blocking is present, which means $w_1^\star < w_2^\star$, then from conditions (4.102) and (4.68), one can show that

$$w_1^\star(1 + d^{1\star}) < w_2^\star(1 + e^{1\star}), \tag{4.103}$$

thus this choice of parameters satisfies the fully stochastic blocking case.

We now pass to analyse the influence on motion of an RNAP by its left neighbor. Our nomenclature will be similar to the one that we have introduced when we considered the influence of the right neighbor. Namely, we call the case $e^{10\star} < 0$ and $e^{1\star}, d^{1\star} < 0$ (left) *next-nearest* and *nearest stochastic attraction* respectively since it reduces the translocation rate. We call the case $\omega_1^\star/\omega_2^\star > 1$ is (ahead) stochastic attraction. If this case holds then the rate with which an RNAP approaches a paused RNAP increases. We will

say the attraction is weak or strong depending on whether the ratio is close to 1 or significantly larger than 1, respectively.

4.4.2 Cooperative pushing

Let us now discuss the cooperative pushing phenomenon that might occur as it is suggested by the plots of average velocity and flux exhibited in Subsection 4.3.4.

Fully repulsive case: We note that in this case one has $y_1 > y_2 > 1$ and all the plots in the Subsection 4.3.4 for this case we used the blocking strength $\omega_1^\star/\omega_2^\star$ less than 1 (stochastic blocking enhancement is assumed). First, from Fig. 4.6, we see that for the case when the repulsive strengths y_1, y_2 are small, even very weak blocking enhancement does not lead to the cooperative pushing. Fig. 4.7 shows that when repulsive strengths y_1 and y_2 are, respectively, strong and weak then the cooperative pushing occurs only if the blocking enhancement strength is weak.

It is interesting to see what happens when repulsive strengths y_1 is very strong and, at the same time, y_2 is very weak. Fig. 4.8 shows that a new phenomenon appears. It is similar to what has been noticed in [4], but in our case, it is not required that the blocking is too strong. In this case, the cooperative pushing at low RNAP densities is suppressed. Furthermore, the speed of an RNAP has an intermediate minimum at a density ρ_{min} which is outside the range of cooperative pushing. The local minimum deepens when the blocking strength decreases. However, at higher densities there is an entrance to a cooperative regime. After reaching a maximum at a very high density ρ_{max} which is greater than ρ_{min}, the speed and also average elongation rate drop down to zero.

The third scenario is when both repulsive strengths y_1 and y_2 are strong, see Figs. 4.9, 4.10, and 4.11. The cooperative pushing always appears until the jamming takes over, that happens at very high densities. The figures also show that the pushing is not sensitive to the blocking strength $\omega_1^\star/\omega_2^\star$. Furthermore, if y_1 is arbitrarily large then, as Fig. 4.11 shows, at moderate densities the speed is almost the same as it would be in the non–interacting RNAPs case. However at high densities, the speed and also the average elongation rate increase "very fast" until they reach a maximum and drop then down due to steric hard core repulsion.

In general, the interplay between stochastic pushing and blocking contribute to the average elongation rate in a way that is similar to that described in [4].

Lennard Jones potential: In this case one requires $y_2 < y_1, y_2 < 1$. Since $y_2 < 1$ and taking into account (4.47), one deduces that $e^{10\star} < 0$ which means that the next-nearest attraction takes place. If the repulsive strength y_1 is small, see Fig. 4.12, then only at a very large values (greater than 1) of the ratio $\omega_1^\star/\omega_2^\star$ the cooperative pushing will occur. Notice that in the case when the ratio is large, one has $e^{1\star} > 0$ which implies $d^{1\star} > 0$

as well. This means that the nearest pushing takes place. As for the case when $\omega_1^\star/\omega_2^\star$ is less than 1, i.e., when the stochastic blocking occurs, one has $d^{1\star}, e^{1\star} < 0$. Thus, in this case, the translocation rate at which an RNAP approaches a paused RNAP is reduced. The reduction is due to the effective attraction of its trailing RNAP and the blocking of the paused RNAP as well.

If the static repulsion y_1 is large, see Figs. 4.13 and 4.14, then the nearest pushing occurs. Depending on strength of blocking $\omega_1^\star/\omega_2^\star$, one has two situations. First, if the blocking is strong, we get a phenomenon that is similar to the one exhibited in Fig. 4.8. Thus, the cooperative pushing appears at a high density. However, in the fully repulsive case, one does not require the extreme strength of the stochastic blocking as in this case. Second, if the blocking is weak, one recovers the phenomenon similar to that exhibited in Fig. 4.11. Thus, cooperative pushing occurs even at a low density. One recognizes that next-nearest pushing or attraction (indicated by $e^{10\star}$) affects the average elongation rate. Namely, if the case is the pushing then the average elongation is not sensitive to the blocking strength, however, if the case is of the next-nearest attraction, the strength is an important factor that leads cooperative pushing.

DLVO theory: First, we consider the case $y_1 < 1$, see Figs. 4.15, 4.16, and 4.17. They show that only if the ratio $\omega_1^\star/\omega_2^\star$ is big enough (greater than 1), which means the stochastic attraction takes place, then there is possible to have cooperative pushing. Notice that in this case, the next-nearest stochastic pushing takes place since $e^{10\star} > 0$. Depending on the value of ratio $\omega_1^\star/\omega_2^\star$, one has $d^{1\star}, e^{1\star} < 0$, if the ratio is small, and one has $e^{1\star} > 0$, if the ratio is big enough. One recognizes that the former case performs the nearest attraction, meanwhile the latter performs partially nearest pushing, since $d^{1\star}$ can be positive or negative. We conjecture that in this case, a necessary condition for cooperative pushing is $e^{1\star} > 0$. It is interesting to see Fig. 4.17, the case $\omega_1^\star/\omega_2^\star = 5$ ("small"), the average speed (left panel) drops faster than the speed of the model with hard core repulsion along with the decrease of the density. Nevertheless, the average elongation rate still increases at low densities.

Second, we consider the case $y_2 > y_1 > 1$, see Figs. 4.18 and 4.19. The pictures show that the cooperative pushing occurs even at low densities and it is not sensitive to the ratio $\omega_1^\star/\omega_2^\star$. In this case the average speed and also the average elongation rate increase until they reach their respective maxima; after the maximum is achieved, both will drop down due to the traffic jam that takes place at high densities.

4.5   Conclusion

Our model is a generalization of the model proposed by Belistky and Gunter [4] in the sense that we have added the nearest interaction energy to the hard core repulsion and we also added one term that is a o-called next-nearest interaction energy. Moreover, on the microscopic scale, we also widened the range of interaction among

RNAPs. By doing so, one hopes to obtain a more detailed biological description of the mechanochemical cycle of the RNAP during elongation and also of the mutual incorporation of RNAPs on the same DNA track.

It turns out that when repulsive strengths y_1 and y_2 are strong enough (both must be greater than 1), the cooperative pushing always occurs even at low RNAP densities and it is not sensitive to stochastic blocking or attraction. Meanwhile, if either y_1 or y_2 is less than 1, the cooperative pushing requires a very strong stochastic blocking or attraction. Thus, the next–nearest interaction energy plays an important role in the prediction of collective pushing and jamming of RNAP motors on the DNA template.

Chapter 5

Modeling by an exclusion process with two degrees of freedom and nearest neighbor long-range interaction

5.1 The model dynamics and stationary distribution

In this chapter, we shall propose invariant measure as in (5.3) for RNAP model whose interaction energy $U(\mathbf{x})$ (5.1) has general interaction range indicated by parameter d. Notice that $d = 1$ and $d = 2$ are the cases considered in Chapters 3 and 4 respectively. Since the range is wider, on the microscopic scale, the interaction range among RNAPs in transition rates might be widened as well. To see the relation between two kinds of interaction, we shall propose two models which will be called **Model 1** (with rates (5.8) and (5.9)) and **Model 2** (with rates (5.10) and (5.11)). The difference between the two models is the following. The translocation rate (5.8) of an RNAP of Model 1 depends only on the occupancy of its nearest neighboring lattice site on the left, meanwhile, the corresponding one (5.10) of Model 2 depends on the position of the leftmost RNAP neighbor. As Model 1 shows, if the translocation rate (5.8) of an RNAP depends on the occupancy of its nearest neighboring lattice site on the left, then the interaction range d must be equal to 1. Otherwise, the rate depends only on the position of the rightmost RNAP neighbor. We stress that although the models' dynamics are different, the processes corresponding to each model have invariant distributions of the same form (5.3).

We consider the reaction scheme of RNAP translocation as in Fig. 5.1. It means that we continue neglecting the reverse processes in the sense explained in the previous chapter.
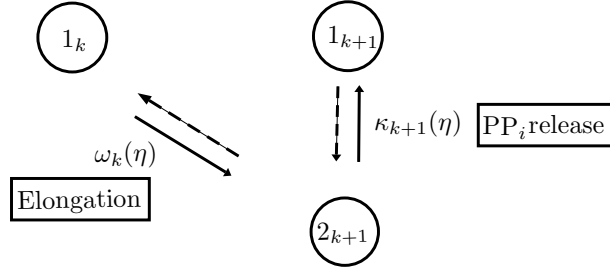
Figure 5.1: *Minimal reaction scheme of RNAP translocation. Reverse reactions (not considered here) are indicated with dashed arrows.*

5.1.1   The model stationary distribution

An allowed configuration of N RNAPs, which we denote by $\boldsymbol{\eta}$, is thus specified by a coordinate vector $\mathbf{x} = (x_1, ..., x_N)$ with ordered integer coordinates and a state vector $\mathbf{s} = (s_1, ..., s_N)$ with state variables $s_i \in \{1, 2\}$.

As for the stationary distribution of the interacting RNAPs, we define effective long-range interaction energy

$$U(\mathbf{x}) = J_1 \sum_{i=1}^{L} \delta^L_{x_{i+1}, x_i + \ell} + J_2 \sum_{i=1}^{L} \delta^L_{x_{i+1}, x_i + \ell + 1} + ... + J_d \sum_{i=1}^{L} \delta^L_{x_{i+1}, x_i + \ell + d - 1}. \tag{5.1}$$

and the excess $B(\mathbf{s}) = N^1 - N^2$ where N^α the fluctuating number of RNAPs in state $\alpha \in \{1, 2\}$. One has $N = N^1 + N^2$ and

$$B(\mathbf{s}) = \sum_{i=1}^{N} (3 - 2s_i) \tag{5.2}$$

Positive J_k for $k = 1, ..., d$ correspond to repulsion. For $k > d$, set $J_k = 0$. The stationary distribution for allowed configurations acquires thus, the following form

$$\hat{\pi}_d(\boldsymbol{\eta}) = \frac{1}{Z_{d,L}} \pi(\boldsymbol{\eta}) \tag{5.3}$$

with the Boltzmann weights

$$\pi_d(\boldsymbol{\eta}) = \exp\left[-\frac{1}{k_B T} (U + \lambda B) \right] \tag{5.4}$$

and the partition function

$$Z_{d,L} = \sum_{\boldsymbol{\eta}} \pi_d(\boldsymbol{\eta}). \tag{5.5}$$

One introduces

$$x = e^{\frac{2\lambda}{k_B T}}, \quad y_k = e^{-\frac{J_k}{k_B T}}, \quad \text{for } k = 1, ..., d \tag{5.6}$$

so that $x > 1$ corresponds to an excess of RNAP in state 1. The normalized stationary distribution for allowed configurations is then given by

$$\hat{\pi}_d(\boldsymbol{\eta}) = \frac{1}{Z_{d,L}} \prod_{i=1}^{N} x^{-3/2+s_i} y_1^{\delta^L_{x_{i+1},x_i+\ell}} \cdots y_d^{\delta^L_{x_{i+1},x_i+\ell+d-1}}. \tag{5.7}$$

5.1.2   The model dynamics

As mentioned above, we propose two models called Model 1 and Model 2. Model 1 has translocation rate $w_i(\boldsymbol{\eta})$ (see (5.8)) of an RNAP which depends only on the occupancy of the nearest neighboring lattice site on the left, meanwhile the rate $w_i(\boldsymbol{\eta})$ (see (5.10)) on the left depends on the position of leftmost RNAP neighbor. We also notice that the PP_i release rates $\kappa_i(\boldsymbol{\eta})$ ((5.9) for Model 1 and (5.11) for Model 2) of an RNAP for both models depend on the positions of its leftmost and rightmost RNAP neighbors. We would like to emphasize again here that although the dynamics of the two models are different, the processes admit the same form of invariant distributions (5.3).

Model 1: The configuration-dependent translocation rate and the rate for PP_i release for rod i are of the forms

$$w_i(\boldsymbol{\eta}) = \omega^\star \delta_{s_i,1} (1 + e^{1\star} \delta_{x_i,x_{i-1}+\ell} + \sum_{k=1}^{d} e^{\star \bar{k} 1} \delta_{x_{i+1},x_i+\ell+k})(1 - \delta_{x_{i+1},x_i+\ell}), \tag{5.8}$$

$$\kappa_i(\boldsymbol{\eta}) = \kappa^\star \delta_{s_i,2} (1 + \sum_{k=0}^{d} f^{1\bar{k}\star} \delta_{x_i,x_{i-1}+\ell+k} + \sum_{k=0}^{d} f^{\star \bar{k} 1} \delta_{x_{i+1},x_i+\ell+k}). \tag{5.9}$$

It means that the interaction range in the rates is d. The parameters must be chosen to ensure positivity for all rates. Namely, the parameter range is $\omega^\star, \kappa^\star > 0$, $e^{1\star} \geq -1, e^{\star \bar{k} 1} \geq -1, e^{1\star} + e^{\star \bar{k} 1} \geq -1$ for $k = 1, ..., d$ and $f^{1\bar{k}\star} + f^{\star \bar{l} 1} \geq -1$ for $k, l = 0, ..., d$. For the convenience, we set that $e^{\star \bar{k} 1} = f^{\star \bar{k} 1} = f^{1\bar{k}\star} = 0$ for $k > d$.

Model 2: The configuration-dependent translocation rate and the rate for PP_i release are of the forms

$$w_i(\boldsymbol{\eta}) = \delta_{s_i,1} (\omega_i^1(\boldsymbol{\eta}) + ... + \omega_i^d(\boldsymbol{\eta})) \tag{5.10}$$

$$\kappa_i(\boldsymbol{\eta}) = \delta_{s_i,2} (\kappa_i^1(\boldsymbol{\eta}) + ... + \kappa_i^d(\boldsymbol{\eta})) \tag{5.11}$$

where

$$\omega_i^k(\boldsymbol{\eta}) = \omega_k^\star \left(1 + \sum_{j=0}^{d-1} e_k^{1\bar{j}\star} \delta_{x_i,x_{i-1}+\ell+j}\right) (1 - \delta_{x_{i+1},x_i+\ell})(1 - \delta_{x_{i+1},x_i+\ell+1}) \cdots (1 - \delta_{x_{i+1},x_i+\ell+k-1})$$

$$\times \, \delta_{x_{i+1},x_i+\ell+k}, \text{ for } 1 \leq k \leq d-1, \tag{5.12}$$

$$\omega_i^d(\boldsymbol{\eta}) = \omega_d^\star \left(1 + \sum_{j=0}^{d-1} e_d^{1\bar{j}\star} \delta_{x_i,x_{i-1}+\ell+j}\right) (1 - \delta_{x_{i+1},x_i+\ell})(1 - \delta_{x_{i+1},x_i+\ell+1}) \cdots (1 - \delta_{x_{i+1},x_i+\ell+d-1})$$

$$\times \, (1 - \delta_{x_{i+1},x_i+\ell+d}). \tag{5.13}$$

and

$$\kappa_i^k(\boldsymbol{\eta}) = \kappa^\star \left(1 + \sum_{j=0}^{d-1} f_k^{1\bar{j}\star} \delta_{x_i,x_{i-1}+\ell+j} + f_k^{\star\bar{k}1} \delta_{x_{i+1},x_i+\ell+k}\right) (1 - \delta_{x_{i+1},x_i+\ell})$$

$$\times \, (1 - \delta_{x_{i+1},x_i+\ell+1}) \cdots (1 - \delta_{x_{i+1},x_i+\ell+k-1}) \delta_{x_{i+1},x_i+\ell+k}, \text{ for } 0 \leq k \leq d-1, \tag{5.14}$$

$$\kappa_i^d(\boldsymbol{\eta}) = \kappa^\star \left(1 + \sum_{j=0}^{d-1} f_d^{1\bar{j}\star} \delta_{x_i,x_{i-1}+\ell+j}\right) (1 - \delta_{x_{i+1},x_i+\ell})(1 - \delta_{x_{i+1},x_i+\ell+1}) \cdots (1 - \delta_{x_{i+1},x_i+\ell+d-1})$$

$$\times \, (1 - \delta_{x_{i+1},x_i+\ell+d}). \tag{5.15}$$

The parameter range is $\kappa^\star > 0, \omega_k^\star > 0$ for $k = 1, ..., d$, $e_k^{1\bar{j}\star} \geq -1$ for $k = 1, ..., d; j = 0, ..., d-1$, $f_k^{1\bar{j}\star} + f_k^{\star\bar{k}1} \geq -1$ for $k, j = 0, ..., d-1$, and $f_d^{1\bar{j}\star} \geq -1$ to ensure positivity of all jump rates.

Remark 5.1. *The single-RNAP PP_i release rate is denoted by $\kappa^\star$ in both models.*

5.2 The conditions for the existence

5.2.1 Master equation

The master equation for the probability $\mathbb{P}_t(\boldsymbol{\eta})$ of finding the rods at time t in the configuration $\boldsymbol{\eta}$

$$\frac{d}{dt}\mathbb{P}(\boldsymbol{\eta}, t) = \sum_{i=1}^{N} [\omega_i(\boldsymbol{\eta}_{tl}^i)\mathbb{P}(\boldsymbol{\eta}_{tl}^i, t) + \kappa_i(\boldsymbol{\eta}_{rel}^i)\mathbb{P}(\boldsymbol{\eta}_{rel}^i, t) - (\omega_i(\boldsymbol{\eta}) + \kappa_i(\boldsymbol{\eta}))\mathbb{P}(\boldsymbol{\eta}, t)], \tag{5.16}$$

where $\boldsymbol{\eta}_{tl}^i$ is the configuration that leads to $\boldsymbol{\eta}$ before a translocation of RNAP i (i.e., with coordinate $x_i^{tl} = x_i - 1$ and state $s_i^{tl} = 3 - s_i$), $\boldsymbol{\eta}_{rel}^i$ is the configuration $\boldsymbol{\eta}$ before PP_i release at RNAP i (i.e., $x_i^{rel} = x_i$ and $s_i^{rel} = 3 - s_i$). Due to periodicity, the positions x_i of the rods are counted modulo L and labels i are counted modulo N.

Dividing (5.16) by the stationary distribution (5.3), the stationary condition becomes

$$\sum_{i=1}^{N} \left(\omega_i(\boldsymbol{\eta}_{tl}^i) \frac{\pi_d(\boldsymbol{\eta}_{tl}^i)}{\pi_d(\boldsymbol{\eta})} - \omega_i(\boldsymbol{\eta}) + \kappa_i(\boldsymbol{\eta}_{rel}^i) \frac{\pi_d(\boldsymbol{\eta}_{rel}^i)}{\pi_d(\boldsymbol{\eta})} - \kappa_i(\boldsymbol{\eta}) \right) = 0. \qquad (5.17)$$

Now we introduce the quantities

$$D_i(\boldsymbol{\eta}) = \omega_i(\boldsymbol{\eta}_{tl}^i) \frac{\pi_d(\boldsymbol{\eta}_{tl}^i)}{\pi_d(\boldsymbol{\eta})} - \omega_i(\boldsymbol{\eta}), \qquad (5.18)$$

$$F_i(\boldsymbol{\eta}) = \kappa_i(\boldsymbol{\eta}_{rel}^i) \frac{\pi_d(\boldsymbol{\eta}_{rel}^i)}{\pi_d(\boldsymbol{\eta})} - \kappa_i(\boldsymbol{\eta}). \qquad (5.19)$$

Taking into account periodicity, the stationarity condition (5.17) is satisfied if the lattice divergence condition

$$D_i(\boldsymbol{\eta}) + F_i(\boldsymbol{\eta}) = \Phi_i(\boldsymbol{\eta}) - \Phi_{i+1}(\boldsymbol{\eta}) \qquad (5.20)$$

holds for all allowed configurations with a family of functions $\Phi_i(\boldsymbol{\eta})$ satisfying $\Phi_{N+1}(\boldsymbol{\eta}) = \Phi_1(\boldsymbol{\eta})$.

5.2.2   Mapping to the headway process

One can write the stationary distribution (5.3) in terms of the parameters (5.6) and the distance variables θ_i^p as follows

$$\tilde{\pi}_d(\boldsymbol{\zeta}) = \frac{1}{Z} \prod_{i=i}^{N} \left(x^{-3/2+s_i} y_1^{\theta_i^0} y_2^{\theta_i^1} \cdots y_d^{\theta_i^{d-1}} \right). \qquad (5.21)$$

One also can rewrite the transition rates of the two models in terms of the stochastic variables $\boldsymbol{\zeta} = (\mathbf{m}, \mathbf{s})$ that are given by the distance vector $\mathbf{m}$ and the state vector $\mathbf{s}$.

Transition rates of Model 1: The transition rates (5.8) and (5.9) can be rewritten as follows

$$\tilde{\omega}_i(\boldsymbol{\zeta}) = \omega^\star \delta_{s_1,1}(1 + e^{1\star}\theta_{i-1}^0 + \sum_{k=1}^{d} e^{\star\bar{k}1}\theta_i^k)(1 - \theta_i^0), \qquad (5.22)$$

$$\tilde{\kappa}_i(\boldsymbol{\zeta}) = \kappa^\star \delta_{s_i,2}(1 + \sum_{k=1}^{d} f^{1\bar{k}\star}\theta_{i-1}^k + \sum_{k=1}^{d} f^{\star\bar{k}1}\theta_i^k). \qquad (5.23)$$

Transition rates of Model 2: The transition rates (5.10) and (5.11) can be rewritten as follows

$$\tilde{w}_i(\boldsymbol{\zeta}) = \delta_{s_i,1}(\tilde{\omega}_i^1(\boldsymbol{\zeta}) + ... + \tilde{\omega}_i^d(\boldsymbol{\zeta})), \qquad (5.24)$$

$$\tilde{\kappa}_i(\boldsymbol{\zeta}) = \delta_{s_i,2}(\tilde{\kappa}_i^1(\boldsymbol{\zeta}) + \dots + \tilde{\kappa}_i^d(\boldsymbol{\zeta})), \tag{5.25}$$

where

$$\tilde{\omega}_i^k(\boldsymbol{\zeta}) = \omega_k^\star \left(1 + \sum_{j=0}^{d-1} e_k^{1\bar{j}\star} \theta_{i-1}^j\right)(1 - \theta_i^0)\cdots(1 - \theta_i^{k-1})\theta_i^k, \text{ for } 1 \le k \le d-1, \tag{5.26}$$

$$\tilde{\omega}_i^d(\boldsymbol{\zeta}) = \omega_d^\star \left(1 + \sum_{j=0}^{d-1} e_d^{1\bar{j}\star} \theta_{i-1}^j\right)(1 - \theta_i^0)\cdots(1 - \theta_i^{d-1})(1 - \theta_i^d), \tag{5.27}$$

$$\tilde{\kappa}_i^k(\boldsymbol{\zeta}) = \kappa^\star \left(1 + \sum_{j=0}^{d-1} f_k^{1\bar{j}\star} \theta_{i-1}^j + f_k^{\star\bar{k}1} \theta_i^k\right)(1 - \theta_i^0)\cdots(1 - \theta_i^{k-1})\theta_i^k, \text{ for } 1 \le k \le d-1, \tag{5.28}$$

$$\tilde{\kappa}_i^d(\boldsymbol{\zeta}) = \kappa^\star \left(1 + \sum_{j=0}^{d-1} f_d^{1\bar{j}\star} \theta_{i-1}^j\right)(1 - \theta_i^0)\cdots(1 - \theta_i^{d-1})(1 - \theta_i^d). \tag{5.29}$$

Master equation for the headway process: In order to write the master equation, we need to introduce notation for the configuration that leads to a given configuration $\boldsymbol{\zeta}$, viz. $\boldsymbol{\zeta}^{i-1,i}$ for translocation and $\boldsymbol{\zeta}^i$ for PP$_i$ release. For a fixed $\boldsymbol{\zeta}$ these configurations are defined by

$$s_j^{i-1,i} = s_j + (3 - 2s_j)\delta_{j,i}, \quad m_j^{i-1,i} = m_j + \delta_{j,i} - \delta_{j,i-1}, \tag{5.30}$$

$$s_j^i = s_j + (3 - 2s_j)\delta_{j,i}, \quad m_j^i = m_j. \tag{5.31}$$

This yields the master equation

$$\frac{d\mathbb{P}(\boldsymbol{\zeta}, t)}{dt} = \sum_{i=1}^N Q_i(\boldsymbol{\zeta}, t), \tag{5.32}$$

with

$$Q_i(\boldsymbol{\zeta}, t) = \tilde{\omega}_i(\boldsymbol{\zeta}^{i-1,i})\mathbb{P}(\boldsymbol{\zeta}^{i-1,i}, t) - \tilde{\omega}_i(\boldsymbol{\zeta})\mathbb{P}(\boldsymbol{\zeta}, t) + \tilde{\kappa}_i(\boldsymbol{\zeta}^i)\mathbb{P}(\boldsymbol{\zeta}^i, t) - \tilde{\kappa}_i(\boldsymbol{\zeta})\mathbb{P}(\boldsymbol{\zeta}, t) \tag{5.33}$$

where the rates $\tilde{\omega}_i(\boldsymbol{\zeta}^{i-1,i})$ and $\tilde{w}_i(\boldsymbol{\zeta}^{i-1,i})$ correspond to Model 1 and Model 2 in the following.

Model 1: One has

$$\tilde{\omega}_i(\boldsymbol{\zeta}^{i-1,i}) = \omega^\star \delta_{s_i,2}(1 + e^{1\star}\theta_{i-1}^1 + \sum_{k=1}^{d-1} e^{\star\overline{k+11}}\theta_i^k)(1 - \theta_{i-1}^0), \tag{5.34}$$

$$\tilde{\kappa}_i(\boldsymbol{\zeta}^i) = \kappa^\star \delta_{s_i,1}(1 + \sum_{k=1}^d f^{1\bar{k}\star}\theta_{i-1}^k + \sum_{k=1}^d f^{\star\bar{k}1}\theta_i^k). \tag{5.35}$$

Model 2: One has

$$\tilde{w}_i(\boldsymbol{\zeta}^{i-1,i}) = \delta_{s_i,2}(\tilde{\omega}_i^1(\boldsymbol{\zeta}^{i-1,i}) + ... + \tilde{\omega}_i^d(\boldsymbol{\zeta}^{i-1,i})), \tag{5.36}$$

$$\tilde{\kappa}_i(\boldsymbol{\zeta}^i) = \delta_{s_i,1}(\tilde{\kappa}_i^1(\boldsymbol{\zeta}^i) + ... + \tilde{\kappa}_i^d(\boldsymbol{\zeta}^i)), \tag{5.37}$$

where

$$\tilde{\omega}_i^k(\boldsymbol{\zeta}^{i-1,i}) = \omega_{k+1}^\star \left(1 + \sum_{j=1}^{d-1} e_{k+1}^{1\overline{j-1}\star} \theta_{i-1}^j\right)(1 - \theta_{i-1}^0)(1 - \theta_i^0) \cdots (1 - \theta_i^{k-1})\theta_i^k, \text{ for } 1 \leq k \leq d-1, \tag{5.38}$$

$$\tilde{\omega}_i^d(\boldsymbol{\zeta}^{i-1,i}) = \omega_d^\star \left(1 + \sum_{j=1}^{d-1} e_d^{1\overline{j-1}\star} \theta_{i-1}^j\right)(1 - \theta_{i-1}^0)(1 - \theta_i^0) \cdots (1 - \theta_i^{d-1}), \tag{5.39}$$

$$\tilde{\kappa}_i^k(\boldsymbol{\zeta}^i) = \kappa^\star \left(1 + \sum_{j=0}^{d-1} f_k^{1\overline{j}\star} \theta_{i-1}^j + f_k^{\star\overline{k}1} \theta_i^k\right)(1 - \theta_i^0) \cdots (1 - \theta_i^{k-1})\theta_i^k, \text{ for } 1 \leq k \leq d-1, \tag{5.40}$$

$$\tilde{\kappa}_i^d(\boldsymbol{\zeta}^i) = \kappa^\star \left(1 + \sum_{j=0}^{d-1} f_d^{1\overline{j}\star} \theta_{i-1}^j\right)(1 - \theta_i^0) \cdots (1 - \theta_i^{d-1})(1 - \theta_i^d). \tag{5.41}$$

5.2.3 Stationary conditions

Since $\tilde{\pi}_d$ in (5.21) is the invariant measure of the headway process, (5.32) can be written as follows

$$\sum_{i=1}^N \left(\tilde{D}_i(\boldsymbol{\zeta}) + \tilde{F}_i(\boldsymbol{\zeta})\right) = 0 \tag{5.42}$$

where

$$\tilde{D}_i(\boldsymbol{\zeta}) := \tilde{\omega}_i(\boldsymbol{\zeta}^{i-1,i}) \frac{\tilde{\pi}_d(\boldsymbol{\zeta}^{i-1,i})}{\tilde{\pi}_d(\boldsymbol{\zeta})} - \tilde{\omega}_i(\boldsymbol{\zeta}), \tag{5.43}$$

$$\tilde{F}_i(\boldsymbol{\zeta}) := \tilde{\kappa}_i(\boldsymbol{\zeta}^i) \frac{\tilde{\pi}_d(\boldsymbol{\zeta}^i)}{\tilde{\pi}_d(\boldsymbol{\zeta})} - \tilde{\kappa}_i(\boldsymbol{\zeta}). \tag{5.44}$$

We can therefore rephrase the stationarity condition in a local divergence form equivalent to (5.20). Notice that

$$\theta_j^p(\boldsymbol{\zeta}^{i-1,i}) = \delta_{m_j + \delta_{j,i} - \delta_{j,i-1},p} = \theta_j^{p - \delta_{j,i} + \delta_{j,i-1}}(\boldsymbol{\zeta}) \text{ and } \delta_{s_i^{i-1,i},\alpha} = \delta_{s_i,3-\alpha}; \tag{5.45}$$

$$\theta_j^p(\boldsymbol{\zeta}^i) = \theta_j^p(\boldsymbol{\zeta}) \text{ and } \delta_{s_i^i,\alpha} = \delta_{s_i,3-\alpha}. \tag{5.46}$$

One has

$$\frac{\tilde{\pi}_d(\boldsymbol{\zeta}^{i-1,i})}{\tilde{\pi}_d(\boldsymbol{\zeta})} = x^{-1}y_{m_{i-1}}y^{-1}_{m_{i-1}+1}y^{-1}_{m_i+1}y_{m_i+2} \tag{5.47}$$

$$\frac{\tilde{\pi}_d(\boldsymbol{\zeta}^{i})}{\tilde{\pi}_d(\boldsymbol{\zeta})} = x^{3-2s_i}. \tag{5.48}$$

For the detailed computation of (5.47), we refer a reader to Lemma 6.1 in Chapter 6. Hence,

$$\tilde{D}_i(\boldsymbol{\zeta}) = x^{-1}y_{m_{i-1}}y^{-1}_{m_{i-1}+1}y^{-1}_{m_i+1}y_{m_i+2}\tilde{\omega}_i(\boldsymbol{\zeta}^{i-1,i}) - \tilde{\omega}_i(\boldsymbol{\zeta}), \tag{5.49}$$

$$\tilde{F}_i(\boldsymbol{\zeta}) = x^{3-2s_i}\tilde{\kappa}_i(\boldsymbol{\zeta}^{i}) - \tilde{\kappa}_i(\boldsymbol{\zeta}). \tag{5.50}$$

One requires

$$\tilde{D}_i + \tilde{F}_i = \tilde{\Phi}_{i-1} - \tilde{\Phi}_i, \tag{5.51}$$

and notices that the left hand side of (5.51) is a function of variables $\theta_i^k, \theta_{i-1}^l$ taking values 0 or 1, therefore the form of Φ_i is the following

$$\Phi_i(\boldsymbol{\eta}) = a_0 + a_1\theta_i^0 + a_2\theta_i^1 + ... + a_{d+1}\theta_i^d. \tag{5.52}$$

Thus, instead of finding stationary conditions based on the master equation (5.42), we shall deal with equation (5.51). The method used here is similar to the one already exposed in the previous chapter. Namely, one first finds coefficients a_k for $k = 1, ..., d+1$ of function Φ_i in (5.52), next finds values y_k in terms of parameters appearing in the transition rates and then finds the relations among the parameters. For convenience, in the sequel, we set $a_k = 0$ for $k > d + 1$.

5.2.3.1   Stationary conditions for Model 1:

In this subsection, we shall deal with Model 1. For convenience, we set $e^{\star\bar{k}1} = f^{1\bar{k}1} = f^{\star\bar{k}1} = 0$ for $k \geq d + 1$. Suppose that $m_{i-1} = m, m_i = n$. The lattice divergence condition (5.51) becomes

$$
\begin{aligned}
&x^{-1}y_m y^{-1}_{m+1} y^{-1}_{n+1} y_{n+2}\omega^{\star}\delta_{s_i,2}(1 + e^{1\star}\theta^1_{i-1} + e^{\star\overline{n+1}1}\theta^{n-1}_i)(1 - \theta^0_{i-1}) \\
&- \omega^{\star}\delta_{s_i,1}(1 + e^{1\star}\theta^0_{i-1} + e^{\star\bar{n}1})(1 - \theta^0_i) \\
&+ x\kappa^{\star}\delta_{s_i,1}(1 + f^{1\overline{m}\star}\theta^m_{i-1} + f^{\star\bar{n}1}\theta^n_i) \\
&- \kappa^{\star}\delta_{s_i,2}(1 + f^{1\overline{m}\star}\theta^m_{i-1} + f^{\star\bar{n}1}\theta^{m_i}_i) \\
&= a_{m+1} - a_{n+1}. \tag{5.53}
\end{aligned}
$$

By plugging $s_i = 1, 2$ into the equation above, one has the following system of equations.

– If $s_1 = 1$, one has

$$-\omega^\star(1 + e^{1\star}\theta_{i-1}^0 + e^{\star\overline{n}1})(1 - \theta_i^0) + x\kappa^\star(1 + f^{1\overline{m}\star} + f^{\star\overline{n}1}) = a_{m+1} - a_{n+1}. \quad (5.54)$$

– If $s_1 = 2$, one has

$$x^{-1}y_m y_{m+1}^{-1} y_{n+1}^{-1} y_{n+2}\omega^\star(1 + e^{1\star}\theta_{i-1}^1 + e^{\star\overline{n+1}1})(1 - \theta_{i-1}^0) - \kappa^\star(1 + f^{1\overline{m}\star} + f^{\star\overline{n}1})$$
$$= a_{m+1} - a_{n+1}. \quad (5.55)$$

The system of equations (5.54)–(5.55) is equivalent to the system (5.56)–(5.57) below

$$y_m y_{m+1}^{-1} y_{n+1}^{-1} y_{n+2}\omega^\star(1 + e^{1\star}\theta_{i-1}^1 + e^{\star\overline{n+1}1})(1 - \theta_{i-1}^0) - \omega^\star(1 + e^{1\star}\theta_{i-1}^0 + e^{\star\overline{n}1})(1 - \theta_i^0)$$
$$= (1 + x)(a_{m+1} - a_{n+1}), \quad (5.56)$$
$$-\omega^\star(1 + e^{1\star}\theta_{i-1}^0 + e^{\star\overline{n}1})(1 - \theta_i^0) + x\kappa^\star(1 + f^{1\overline{m}\star} + f^{\star\overline{n}1}) = a_{m+1} - a_{n+1}. \quad (5.57)$$

We shall find the values a_k for $k = 1, ..., d+1$ and y_k for $k = 1, ..., d$ from (5.56).

- Consider the case $m = 0$: (5.56) becomes

$$-\omega^\star(1 + e^{1\star} + e^{\star\overline{n}1})(1 - \theta_i^0) = (1 + x)(a_1 - a_{n+1}), \quad (5.58)$$

• If $n > d$, one gets

$$a_1 = -\frac{\omega^\star}{1 + x}(1 + e^{1\star}). \quad (5.59)$$

• If $n = k$ with $1 \leq k \leq d$, one gets

$$a_{k+1} = \frac{\omega^\star}{1 + x}e^{\star\overline{k}1}. \quad (5.60)$$

Therefore, one obtains

$$\begin{cases} a_1 &= -\dfrac{\omega^\star}{1 + x}(1 + e^{1\star}), \\ a_k &= \dfrac{\omega^\star}{1 + x}e^{\star\overline{k-1}1}, \text{ for } k = 2, ..., d+1. \end{cases} \quad (5.61)$$

- Consider the case $m = 1$: (5.56) becomes

$$y_1 y_2^{-1} y_{n+1}^{-1} y_{n+2}\omega^\star(1 + e^{1\star} + e^{\star\overline{n+1}1}) - \omega^\star(1 + e^{\star\overline{n}1})(1 - \theta_i^0) = (1 + x)(a_2 - a_{n+1}). \quad (5.62)$$

• If $n > d$, one gets

$$y_1 y_2^{-1} = \frac{1 + e^{\star\overline{1}1}}{1 + e^{1\star}}. \quad (5.63)$$

- If $n = k$ with $1 \leq k \leq d$, one gets

$$y_{k+1}^{-1} y_{k+2} = \frac{1 + e^{1\star}}{1 + e^{1\star} + e^{\star \overline{k+1}1}}. \tag{5.64}$$

- Consider the case $m > d$: (5.56) becomes

$$y_{n+1}^{-1} y_{n+2} \omega^{\star} (1 + e^{\star \overline{n+1}1}) - \omega^{\star} (1 + e^{\star \overline{n}1})(1 - \theta_i^0) = -(1 + x)a_{n+1}, \tag{5.65}$$

which yields

$$y_{k+1}^{-1} y_{k+2} = \frac{1}{1 + e^{\star \overline{k+1}1}} \text{ for } k \geq 1. \tag{5.66}$$

From (5.64) and (5.66), one has $e^{1\star} e^{\star \overline{k}1} = 0$ for all $k \geq 2$. It means that if $e^{1\star} \neq 0$ then $e^{\star \overline{k}1} = 0$ for all $k \geq 2$. From (5.63) and (5.66), one obtains

$$\begin{cases} y_1 & = \dfrac{\prod_{k=1}^{d}(1 + e^{\star \overline{k}1})}{1 + e^{1\star}}, \\ y_k & = \prod_{j=1}^{d-k+1}(1 + e^{\star \overline{d-j+1}1}), \text{ for } k \geq 2. \end{cases} \tag{5.67}$$

From here, it is easy to prove the following lemma.

Lemma 5.1. *With the values a_k for $k = 1, ..., d+1$ from (5.61) and y_k for $k = 1, ..., d$ from (5.67), the equation (5.56) holds for all configurations.*

Next we shall find the values $f^{1\overline{k}\star}$ and $f^{\star \overline{k}1}$ for $k = 0, ..., d$ from (5.57).

- If $n > d$ then equation (5.57) becomes

$$-\omega^{\star}(1 + e^{1\star} \theta_{i-1}^0) + x\kappa^{\star}(1 + f^{1\overline{m}\star}) = a_{m+1}. \tag{5.68}$$

- If $m > d$ then one gets

$$x = \frac{\omega^{\star}}{\kappa^{\star}}. \tag{5.69}$$

- If $m = 0$ then one gets $f^{1\overline{0}\star} = \dfrac{x}{1+x} e^{1\star} - \dfrac{1}{1+x}$.

- If $1 \leq m \leq d$, one gets $f^{1\overline{m}\star} = \dfrac{1}{1+x} e^{1\overline{m}\star}$.

- If $m > d$ then equation (5.57) becomes

$$-\omega^{\star}(1 + e^{\star \overline{n}1})(1 - \theta_i^0) + x\kappa^{\star}(1 + f^{\star \overline{n}1}) = -a_{n+1}. \tag{5.70}$$

- If $n = 0$, one gets $f^{\star \overline{0}1} = \dfrac{1}{1+x} e^{1\star} - \dfrac{x}{1+x}$.

- If $1 \leq n \leq d$, one gets $f^{\star \overline{n}1} = \dfrac{x}{1+x} e^{\star \overline{n}1}$.

One obtains

$$
\begin{cases}
f^{1\bar{0}\star} & = \dfrac{x}{1+x}e^{1\star} - \dfrac{1}{1+x}, \\[2mm]
f^{\star\bar{0}1} & = \dfrac{1}{1+x}e^{1\star} - \dfrac{x}{1+x}, \\[2mm]
f^{1\bar{k}\star} & = \dfrac{1}{1+x}e^{\star\bar{k}1}, \text{ for } k = 1, ..., d, \\[2mm]
f^{\star\bar{k}1} & = \dfrac{x}{1+x}e^{\star\bar{k}1}, \text{ for } k = 1, ..., d.
\end{cases}
\tag{5.71}
$$

From here, it is easy to prove the following lemma.

Lemma 5.2. *With the values a_k for $k = 1, ..., d+1$ from (5.61), x from (5.69), and $f^{\star\bar{k}1}$, $f^{1\bar{k}\star}$ for $k = 0, ..., d$ from (5.71), the equation (5.57) holds for all configurations.*

Because of the identity $e^{1\star}e^{\star\bar{k}1} = 0$, for $k \geq 2$, thus if $e^{1\star} \neq 0$, then all parameters $e^{\star\bar{k}1}$ for $k \geq 2$ are zero. Consequently, we have two separate cases of the kinetics of a single RNAP.

Case a: Consider the case $e^{1\star} \neq 0$, the transition rates in (5.8) – (5.9) become

$$
w_i(\boldsymbol{\eta}) = \omega^\star \delta_{s_i,1}(1 + e^{1\star}\delta_{x_i,x_{i-1}+\ell})(1 - \delta_{x_{i+1},x_i+\ell}),
\tag{5.72}
$$

$$
\kappa_i(\boldsymbol{\eta}) = \kappa^\star \delta_{s_i,2}(1 + f^{1\bar{0}\star}\delta_{x_i,x_{i-1}+\ell} + f^{\star\bar{0}1}\delta_{x_{i+1},x_i+\ell} + f^{1\bar{1}\star}\delta_{x_i,x_{i-1}+\ell} + f^{\star\bar{1}1}\delta_{x_{i+1},x_i+\ell}).
\tag{5.73}
$$

where

$$
\begin{cases}
f^{1\bar{0}\star} & = \dfrac{x}{1+x}e^{1\star} - \dfrac{1}{1+x}, \\[2mm]
f^{\star\bar{0}1} & = \dfrac{1}{1+x}e^{1\star} - \dfrac{x}{1+x}, \\[2mm]
f^{1\bar{1}\star} & = \dfrac{1}{1+x}e^{1\star}, \\[2mm]
f^{\star\bar{1}1} & = \dfrac{x}{1+x}e^{1\star}.
\end{cases}
\tag{5.74}
$$

with $x = \dfrac{\omega^\star}{\kappa^\star}$.

Notice that the constraints in (5.74) must be satisfied to ensure the stationarity. This is the contents of Theorem 1.3 which is now restated as follows.

Theorem 5.1. *For the process defined in **Case a** above, the conditions (5.74) upon its dynamics rates (5.72) – (5.73) are sufficient for its stationary distribution be of the form (5.3). In this case, the stationary distribution acquires the following expression*

$$
\hat{\pi}_1(\boldsymbol{\eta}) = \frac{1}{Z_{1,L}} \left(\frac{\omega^\star}{\kappa^\star}\right)^{\sum_{i=1}^{N} -3/2+s_i} \left(\frac{1+e^{1\star}}{1+e^{\star\bar{1}1}}\right)^{-\sum_{i=1}^{N} \delta^L_{x_{i+1},x_i+\ell}}
\tag{5.75}
$$

where $Z_{1,L}$ is the partition function.

Remark 5.2. *The results that have been obtained for the current case are almost the same as*

in the paper [4]. There is only one difference which comes from the fact that we did not add the term $f^{1\star\bar{1}}$ into the release rate since its role in contributing to the rate can be compensated by the roles of parameters $f^{1\bar{0}\star}$ and $f^{\star\bar{0}1}$.

Case b: Consider the case $e^{1\star} = 0$. The transition rates in (5.8) become

$$w_i(\boldsymbol{\eta}) = \omega^\star \delta_{s_i,1}(1 + \sum_{k=1}^{d} e^{\star\bar{k}1}\delta_{x_{i+1},x_i+\ell+k})(1 - \delta_{x_{i+1},x_i+\ell}), \qquad (5.76)$$

$$\kappa_i(\boldsymbol{\eta}) = \kappa^\star \delta_{s_i,2}(1 + \sum_{k=0}^{d} f^{1\bar{k}\star}\delta_{x_i,x_{i-1}+\ell+k} + \sum_{k=0}^{d} f^{\star\bar{k}1}\delta_{x_{i+1},x_i+\ell+k}). \qquad (5.77)$$

where

$$\begin{cases} f^{1\bar{0}\star} &= -\dfrac{1}{1+x}, \\ f^{\star\bar{0}1} &= -\dfrac{x}{1+x}, \\ f^{1\bar{k}\star} &= \dfrac{1}{1+x}e^{\star\bar{k}1}, \text{ for } k = 1, ..., d, \\ f^{\star\bar{k}1} &= \dfrac{x}{1+x}e^{\star\bar{k}1}, \text{ for } k = 1, ..., d. \end{cases} \qquad (5.78)$$

Similarly, one gets Theorem 1.4 as follows.

Theorem 5.2. *For the process defined in **Case b** above, the conditions (5.78) upon its dynamics rates (5.76) – (5.77) are sufficient for its stationary distribution be of the form (5.3). In this case, the stationary distribution acquires the following expression*

$$\hat{\pi}_d(\boldsymbol{\eta}) = \frac{1}{Z_{d,L}}\left(\frac{\omega^\star}{\kappa^\star}\right)^{\sum_{i=1}^{N} -3/2+s_i} \prod_{k=1}^{d}\left(\prod_{j=1}^{d-k+1}\frac{1}{1+e^{\star\overline{d-j+1}1}}\right)^{-\sum_{i=1}^{N}\delta^L_{x_{i+1},x_i+\ell+k-1}} \qquad (5.79)$$

where $Z_{d,L}$ is the partition function.

5.2.3.2 Stationary conditions for Model 2:

In this subsection, we shall deal with Model 2. For convenience, we set $f^{\star\bar{k}1}_k = 0$ for $k \geq d$, and $f^{1\bar{j}\star}_k = 0$ for all j and $k \geq d$. If $m_{i-1} = m$ and $m_i = n$, the lattice divergence condition (5.51) becomes

$$\begin{aligned} &x^{-1}y_m y^{-1}_{m+1}y^{-1}_{n+1}y_{n+2}\delta_{s_i,2}\omega^{n+1}_i(\boldsymbol{\eta}^{i-1,i}) - \delta_{s_i,1}\omega^n_i(\boldsymbol{\eta}) \\ &+ x\kappa^\star\delta_{s_i,1}(1 + f^{1\overline{m}\star}_n\theta^m_{i-1} + f^{\star\overline{n}1}_n\theta^n_i) - \kappa^\star\delta_{s_i,2}(1 + f^{1\overline{m}\star}_n\theta^m_{i-1} + f^{\star\overline{n}1}_n\theta^n_i) \\ &= a_{m+1} - a_{n+1}. \end{aligned} \qquad (5.80)$$

By plugging $s_i = 1, 2$ into the above equation, one has the following system of equations (5.81)–(5.82).

– If $s_1 = 1$, one has

$$-\omega_i^n(\boldsymbol{\eta}) + x\kappa^\star(1 + f_n^{1\overline{m}\star} + f_n^{\star\overline{n}1}) = a_{m+1} - a_{n+1}. \tag{5.81}$$

– If $s_1 = 2$, one has

$$x^{-1}y_m y_{m+1}^{-1} y_{n+1}^{-1} y_{n+2} \omega_i^{n+1}(\boldsymbol{\eta}^{i-1,i}) - \kappa^\star(1 + f_n^{1\overline{m}\star} + f_n^{\star\overline{n}1}) = a_{m+1} - a_{n+1}. \tag{5.82}$$

The system of equations (5.81)–(5.82) is equivalent to the system (5.84)–(5.83) below

$$-\omega_i^n(\boldsymbol{\eta}) + x\kappa^\star(1 + f_n^{1\overline{m}\star} + f_n^{\star\overline{n}1}) = a_{m+1} - a_{n+1}, \tag{5.83}$$

$$y_m y_{m+1}^{-1} y_{n+1}^{-1} y_{n+2} \omega_i^{n+1}(\boldsymbol{\eta}^{i-1,i}) - \omega_i^n(\boldsymbol{\eta}) = (1+x)(a_{m+1} - a_{n+1}). \tag{5.84}$$

Finding values a_k for $k = 1, ..., d+1$: Before starting, we set that $\omega_0^\star = 0$ and $w_k^\star = w_d^\star$ for $k \geq d$.

We consider the case $m = 0$, (5.84) becomes

$$-\omega_i^n(\boldsymbol{\eta}) = (1+x)(a_1 - a_{n+1}), \tag{5.85}$$

• If $n > d$, one has $\omega_i^n(\boldsymbol{\eta}) = \omega_d^\star(1 + e_d^{1\overline{0}\star})$, $a_{n+1} = 0$ and gets

$$a_1 = \frac{-\omega_d^\star(1 + e_d^{1\overline{0}\star})}{1+x}. \tag{5.86}$$

• If $1 \leq n \leq d$, one has $\omega_i^n(\boldsymbol{\eta}) = \omega_n^\star(1 + e_n^{1\overline{0}\star})$ and gets

$$a_{n+1} = \frac{\omega_n^\star(1 + e_n^{1\overline{0}\star}) - \omega_d^\star(1 + e_d^{1\overline{0}\star})}{1+x} \tag{5.87}$$

Therefore, one obtains

$$a_{k+1} = \frac{\omega_k^\star(1 + e_k^{1\overline{0}\star}) - \omega_d^\star(1 + e_d^{1\overline{0}\star})}{1+x}, \quad \text{for } k = 0, ..., d. \tag{5.88}$$

Notice here that $a_{d+1} = 0$.

Finding values y_k for $k = 1, ..., d$: Consider equation (5.84) with some choices of m and n.

– If $m = d$ and $n \geq d$, from (5.84), one has $y_d \omega_d^\star(1 + e_d^{1\overline{d-1}\star}) - \omega_d^\star = 0$ which implies

$$y_d = \frac{1}{1 + e_d^{1\overline{d-1}\star}}. \tag{5.89}$$

– If $m = d$ and $n = d - 1$, one has

$$\omega_d^\star(1 + e_d^{1\overline{d-1}\star}) - \omega_{d-1}^\star = -(1 + x)a_d, \tag{5.90}$$

thus

$$e_{d-1}^{1\overline{0}\star} = \frac{\omega_d^\star}{\omega_{d-1}^\star}(e_d^{1\overline{0}\star} - e_d^{1\overline{d-1}\star}). \tag{5.91}$$

– If $0 \le m \le d - 1$ and $n \ge d$, one has

$$y_m y_{m+1}^{-1}\omega_d^\star(1 + e_d^{1\overline{m-1}\star}) - \omega_d^\star(1 + e_d^{1\overline{m}\star}) = (1 + x)a_{m+1} \tag{5.92}$$

which yields

$$y_m y_{m+1}^{-1} = \frac{\omega_m^\star(1 + e_m^{1\overline{0}\star}) + \omega_d^\star(e_d^{1\overline{m}\star} - e_d^{1\overline{0}\star})}{\omega_d^\star(1 + e_d^{1\overline{m-1}\star})}. \tag{5.93}$$

– If $m > d$ and for $n \ge 0$, one has

$$y_{n+1}^{-1}y_{n+2}\omega_{n+1}^\star - \omega_n^\star = -(1 + x)a_{n+1} \tag{5.94}$$

which yields

$$y_{n+1}^{-1}y_{n+2} = \frac{-\omega_n^\star e_n^{1\overline{0}\star} + \omega_d^\star(1 + e_d^{1\overline{0}\star})}{\omega_{n+1}^\star}. \tag{5.95}$$

From (5.89), (5.91), (5.93), and (5.95) one gets

$$y_k = \frac{\omega_k^\star \cdots \omega_{d-1}^\star \omega_d^\star}{(\omega_d^\star)^{d-k+1}} \frac{1}{(1 + e_d^{1\overline{k-1}\star})\cdots(1 + e_d^{1\overline{d-1}\star})}, \quad \text{for } k = 1, ..., d, \tag{5.96}$$

and

$$e_k^{1\overline{0}\star} = \frac{\omega_d^\star}{\omega_k^\star}(e_d^{1\overline{0}\star} - e_d^{1\overline{k}\star}), \quad \text{for } k = 1, 2, ..., d - 1. \tag{5.97}$$

Notice that we already found the representations of $e_k^{1\overline{0}\star}$ for $k = 1, ..., d - 1$ through parameters $\omega_k^\star$ and $e_d^{1\overline{k}\star}$ for $k = 0, ..., d - 1$. We will continue finding representations of $e_j^{1\overline{k}\star}$ for $j = 1, ..., d - 1$ and $k = 1, .., d - 2$ through those parameters.

Finding values $e_n^{1\overline{m}\star}$ for $m, n = 1, ..., d - 1$: Notice that we have considered all cases of m, n except for $0 \le m \le d$ and $0 \le n \le d - 1$. One has from (5.84) that

$$e_n^{1\overline{m}\star} = y_m y_{m+1}^{-1} y_{n+1}^{-1} y_{n+2} \frac{\omega_{n+1}^\star}{\omega_n^\star}(1 + e_{n+1}^{1\overline{m-1}\star}) - \frac{(1 + x)(a_{m+1} - a_{n+1})}{\omega_n^\star} - 1. \tag{5.98}$$

From (5.96), one gets

$$y_m y_{m+1}^{-1} y_{n+1}^{-1} y_{n+2} = \frac{\omega_m^\star}{\omega_{n+1}^\star} \frac{1 + e_d^{1\overline{n}\star}}{1 + e_d^{1\overline{m-1}\star}}, \tag{5.99}$$

and from (5.88), (5.97) one gets

$$(1+x)(a_{m+1} - a_{n+1}) = \omega_m^\star(1 + e_m^{1\overline{0}\star}) - \omega_n^\star(1 + e_n^{1\overline{0}\star}) \tag{5.100}$$

$$= \omega_m^\star - \omega_n^\star - \omega_d^\star(e_d^{1\overline{m}\star} - e_d^{1\overline{n}\star}). \tag{5.101}$$

Therefore, one can compute $e_n^{1\overline{m}\star}$ by using values $e_k^{1\overline{0}\star}$ for $k = 1, ..., d-1$ in (5.97) and the following recurrence relation

$$e_n^{1\overline{m}\star} = \frac{\omega_m^\star}{\omega_n^\star} \frac{1 + e_d^{1\overline{n}\star}}{1 + e_d^{1\overline{m-1}\star}}(1 + e_{n+1}^{1\overline{m-1}\star}) + \frac{\omega_d^\star}{\omega_n^\star}(e_d^{1\overline{m}\star} - e_d^{1\overline{n}\star}) - \frac{\omega_m^\star}{\omega_n^\star}. \tag{5.102}$$

Thus, in order to ensure the stationarity, the parameters appearing in the translocation rate must satisfy the following relations

$$\begin{cases} e_k^{1\overline{0}\star} = \dfrac{\omega_d^\star}{\omega_k^\star}(e_d^{1\overline{0}\star} - e_d^{1\overline{k}\star}), \text{ for } k = 1, 2, ..., d-1, \\[4mm] e_k^{1\overline{j}\star} = \dfrac{\omega_j^\star}{\omega_k^\star} \dfrac{1 + e_d^{1\overline{k}\star}}{1 + e_d^{1\overline{j-1}\star}}(1 + e_{k+1}^{1\overline{j-1}\star}) - \dfrac{\omega_d^\star}{\omega_k^\star}(e_d^{1\overline{j}\star} - e_d^{1\overline{k}\star}) - \dfrac{\omega_j^\star}{\omega_k^\star}, \end{cases} \tag{5.103}$$

where in the last equation the indexes k, j run from 1 to $d-1$.

Remark 5.3. *By plugging $m = d$ into (5.102) with noticing that the left hand side of (5.102) is 0, one gets $e_{n+1}^{1\overline{d-1}\star} = e_d^{1\overline{d-1}\star}$ for $n = 0, ..., d-1$.*

Notice that we have considered all cases of m_{i-1} and m_i in finding values $a_k, y_k, e_k^{1\overline{j}\star}$ for ensuring stationarity, in other words, one has the following lemma.

Lemma 5.3. *With the values y_k for $k = 1, ..., d$ in (5.96) and $e_n^{1\overline{m}\star}$ for $n = 1, ..., d$ and $m = 0, ..., d-1$ in (5.103), equation (5.84) holds for all allowed configurations.*

Next we shall find representations of $f_k^{1\overline{j}\star}$ and $f_k^{\star\overline{k}1}$ for $k, j = 0, ..., d-1$ through $e_d^{1\overline{j}\star}$ for $j = 1, ..., d-1$ by using equation (5.83). Again, we suppose that $m_{i-1} = m$ and $m_i = n$ and use the convention $\omega_0^\star = 0$.

– Consider the case $n > d$: equation (5.83) becomes $-\omega_i^d(\boldsymbol{\eta}) + x\kappa_i^d(\boldsymbol{\eta}) = a_{m+1}$.

• If $m \geq d$, one has $-\omega_d^\star + x\kappa^\star = 0$ and gets

$$x = \frac{\omega_d^\star}{\kappa^\star}. \tag{5.104}$$

- If $0 \leq m \leq d - 1$, one has $\omega_i^d(\boldsymbol{\eta}) = \omega_d^\star(1 + e_d^{1\overline{m}\star})$ and gets

$$f_d^{1\overline{m}\star} = \frac{x}{1+x}e_d^{1\overline{m}\star} + \frac{\omega_m^\star}{\omega_d^\star}\frac{1}{1+x} - \frac{1}{1+x}. \tag{5.105}$$

– Consider the case $0 \leq n \leq d - 1$: equation (5.83) becomes $-\omega_i^n(\boldsymbol{\eta}) + x\kappa_i^n(\boldsymbol{\eta}) = a_{m+1} - a_{n+1}$.

- If $m \geq d$, one has $-\omega_n^\star + x\kappa^\star(1 + f_n^{\star\overline{n}1}) = -a_{n+1}$ and gets

$$f_n^{\star\overline{n}1} = \frac{1}{1+x}e_d^{1\overline{n}\star} + \frac{\omega_n^\star}{\omega_d^\star}\frac{x}{1+x} - \frac{x}{1+x}. \tag{5.106}$$

- If $0 \leq m \leq d - 1$, one has $-\omega_n^\star(1 + e_n^{1\overline{m}\star}) + x\kappa^\star(1 + f_n^{\star\overline{m}1} + f_n^{\star\overline{n}1}) = a_{m+1} - a_{n+1}$. Notice in the previous case that $-\omega_n^\star + x\kappa^\star(1 + f_n^{\star\overline{n}1}) = -a_{n+1}$. Thus, $-\omega_n^\star e_n^{1\overline{m}\star} + x\kappa^\star f_n^{\star\overline{m}1} = a_{m+1}$ which gives

$$f_n^{\star\overline{m}1} = -\frac{1}{1+x}e_d^{1\overline{m}\star} + \frac{\omega_n^\star}{\omega_d^\star}e_n^{1\overline{m}1} + \frac{\omega_n^\star}{\omega_d^\star}\frac{1}{1+x} - \frac{1}{1+x} \tag{5.107}$$

where $e_n^{1\overline{m}1}$ can be computed by the recurrence relation (5.102).

Thus, one obtains

$$\begin{cases} f_d^{1\overline{k}\star} = \dfrac{x}{1+x}e_d^{1\overline{k}\star} + \dfrac{\omega_k^\star}{\omega_d^\star}\dfrac{1}{1+x} - \dfrac{1}{1+x}, & \text{for } k = 0, ..., d-1, \\[3mm] f_k^{\star\overline{k}1} = \dfrac{1}{1+x}e_d^{1\overline{k}\star} + \dfrac{\omega_k^\star}{\omega_d^\star}\dfrac{x}{1+x} - \dfrac{x}{1+x}, & \text{for } k = 0, ..., d-1, \\[3mm] f_k^{\star\overline{j}1} = -\dfrac{1}{1+x}e_d^{1\overline{j}\star} + \dfrac{\omega_k^\star}{\omega_d^\star}e_k^{1\overline{j}1} + \dfrac{\omega_k^\star}{\omega_d^\star}\dfrac{1}{1+x} - \dfrac{1}{1+x}, & \text{for } k, j = 0, ..., d-1. \end{cases} \tag{5.108}$$

where $x = \dfrac{\omega_d^\star}{\kappa^\star}$.

We have considered all the cases of m_{i-1} and m_i that are related to finding values of parameters appearing in the release rate (5.83). Hence if those parameters satisfy the constraints in (5.108) then (5.83) holds for all allowed configurations. In other words, we have the following lemma.

Lemma 5.4. *With values $f_k^{1\overline{j}\star}$, $f_k^{\star\overline{k}1}$ for $k, j = 0, ..., d-1$, satisfying constraints in (5.108), equation (5.83) holds for all allowed configurations.*

Notice that the constraints in (5.103) and (5.108) must be satisfied to ensure the stationarity. This and Lemmas 5.3 and 5.4 yield altogether Theorem 1.5; we formulate it below:

Theorem 5.3. *For the process defined in **Model 2** in this chapter, the conditions (5.103) and (5.108) upon its dynamics rates (5.10) and (5.11) are sufficient for its stationary distribution to*

be of the form (5.3). In this case, the stationary distribution acquires the following expression

$$\hat{\pi}(\boldsymbol{\eta}) = \frac{1}{Z_{d,L}} \left(\frac{\omega_d^\star}{\kappa^\star}\right)^{\sum_{i=1}^N -3/2 + s_i} \prod_{k=1}^d \left(\prod_{j=k}^d \frac{\omega_d^\star}{\omega_j^\star} \left(1 + e_d^{1\overline{j-1}\star}\right)\right)^{-\sum_{i=1}^N \delta_{x_{i+1}, x_i + \ell + k - 1}^L} \tag{5.109}$$

where $Z_{d,L}$ is the partition function.

5.3   Properties of RNAP model

In this section, it is convenient to work with the grand-canonical ensemble defined by

$$\tilde{\pi}_{gc}(\boldsymbol{\zeta}) = \frac{1}{Z_{gc}} \prod_{i=1}^N (x^{-3/2 + s_i} y_1^{\theta_i^0} y_2^{\theta_i^1} \cdots y_d^{\theta_i^{d-1}} z^{m_i}), \tag{5.110}$$

where $Z_{gc} = (Z_1 Z_2)^N$ with

$$Z_1 = y_1 + y_2 z + \dots + y_d z^{d-1} + \frac{z^d}{1 - z}, \quad Z_2 = x^{1/2} + x^{-1/2}. \tag{5.111}$$

We shall show that the grand-canonical ensemble is well-defined in the sense that one can always select a value of fugacity z such that for a given density of RNAP it will hold that $Z_{gc} < \infty$. This amounts to finding z which satisfies $0 \le z < 1$.

Remark 5.4. *Notice that the processes defined for Model 1 and Model 2 have invariant distributions with the same form (5.3). Hence, the grand-canonical measure (5.110) above is defined for both models as well. However, for each model, the values of x and $y_1, ..., y_k$ are different because of the difference in the transition rates.*

5.3.1   Mean headway

Lemma 5.5. *The stationary mean headway of the process is the following*

$$\langle m_i \rangle = \frac{\left(y_2 z + 2 y_3 z^2 + \dots + (d-1) y_d z^{d-1}\right)(1-z)^2 + (d z^d - (d-1) z^{d+1})}{(y_1 + y_2 z + \dots + y_d z^{d-1})(1-z)^2 + z^d(1-z)}. \tag{5.112}$$

Proof. From the grand-canonical distribution (5.110), one obtains the mean headway. Namely, for $i = 1, ..., N$, one has

$$\langle m_i \rangle = \sum_{\boldsymbol{\zeta}} m_i \tilde{\pi}_{gc}(\boldsymbol{\zeta})$$

$$= \sum_{\boldsymbol{\zeta}} m_i \frac{1}{Z_{gc}} \prod_{j=1}^N (x^{-3/2 + s_j} y_1^{\theta_j^0} y_2^{\theta_j^1} \cdots y_d^{\theta_j^{d-1}} z^{m_j})$$

$$= \frac{z}{Z_{gc}} \sum_{\zeta} \prod_{j=1,j\neq i}^{N} (x^{-3/2+s_j} y_1^{\theta_j^0} y_2^{\theta_j^1} \cdots y_d^{\theta_j^{d-1}} z^{m_j})(x^{-3/2+s_i} y_1^{\theta_i^0} y_2^{\theta_i^1} \cdots y_d^{\theta_i^{d-1}})(m_i z^{m_i-1})$$

$$= \frac{z}{Z_{gc}} \sum_{\zeta} \prod_{j=1,j\neq i}^{N} (x^{-3/2+s_j} y_1^{\theta_j^0} y_2^{\theta_j^1} \cdots y_d^{\theta_j^{d-1}} z^{m_j})(x^{-3/2+s_i} y_1^{\theta_i^0} y_2^{\theta_i^1} \cdots y_d^{\theta_i^{d-1}})(z^{m_i})'.$$

Notice that $\langle m_1 \rangle = \cdots = \langle m_N \rangle$ which implies

$$N \langle m_i \rangle = \frac{z}{Z_{gc}} \sum_{i=1}^{N} \sum_{\zeta} \prod_{j=1,j\neq i}^{N} (x^{-3/2+s_j} y_1^{\theta_j^0} y_2^{\theta_j^1} \cdots y_d^{\theta_j^{d-1}} z^{m_j})(x^{-3/2+s_i} y_1^{\theta_i^0} y_2^{\theta_i^1} \cdots y_d^{\theta_i^{d-1}})(z^{m_i})'.$$

From the fact that

$$\sum_{i=1}^{N} \sum_{\zeta} \prod_{j=1,j\neq i}^{N} (x^{-3/2+s_j} y_1^{\theta_j^0} y_2^{\theta_j^1} \cdots y_d^{\theta_j^{d-1}} z^{m_j})(x^{-3/2+s_i} y_1^{\theta_i^0} y_2^{\theta_i^1} \cdots y_d^{\theta_i^{d-1}})(z^{m_i})' = (Z_{gc})'_z.$$

which yields

$$\langle m_i \rangle = \frac{1}{N} z \frac{\mathrm{d}}{\mathrm{d}z} \ln Z_{gc}. \tag{5.113}$$

Thus, one obtains

$$\langle m_i \rangle = \frac{\left(y_2 z + 2y_3 z^2 + \ldots + (d-1)y_d z^{d-1}\right)(1-z)^2 + (dz^d - (d-1)z^{d+1})}{(y_1 + y_2 z + \ldots + y_d z^{d-1})(1-z)^2 + z^d(1-z)}. \tag{5.114}$$

This competes the proof. $\square$

Lemma 5.6. *The grand-canonical ensemble* (5.110) *is well-defined.*

Proof. On the one hand, one has the mean headway quantity (5.112). On the other hand, this is the mean available empty space on the lattice $L - \ell N$ per rod which gives

$$\langle m_i \rangle = \frac{L - \ell N}{N} = \frac{1}{\rho} - \ell, \tag{5.115}$$

where $\rho = \frac{N}{L}$ is the RNAP density.

Comparing (5.112) and (5.115) gives us the auxiliary variable z which is the solution of the following equation

$$\frac{\left(y_2 z + 2y_3 z^2 + \ldots + (d-1)y_d z^{d-1}\right)(1-z)^2 + (dz^d - (d-1)z^{d+1})}{(y_1 + y_2 z + \ldots + y_d z^{d-1})(1-z)^2 + z^d(1-z)} = \frac{1}{\rho} - \ell \tag{5.116}$$

We prove that the above equation has a solution $0 \le z < 1$. Set

$$f(z) = \frac{\left(y_2 z + 2y_3 z^2 + ... + (d-1)y_d z^{d-1}\right)(1-z)^2 + (dz^d - (d-1)z^{d+1})}{(y_1 + y_2 z + ... + y_d z^{d-1})(1-z)^2 + z^d(1-z)} - \left(\frac{1}{\rho} - \ell\right).$$
(5.117)

One notice that $f(0)f(1^-) < 0$. Thus, (5.116) has a solution belonging to $(0,1)$ which implies that the grand-canonical ensemble is well-defined. This completes the proofs. $\square$

Remark 5.5. *Since for any given RNAP density ρ, one can find the fugacity z that solves the equation (5.116), thus z is as a function of $\rho, y_1, ..., y_d$. Since it is difficult to find the close form of the dependence of z upon the model parameters, we shall use numerical methods; all the plots in this chapter come from numeric computer calculations.*

5.3.2   Average excess and dwell time

As in Chapters 3 and 4, from the grand-canonical stationary distribution (5.110) one can compute the average excess density

$$\sigma = \frac{\langle N^1 \rangle - \langle N^2 \rangle}{L} = -\frac{k_B T}{L}\frac{d}{d\lambda}\ln Z_{gc} = \frac{1-x}{1+x}\rho.$$
(5.118)

Thus one gets the densities of each RNAP state

$$\rho^1 = \langle \delta_{s_i,1} \rangle = \frac{1}{1+x}\rho, \qquad \rho^2 = \langle \delta_{s_i,2} \rangle = \frac{x}{1+x}\rho.$$
(5.119)

Due to ergodicity, this ensemble average is proportional to the average fraction of dwell times $\tau^\alpha = \rho^\alpha/\rho$ that the RNAP spends in state $1, 2$. Thus

$$\tau^1 = \frac{1}{1+x}, \quad \tau^2 = \frac{x}{1+x}.$$
(5.120)

Using the expression for x that followed from the requirement of stationary we arrive at the balance equation

$$\frac{\rho^1}{\rho^2} = \frac{\tau^1}{\tau^2} = \frac{\kappa^\star}{\omega^\star}$$
(5.121)

for Model 1 and

$$\frac{\rho^1}{\rho^2} = \frac{\tau^1}{\tau^2} = \frac{\kappa^\star}{\omega_d^\star}$$
(5.122)

for Model 2, which expresses the ensemble ratio in terms of the single-RNAP translocation rate $\omega^\star$ (Model 1), $\omega_d^\star$ (Model 2), and the single-RNAP PP_i release rate $\kappa^\star$ (for both models).

5.3.3   RNAP headway distribution

Denote by $P_h(r)$ the distribution of the headway between the front of a trailing rod i and the back of a leading rod $i+1$. It means $P_h(r) = \frac{1}{\rho} \left\langle \delta_{x_{i+1}-x_i-\ell,r} \right\rangle = \langle \theta_i^r \rangle$.

Lemma 5.7. *The distribution of the headway of the process is the following*

$$P_h(r) = \begin{cases} \dfrac{y_{r+1}z^r(1-z)}{(y_1 + y_2 z + \ldots + y_d z^{d-1})(1-z) + z^d} & \text{for } r = 0, \ldots, d-1, \\ \dfrac{z^r(1-z)}{(y_1 + y_2 z + \ldots + y_d z^{d-1})(1-z) + z^d} & \text{for } r \geq d. \end{cases} \tag{5.123}$$

Proof. Denote by $\boldsymbol{\zeta} = (\zeta_1, \ldots, \zeta_N)$ the configuration of RNAPs and $f = Z_1 Z_2$. For $r = 0, \ldots, d-1$, one gets

$$\langle \theta_i^r \rangle = \sum_{\boldsymbol{\zeta}} \theta_i^r \tilde{\pi}_{gc}(\boldsymbol{\zeta})$$

$$= \frac{1}{Z_{gc}} \sum_{\boldsymbol{\zeta}} \theta_i^r \prod_{j=1}^N (x^{-3/2+s_j} y_1^{\theta_j^0} y_2^{\theta_j^1} \cdots y_d^{\theta_j^{d-1}} z^{m_j})$$

$$= \frac{1}{Z_{gc}} \sum_{\zeta_1} \cdots \sum_{\zeta_N} \theta_i^r \prod_{j=1}^N (x^{-3/2+s_j} y_1^{\theta_j^0} y_2^{\theta_j^1} \cdots y_d^{\theta_j^{d-1}} z^{m_j})$$

$$= \frac{1}{f^N} \sum_{\zeta_1} \cdots \sum_{\zeta_N} \theta_i^r \prod_{j=1}^N (x^{-3/2+s_j} y_1^{\theta_j^0} y_2^{\theta_j^1} \cdots y_d^{\theta_j^{d-1}} z^{m_j})$$

$$= \prod_{j=1, j\neq i}^N \left(\frac{1}{f} \sum_{\zeta_j} x^{-3/2+s_j} y_1^{\theta_j^0} y_2^{\theta_j^1} \cdots y_d^{\theta_j^{d-1}} z^{m_j} \right) \left(\frac{1}{f} \sum_{\zeta_i} \theta_i^r x^{-3/2+s_i} y_1^{\theta_i^0} y_2^{\theta_i^1} \cdots y_d^{\theta_i^{d-1}} z^{m_i} \right).$$

One has here that

$$\frac{1}{f} \sum_{\zeta_j} x^{-3/2+s_j} y_1^{\theta_j^0} y_2^{\theta_j^1} \cdots y_d^{\theta_j^{d-1}} z^{m_j} = 1, \text{ for all } j. \tag{5.124}$$

and

$$\frac{1}{f} \sum_{\zeta_i} \theta_i^r x^{-3/2+s_i} y_1^{\theta_i^0} y_2^{\theta_i^1} \cdots y_d^{\theta_i^{d-1}} z^{m_i} = \frac{1}{f} \left(y_{r+1} \frac{\mathrm{d}}{\mathrm{d} y_{r+1}} \right) \sum_{\zeta_i} x^{-3/2+s_i} y_1^{\theta_i^0} y_2^{\theta_i^1} \cdots y_d^{\theta_i^{d-1}} z^{m_i}$$

$$= y_{r+1} \frac{1}{f} \frac{\mathrm{d}}{\mathrm{d} y_{r+1}} f.$$

Hence,

$$\langle \theta_i^r \rangle = y_{r+1} \frac{1}{f} \frac{\mathrm{d}}{\mathrm{d} y_{r+1}} f = \frac{y_{r+1} z^r}{Z_1} = \frac{y_{r+1} z^r (1-z)}{(y_1 + y_2 z + \ldots + y_d z^{d-1})(1-z) + z^d}. \tag{5.125}$$

Now we compute $\langle \theta_i^r \rangle$ for $r \geq d$.

$$\langle \theta_i^r \rangle = \sum_{\boldsymbol{\zeta}} \theta_i^r(\boldsymbol{\zeta}) \tilde{\pi}_{gc}(\boldsymbol{\zeta})$$

$$= \frac{1}{Z_{gc}} \sum_{\boldsymbol{\zeta}} \theta_i^r \prod_{j=1}^{N} (x^{-3/2+s_j} y_1^{\theta_j^0} y_2^{\theta_j^1} \cdots y_d^{\theta_j^{d-1}} z^{m_j})$$

$$= \frac{1}{Z_{gc}} \sum_{\zeta_1} \cdots \sum_{\zeta_N} \theta_i^r \prod_{j=1}^{N} (x^{-3/2+s_j} y_1^{\theta_j^0} y_2^{\theta_j^1} \cdots y_d^{\theta_j^{d-1}} z^{m_j})$$

$$= \frac{1}{f^N} \sum_{\zeta_1} \cdots \sum_{\zeta_N} \theta_i^r \prod_{j=1}^{N} (x^{-3/2+s_j} y_1^{\theta_j^0} y_2^{\theta_j^1} \cdots y_d^{\theta_j^{d-1}} z^{m_j})$$

$$= \prod_{j=1,j\neq i}^{N} \left(\frac{1}{f} \sum_{\zeta_j} x^{-3/2+s_j} y_1^{\theta_j^0} y_2^{\theta_j^1} \cdots y_d^{\theta_j^{d-1}} z^{m_j} \right) \left(\frac{1}{f} \sum_{\zeta_i} \theta_i^r x^{-3/2+s_i} y_1^{\theta_i^0} y_2^{\theta_i^1} \cdots y_d^{\theta_i^{d-1}} z^{m_i} \right).$$

Using again identity (5.124) and noticing that $\theta_i^r = 1$ implies $\theta_i^k = 0$ for $k = 0, ..., d-1$ and $z^{m_i} = z^r$, one gets

$$\langle \theta_i^r \rangle = \frac{1}{f} \sum_{\zeta_i} \theta_i^r x^{-3/2+s_i} y_1^{\theta_i^0} y_2^{\theta_i^1} \cdots y_d^{\theta_i^{d-1}} z^{m_i} \tag{5.126}$$

$$= \frac{1}{f} z^r \sum_{\zeta_i} x^{-3/2+s_i}. \tag{5.127}$$

Finally, one notices that

$$\sum_{\zeta_i} x^{-3/2+s_i} = x^{-1/2} + x^{1/2}. \tag{5.128}$$

Therefore,

$$\langle \theta_i^r \rangle = \frac{z^r}{Z_1} = \frac{z^r(1-z)}{(y_1 + y_2 z + ... + y_d z^{d-1})(1-z) + z^d}. \tag{5.129}$$

From the above computations, one gets

$$P_h(r) = \begin{cases} \dfrac{y_{r+1} z^r(1-z)}{(y_1 + y_2 z + ... + y_d z^{d-1})(1-z) + z^d} & \text{for } r = 0, ..., d-1, \\[3mm] \dfrac{z^r(1-z)}{(y_1 + y_2 z + ... + y_d z^{d-1})(1-z) + z^d} & \text{for } r \geq d. \end{cases} \tag{5.130}$$

This completes the proof. □

We now proceed to plotting the headway distribution. Since the cases $d = 1, 2$ have been considered in the previous chapters, we only focus on the case $d = 3$. Let us

rewrite the headway distribution for the case $d = 3$ as follows

$$P_h(r) = \begin{cases} \dfrac{y_{r+1}z^r(1-z)}{(y_1 + y_2 z + y_3 z^2)(1-z) + z^3} & \text{for } r = 0, 1, 2, \\[4mm] \dfrac{z^r(1-z)}{(y_1 + y_2 z + y_3 z^2)(1-z) + z^3} & \text{for } r \geq 3. \end{cases} \tag{5.131}$$

One can see from (5.131) that $P_h(r)$ decreases when $r \geq 3$ since $z \leq 1$. Let us plot some graphs of the headway distribution function with some choices of parameters y_1, y_2, and y_3.

– Case $y_1 > y_2 > y_3$: See the Fig.5.2.

(a) $y_1 = 20, y_2 = 5, y_3 = 2$

(b) $y_1 = 10, y_2 = 9, y_3 = 3$

(c) $y_1 = 1.5, y_2 = 0.7, y_3 = 0.2$

(d) $y_1 = 0.9, y_2 = 0.7, y_3 = 0.5$

Figure 5.2: *RNAP headway distribution $P_h(r)$ for different interaction strengths $y_1 > y_2 > y_3$ as a function of the integer lattice distance. The curves joining the data points are guides to the eye.*

Remark 5.6. *Using (5.131) for $P_h(r)$ and the fact that $P_h(r)$ decreases when $r \geq 3$, as it happens for $z < 1$, one has also in this case $y_1 > y_2 > y_3$, $P_h(0) > P_h(1) > P_h(2)$.*

– Case $y_1 < y_2 < y_3$: See the Fig. 5.3 and 5.4.

Figure 5.3: *RNAP headway distribution $P_h(r)$ for different interaction strengths $y_1 < y_2 < y_3$ with $y_3 < 1$ as a function of the integer lattice distance. The curves joining the data points are guides to the eye.*

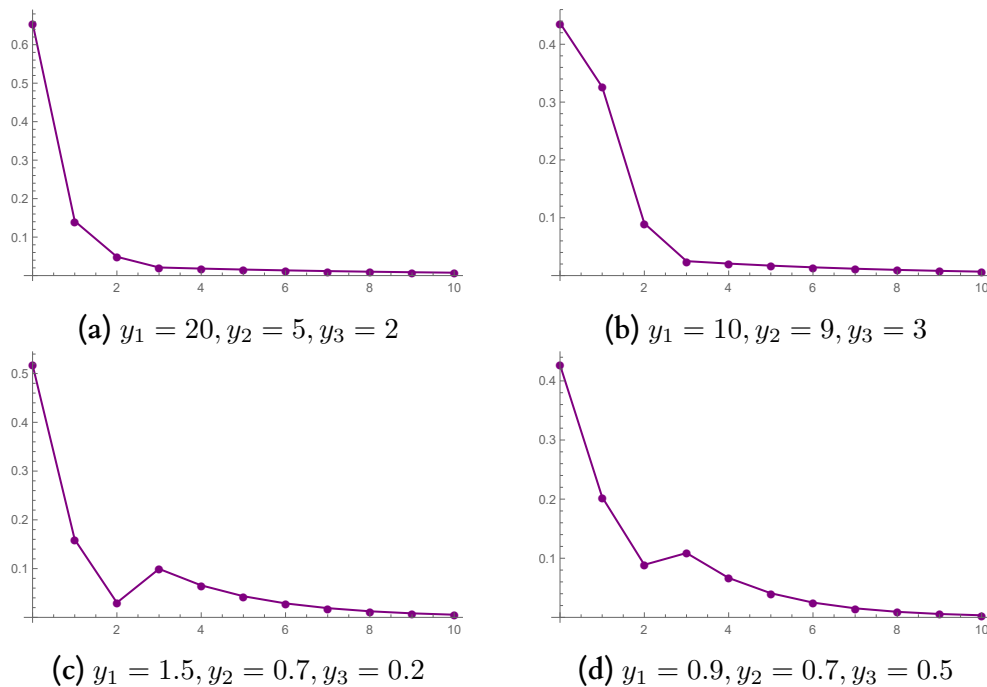**Figure 5.4:** *RNAP headway distribution $P_h(r)$ for different interaction strengths $y_1 < y_2 < y_3$ with $y_1 > 1$ as a function of the integer lattice distance. The curves joining the data points are guides to the eye.*

- The case in which y_2 is the greatest distance among those expressed by y_1, y_2, y_3: See the Fig. 5.5.

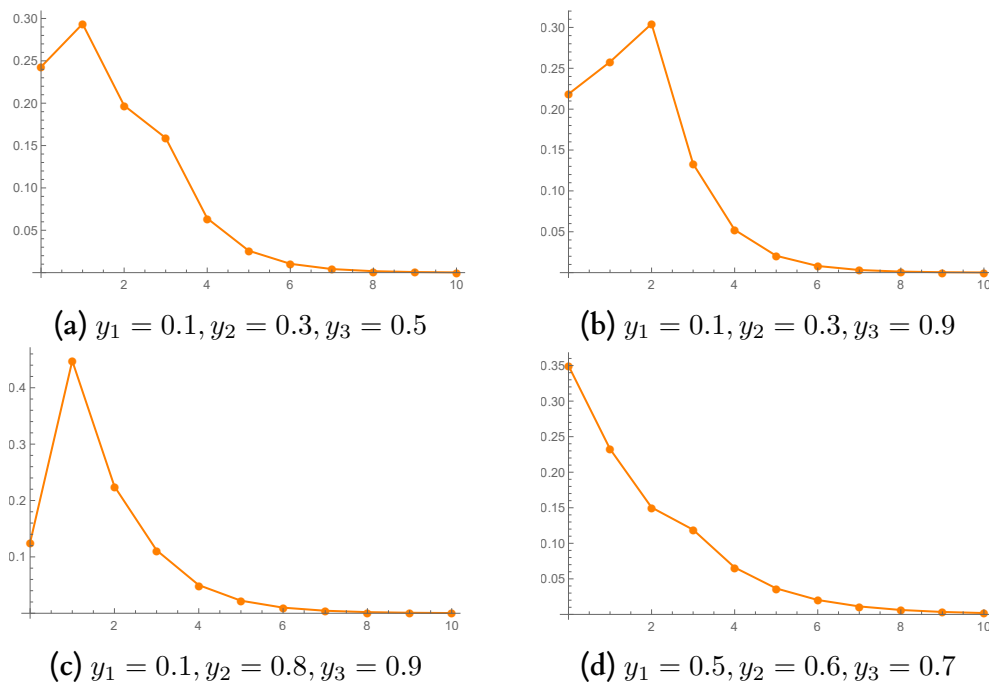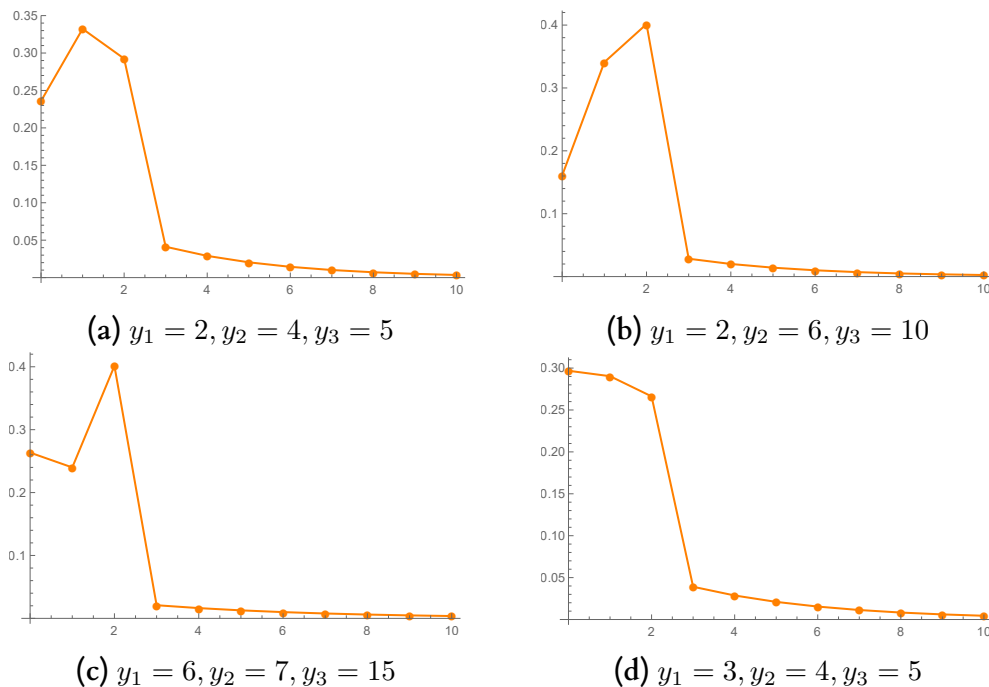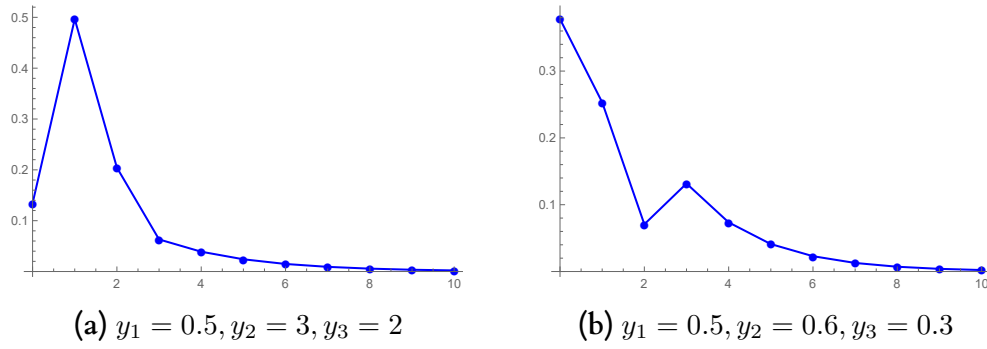(a) $y_1 = 0.5, y_2 = 3, y_3 = 2$ (b) $y_1 = 0.5, y_2 = 0.6, y_3 = 0.3$

Figure 5.5: *RNAP headway distribution $P_h(r)$ for different interaction strengths y_1, y_2, y_3 where y_2 is the greatest as a function of the integer lattice distance. The curves joining the data points are guides to the eye.*

5.3.4 Elongation rate

Since Model 2 for the case $d = 2$ and Model 1 for the case $e^{1\star} \neq 0$ are considered intensively in Chapter 4 and paper [4] respectively, we only focus on Model 1 with $e^{1\star} = 0$ for the cases $d = 2$ and $d = 3$.

Recall that the average flux and the average speed are related by

$$j = \rho\nu \tag{5.132}$$

Here the average flux j is the expectation of translocation rate $\omega_i(\boldsymbol{\eta})$ in the stationary distribution (5.3) which gives the total elongation rate.

From the work of Wang et al [32] one can compute the mean velocity of an isolated RNAP

$$\nu^\star = \frac{\omega^\star \kappa^\star}{\omega^\star + \kappa^\star} = \frac{1}{1+x}\omega^\star. \tag{5.133}$$

It is important to notice that the velocity of a single random walk is $\nu_0^\star = \omega^\star$ and that it is different from the expression (5.133) by the prefactor $1/(1+x)$ which is the mean dwell time that RNAP spent in the mobile state 1.

Using the factorization property of the stationary distribution, one can compute the average velocity and flux of the process.

$$j = \rho^1 \omega^\star \langle (1 + \sum_{k=1}^{d} e^{\star \overline{k} 1} \theta_i^k)(1 - \theta_i^0) \rangle \tag{5.134}$$

$$= \rho^1 \omega^\star (1 + \sum_{k=1}^{d} e^{\star \overline{k} 1} \langle \theta_i^k \rangle)(1 - \langle \theta_i^0 \rangle). \tag{5.135}$$

One has $\nu^\star = \dfrac{\rho^1}{\rho}\omega^\star$ and

$$\nu = A(e^{\star\overline{1}1}, ..., e^{\star\overline{d}1}, \rho)\nu^\star. \tag{5.136}$$

where $A(e^{\star\overline{1}1}, ..., e^{\star\overline{d}1}, \rho) = \langle(1 + \sum_{k=1}^{d} e^{\star\overline{k}1}\theta_i^k)(1 - \theta_i^0)\rangle$ is RNAP velocity amplitude.

– Case $d = 2$**:** One has

$$\nu = \langle(1 + e^{\star\overline{1}1}\theta_i^1 + e^{\star\overline{2}1}\theta_i^2)(1 - \theta_i^0)\rangle$$
$$= (1 + e^{\star\overline{1}1}\langle\theta_i^1\rangle + e^{\star\overline{2}1}\langle\theta_i^2\rangle)(1 - \langle\theta_i^0\rangle). \tag{5.137}$$

Recall that $y_1 = (1 + e^{\star\overline{1}1})(1 + e^{\star\overline{2}1})$, $y_2 = 1 + e^{\star\overline{2}1}$. Thus, the average velocity amplitude is a function of y_1, y_2 and RNAP density ρ.

(a) *Velocity amplitude*   (b) *Flux amplitude*

Figure 5.6: *RNAP velocity and flux amplitudes with interaction strength $y_1^{-1} = 1.5$, $y_2^{-1} = 1.2$. The dotted reference line corresponds to non-interacting RNAPs.*

(a) *Velocity amplitude*   (b) *Flux amplitude*

Figure 5.7: *RNAP velocity and flux amplitudes with interaction strength $y_1^{-1} = 5$, $y_2^{-1} = 1.2$. The dotted reference line corresponds to non-interacting RNAPs.*

(a) *Velocity amplitude*   (b) *Flux amplitude*

Figure 5.8: *RNAP velocity and flux amplitudes with interaction strength $y_1^{-1} = 20, y_2^{-1} = 1.2$. The dotted reference line corresponds to non-interacting RNAPs.*

(a) *Velocity amplitude*   (b) *Flux amplitude*
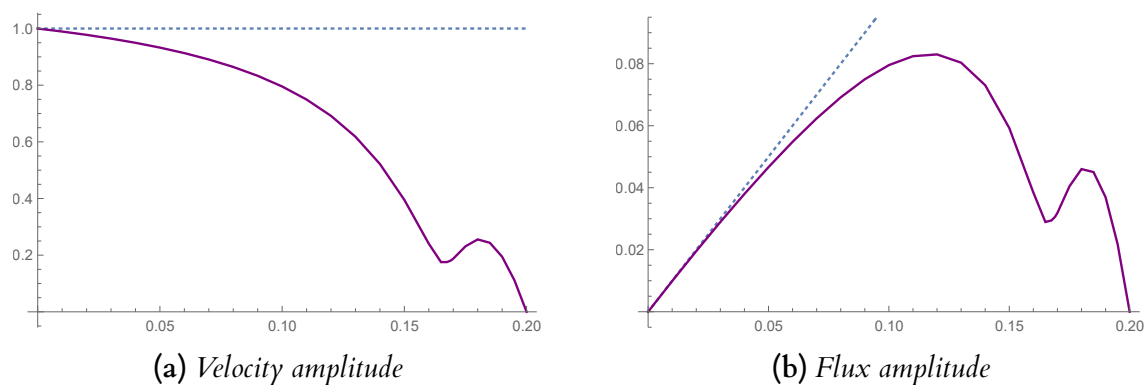
Figure 5.9: *RNAP velocity and flux amplitudes with interaction strengths $y_1^{-1} = 100, y_2^{-1} = 1.2$. The dotted reference line corresponds to non-interacting RNAPs.*

(a) *Velocity amplitude*   (b) *Flux amplitude*
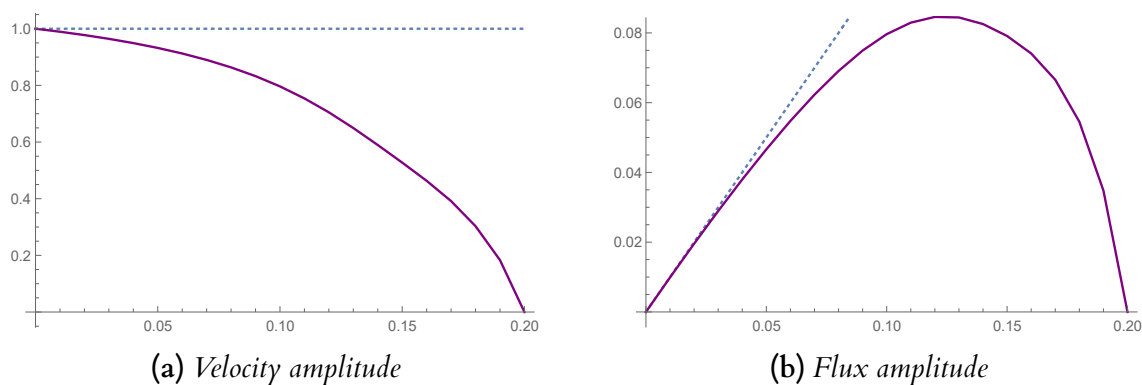
Figure 5.10: *RNAP velocity and flux amplitudes with interaction strengths $y_1^{-1} = 5, y_2^{-1} = 3$. The dotted reference line corresponds to non-interacting RNAPs.*

(a) *Velocity amplitude*   (b) *Flux amplitude*
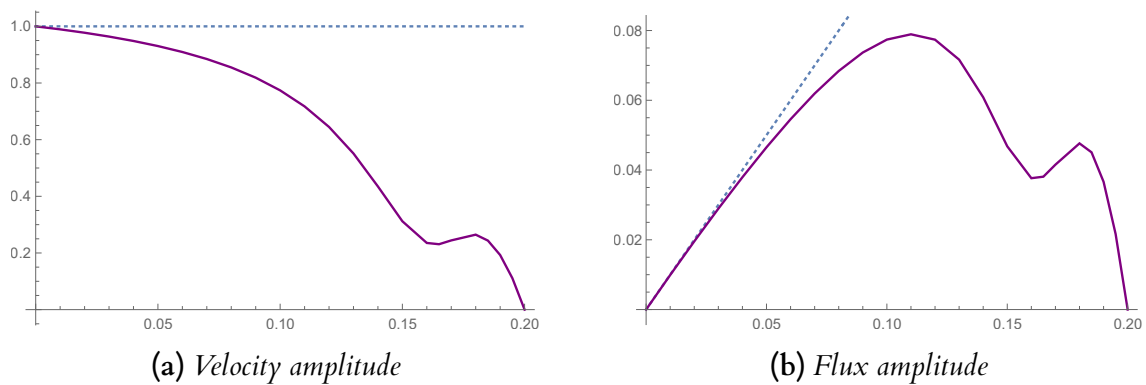
Figure 5.11: *RNAP velocity and flux amplitudes with interaction strengths $y_1^{-1} = 100, y_2^{-1} = 3$. The dotted reference line corresponds to non-interacting RNAPs.*

The following plots correspond to cases with some other choices of the parameters.

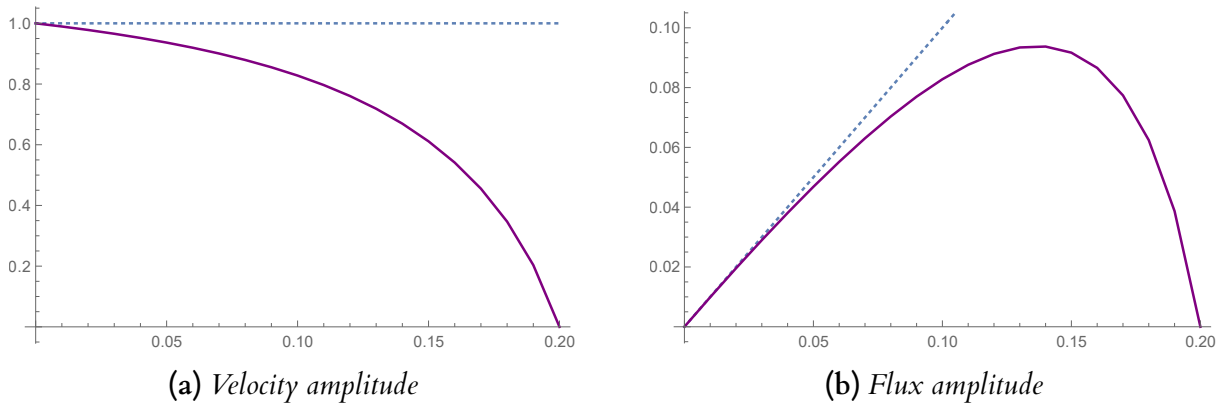(a) *Velocity amplitude*   (b) *Flux amplitude*

Figure 5.12: *RNAP velocity and flux amplitudes with interaction strengths $y_1^{-1} = 5, y_2^{-1} = 100$. The dotted reference line corresponds to non-interacting RNAPs.*

(a) *Velocity amplitude*   (b) *Flux amplitude*

Figure 5.13: *RNAP velocity and flux amplitudes with interaction strengths $y_1^{-1} = 0.4, y_2^{-1} = 100$. The dotted reference line corresponds to non-interacting RNAPs.*
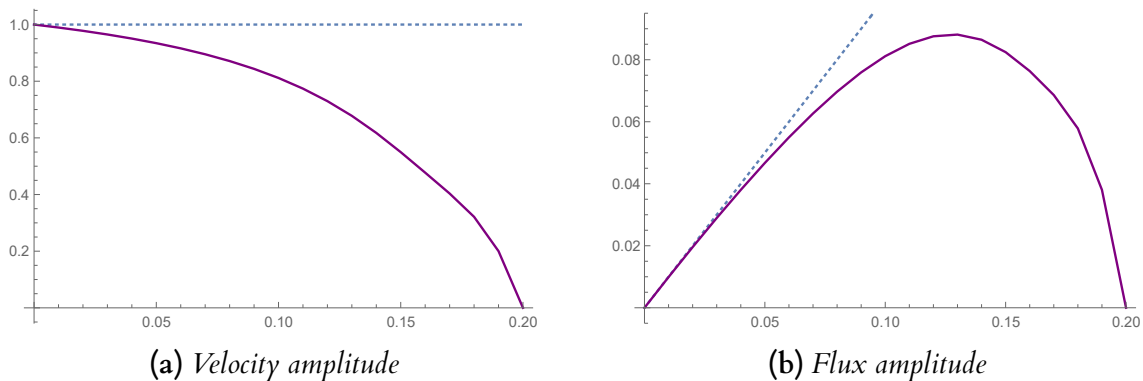
(a) *Velocity amplitude* (b) *Flux amplitude*

Figure 5.14: *RNAP velocity and flux amplitudes with interaction strengths $y_1^{-1} = 100, y_2^{-1} = 0.85$. The dotted reference line corresponds to non-interacting RNAPs.*
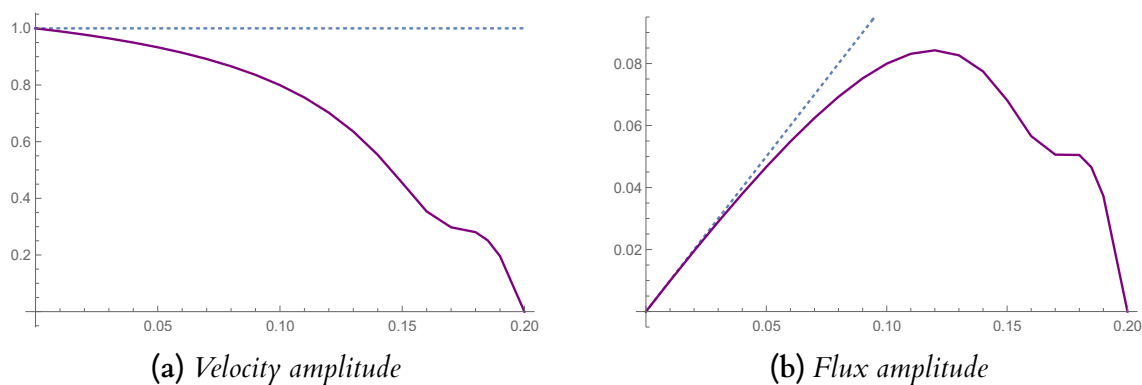

(a) *Velocity amplitude* (b) *Flux amplitude*

Figure 5.15: *RNAP velocity and flux amplitudes with interaction strengths $y_1^{-1} = 100, y_2^{-1} = 0.01$. The dotted reference lines correspond to non-interacting RNAPs.*

– Case $d = 3$**:** One has

$$\nu = \langle (1 + e^{\star \bar{1}1}\theta_i^1 + e^{\star \bar{2}1}\theta_i^2 + e^{\star \bar{3}1}\theta_i^3)(1 - \theta_i^0) \rangle \tag{5.138}$$

$$= (1 + e^{\star \bar{1}1}\langle \theta_i^1 \rangle + e^{\star \bar{2}1}\langle \theta_i^2 \rangle + e^{\star \bar{3}1}\langle \theta_i^3 \rangle)(1 - \langle \theta_i^0 \rangle) \tag{5.139}$$

Recall that $y_1 = (1 + e^{\star \bar{1}1})(1 + e^{\star \bar{2}1})(1 + e^{\star \bar{3}1})$, $y_2 = (1 + e^{\star \bar{2}1})(1 + e^{\star \bar{3}1})$, $y_3 = (1 + e^{\star \bar{3}1})$. Thus, the average velocity amplitude is a function of y_1, y_2, y_3 and RNAP density ρ.

(a) *Velocity amplitude*

(b) *Flux amplitude*

Figure 5.16: *RNAP velocity and flux amplitudes with interaction strengths $y_1^{-1} = 5, y_2^{-1} = 3, y_3^{-1} = 2$. The dotted reference line corresponds to non-interacting RNAPs.*

(a) *Velocity amplitude*
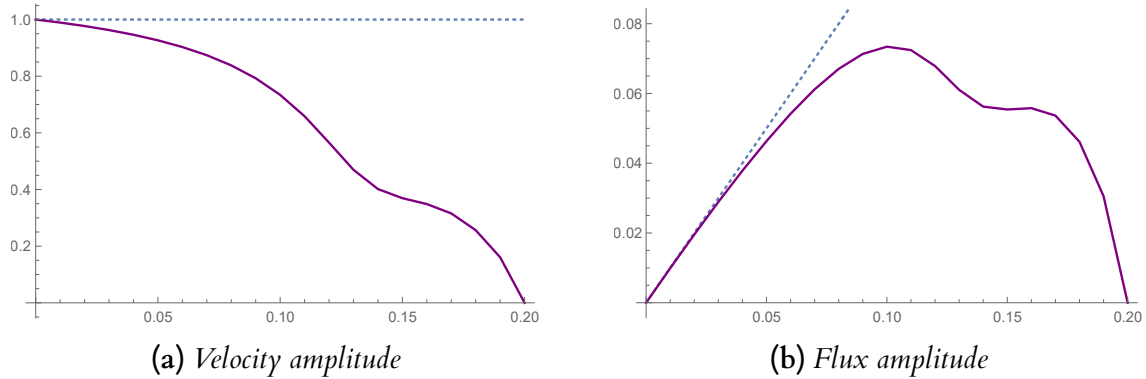
(b) *Flux amplitude*

Figure 5.17: *RNAP velocity and flux amplitudes with interaction strengths $y_1^{-1} = 50, y_2^{-1} = 20, y_3^{-1} = 2$. The dotted reference line corresponds to non-interacting RNAPs.*

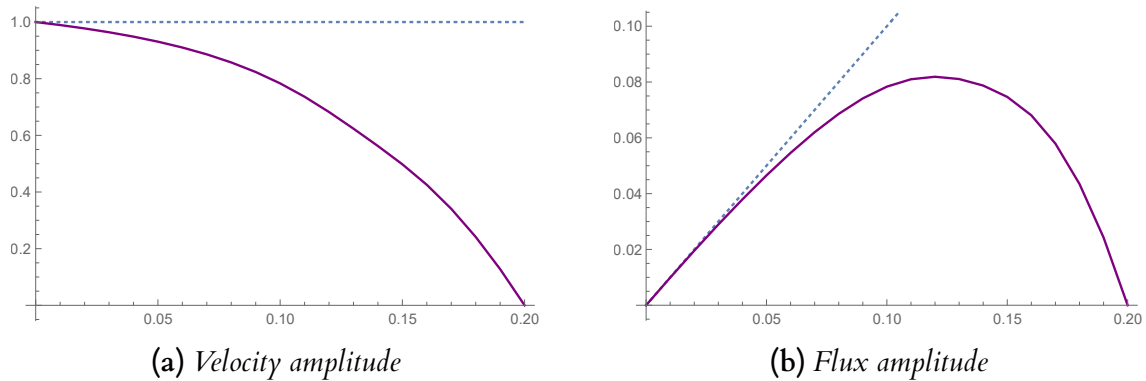(a) *Velocity amplitude*

(b) *Flux amplitude*

Figure 5.18: *RNAP velocity and flux amplitudes with interaction strengths $y_1^{-1} = 100, y_2^{-1} = 5, y_3^{-1} = 2$. The dotted reference line corresponds to non-interacting RNAPs.*
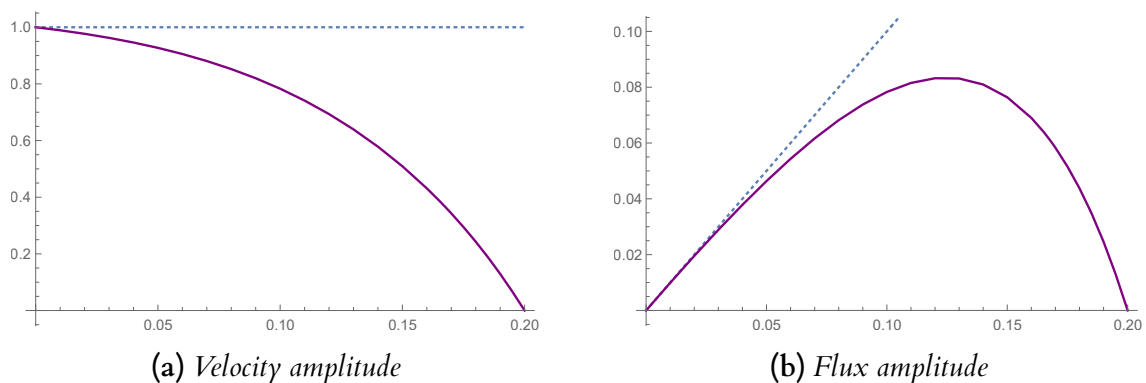
(a) *Velocity amplitude*   (b) *Flux amplitude*
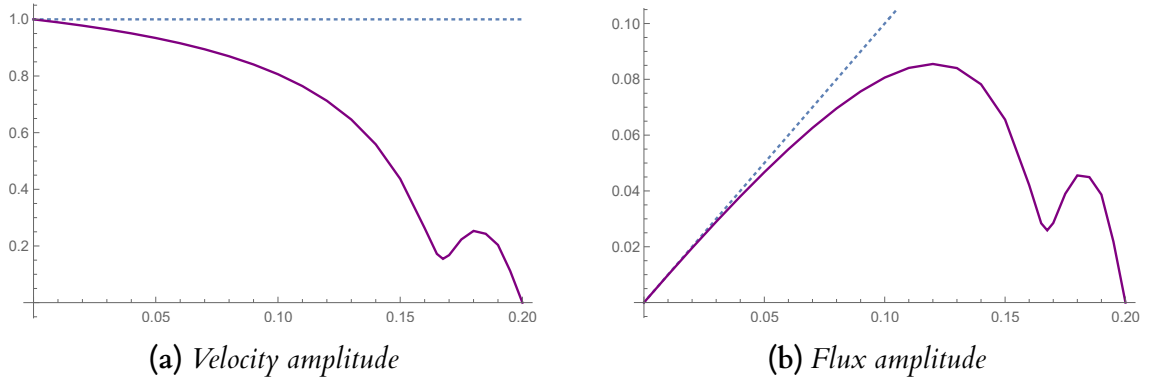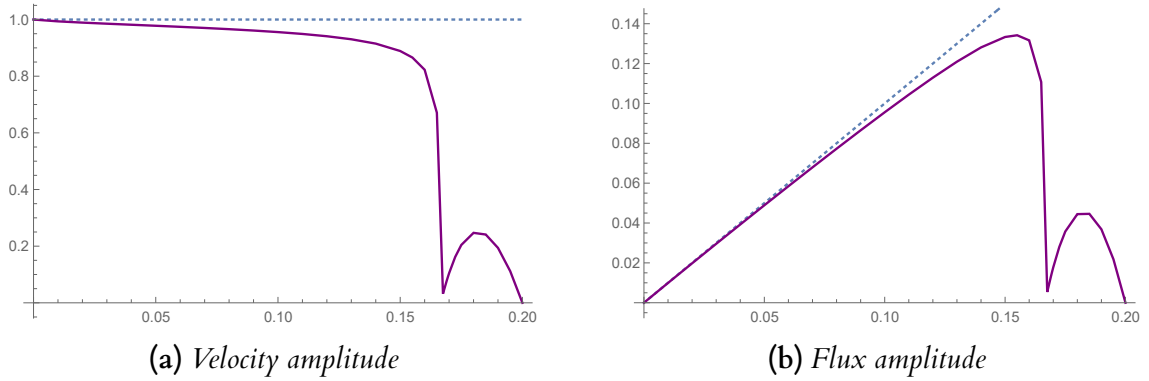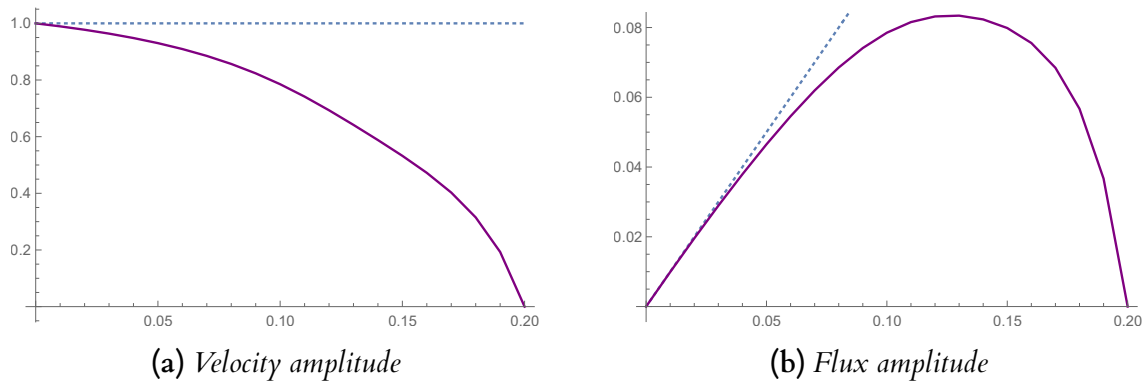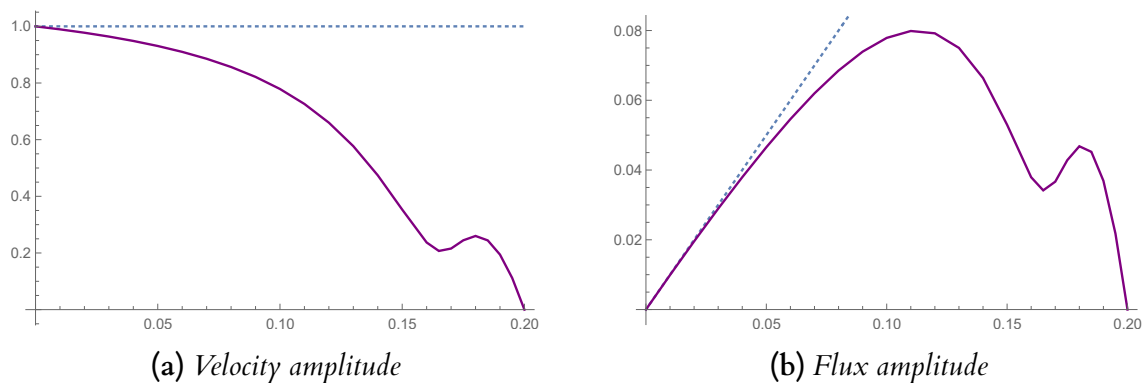
Figure 5.19: *RNAP velocity and flux amplitudes with interaction strengths* $y_1^{-1} = 100, y_2^{-1} = 1.9, y_3^{-1} = 1.2$. *The dotted reference line corresponds to non-interacting RNAPs.*
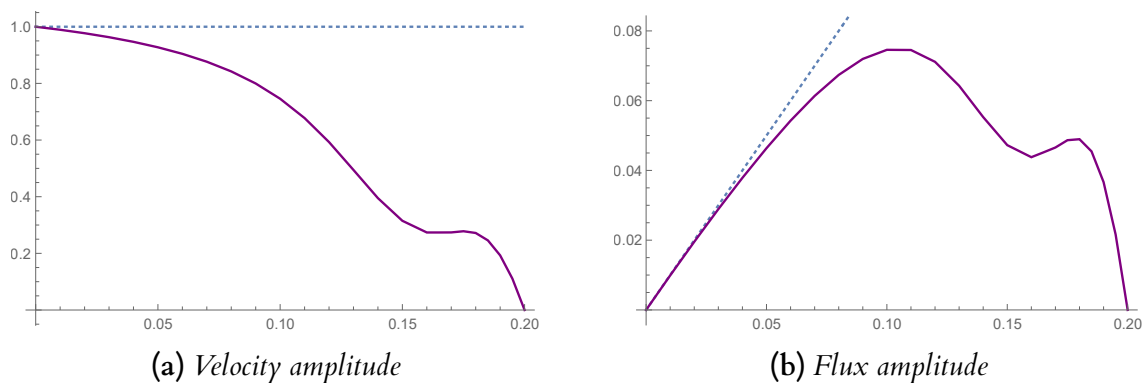
5.4   Discussion

We only discuss the case $d = 2$ for Model 1 with the choice $e^{1\star} = 0$ corresponding to the **Case b** of Model 1. The reasons to do that are the following. Firstly, the case $e^{1\star} \neq 0$ has been already considered in [4]. Secondly, the case $d = 2$ for Model 2 is the content of the previous chapter. Finally, as shown in the plots above for the cases $d = 2, 3$ of Model 1 with $e^{1\star} = 0$, the average speed and flux amplitudes are similar in both cases.

Stochastic blocking: Let us consider three situations in respect to the translocation rate $\omega_i(\boldsymbol{\eta})$ of ith RNAP when it is in state 1. The situations depend upon the position of leading RNAP, i.e., depend on distance m_i. One has that either $\omega_i(\boldsymbol{\eta}) = w^\star$ if $m_i > 2$, or $\omega_i(\boldsymbol{\eta}) = w^\star(1 + e^{\star\bar{2}1})$ if $m_i = 2$, or, finally, if $m_i = 1$ then one has $\omega_i(\boldsymbol{\eta}) = w^\star(1 + e^{\star\bar{1}1})$. The case $e^{\star\bar{1}1} < e^{\star\bar{2}1} < 0$ will be referred to as stochastic blocking enhancement or simply jamming, since, in this range of the interaction parameters $e^{\star\bar{1}1}$ and $e^{\star\bar{2}1}$, the rate of approaching to a leading RNAP is reduced as compared to the translocation rate of a single RNAP that moves in the non-interacting environment.

Cooperative pushing: Firstly, a general observation that follows from the plots presented in section 5.3.4 is that the average velocity and flux amplitudes are smaller than what they would have been if they were generated by the same number of single RNAP (dotted cure in the right panels). Secondly, if the repulsion strengths y_1^{-1} and y_2^{-1} relate to each other by $y_1^{-1} < y_2^{-1}$, see Figs. 5.12 and 5.13, then it does not lead to cooperative pushing at any density. Moreover, the average speed amplitude (left panels) is reduced as the density increases, as does also the pure hard-core repulsion. However, the total average elongation rate increases until the jamming take over at high density (right panels). Accordingly, in what follows, we shall only discuss the case $y_1^{-1} > y_2^{-1}$.

From Figs. 5.6 and 5.7, one can see that when the repulsive strengths y_1^{-1}, y_2^{-1} are "small", there is no cooperative pushing at any density. However, similar to the case $y_1^{-1} < y_2^{-1}$, the total average elongation rate increases until the jamming takes over at

high density, see Fig. 5.6 and 5.7, right panels.

When repulsive strength y_1^{-1} is large, the speed of an RNAP has an intermediate minimum at a density ρ_m. If the strength y_1^{-1} is fixed, the local minimum deepens as strength y_2^{-1} decreases. At higher densities, there is an entrance to a cooperative pushing regime, see Figs. 5.9, 5.11, 5.14, and 5.15. It is interesting that when y_1^{-1} is large and y_2^{-1} is small (close to 0), a new phenomenon appears, as Fig. 5.15 indicates. At not-so-high densities, the average velocity and flux amplitudes behave almost the same as the ones generated by a single non-interacting RNAP (dotted curves) respectively. After reaching a maximum at a density, the average flux amplitude drops quickly to an intermediate minimum which is very close to 0, and immediately after that, the cooperative pushing appears which leads to another local maximum. We suggest that the local minimums for average velocity and flux are singular points in this case.

Part III

Exclusion processes with many speeds

Chapter 6

A family of generalized Ising measures as invariant distributions for exclusion processes with many speeds

The problem addressed in this chapter is motivated by the study of Case b of Model 1 from Chapter 5. Namely, we shall consider here that model but with the length of the rod being comparable to the interaction range, i.e. $\ell = 1$, and we shall focus only at the translocation dynamics. The reason to do so is to get an insight at the RNAP density correlations. Once we achieve this aim, we shall get the information about the stationary current of the model. We stress that the model in this chapter is a generalization of the model that has been studied in Section II of [1]. We also would like to stress that instead of making an ansatz for the translocation rates, as in Chapter 5 (which means we assume that the rates have specific forms), we find the answer (to the question posed in Section 6.1.2) in the most general form. It turns out that in one special case (repulsive interaction) our model becomes the slowing-down traffic model.

6.1 A family of generalized Ising measures for a one-dimensional lattice gas

6.1.1 Totally asymmetric exclusion processes with one and two speeds

The totally asymmetric simple exclusion process (TASEP) is a system of particles hopping unidirectionally on the sites of a lattice, see [13, 20, 22, 26]. The dynamics can be represented as follows

$$10 \rightarrow 01 \text{ with rate } 1. \tag{6.1}$$

Here 1 represents a site occupied by a particle and 0 represents a vacant site. The invariant measure of this model on the finite ring $\mathbb{T}_L := \mathbb{Z}/L\mathbb{Z}$ is the uniform distribution. In the thermodynamic limit, the stationary particle current j is the following

$$j = \rho(1 - \rho). \tag{6.2}$$

where ρ is the particle density.
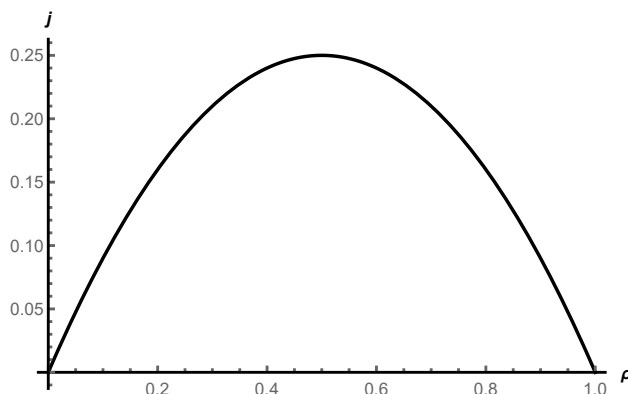
Figure 6.1: *Stationary current j as a function of the density.*

One notices, as mentioned in [1], that the dynamic (6.1) is too simple to be a realistic model for traffic flow since the average current j (6.2) is symmetric, see Fig. 6.1. In that paper, the authors introduced a next-nearest-neighbor interaction model which is a special case in the class of driven lattice gases studied in [13]. Namely, the dynamics of the process is as follows. A particle hops to the right with rate r, if the next-nearest-neighboring site is empty, and with rate q, if it is occupied. The dynamics can be represented as follows

$$
\begin{aligned}
100 &\to 010 \text{ with rate } r, \\
101 &\to 011 \text{ with rate } q.
\end{aligned}
\tag{6.3}
$$

As for the repulsive interaction, i.e., $q < r$, the model is an interpretation of the slowing-down traffic model. This means that a particle reduces its "speed", if there is another particle in front of (on the right) and close enough to (next-nearest neighboring site) it. The current-density relation of this model is asymmetric that suggests that the model describes the traffic flow more accurately, see Figure 6.3. As for the $q > r$, the dynamics describes hard-core particles with attractive short-range interactions which are driven by an external field. Note that for the case $q = r$, one recovers model (6.1).

On the ring $\mathbb{T}_L$, the stationary distribution of the process turns out to be the Ising measure with nearest-neighbor interaction energy, see [1, 23]. Namely, the stationary probability of finding the system in state $\boldsymbol{\eta} = (\eta_1, ..., \eta_L)$ where $\eta_i \in \{0, 1\}$, is given by

$$\hat{\pi}(\boldsymbol{\eta}) = \frac{1}{Z_L} \left(\frac{q}{r}\right)^{\sum_{i=1}^{L}(\eta_i \eta_{i+1} + h\eta_i)}. \tag{6.4}$$

Here Z_L is the partition function and parameter h plays the role of a chemical potential which controls the particle density. Although, grand-canonical ensemble (6.4) is the same as the Ising distribution for equilibrium system, it does not satisfy detailed balance with respect to the dynamics.

Let us say that (6.1) is a one-speed-model and (6.3) is a two-speed-model. In the same manner, we will deal with the process with many speeds which admits a generalized Ising measure as its invariant distribution. We refer a reader to [1, 4, 6, 13, 14, 21, 26] for more details about effects of different speeds observed in traffic models.

6.1.2 A family of generalized Ising measures and the question considered

We consider totally asymmetric exclusion process on the ring $\mathbb{T}_L$. We denote configurations by the array of occupation numbers $\boldsymbol{\eta} = \{\eta_1, ..., \eta_L\}$ where $\eta_k \in \{0, 1\}$. Because of periodic boundary conditions, one has $\eta_{i+mL} := \eta_i$ for $i \in \{1, ..., L\}$ and any integer $m \in \mathbb{Z}$.

A family of generalized Ising measures: Let us now introduce a family of generalized Ising measures $\hat{\pi}_d$ where $d \in \{1, 2, ..., L-1\}$ on the ring $\mathbb{T}_L$. Denote by π_d the unnormalized measure corresponding to $\hat{\pi}_d$ which is of the following form

$$\pi_d(\boldsymbol{\eta}) = \exp\left\{-\beta \sum_{i=1}^{L}\left\{\sum_{n=1}^{d} J_n \eta_i (1-\eta_{i+1})(1-\eta_{i+2})\cdots(1-\eta_{i+n-1})\eta_{i+n} + h\eta_i\right\}\right\},$$
(6.5)

where $J_1, ..., J_d$ are real numbers. The constants $\beta \in \mathbb{R}_+$ and $h \in \mathbb{R}$ play the roles of inverse temperature and of a chemical potential, respectively. Denote by $Z_{d,L}$ the partition function of measure $\hat{\pi}_d$. One has

$$Z_{d,L} = \sum_{\boldsymbol{\eta}} \pi_d(\boldsymbol{\eta}) \quad \text{and} \quad \hat{\pi}_d(\boldsymbol{\eta}) = \frac{1}{Z_{d,L}} \pi_d(\boldsymbol{\eta}).$$
(6.6)

Jump rates: Let us introduce the following notations for the jump rates: r_k is the rate of a jump to the right at distance 1 (i.e., to the nearest site on the right) of a particle of the process, when the nearest particle to its right is at the distance $k+1$ which means that the number of vacant sites between the two particles is k. Thus, r_0 is the jump rate of a particle when its rightmost nearest site is occupied by another particle. Certainly, r_0 is always 0 since we want the exclusion rule to hold true, r_1 is the jump rate of a particle when its rightmost neighboring site is free but the next site is occupied by another particle, etc.

The question addressed: Our question at hand is to find a one-dimensional totally asymmetric exclusion process on the ring $\mathbb{T}_L$ with jump rates $r_0, r_1, r_2, \ldots, r_d$, such
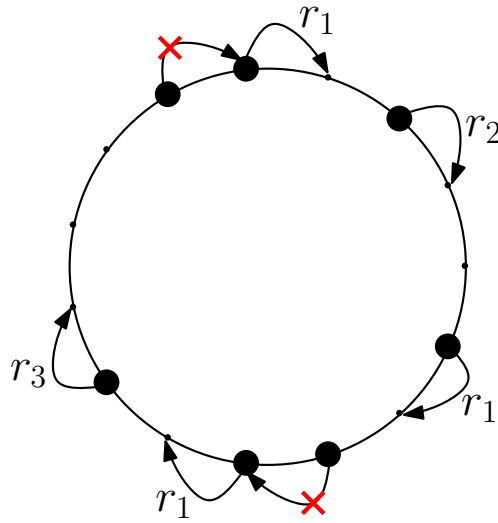
Figure 6.2: *A configuration on ring $\mathbb{T}_{15}$ with 7 particles.*

that the invariant measure of the process is $\hat{\pi}_d$.

Remark: Regarding the case where $d = 1$, our model is equivalent to the two–speed model mentioned earlier, and a solution to our question can be found in [1]. Specifically, we can set $r_1 = r \exp(-\beta J_1)$ and $r_2 = r$, where r is a free parameter. This selection of jump rates ensures that the process admits $\hat{\pi}_1$ as its invariant measure. In the more general case where d can take any value, we note that $\hat{\pi}_d$ is a special case of the measure considered in [26]. However, the process analyzed in that paper (Section 5a) is a symmetric exclusion process, which differs from the totally asymmetric exclusion process studied in this chapter. It is worth emphasizing that our process with invariant distribution $\hat{\pi}_d$ requires a model with $d + 1$ speeds, as our proof indicates that r_k for $k \geq d + 1$ must be all equal.

6.1.3   Idea for solution

Due to the periodicity, the number of particles is conserved. Assume that $\sum_{i=1}^{L} \eta_i = N$. Denote by $\mathbf{x} = (x_1, ..., x_N)$ the coordinate vector of positions of the particles in a configuration $\boldsymbol{\eta}$. Notice that the jump rate of the particle at the position x_i to the right is $r_{x_{i+1}-x_i-1}$.

The master equation finding configuration $\boldsymbol{\eta}$ associated with the coordinate vector $\mathbf{x}$ at time t is the following

$$\frac{d\mathbb{P}(\boldsymbol{\eta}, t)}{dt} = \sum_{\boldsymbol{\eta}'} \omega(\boldsymbol{\eta}' \to \boldsymbol{\eta})\mathbb{P}(\boldsymbol{\eta}', t) - \sum_{\boldsymbol{\eta}''} \omega(\boldsymbol{\eta} \to \boldsymbol{\eta}'')\mathbb{P}(\boldsymbol{\eta}, t)$$

$$= \sum_{i=1}^{N} \omega(\boldsymbol{\eta}^{x_i-1,x_i} \to \boldsymbol{\eta})\mathbb{P}(\boldsymbol{\eta}^{x_i-1,x_i}, t) - \sum_{i=1}^{N} \omega(\boldsymbol{\eta} \to \boldsymbol{\eta}^{x_i})\mathbb{P}(\boldsymbol{\eta}, t), \qquad (6.7)$$

where

- $\boldsymbol{\eta}^{x_i-1,x_i}$ is the configuration that leads to $\boldsymbol{\eta}$ before the particle of $\boldsymbol{\eta}^{x_i-1,x_i}$ at the position $x_i - 1$ hops to the right, i.e., $\eta_j^{x_i-1,x_i} = \eta_j$ for $j \neq x_i - 1, x_i$ and $\eta_j^{x_i-1,x_i} = 1 - \eta_j$ for $j = x_i - 1, x_i$,

- $\boldsymbol{\eta}^{x_i}$ is the configuration led by the configuration $\boldsymbol{\eta}$ after the particle of $\boldsymbol{\eta}$ at the position x_i hops to the right, i.e. $\eta_j^{x_i} = \eta_j$ for $j \neq x_i, x_i + 1$ and $\eta_j^{x_i} = 1 - \eta_j$ for $j = x_i, x_i + 1$.

On the one hand, one has

$$\omega(\boldsymbol{\eta}^{x_i-1,x_i} \rightarrow \boldsymbol{\eta}) = r_{x_{i+1}-x_i}(1 - \delta_{x_i-x_{i-1},1}) \tag{6.8}$$

since there does not exist the configuration $\boldsymbol{\eta}^{x_i-1,x_i}$ if $x_i - x_{i-1} = 1$ and the jump rate of the ith particle of the configuration $\boldsymbol{\eta}^{x_i-1,x_i}$ is $r_{x_{i+1}-x_i}$. On the other hand, one has

$$\omega(\boldsymbol{\eta} \rightarrow \boldsymbol{\eta}^{x_i}) = r_{x_{i+1}-x_i-1}. \tag{6.9}$$

Since π_d is the unnormalized invariant measure of the process, the master equation (6.7) reads

$$\sum_{i=1}^N \omega(\boldsymbol{\eta}^{x_i-1,x_i} \rightarrow \boldsymbol{\eta})\pi_d(\boldsymbol{\eta}^{x_i-1,x_i}) - \sum_{i=1}^N \omega(\boldsymbol{\eta} \rightarrow \boldsymbol{\eta}^{x_i})\pi_d(\boldsymbol{\eta}) = 0. \tag{6.10}$$

Dividing (6.10) by $\pi_d(\boldsymbol{\eta})$, the stationarity condition (6.10) becomes

$$\sum_{i=1}^N \left(r_{x_{i+1}-x_i}(1 - \delta_{x_i-x_{i-1},1})\frac{\pi_d(\boldsymbol{\eta}^{x_i-1,x_i})}{\pi_d(\boldsymbol{\eta})} - r_{x_{i+1}-x_i-1} \right) = 0. \tag{6.11}$$

Notice that the index i is taken modulo N, i.e., $x_{N+1} \equiv x_1$.

Strategy of finding the rates: Due to the fact that the farthest possible distance between two particles is $L-N+1$, the jump rate of a particle belongs to the set $\{r_0, r_1, ..., r_{L-N}\}$. In order to find the rates $r_1, r_2, ..., r_{L-N}$, one considers $L - N$ configurations such that $x_i = i$ for $i = 1, 2, ..., N-1$ and $x_N \in \{N, ..., L-1\}$. Plugging each coordinate vector of these configurations into (6.11) will give us an equation. With the rates found by solving the system of equations, we then prove that (6.11) holds for all configurations. In order to prove that, one only needs to show if (6.11) holds for a configuration $\boldsymbol{\eta}$ with $\mathbf{x}(\boldsymbol{\eta}) = (x_1, ..., x_N)$, then it also holds for $\bar{\boldsymbol{\eta}}$ with $\mathbf{x}(\bar{\boldsymbol{\eta}}) = (x_1, x_2, ..., x_{i-1}, x_i + 1, x_{i+1}, .., x_N)$. Here we write $\mathbf{x}(\boldsymbol{\eta})$ to indicate the coordinate vector $\mathbf{x}$ of the configuration $\boldsymbol{\eta}$. Notice here that $\mathbf{x}(\boldsymbol{\eta})$ differs from $\mathbf{x}(\bar{\boldsymbol{\eta}})$ only at i^{th} coordinate and notice that the particle x_i of $\boldsymbol{\eta}$ can jump to the right.

6.2   Answer to the question

In this section, we shall provide an answer to the question posed above. The answer is Theorem 6.1 appearing at the end of the section. It will state that the rates must have the form $r_k = r \exp\{J_k' - J_{k+1}'\}$ for $k \geq 1$ where r is a free parameter and $J_k' = -\beta J_k$. To obtain the answer, we shall have to make a series of computations, one of which plays an important role in the present work; it is the key lemma at the end of the next subsection.

6.2.1   Key lemma

As mentioned above, we have to deal with equation (6.11) in which the term $\dfrac{\pi_d(\boldsymbol{\eta}^{x_i-1,x_i})}{\pi_d(\boldsymbol{\eta})}$ needs to be computed. This will be done in the present subsection.

Before going further, let us introduce a convention. If we consider having a fixed specific value of d then $J_k = 0$ for $k > d$ in all the expressions. For example, if we consider the case $d = 1$ then $J_k = 0$ for all $k \geq 2$.

One can rewrite the invariant measure (6.5) in the following form

$$\pi_d = \exp\{h \sum_{i=1}^{L} \eta_i\} \prod_{k=1}^{d} R_k(\boldsymbol{\eta}), \tag{6.12}$$

where $R_k(\boldsymbol{\eta}) = \exp\{-\beta \sum_{i=1}^{L} J_k \eta_i (1 - \eta_{i+1})(1 - \eta_{i+2}) \cdots (1 - \eta_{i+k-1})\eta_{i+k}\}$ for $k = 1, ..., d$. Notice that $\eta_j^{x_i-1,x_i} = \eta_j + \delta_{j,i-1} - \delta_{j,i}$ for $j = 1, ..., L$. One gets

$$\frac{R_1(\boldsymbol{\eta}^{x_i-1,x_i})}{R_1(\boldsymbol{\eta})} = \exp\left\{-\beta J_1(\eta_{x_i-2} - \eta_{x_i+1})\right\}, \tag{6.13}$$

$$\frac{R_2(\boldsymbol{\eta}^{x_i-1,x_i})}{R_2(\boldsymbol{\eta})} = \exp\left\{-\beta J_2 \left[\eta_{x_i-3}(1 - \eta_{x_i-2}) - \eta_{x_i-2} + \eta_{x_i+1} - (1 - \eta_{x_i+1})\eta_{x_i+2}\right]\right\}, \tag{6.14}$$

$$\frac{R_k(\boldsymbol{\eta}^{x_i-1,x_i})}{R_k(\boldsymbol{\eta})} = \exp\left\{ - \beta J_k \left[(1 - \eta_{x_i-k+1})...(1 - \eta_{x_i-2}) \left[\eta_{x_i-k-1}(1 - \eta_{x_i-k}) - \eta_{x_i-k}\right] \right.\right.$$
$$\left.\left. + (1 - \eta_{x_i+1})...(1 - \eta_{x_i+k-2}) \left[\eta_{x_i+k-1} - (1 - \eta_{x_i+k-1})\eta_{x_i+k}\right]\right]\right\}, \text{ for } k > 2. \tag{6.15}$$

Suppose that $x_i - x_{i-1} = m$ and $x_{i+1} - x_i = n$ for $m \geq 2$ and $n \geq 1$. As for $k = 1$, one

has

$$
\frac{R_1(\boldsymbol{\eta}^{x_i-1,x_i})}{R_1(\boldsymbol{\eta})} = \begin{cases} 1, & m > 2, \ n > 1 \\ \exp(\beta J_1), & m > 2, \ n = 1 \\ \exp(-\beta J_1), & m = 2, \ n > 1 \\ 1, & m = 2, \ n = 1 \end{cases} \tag{6.16}
$$

As for $k = 2$, one has

$$
\frac{R_2(\boldsymbol{\eta}^{x_i-1,x_i})}{R_2(\boldsymbol{\eta})} = \begin{cases} 1, & m > 3, \ n > 2 \\ \exp(-\beta J_2), & m > 3, \ n = 2 \\ \exp(-\beta J_2), & m > 3, \ n = 1 \\ \exp(-\beta J_2), & m = 3, \ n > 2 \\ 1, & m = 3, \ n = 2 \\ \exp(-2\beta J_2), & m = 3, \ n = 1 \\ \exp(\beta J_2), & m = 2, \ n > 2 \\ \exp(2\beta J_2), & m = 2, \ n = 2 \\ 1, & m = 2, \ n = 1 \end{cases} \tag{6.17}
$$

As for $k > 2$, one can get the values of $\dfrac{R_k(\boldsymbol{\eta}^{x_i-1,x_i})}{R_k(\boldsymbol{\eta})}$ as follows.

- If $m > k + 1$, one obtains

$$
\frac{R_k(\boldsymbol{\eta}^{x_i-1,x_i})}{R_k(\boldsymbol{\eta})} = \begin{cases} 1, & 1 \leq n \leq k - 2 \\ \exp(-\beta J_k), & n = k - 1 \\ \exp(\beta J_k), & n = k \\ 1, & n > k \end{cases} \tag{6.18}
$$

- If $m = k + 1$, one obtains

$$
\frac{R_k(\boldsymbol{\eta}^{x_i-1,x_i})}{R_k(\boldsymbol{\eta})} = \begin{cases} \exp(-\beta J_k), & 1 \leq n \leq k - 2 \\ \exp(-2\beta J_k), & n = k - 1 \\ 1, & n = k \\ \exp(-\beta J_k), & n > k \end{cases} \tag{6.19}
$$

- If $m = k$, one obtains

$$
\frac{R_k(\boldsymbol{\eta}^{x_i-1,x_i})}{R_k(\boldsymbol{\eta})} = \begin{cases} \exp(\beta J_k), & 1 \leq n \leq k - 2 \\ 1, & n = k - 1 \\ \exp(2\beta J_k), & n = k \\ \exp(\beta J_k), & n > k \end{cases} \tag{6.20}
$$

- If $2 \leq m \leq k-1$, one obtains

$$\frac{R_k(\boldsymbol{\eta}^{x_i-1,x_i})}{R_k(\boldsymbol{\eta})} = \begin{cases} 1, & 1 \leq n \leq k-2 \\ \exp(-\beta J_k), & n = k-1 \\ \exp(\beta J_k), & n = k \\ 1, & n > k \end{cases} \tag{6.21}$$

Therefore, one can get the values of $\dfrac{\pi_d(\boldsymbol{\eta}^{x_i-1,x_i})}{\pi_d(\boldsymbol{\eta})}$ as follows.

- If $m > d+1$, one obtains

$$\frac{\pi_d(\boldsymbol{\eta}^{x_i-1,x_i})}{\pi_d(\boldsymbol{\eta})} = \begin{cases} 1, & n > d, \\ \exp(\beta J_d), & n = d, \\ \exp(\beta J_n - \beta J_{n+1}), & n \in \{1, ..., d-1\}. \end{cases} \tag{6.22}$$

- If $m = d+1$, one obtains

$$\frac{\pi_d(\boldsymbol{\eta}^{x_i-1,x_i})}{\pi_d(\boldsymbol{\eta})} = \begin{cases} \exp(-\beta J_d), & n > d, \\ 1, & n = d, \\ \exp(\beta J_n - \beta J_{n+1} - \beta J_d), & n \in \{1, ..., d-1\}. \end{cases} \tag{6.23}$$

- If $m \in \{2, ..., d\}$, one obtains

$$\frac{\pi_d(\boldsymbol{\eta}^{x_i-1,x_i})}{\pi_d(\boldsymbol{\eta})} = \begin{cases} \exp(-\beta J_{m-1} + \beta J_m), & n > d, \\ \exp(-\beta J_{m-1} + \beta J_m + \beta J_d), & n = d, \\ \exp(\beta J_n - \beta J_{n+1} - \beta J_{m-1} + \beta J_m), & n \in \{1, ..., d-1\}. \end{cases} \tag{6.24}$$

Denote by $\mathbf{m} = (m_1, m_2, ..., m_N)$ the headway distance vector where m_i is the number of empty sites between neighboring sites i^{th} and $(i+1)^{th}$, i.e., $m_i = x_{i+1} - x_i - 1 \mod L$. We denote $y_k = \exp\{-\beta J_k\}$ for $k = 1, .., d$. For convenience, we set that $y_k = 1$ for $k > d$ or $k = 0$. By the computations above, one has the following lemma which plays an important role in the present work (the variables m and n defined above are equal to $m_{i-1} + 1$ and $m_i + 1$, respectively, in the lemma).

Lemma 6.1. *One has*

$$\frac{\pi_d(\boldsymbol{\eta}^{x_i-1,x_i})}{\pi_d(\boldsymbol{\eta})} = y_{m_{i-1}} y_{m_{i-1}+1}^{-1} y_{m_i+1}^{-1} y_{m_i+2}. \tag{6.25}$$

Proof. The lemma follows from (6.22), (6.23), and (6.24). $\qquad \square$

6.2.2   Stationary conditions

We are now in the position to state a necessary condition such that $\hat{\pi}_d$ (6.6) would be the invariant distribution of the process. It is the contents of the following lemma.

Lemma 6.2. *Suppose that π_d for $d \geq 1$ in (6.5) is the unnormalized invariant measure of the process. Then the rates r_k must be of the form*

$$r_k = r \exp\{-\beta J_k + \beta J_{k+1}\} = r y_k y_{k+1}^{-1}, \quad \text{for } k \geq 1 \tag{6.26}$$

where r is a free parameter.

Proof. Consider $L - N$ configurations such that $x_i = i$ for $i = 1, 2, ..., N - 1$ and $x_N \in \{N, ..., L - 1\}$ and note that plugging each coordinate vector of these configurations into (6.11) gives us an equation. One obtains the following system of equations

$$\begin{cases}
r_1 y_1^{-1} y_2 - r_{L-N} & = 0 \\
r_1 y_1^{-1} y_2 - r_1 + r_{L-N} y_1 y_2^{-1} - r_{L-N-1} & = 0 \\
r_1 y_1^{-1} y_2 - r_2 + r_{L-N-1} y_2 y_3^{-1} - r_{L-N-2} & = 0 \\
\vdots \\
r_1 y_1^{-1} y_2 - r_{d-1} + r_{L-N-d+2} y_{d-1} y_d^{-1} - r_{L-N-d+1} & = 0 \\
r_1 y_1^{-1} y_2 - r_d + r_{L-N-d+1} y_d - r_{L-N-d} & = 0 \\
r_1 y_1^{-1} y_2 - r_{d+1} + r_{L-N-d} - r_{L-N-d-1} & = 0 \\
r_1 y_1^{-1} y_2 - r_{d+2} + r_{L-N-d-1} - r_{L-N-d-2} & = 0 \\
\vdots \\
r_1 y_1^{-1} y_2 - r_{L-N-d-1} + r_{d+2} - r_{d+1} & = 0 \\
r_1 y_1^{-1} y_2 y_d - r_{L-N-d} + r_{d+1} - r_d & = 0 \\
r_1 y_1^{-1} y_2 y_{d-1} y_d^{-1} - r_{L-N-d+1} + r_d y_d^{-1} - r_{d-1} & = 0 \\
r_1 y_1^{-1} y_2 y_{d-2} y_{d-1}^{-1} - r_{L-N-d} + r_{d-1} y_{d-1}^{-1} y_d - r_{d-2} & = 0 \\
\vdots \\
r_1 y_1^{-1} y_2 y_3 y_4^{-1} - r_{L-N-3} + r_4 y_4^{-1} y_5 - r_3 & = 0 \\
r_1 y_1^{-1} y_2^2 y_3^{-1} - r_{L-N-2} + r_3 y_3^{-1} y_4 - r_2 & = 0 \\
r_1 - r_{L-N-1} + r_2 y_2^{-1} y_3 - r_1 & = 0
\end{cases} \tag{6.27}$$

It is easy to solve the system of equations above which has a unique solution with the form (6.26). This completes the proof. $\qquad\square$

Next, we shall prove that the process with jump rates (6.26) admits $\hat{\pi}_d$ as its invariant measure. Let $\mathbf{x} = (x_1, ..., x_N)$ be the coordinate vector of particles of configuration $\boldsymbol{\eta}$. Denote by

$$S(\boldsymbol{\eta}) = \sum_{i=1}^{N} A_i \tag{6.28}$$

the left-hand side of (6.11), where

$$A_i = r_{x_{i+1}-x_i}(1 - \delta_{x_i-x_{i-1},1})\frac{\pi_d(\boldsymbol{\eta}^{x_i-1,x_i})}{\pi_d(\boldsymbol{\eta})} - r_{x_{i+1}-x_i-1}. \tag{6.29}$$

In the terms of headway distance $m_i, i = 1..N$, one can rewrite A_i as follows

$$A_i = r_{m_i+1}(1 - \delta_{m_{i-1},0})\frac{\pi_d(\boldsymbol{\eta}^{x_i-1,x_i})}{\pi_d(\boldsymbol{\eta})} - r_{m_i}. \tag{6.30}$$

Suppose that there exists i such that $\boldsymbol{\eta}_{x_i+1} = 0$ which means the particle x_i can hop to the right. It also means that $m_i \geq 1$. Let $\bar{\boldsymbol{\eta}}$ be the configuration with its coordinate vector $\bar{\mathbf{x}} := (\bar{x}_1, ..., \bar{x}_N)$. The difference between $\mathbf{x}$ and $\bar{\mathbf{x}}$ is i^{th} coordinate. Namely, $\bar{x}_i = x_i + 1$. We will prove that $S(\boldsymbol{\eta}) = S(\bar{\boldsymbol{\eta}})$. From this, one can conclude that (6.11) holds for all configurations. In order to show this we need the following lemmas. Before doing so, let us denote by $\bar{\mathbf{m}} = (\bar{m}_1, ..., \bar{m}_N)$ the headway vector of configuration $\bar{\boldsymbol{\eta}}$. Note that $m_j = \bar{m}_j$ for $j \neq i-1, i$, $\bar{m}_{i-1} = m_i + 1$, and $\bar{m}_i = m_i - 1$.

Lemma 6.3. *The value of $S(\boldsymbol{\eta}) - S(\bar{\boldsymbol{\eta}})$ is the following*

$$S(\boldsymbol{\eta}) - S(\bar{\boldsymbol{\eta}}) = \sum_{j=i-1}^{i+1} (A_j(\boldsymbol{\eta}) - A_j(\bar{\boldsymbol{\eta}})). \tag{6.31}$$

Proof. By Lemma 6.1, the value of $\frac{\pi_d(\boldsymbol{\eta}^{x_j-1,x_j})}{\pi_d(\boldsymbol{\eta})}$ depends only on m_j and m_{j-1}, one has

$$\frac{\pi_d(\boldsymbol{\eta}^{x_j-1,x_j})}{\pi_d(\boldsymbol{\eta})} = \frac{\pi_d(\bar{\boldsymbol{\eta}}^{x_j-1,x_j})}{\pi_d(\bar{\boldsymbol{\eta}})} \tag{6.32}$$

and thus $A_j(\boldsymbol{\eta}) = A_j(\bar{\boldsymbol{\eta}})$ for $j \neq i-1, i, i+1$. This completes the proof. $\square$

Lemma 6.4. *Under condition (6.26), one has*

$$A_{i+1}(\boldsymbol{\eta}) - A_{i+1}(\bar{\boldsymbol{\eta}}) = r_{m_i} - r_{m_i-1}. \tag{6.33}$$

Proof. One has

$$A_{i+1}(\boldsymbol{\eta}) - A_{i+1}(\bar{\boldsymbol{\eta}}) = r_{m_{i+1}+1}\frac{\pi_d(\boldsymbol{\eta}^{x_{i+1}-1,x_{i+1}})}{\pi_d(\boldsymbol{\eta})}$$
$$- r_{m_{i+1}+1}(1 - \delta_{m_i,1})\frac{\pi_d(\bar{\boldsymbol{\eta}}^{x_{i+1}-1,x_{i+1}})}{\pi_d(\bar{\boldsymbol{\eta}})}. \tag{6.34}$$

By condition (6.26) and Lemma 6.1, one has

$$r_{m_{i+1}+1}\frac{\pi_d(\boldsymbol{\eta}^{x_{i+1}-1,x_{i+1}})}{\pi_d(\boldsymbol{\eta})} = \left(ry_{m_{i+1}+1}y_{m_{i+1}+2}^{-1}\right)\left(y_{m_i}y_{m_i+1}^{-1}y_{m_{i+1}+1}^{-1}y_{m_{i+1}+2}\right)$$

$$= r y_{m_i} y_{m_i+1}^{-1} \tag{6.35}$$
$$= r_{m_i}$$

and

$$r_{m_{i+1}+1} \frac{\pi_d(\bar{\boldsymbol{\eta}}^{x_{i+1}-1,x_{i+1}})}{\pi_d(\bar{\boldsymbol{\eta}})} = \left(r y_{m_{i+1}+1} y_{m_{i+1}+2}^{-1} \right) \left(y_{\bar{m}_i} y_{\bar{m}_i+1}^{-1} y_{\bar{m}_{i+1}+1}^{-1} y_{\bar{m}_{i+1}+2} \right)$$
$$= r y_{m_{i+1}+1} y_{m_{i+1}+2}^{-1} y_{m_i-1} y_{m_i}^{-1} y_{m_{i+1}+1}^{-1} y_{m_{i+1}+2} \tag{6.36}$$
$$= r_{m_i-1}.$$

The proof is complete. $\qquad \square$

Lemma 6.5. *Under condition* (6.26), *one has*

$$A_{i-1}(\boldsymbol{\eta}) - A_{i-1}(\bar{\boldsymbol{\eta}}) = r_{m_{i-1}+1} - r_{m_{i-1}}. \tag{6.37}$$

Proof. One has

$$A_{i-1}(\boldsymbol{\eta}) - A_{i-1}(\bar{\boldsymbol{\eta}}) = r_{m_{i-1}+1}(1 - \delta_{m_{i-2},0}) \frac{\pi_d(\boldsymbol{\eta}^{x_{i-1}-1,x_{i-1}})}{\pi_d(\boldsymbol{\eta})} - r_{m_{i-1}}$$
$$- r_{m_{i-1}+2}(1 - \delta_{m_{i-2},0}) \frac{\pi_d(\bar{\boldsymbol{\eta}}^{x_{i-1}-1,x_{i-1}})}{\pi_d(\bar{\boldsymbol{\eta}})} + r_{m_{i-1}+1}. \tag{6.38}$$

In order to prove (6.37), we only need to prove that

$$r_{m_{i-1}+1} \frac{\pi_d(\boldsymbol{\eta}^{x_{i-1}-1,x_{i-1}})}{\pi_d(\boldsymbol{\eta})} = r_{m_{i-1}+2} \frac{\pi_d(\bar{\boldsymbol{\eta}}^{x_{i-1}-1,x_{i-1}})}{\pi_d(\bar{\boldsymbol{\eta}})}. \tag{6.39}$$

By condition (6.26) and Lemma 6.1, one has

$$r_{m_{i-1}+1} \frac{\pi_d(\boldsymbol{\eta}^{x_{i-1}-1,x_{i-1}})}{\pi_d(\boldsymbol{\eta})} = \left(r y_{m_{i-1}+1} y_{m_{i-1}+2}^{-1} \right) \left(y_{m_{i-2}} y_{m_{i-2}+1}^{-1} y_{m_{i-1}+1}^{-1} y_{m_{i-1}+2} \right)$$
$$= r y_{m_{i-2}} y_{m_{i-2}+1}^{-1} \tag{6.40}$$
$$= r_{m_{i-2}}$$

and

$$r_{m_{i-1}+2} \frac{\pi_d(\bar{\boldsymbol{\eta}}^{x_{i-1}-1,x_{i-1}})}{\pi_d(\bar{\boldsymbol{\eta}})} = \left(r y_{m_{i-1}+2} y_{m_{i-1}+3}^{-1} \right) \left(y_{\bar{m}_{i-2}} y_{\bar{m}_{i-2}+1}^{-1} y_{\bar{m}_{i-1}+1}^{-1} y_{\bar{m}_{i-1}+2} \right)$$
$$= r y_{m_{i-1}+2} y_{m_{i-1}+3}^{-1} y_{m_{i-2}} y_{m_{i-2}+1}^{-1} y_{m_{i-1}+2}^{-1} y_{m_{i-1}+3} \tag{6.41}$$
$$= r_{m_{i-2}}.$$

Thus, the proof is complete. $\qquad \square$

Lemma 6.6. *Under condition* (6.26), *one has*

$$A_i(\boldsymbol{\eta}) - A_i(\bar{\boldsymbol{\eta}}) = r_{m_{i-1}} - r_{m_i} - r_{m_{i-1}+1} + r_{m_i-1}. \tag{6.42}$$

Proof. Since

$$A_i(\boldsymbol{\eta}) - A_i(\bar{\boldsymbol{\eta}}) = \left(r_{m_i+1}(1 - \delta_{m_{i-1},0}) \frac{\pi_d(\boldsymbol{\eta}^{x_i-1,x_i})}{\pi_d(\boldsymbol{\eta})} - r_{m_i} \right)$$
$$- \left(r_{m_i} \frac{\pi_d(\bar{\boldsymbol{\eta}}^{x_i-1,x_i})}{\pi_d(\bar{\boldsymbol{\eta}})} - r_{m_{i-1}} \right), \tag{6.43}$$

we only need to prove that

$$r_{m_i+1}(1 - \delta_{m_{i-1},0}) \frac{\pi_d(\boldsymbol{\eta}^{x_i-1,x_i})}{\pi_d(\boldsymbol{\eta})} - r_{m_i} \frac{\pi_d(\bar{\boldsymbol{\eta}}^{x_i-1,x_i})}{\pi_d(\bar{\boldsymbol{\eta}})} = r_{m_{i-1}} - r_{m_{i-1}+1}. \tag{6.44}$$

By condition (6.26) and Lemma 6.1, one has

$$r_{m_i+1} \frac{\pi_d(\boldsymbol{\eta}^{x_i-1,x_i})}{\pi_d(\boldsymbol{\eta})} = \left(r y_{m_i+1} y_{m_i+2}^{-1} \right) \left(y_{m_{i-1}} y_{m_{i-1}+1}^{-1} y_{m_i+1}^{-1} y_{m_i+2} \right)$$
$$= r y_{m_{i-1}} y_{m_{i-1}+1}^{-1} \tag{6.45}$$
$$= r_{m_{i-1}}$$

and

$$r_{m_i} \frac{\pi_d(\bar{\boldsymbol{\eta}}^{x_i-1,x_i})}{\pi_d(\bar{\boldsymbol{\eta}})} = \left(r y_{m_i} y_{m_i+1}^{-1} \right) \left(y_{\bar{m}_{i-1}} y_{\bar{m}_{i-1}+1}^{-1} y_{\bar{m}_i+1}^{-1} y_{\bar{m}_i+2} \right)$$
$$= r y_{m_i} y_{m_i+1}^{-1} y_{m_{i-1}+1} y_{m_{i-1}+2}^{-1} y_{m_i}^{-1} y_{m_i+1} \tag{6.46}$$
$$= r_{m_{i-1}+1}.$$

Thus, the proof is complete. □

From Lemmas 6.3, 6.4 and 6.5, one obtains Theorem 1.6 as follows.

Theorem 6.1. *$\hat{\pi}_d$ is the invariant measure of the process if only if*

$$r_k = r \exp\{-\beta J_k + \beta J_{k+1}\}, \quad \text{for } k \geq 1. \tag{6.47}$$

where r is a free parameter.

Proof. By Lemma 6.2, the conditions (6.47) are satisfied. Suppose that we have two sets of parameters $r_1, r_2, ..., r_{L-N}$ and $r'_1, r'_2, ..., r'_{L-N}$. If $r_1 = r'_1$, since the system of equation (6.27) has a unique solution of the form (6.47), then $r_k = r'_k$ for $k = 1, ..., L - N$. This means that if r_1 is given, then there is only one set of rates $r_1, ..., r_{L-N}$ which is the unique solution of the considered problem.

Conversely, under conditions (6.47), we prove that (6.11) holds for all configurations by showing that $S(\boldsymbol{\eta}) - S(\bar{\boldsymbol{\eta}})$ in Lemma 6.3 is 0. One has

$$S(\boldsymbol{\eta}) - S(\bar{\boldsymbol{\eta}}) = \sum_{j=i-1}^{i+1} (A_j(\boldsymbol{\eta}) - A_j(\bar{\boldsymbol{\eta}})). \tag{6.48}$$

By Lemmas 6.4, 6.5, and 6.6 one gets

$$A_{i-1}(\boldsymbol{\eta}) - A_{i-1}(\bar{\boldsymbol{\eta}}) = r_{m_{i-1}+1} - r_{m_{i-1}} \tag{6.49}$$

$$A_i(\boldsymbol{\eta}) - A_i(\bar{\boldsymbol{\eta}}) = r_{m_{i-1}} - r_{m_i} - r_{m_{i-1}+1} + r_{m_i-1} \tag{6.50}$$

$$A_{i+1}(\boldsymbol{\eta}) - A_{i+1}(\bar{\boldsymbol{\eta}}) = r_{m_i} - r_{m_i-1} \tag{6.51}$$

which implies $S(\boldsymbol{\eta}) - S(\bar{\boldsymbol{\eta}}) = 0$. Thus, one can conclude that the master equation (6.11) holds for all configurations $\boldsymbol{\eta}$. This means $\hat{\pi}_d$ is the invariant measure of the process. This completes the proof. □

6.3 Stationary particle current

In this section, we shall investigate stationary particle current for the cases $d = 1, 2$. Notice that the case $d = 1$ has been studied in [1]. One recognizes in (6.6) a generalized Ising measure that can be treated by the transfer matrix technique. For more details regarding the use of this technique, see [5, 15, 16, 25].

We consider the mean density

$$\rho_{d,L} := \langle \eta_i \rangle_{\hat{\pi}_d} = \frac{1}{Z_{d,L}} \sum_{\boldsymbol{\eta}} \eta_i \pi_d(\boldsymbol{\eta}), \tag{6.52}$$

and for $r_i \geq 1$ the joint expectations

$$G_{d,L}(r_1, ..., r_k) := \langle \eta_i \eta_{i+r_1} \eta_{i+r_1+r_2} ... \eta_{i+r_1+...+r_k} \rangle_{\hat{\pi}_d}$$

$$= \frac{1}{Z_{d,L}} \sum_{\boldsymbol{\eta}} \eta_i \eta_{i+r_1} \eta_{i+r_1+r_2} \cdots \eta_{i+r_1+...+r_k} \pi_d(\boldsymbol{\eta}), \tag{6.53}$$

with the constraint that $\sum_{i=1}^{k} r_k < L$. Here $\langle \cdot \rangle_{\hat{\pi}_d}$ is the expectation with respect to measure $\hat{\pi}_d$. Because of translation invariance, the joint expectations do not depend on i. In order to compute these values, one can express the invariant measures in terms of transfer matrices that we present in Appendices A and B.

6.3.1   Case $d = 1$: two speeds

In this case, one has $r_2 = ... = r_{L-N} = r_1 \exp\{\beta J_1\}$. The stationary current between sites $(i, i+1)$ denoted by $j_{1,i}$ is the following

$$j_{1,i} = \langle \eta_i(1 - \eta_{i+1})[r_1\eta_{i+2} + r_2(1 - \eta_{i+2})]\rangle_{\hat{\pi}_1}$$
$$= r_2\rho_{1,L} + (r_1 - r_2)G_{1,L}(2) + (r_2 - r_1)G_{1,L}(1,1). \tag{6.54}$$

In the thermodynamic limit $L \to \infty$, one obtains

$$j_1 := \lim_{L\to\infty} j_{1,L} = r_2\rho - r_2 G_1(1) + (r_1 - r_2)G_1(2) + (r_2 - r_1)G_1(1,1), \tag{6.55}$$

where $\rho = \lim_{L\to\infty}\rho_{1,L}, G_1(r) = \lim_{L\to\infty} G_{1,L}(r)$, and $G_1(r_1, r_2) = \lim_{L\to\infty} G_{1,L}(r_1, r_2)$.

Denote

$$\chi := \frac{\lambda_2}{\lambda_1} \tag{6.56}$$

where λ_1 and λ_2 are eigenvalues (A.15) of the transfer matrix T_1 (A.4). To compute the mean density and the joint expectations we introduce the projectors

$$\hat{n} := |1\rangle\langle 1| = \begin{pmatrix} 0 & 0 \\ 0 & 1 \end{pmatrix}, \qquad \hat{v} := |0\rangle\langle 0| = \begin{pmatrix} 1 & 0 \\ 0 & 0 \end{pmatrix} \tag{6.57}$$

and observe that $\hat{n}|\eta\rangle = \eta|\eta\rangle$ for $\eta \in \{0, 1\}$ where $|\eta\rangle$ is denoted in (A.6). With the normalized left and right eigenvectors $\langle\lambda_i|, |\lambda_i\rangle$ for $i \in \{1, 2\}$ defined in (A.13), the mean density and some needed cases of joint expectations are the following

$$\rho_{1,L} = \frac{1}{Z_{1,L}}\mathrm{Tr}T_1^{i-1}\hat{n}T_1^{L-i+1} = \sum_{i=1}^{2}\frac{1}{Z_{1,L}}\mathrm{Tr}\lambda_i^L \langle\lambda_i|\hat{n}|\lambda_i\rangle$$
$$= \frac{w_2(1)v_2(1) + \chi^L w_2(2)v_2(2)}{1 + \chi^L}, \tag{6.58}$$

$$G_{1,L}(r) = \frac{1}{Z_{1,L}}\mathrm{Tr}T_1^{i-1}\hat{n}T_1^r\hat{n}T_1^{L-i-r+1}$$
$$= \frac{w_2^2(1)v_2^2(1) + (\chi^r + \chi^{L-r})w_2(1)w_2(2)v_2(1)v_2(2) + \chi^L w_2^2(2)v_2^2(2)}{1 + \chi^L}. \tag{6.59}$$

$$G_{1,L}(r_1, r_2) = \frac{1}{Z_{1,L}}\mathrm{Tr}T_1^{i-1}\hat{n}T_1^{r_1}\hat{n}T_1^{r_2}\hat{n}T_1^{L-i-r_1-r_2+1}$$
$$= \frac{\begin{aligned}&\omega_2^3(1)v_2^3(1) + (\chi^{L-r_1-r_2} + \chi^{r_1} + \chi^{r_2})\omega_2^2(1)v_2^2(1)\omega_2(2)v_2(2)\\&\quad + (\chi^{L-r_1} + \chi^{L-r_2} + \chi^{r_1+r_2})\omega_2(1)v_2(1)\omega_2^2(2)v_2^2(2) + \chi^L w_2^3(2)v_2^3(2)\end{aligned}}{1 + \chi^L}. \tag{6.60}$$

Since $\chi = \dfrac{1 + xy - \sqrt{(xy-1)^2 + 4x}}{1 + xy + \sqrt{(xy-1)^2 + 4x}}$, it is easy to show that $-1 < \chi < 1$. Thus, in the thermodynamic limit $L \to \infty$, one gets

$$\rho = w_2(1)v_2(1), \tag{6.61}$$

$$G_1(r) = w_2^2(1)v_2^2(1) + \chi^r w_2(1)w_2(2)v_2(1)v_2(2), \tag{6.62}$$

$$G_1(r_1, r_2) = \omega_2^3(1)v_2^3(1) + (\chi^{r_1} + \chi^{r_2})\omega_2^2(1)v_2^2(1)\omega_2(2)v_2(2) + \chi^{r_1+r_2}\omega_2(1)v_2(1)\omega_2^2(2)v_2^2(2). \tag{6.63}$$

Thus, one has from (6.61) – (6.63) that

$$\rho = \frac{x}{(\lambda_1 - xy)^2 + x}, \tag{6.64}$$

$$G_1(1) = \rho^2 + \chi\rho\frac{x}{(\lambda_2 - xy)^2 + x}, \tag{6.65}$$

$$G_1(2) = \rho^2 + \chi^2\rho\frac{x}{(\lambda_2 - xy)^2 + x}, \tag{6.66}$$

$$G_1(1, 1) = \rho^3 + 2\chi\rho^2\frac{x}{(\lambda_2 - xy)^2 + x} + \chi^2\rho\frac{x^2}{((\lambda_2 - xy)^2 + x)^2}. \tag{6.67}$$

From (6.64), one gets

$$x = \begin{cases} \dfrac{2\rho y(\rho - 1) - (2\rho - 1)^2 - \sqrt{(2\rho y(\rho - 1) - (2\rho - 1)^2)^2 - 4\rho^2 y^2(\rho - 1)^2}}{2(\rho - 1)\rho y^2} & \text{if } \rho \geq 0.5, \\[3mm] \dfrac{2\rho y(\rho - 1) - (2\rho - 1)^2 + \sqrt{(2\rho y(\rho - 1) - (2\rho - 1)^2)^2 - 4\rho^2 y^2(\rho - 1)^2}}{2(\rho - 1)\rho y^2} & \text{if } 0 < \rho < 0.5. \end{cases} \tag{6.68}$$

Thus, one can express j_1 in terms of particle density ρ, see Figure 6.3.
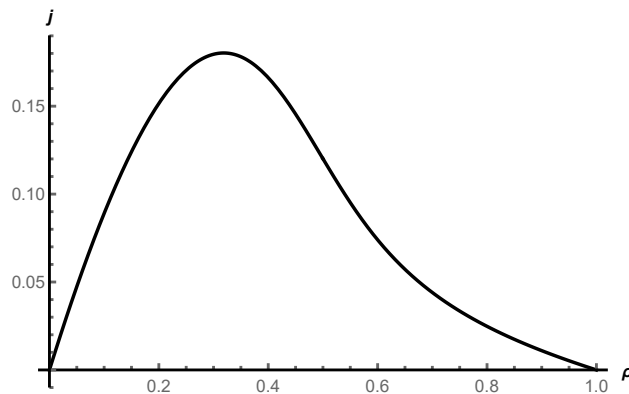
Figure 6.3: *Stationary current j_1 as a function of the density ρ for $r_1 = 0.1, r_2 = 1$ (repulsive interaction).*

6.3.2   Case $d = 2$: three speeds

In this case, one has $r_2 = r_1 \exp\{\beta J_1 - 2\beta J_2\}$ and $r_3 = ... = r_{L-N} = r_1 \exp\{\beta J_1 - \beta J_2\}$. The stationary current between sites $(i, i+1)$ is following

$$
\begin{aligned}
j_{2,i} &= \langle \eta_i (1 - \eta_{i+1})[r_1 \eta_{i+2} + r_2(1 - \eta_{i+2})\eta_{i+3} + r_3(1 - \eta_{i+2})(1 - \eta_{i+3})]\rangle_{\hat{\pi}_2} \\
&= r_3 \rho_{2,L} - r_3 G_{2,L}(1) + (r_1 - r_3)G_{2,L}(2) + (r_2 - r_3)G_{2,L}(3) - (r_1 - r_3)G_{2,L}(1,1) \\
&\quad - (r_2 - r_3)G_{2,L}(1,2) - (r_2 - r_3)G_{2,L}(2,1) + (r_2 - r_3)G_{2,L}(1,1,1).
\end{aligned}
\tag{6.69}
$$

In the thermodynamic limit, one obtains

$$
\begin{aligned}
j_2 &:= \lim_{L \to \infty} j_{2,L} = r_3 \rho - r_3 G_2(1) + (r_1 - r_3)G_2(2)(r_2 - r_3)G_2(3) - (r_1 - r_3)G_2(1,1) \\
&\quad - (r_2 - r_3)G_2(1,2) - (r_2 - r_3)G_2(2,1) + (r_2 - r_3)G_2(1,1,1)
\end{aligned}
\tag{6.70}
$$

where $\rho, G_2(1), G_2(2), G_2(3), G_2(1,1), G_2(1,2), G_2(2,1)$, and $G_2(1,1,1)$ are limits of $\rho_{2,L}, G_{2,L}(1), G_{2,L}(2), G_{2,L}(3), G_{2,L}(1,1), G_{2,L}(1,2), G_{2,L}(2,1)$, and $G_{2,L}(1,1,1)$ respectively as L goes to infinity.

Denote

$$
\chi_i := \frac{\lambda_i}{\lambda_1}, \text{ for } i = 1, 2, 3, 4,
\tag{6.71}
$$

where $\lambda_i, i = 1, 2, 3, 4$, are the eigenvectors of transfer matrix T_2 (B.4) presented in Appendix B. To compute the mean density and the joint expectations, with the two-dimensional unit matrix $\mathbb{1}$, one constructs projectors

$$
\hat{n}_1 := \hat{n} \otimes \mathbb{1}, \qquad \hat{n}_2 := \mathbb{1} \otimes \hat{n}
\tag{6.72}
$$

where $\hat{n}$ is in (6.57) and observes that

$$
\hat{n}_1 |\eta_{2i-1}, \eta_{2i}\rangle = \eta_{2i-1} |\eta_{2i-1}, \eta_{2i}\rangle, \qquad \hat{n}_2 |\eta_{2i-1}, \eta_{2i}\rangle = \eta_{2i} |\eta_{2i-1}, \eta_{2i}\rangle.
\tag{6.73}
$$

Here, ket-vectors $|i, j\rangle$ for $i, j \in \{0, 1\}$ are defined in (B.7). Identities in (6.73) allow one to replace the occupation variables η_i in the product $\eta_i \pi_2(\boldsymbol{\eta})$ by projectors at appropriately chosen positions in the string (B.12).

The normalized left and right eigenvectors are denoted by

$$
\langle \lambda_i | = (w_1(i), w_2(i), w_3(i), w_4(i)), \qquad |\lambda_i\rangle = \begin{pmatrix} v_1(i) \\ v_2(i) \\ v_3(i) \\ v_4(i) \end{pmatrix}, \text{ for } i = 1, 2, 3, 4
\tag{6.74}
$$

and we recall the completeness relation

$$\sum_{i=1}^{4} |\lambda_i\rangle \langle\lambda_i| = \mathbb{1}. \tag{6.75}$$

The mean density (6.52) and the joint expectations (6.53) with respect to $\hat{\pi}_2$ that we shall later need acquire the following form:

$$
\begin{aligned}
\rho_{2,L} &= \frac{1}{Z_{2,L}} \mathrm{Tr}\hat{n}_2 T_2^{L/2} \\
&= \frac{\sum_{k=1}^{4} \lambda_k^{L/2} \langle\lambda_k| \hat{n}_2 |\lambda_k\rangle}{\sum_{k=1}^{4} \lambda_k^{L/2}},
\end{aligned}
\tag{6.76}
$$

$$
\begin{aligned}
G_{2,L}(2m) &= \frac{1}{Z_{2,L}} \mathrm{Tr}T_2^{i-1}\hat{n}_2 T_2^{m}\hat{n}_2 T_2^{L/2-i-m+1} \\
&= \frac{\sum_{k=1}^{4} \sum_{l=1}^{4} \lambda_k^{L/2-m} \lambda_l^{m} \langle\lambda_k| \hat{n}_2 |\lambda_l\rangle \langle\lambda_l| \hat{n}_2 |\lambda_k\rangle}{\sum_{k=1}^{4} \lambda_k^{L/2}},
\end{aligned}
\tag{6.77}
$$

$$
\begin{aligned}
G_{2,L}(2m+1) &= \frac{1}{Z_{2,L}} \mathrm{Tr}T_2^{i-1}\hat{n}_2 T_2^{m+1}\hat{n}_1 T_2^{L/2-i-m} \\
&= \frac{\sum_{k=1}^{4} \sum_{l=1}^{4} \lambda_k^{L/2-m-1} \lambda_l^{m+1} \langle\lambda_k| \hat{n}_2 |\lambda_l\rangle \langle\lambda_l| \hat{n}_1 |\lambda_k\rangle}{\sum_{k=1}^{4} \lambda_k^{L/2}},
\end{aligned}
\tag{6.78}
$$

$$
\begin{aligned}
G_{2,L}(2m, 2n+1) &= \frac{1}{Z_{2,L}} \mathrm{Tr}T_2^{i-1}\hat{n}_2 T_2^{m}\hat{n}_2 T_2^{n+1}\hat{n}_1 T_2^{L/2-i-m-n} \\
&= \frac{\begin{aligned}\sum_{j=1}^{4} \sum_{k=1}^{4} \sum_{l=1}^{4} &\lambda_j^{L/2-m-n-1} \lambda_k^{m} \lambda_l^{n+1} \\ &\times \langle\lambda_j| \hat{n}_2 |\lambda_k\rangle \langle\lambda_k| \hat{n}_2 |\lambda_l\rangle \langle\lambda_l| \hat{n}_1 |\lambda_j\rangle\end{aligned}}{\sum_{j=1}^{4} \lambda_j^{L/2}},
\end{aligned}
\tag{6.79}
$$

$$G_{2,L}(2m+1, 2n) = \frac{1}{Z_{2,L}} \mathrm{Tr}T_2^{i-1}\hat{n}_2 T_2^{m+1}\hat{n}_1 T_2^{n}\hat{n}_1 T_2^{L/2-i-m-n} \tag{6.80}$$

$$
= \frac{\begin{aligned}\sum_{j=1}^{4} \sum_{k=1}^{4} \sum_{l=1}^{4} &\lambda_j^{L/2-m-n-1} \lambda_k^{m+1} \lambda_l^{n} \\ &\times \langle\lambda_j| \hat{n}_2 |\lambda_k\rangle \langle\lambda_k| \hat{n}_1 |\lambda_l\rangle \langle\lambda_l| \hat{n}_1 |\lambda_j\rangle\end{aligned}}{\sum_{j=1}^{4} \lambda_j^{L/2}}.
\tag{6.81}
$$

We also need $G_{2,L}(1,1)$ and $G_{2,L}(1,1,1)$ to compute the stationary current. One gets

$$
\begin{aligned}
G_{2,L}(1,1) &= \frac{1}{Z_{2,L}} \mathrm{Tr}T_2^{i-1}\hat{n}_2 T_2\hat{n}_1 \hat{n}_2 T_2^{L/2-i} \\
&= \frac{\sum_{k=1}^{4} \sum_{l=1}^{4} \lambda_k^{L/2-1} \lambda_k \langle\lambda_k| \hat{n}_2 |\lambda_l\rangle \langle\lambda_l| \hat{n}_1\hat{n}_2 |\lambda_k\rangle}{\sum_{k=1}^{4} \lambda_k^{L/2}},
\end{aligned}
\tag{6.82}
$$

$$G_{2,L}(1,1,1) = \frac{1}{Z_{2,L}} \mathrm{Tr}T_2^{i-1}\hat{n}_2 T_2\hat{n}_1 \hat{n}_2 T_2\hat{n}_1 T_2^{L/2-i-1}$$

$$
= \frac{\begin{array}{c} \sum_{j=1}^{4} \sum_{k=1}^{4} \sum_{l=1}^{4} \lambda_{j}^{L/2-2} \lambda_{k} \lambda_{l} \\ \times \langle \lambda_{j}| \, \hat{n}_{2} \, |\lambda_{k}\rangle \, \langle \lambda_{k}| \, \hat{n}_{1}\hat{n}_{2} \, |\lambda_{l}\rangle \, \langle \lambda_{l}| \, \hat{n}_{1} \, |\lambda_{j}\rangle \end{array}}{\sum_{j=1}^{4} \lambda_{j}^{L/2}}. \tag{6.83}
$$

One notices that $|\chi_i| < 1$ for $i = 2, 3, 4$ and

$$
\begin{aligned}
\langle \lambda_i| \, \hat{n}_1 \, |\lambda_j\rangle &= w_3(i)v_3(j) + w_4(i)v_4(j), \\
\langle \lambda_i| \, \hat{n}_2 \, |\lambda_j\rangle &= w_2(i)v_2(j) + w_4(i)v_4(j)
\end{aligned} \tag{6.84}
$$

for $i, j = 1, 2, 3, 4$. Thus, in the thermodynamic limit $L \to \infty$, one gets

$$
\rho = \langle \lambda_1| \, \hat{n}_2 \, |\lambda_1\rangle, \tag{6.85}
$$

$$
G_2(1) = \sum_{i=1}^{4} \chi_i \langle \lambda_1| \, \hat{n}_2 \, |\lambda_i\rangle \, \langle \lambda_i| \, \hat{n}_1 \, |\lambda_1\rangle, \tag{6.86}
$$

$$
G_2(2) = \sum_{i=1}^{4} \chi_i \langle \lambda_1| \, \hat{n}_2 \, |\lambda_i\rangle \, \langle \lambda_i| \, \hat{n}_2 \, |\lambda_1\rangle, \tag{6.87}
$$

$$
G_2(3) = \sum_{i=1}^{4} \chi_i^2 \langle \lambda_1| \, \hat{n}_2 \, |\lambda_i\rangle \, \langle \lambda_i| \, \hat{n}_1 \, |\lambda_1\rangle, \tag{6.88}
$$

$$
G_2(1,1) = \sum_{i=1}^{4} \chi_i \langle \lambda_1| \, \hat{n}_2 \, |\lambda_i\rangle \, \langle \lambda_i| \, \hat{n}_1\hat{n}_2 \, |\lambda_1\rangle, \tag{6.89}
$$

$$
G_2(1,2) = \sum_{i=1}^{4} \sum_{j=1}^{4} \chi_i\chi_j \langle \lambda_1| \, \hat{n}_2 \, |\lambda_i\rangle \, \langle \lambda_i| \, \hat{n}_1 \, |\lambda_j\rangle \, \langle \lambda_j| \, \hat{n}_1 \, |\lambda_1\rangle, \tag{6.90}
$$

$$
G_2(2,1) = \sum_{i=1}^{4} \sum_{j=1}^{4} \chi_i\chi_j \langle \lambda_1| \, \hat{n}_2 \, |\lambda_i\rangle \, \langle \lambda_i| \, \hat{n}_2 \, |\lambda_j\rangle \, \langle \lambda_j| \, \hat{n}_1 \, |\lambda_1\rangle, \tag{6.91}
$$

$$
G_2(1,1,1) = \sum_{i=1}^{4} \sum_{j=1}^{4} \chi_i\chi_j \langle \lambda_1| \, \hat{n}_2 \, |\lambda_i\rangle \, \langle \lambda_i| \, \hat{n}_1\hat{n}_2 \, |\lambda_j\rangle \, \langle \lambda_j| \, \hat{n}_1 \, |\lambda_1\rangle. \tag{6.92}
$$

Because of the difficulty in finding the eigensystem of matrix T_2 in close forms, we shall show the stationary current j_2 obtained by numerical method, see Figure 6.4.
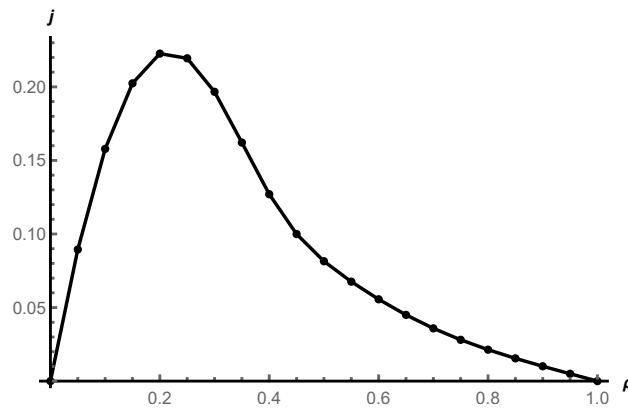
Figure 6.4: *Stationary current j_2 as a function of the density ρ for $r_1 = 0.1, r_2 = 1, r_3 = 2$ (repulsive interaction).*

6.4   Discussion

To begin with, we want to highlight that our results demonstrate that there it is necessary to have $d + 1$ speed in order to maintain the model in the invariate distribution corresponding to the generalized Ising measure $\hat{\pi}_d$. Additionally, it has been noted in [1] that a one-speed model is not realistic, since its average current is symmetric, as illustrated in Fig. 6.1. The paper also considers a two-speed model (equivalent to $d = 1$ in our model) and shows that the current, as seen in Fig. 6.3, is consistent with real traffic flow data. It can be inferred from Figs. 6.1, 6.3 and 6.4 the following property of the current: the more speeds a model has, the more rapidly the current increases. Once it reaches its global maximum, it declines fast to 0; the larger the number of model's speeds, the faster it will fall down.

Chapter 7

A generalization of one-dimensional Katz–Lebowitz–Spohn model

In order to get more information about RNA transcription model in Chapter 3, we consider only translocation dynamics of rods whose length is comparable to the interaction range which is 1. It turns out that our model is a generalized version of Katz–Lebowitz–Spohn model for a one-dimensional lattice gas with periodic boundary conditions in the sense stated in Remark 7.2.

7.1 One-dimensional Katz–Lebowitz–Spohn model

We start with Katz–Lebowitz–Spohn model (KLS) [13, 23] on the ring $\mathbb{T}_L$ with L sites and N particles. KLS model is a generalized version of the asymmetric simple exclusion process in which hopping rates depend on the neighboring sites. Namely, a particle at site i hops to site $i-1$ or $i+1$ with a rate depending on the occupancy of the sites $i-2$ and $i+1$ or $i-1$ and $i+2$, respectively, provided the target site is empty. Thus, the dynamics are the following

$$0\widehat{10}0 \xrightarrow{r(1+\delta)} 0010, \quad 1\widehat{10}0 \xrightarrow{r(1+\epsilon)} 1010, \quad 0\widehat{10}1 \xrightarrow{r(1-\epsilon)} 0011, \quad 1\widehat{10}1 \xrightarrow{r(1-\delta)} 1011$$

$$0\widehat{01}0 \xrightarrow{\ell(1+\delta)} 0100, \quad 1\widehat{01}0 \xrightarrow{\ell(1-\epsilon)} 1100, \quad 0\widehat{01}1 \xrightarrow{\ell(1+\epsilon)} 0101, \quad 1\widehat{01}1 \xrightarrow{\ell(1-\delta)} 1101$$

where $\epsilon, \delta \in (-1, 1)$. The process admits a Gibbs measure with nearest neighbor interaction energy to be invariant distribution given by

$$\hat{\pi}(\boldsymbol{\eta}) = \frac{1}{Z} e^{-\beta J \sum_{i=1}^{L} \eta_i \eta_{i+1} + h \sum_{i=1}^{L} \eta_i} \tag{7.1}$$

where $e^{\beta J} = \dfrac{1+\epsilon}{1-\epsilon}$ and Z is the partition function [13, 23]. In equilibrium thermodynamics, parameter h plays the role of a chemical potential and non-negative real parameter β is proportional to the inverse of experimentally strictly positive temperature T, i.e., $\beta = 1/(k_B T)$, where k_B is the Boltzmann constant.

7.2   Model and main result

We consider a generalized exclusion process with jump rates of a particle being configuration-dependent on the ring $\mathbb{T}_L$ with L sites and N particles. Denote $\mathbf{x} = (x_1, x_2, ..., x_N)$ by positions of the particles. Jump rate of the particle at position x_i which is of the following form

$$\omega_i(\boldsymbol{\eta}) = \omega^\star (1 + d^{1\star} \delta_{x_{i-1}+1, x_i} + d^{\star 01} \delta_{x_i+2, x_{i+1}})(1 - \delta_{x_i+1, x_{i+1}}), \qquad (7.2)$$

$$\phi_i(\boldsymbol{\eta}) = \phi^\star (1 + e^{10\star} \delta_{x_{i-1}+2, x_i} + e^{\star 1} \delta_{x_i+1, x_{i+1}})(1 - \delta_{x_{i-1}+1, x_i}). \qquad (7.3)$$

Notice here that $\omega_i(\boldsymbol{\eta})$ is the jump rate of the particle at x_i to the right, meanwhile $\phi_i(\boldsymbol{\eta})$ is the jump rate of the particle at x_i to the left. These rates are different from the rates that we have considered in Chapter 6 for the case $d = 1$ since these rates depend not only on the nearest particle on the right but also on the presence of a particle at the position $x_i - 1$ on the left; contrary to that, the jump rates of a particle of the model of Chapter 6, case $d = 1$, depend only on the position of the rightmost neighboring particle.

Some cases of the jump rates are presented in Fig. 7.1 (that illustrates the jump rates to the right) and Fig. 7.2 (that illustrates the jump rates to the left).

(a) $\omega_i(\boldsymbol{\eta}) = \omega^\star (1 + d^{1\star} + d^{\star 01})$ **(b)** $\omega_i(\boldsymbol{\eta}) = \omega^\star (1 + d^{1\star})$

(c) $\omega_i(\boldsymbol{\eta}) = \omega^\star (1 + d^{\star 01})$ **(d)** $\omega_i(\boldsymbol{\eta}) = \omega^\star$
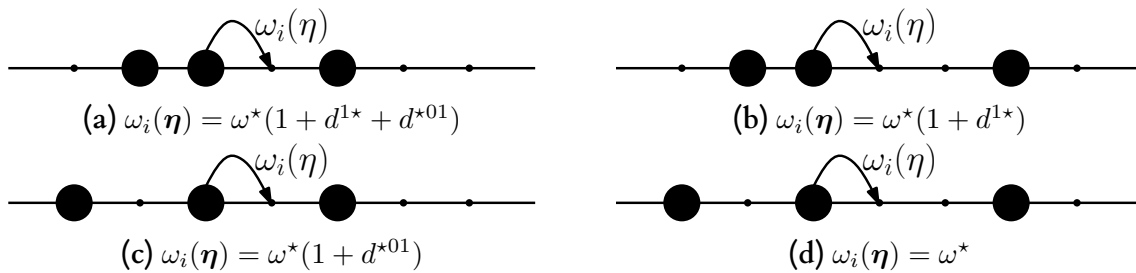
Figure 7.1: *Some examples of the jump rates to the right.*

(a) $\phi_i(\boldsymbol{\eta}) = \phi^\star(1 + e^{\star 1})$

(b) $\phi_i(\boldsymbol{\eta}) = \phi^\star(1 + e^{\star 1} + e^{10\star})$

(c) $\phi_i(\boldsymbol{\eta}) = \phi^\star(1 + e^{10\star})$

(d) $\phi_i(\boldsymbol{\eta}) = \phi^\star$
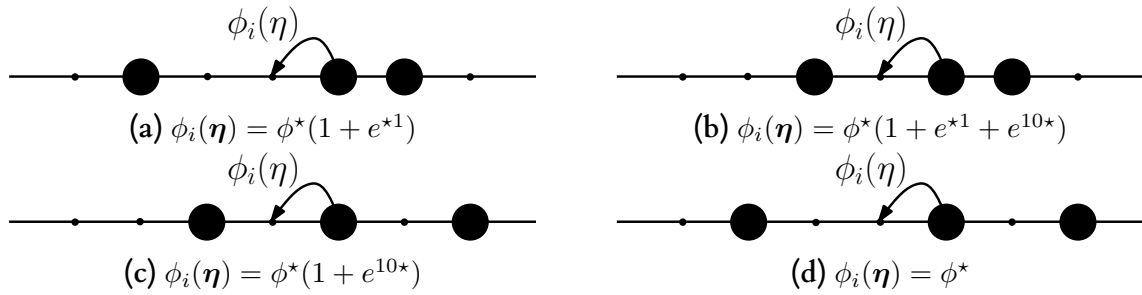
Figure 7.2: *Some examples of the jump rates to the left.*

We shall now employ the approach developed in Chapter 3 but we shall apply it only to the translocation dynamics. This will give us the main result of this chapter which is the content of Theorem 1.7. We will give a direct proof of the theorem.

Theorem 7.1. *If parameters $d^{1\star}, d^{\star 01}, e^{\star 1}$ and $d^{\star 10}$ of the model satisfy the following constraint*

$$\frac{1 + d^{1\star}}{1 + d^{\star 01}} = \frac{1 + e^{\star 1}}{1 + e^{10\star}}, \tag{7.4}$$

then the invariant distribution of the process is the following

$$\hat{\pi}(\boldsymbol{\eta}) = \frac{1}{Z_L}\left(\frac{1 + d^{1\star}}{1 + d^{\star 10}}\right)^{-\sum_{i=1}^{L}\eta_i\eta_{i+1}} \tag{7.5}$$

where Z_L is the partition function.

Before giving proof to the theorem, let us list below some remarks.

Remark 7.1. *By setting*

$$e^{\beta J} := \frac{1 + d^{1\star}}{1 + d^{\star 10}} \tag{7.6}$$

where β has the same definition as in (7.1), the invariant measure (7.5) acquires the form of the Ising measure with a nearest neighbor interaction energy as outlined in (7.1). A repulsive interaction corresponds to $J > 0$ (or $d^{1\star} > d^{\star 10}$), a non-interacting interaction takes place when $J = 0$ (or $d^{1\star} = d^{\star 10}$), and an attractive interaction is present when $J < 0$ (or $d^{1\star} < d^{\star 10}$).

Remark 7.2. *Our model is a generalization of KLS model. Indeed, let us compare the rates*

of our model to the ones of KLS model. One has

$$
\begin{cases}
r(1+\delta) = \omega^\star \\
r(1+\epsilon) = \omega^\star(1+d^{1\star}) \\
r(1-\epsilon) = \omega^\star(1+d^{\star 01}) \\
r(1-\delta) = \omega^\star(1+d^{1\star}+d^{\star 01}) \\
\ell(1+\delta) = \phi^\star \\
\ell(1-\epsilon) = \phi^\star(1+e^{10\star}) \\
\ell(1+\epsilon) = \phi^\star(1+e^{\star 1}) \\
\ell(1-\delta) = \phi^\star(1+e^{\star 1}+e^{10\star}).
\end{cases}
\tag{7.7}
$$

One gets

$$
\begin{cases}
\omega^\star & = r(1+\delta) \\
d^{1\star} & = \dfrac{1+\epsilon}{1+\delta} - 1 \\
d^{\star 01} & = \dfrac{1-\epsilon}{1+\delta} - 1 \\
\phi^\star & = \ell(1+\delta) \\
e^{\star 1} & = \dfrac{1+\epsilon}{1+\delta} - 1 \\
e^{10\star} & = \dfrac{1-\epsilon}{1+\delta} - 1.
\end{cases}
\tag{7.8}
$$

One has $d^{1\star} = e^{\star 1}$ and $d^{\star 01} = e^{10\star}$ satisfying the constraint (7.4), thus KLS model for one-dimensional lattice gas with periodic boundary conditions is a special case of our model.

Proof of Theorem 7.1. The master equation for the probability $\mathbb{P}_t(\boldsymbol{\eta})$ of finding the particles at time t in the configuration $\boldsymbol{\eta}$

$$
\frac{d}{dt}\mathbb{P}(\boldsymbol{\eta},t) = \sum_{i=1}^{N}\left[\omega_i(\boldsymbol{\eta}_f^i)\mathbb{P}(\boldsymbol{\eta}_f^i,t) + \phi_i(\boldsymbol{\eta}_b^i)\mathbb{P}(\boldsymbol{\eta}_b^i,t) - (\omega_i(\boldsymbol{\eta})+\phi_i(\boldsymbol{\eta}))\mathbb{P}(\boldsymbol{\eta},t)\right]
\tag{7.9}
$$

where $\boldsymbol{\eta}_f^i$ is the configuration that leads to $\boldsymbol{\eta}$ before a forward translocation of ith particle (i.e., with coordinate $x_j^f = x_j - \delta_{j,i}$), $\boldsymbol{\eta}_b^i$ is the configuration that leads to $\boldsymbol{\eta}$ before a backward translocation of ith particle (i.e., $x_j^b = x_j + \delta_{j,i}$). Notice here that due to periodicity, the positions x_i of the particles are counted modulo L and labels i are counted modulo N.

If a measure π is invariant of the process then by dividing (7.9) by the stationary distribution $\pi(\boldsymbol{\eta})$ we get the stationary condition in the following form:

$$
\sum_{i=1}^{N}\left[\omega_i(\boldsymbol{\eta}_f^i)\frac{\pi(\boldsymbol{\eta}_f^i)}{\pi(\boldsymbol{\eta})} + \phi_i(\boldsymbol{\eta}_b^i)\frac{\pi(\boldsymbol{\eta}_b^i)}{\pi(\boldsymbol{\eta})} - (\omega_i(\boldsymbol{\eta})+\phi_i(\boldsymbol{\eta}))\right] = 0.
\tag{7.10}
$$

In order to prove the theorem, we only need to show that equation (7.10) holds for measure (7.5). For simplicity of notations, we denote by

$$\theta_i^p := \delta_{x_{i+1}, x_{i+1+p}} \tag{7.11}$$

the indicator functions on a headway of length p with the index i are taken modulo N, i.e., $\theta_0^p \equiv \theta_N^p$.

In terms of new variable θ_i^p and

$$y = \left(\frac{1 + d^{1\star}}{1 + d^{\star 01}} \right)^{-1}, \tag{7.12}$$

the measure (7.5) can be rewritten as follows

$$\hat{\pi}(\boldsymbol{\eta}) = \frac{1}{Z} \prod_{i=1}^{N} y^{\theta_i^0}. \tag{7.13}$$

Moreover, the jump rates appearing in equation (7.10) can be express by using the same variables as above, namely,

$$\omega_i(\boldsymbol{\eta}) = \omega^\star (1 + d^{1\star}\theta_{i-1}^0 + d^{\star 01}\theta_i^1)(1 - \theta_i^0), \tag{7.14}$$

$$\phi_i(\boldsymbol{\eta}) = \phi^\star (1 + e^{10\star}\theta_{i-1}^1 + e^{\star 1}\theta_i^0)(1 - \theta_{i-1}^0), \tag{7.15}$$

$$\omega_i(\boldsymbol{\eta}_f^i) = \omega^\star (1 + d^{1\star}\theta_{i-1}^1 + d^{\star 01}\theta_i^0)(1 - \theta_{i-1}^0), \tag{7.16}$$

$$\phi_i(\boldsymbol{\eta}_b^i) = \phi^\star (1 + e^{10\star}\theta_{i-1}^0 + e^{\star 1}\theta_i^1)(1 - \theta_i^0). \tag{7.17}$$

One has

$$\frac{\hat{\pi}(\boldsymbol{\eta}_f^i)}{\hat{\pi}(\boldsymbol{\eta})} = y^{-\theta_{i-1}^0 - \theta_i^0 + \theta_{i-1}^1}, \tag{7.18}$$

$$\frac{\hat{\pi}(\boldsymbol{\eta}_b^i)}{\hat{\pi}(\boldsymbol{\eta})} = y^{-\theta_i^0 + \theta_i^1 - \theta_{i-1}^0}. \tag{7.19}$$

Let us introduce new variables as follows

$$\begin{cases} a_1 &= -\omega^\star(1 + d^{1\star}) + \phi^\star(1 + e^{\star 1}), \\ a_2 &= \omega^\star d^{\star 01} - \phi^\star e^{10\star}, \\ a_k &= 0, \text{ for } k \geq 3. \end{cases} \tag{7.20}$$

Under condition (7.4), it is easy to check that

$$\omega_i(\boldsymbol{\eta}_f^i)\frac{\hat{\pi}(\boldsymbol{\eta}_f^i)}{\hat{\pi}(\boldsymbol{\eta})} + \phi_i(\boldsymbol{\eta}_b^i)\frac{\hat{\pi}(\boldsymbol{\eta}_b^i)}{\hat{\pi}(\boldsymbol{\eta})} - (\omega_i(\boldsymbol{\eta}) + \phi_i(\boldsymbol{\eta})) = a_{m+1} - a_{n+1}, \tag{7.21}$$

where m, n are the distances between i^{th} particle and its leftmost and rightmost particles respectively. Namely, $m = x_i - x_{i-1} - 1$ and $n = x_{i+1} - x_i - 1$. Thus, due to the periodicity of the lattice, by summing over index i from 1 to N, one has

$$\sum_{i=1}^{N} \left[\omega_i(\boldsymbol{\eta}_f^i) \frac{\hat{\pi}(\boldsymbol{\eta}_f^i)}{\hat{\pi}(\boldsymbol{\eta})} + \phi_i(\boldsymbol{\eta}_b^i) \frac{\hat{\pi}(\boldsymbol{\eta}_b^i)}{\hat{\pi}(\boldsymbol{\eta})} - (\omega_i(\boldsymbol{\eta}) + \phi_i(\boldsymbol{\eta})) \right] = 0. \qquad (7.22)$$

Thus, $\hat{\pi}$ is the invariant measure of the process. The proof is complete. $\qquad \square$

7.3   Stationary current and correlation length

We consider the mean density

$$\rho_L := \langle \eta_i \rangle_{\hat{\pi}} = \frac{1}{Z_L} \sum_{\boldsymbol{\eta}} \eta_i \pi(\boldsymbol{\eta}), \qquad (7.23)$$

and for $r_i \geq 1$ the joint expectations

$$G_L(r_1, ..., r_k) := \langle \eta_i \eta_{i+r_1} \eta_{i+r_1+r_2} ... \eta_{i+r_1+...+r_k} \rangle_{\hat{\pi}}$$
$$= \frac{1}{Z_L} \sum_{\boldsymbol{\eta}} \eta_i \eta_{i+r_1} \eta_{i+r_1+r_2} \cdots \eta_{i+r_1+...+r_k} \pi(\boldsymbol{\eta}), \qquad (7.24)$$

under the constraint $\sum_{i=1}^{k} r_k < L$ and with π meaning the unnormalized measure. Here $\langle \cdot \rangle_{\hat{\pi}}$ is the expectation with respect to measure $\hat{\pi}$. Because of translation invariance, the joint expectations do not depend on i.

Since the number of particles is conserved, the stationary distribution can be expressed in grand-canonical form with a fugacity x which is the following

$$\hat{\pi}_{gc}(\boldsymbol{\eta}) = \frac{1}{\hat{Z}_{gc}} y^{\sum_{i=1}^{L} \eta_i \eta_{i+1}} x^{\sum_{i=1}^{L} \eta_i}. \qquad (7.25)$$

Notice here that variable y in (7.12) corresponds to y^{-1} in the Chapter 6. Thus, we are able to make use of the same transfer matrix (A.4) (see Appendix A) for computing the density (7.23) and the joint expectations (7.24).

7.3.1   Stationary current

One can compute the stationary current between sites i and $i + 1$ as follows

$$j_i = j_{i,i+1} - j_{i+1,i} \qquad (7.26)$$

where

$$j_{i,i+1} = \langle \eta_i(1 - \eta_{i+1})[\omega^\star(1 - \eta_{i-1})(1 - \eta_{i+2}) + \omega^\star(1 + d^{1\star})\eta_{i-1}(1 - \eta_{i+2}) \tag{7.27}$$

$$+ \omega^\star(1 + d^{\star 01})\eta_{i-1}\eta_{i+2} + \omega^\star(1 + d^{\star 01})(1 - \eta_{i-1})\eta_{i+2}]\rangle_{\hat{\pi}_{gc}} \tag{7.28}$$

$$= \omega^\star\rho_L + \omega^\star(d^{1\star} - 1)G_L(1) + \omega^\star d^{\star 01}G_L(2) - \omega^\star(d^{1\star} + d^{\star 01})G_L(1,1) \tag{7.29}$$

and

$$j_{i+1,i} = \langle \eta_{i+1}(1 - \eta_i)[\phi^\star(1 - \eta_{i+2})(1 - \eta_{i-1}) + \phi^\star(1 + e^{\star 1})\eta_{i+2}(1 - \eta_{i-1})+ \tag{7.30}$$

$$\phi^\star(1 + e^{\star 1} + d^{10\star})\eta_{i+2}\eta_{i-1} + \phi^\star(1 + e^{10\star})(1 - \eta_{i+2})\eta_{i-1}]\rangle_{\hat{\pi}_{gc}} \tag{7.31}$$

$$= \phi^\star\rho_L + \phi^\star(e^{\star 1} - 1)G_L(1) + \phi^\star e^{10\star}G_L(2) - \phi^\star(e^{\star 1} + e^{10\star})G_L(1,1). \tag{7.32}$$

Thus, one gets

$$j_i = (\omega^\star - \phi^\star)\rho_L + (\omega^\star d^{1\star} - \phi^\star e^{\star 1} - \omega^\star + \phi^\star)G_L(1) + (\omega^\star d^{\star 01} - \phi^\star e^{10\star})G_L(2)$$
$$- [\omega^\star(d^{1\star} + d^{\star 01}) - \phi^\star(e^{\star 1} + e^{10\star})]G_L(1,1) \tag{7.33}$$

In the thermodynamic limit $L \to \infty$, one obtains

$$j = (\omega^\star - \phi^\star)\rho + (\omega^\star d^{1\star} - \phi^\star e^{\star 1} - \omega^\star + \phi^\star)G(1) + (\omega^\star d^{\star 01} - \phi^\star e^{10\star})G(2)$$
$$- [\omega^\star(d^{1\star} + d^{\star 01}) - \phi^\star(e^{\star 1} + e^{10\star})]G(1,1) \tag{7.34}$$

where $\rho = \lim_{L \to \infty} \rho_L$, $G(1) = \lim_{L \to \infty} G_L(1)$, $G(2) = \lim_{L \to \infty} G_L(2)$, and $G(1.1) = \lim_{L \to \infty} G_L(1,1)$.

Similarly to the previous chapter, let us denote

$$\chi := \frac{\lambda_2}{\lambda_1} \tag{7.35}$$

where λ_1 and λ_2 are eigenvalues (A.15) of the transfer matrix T (A.4). To compute the mean density and the joint expectations we make use of the following projectors

$$\hat{n} := |1\rangle\langle 1| = \begin{pmatrix} 0 & 0 \\ 0 & 1 \end{pmatrix}, \qquad \hat{v} := |0\rangle\langle 0| = \begin{pmatrix} 1 & 0 \\ 0 & 0 \end{pmatrix} \tag{7.36}$$

whereas we observe that $\hat{n}|\eta\rangle = \eta|\eta\rangle$ for $\eta \in \{0,1\}$ where $|\eta\rangle$ is defined in (A.6). With the normalized left and right eigenvectors $\langle \lambda_i|, |\lambda_i\rangle$ for $i \in \{1,2\}$ defined in (A.13), the mean density and some needed cases of joint expectations are the following

$$\rho_L = \frac{1}{Z_{gc}}\text{Tr}T^{i-1}\hat{n}T^{L-i+1} = \sum_{i=1}^{2}\frac{1}{Z_L}\text{Tr}\lambda_i^L\langle \lambda_i|\hat{n}|\lambda_i\rangle$$
$$= \frac{\omega_2(1)v_2(1) + \chi^L\omega_2(2)v_2(2)}{1 + \chi^L}, \tag{7.37}$$

$$G_L(r) = \frac{1}{Z_{gc}} \mathrm{Tr} T^{i-1} \hat{n} T^r \hat{n} T^{L-i-r+1}$$

$$= \frac{\omega_2^2(1)v_2^2(1) + (\chi^r + \chi^{L-r})\omega_2(1)\omega_2(2)v_2(1)v_2(2) + \chi^L \omega_2^2(2)v_2^2(2)}{1 + \chi^L}, \quad (7.38)$$

$$G_L(r_1, r_2) = \frac{1}{Z_{gc}} \mathrm{Tr} T^{i-1} \hat{n} T^{r_1} \hat{n} T^{r_2} \hat{n} T^{L-i-r_1-r_2+1}$$

$$= \frac{\begin{aligned}&\omega_2^3(1)v_2^3(1) + (\chi^{L-r_1-r_2} + \chi^{r_1} + \chi^{r_2})\omega_2^2(1)v_2^2(1)\omega_2(2)v_2(2) \\ &+ (\chi^{L-r_1} + \chi^{L-r_2} + \chi^{r_1+r_2})\omega_2(1)v_2(1)\omega_2^2(2)v_2^2(2) + \chi^L w_2^3(2)v_2^3(2)\end{aligned}}{1 + \chi^L}.$$

$$(7.39)$$

Notice that $\lambda_1 > \lambda_2$, hence $\chi < 1$. Thus, in the thermodynamic limit $L \to \infty$, one gets

$$\rho = \omega_2(1)v_2(1), \quad (7.40)$$

$$G(r) = \omega_2^2(1)v_2^2(1) + \chi^r \omega_2(1)\omega_2(2)v_2(1)v_2(2), \quad (7.41)$$

$$G(r_1, r_2) = \omega_2^3(1)v_2^3(1) + (\chi^{r_1} + \chi^{r_2})\omega_2^2(1)v_2^2(1)\omega_2(2)v_2(2) + \chi^{r_1+r_2}\omega_2(1)v_2(1)\omega_2^2(2)v_2^2(2). \quad (7.42)$$

Thus, one has from (7.40) – (7.42) that

$$\rho = \frac{x}{(\lambda_1 - xy)^2 + x}, \quad (7.43)$$

$$G(1) = \rho^2 + \chi\rho\frac{x}{(\lambda_2 - xy)^2 + x}, \quad (7.44)$$

$$G(2) = \rho^2 + \chi^2\rho\frac{x}{(\lambda_2 - xy)^2 + x}, \quad (7.45)$$

$$G(1,1) = \rho^3 + 2\chi\rho^2\frac{x}{(\lambda_2 - xy)^2 + x} + \chi^2\rho\frac{x^2}{((\lambda_2 - xy)^2 + x)^2}. \quad (7.46)$$

where $\chi = \dfrac{1 + xy - \sqrt{(xy-1)^2 + 4x}}{1 + xy + \sqrt{(xy-1)^2 + 4x}}$.

Before drawing graphs of the stationary current, one notices from (7.43) that

$$x = \begin{cases} \dfrac{2\rho y(\rho - 1) - (2\rho - 1)^2 - \sqrt{(2\rho y(\rho - 1) - (2\rho - 1)^2)^2 - 4\rho^2 y^2(\rho - 1)^2}}{2(\rho - 1)\rho y^2} & \text{if } \rho \geq 0.5, \\[4mm] \dfrac{2\rho y(\rho - 1) - (2\rho - 1)^2 + \sqrt{(2\rho y(\rho - 1) - (2\rho - 1)^2)^2 - 4\rho^2 y^2(\rho - 1)^2}}{2(\rho - 1)\rho y^2} & \text{if } 0 < \rho < 0.5. \end{cases}$$

$$(7.47)$$

Remark 7.3. *Since one has the relation (7.4), the stationary current is a function of the particle density ρ and $y, \omega^\star, \phi^\star, d^{1\star}, e^{\star 1}$. As for KLS model, one requires $d^{1\star} = e^{\star 1}$, thus the current depends only on $\rho, y, \omega^\star, \phi^\star, d^{1\star}$.*

We are now able to plot some graphs of the stationary current. Observe that in the

stationary current figures, the value of $d^{1\star} = e^{\star 1}$ corresponds to the KLS model (represented by blue curves). The repulsive interaction case $(y < 1)$ can be seen in Fig. 7.5, while the attractive case $(y > 1)$ can be viewed in Figs. 7.3 and 7.4.
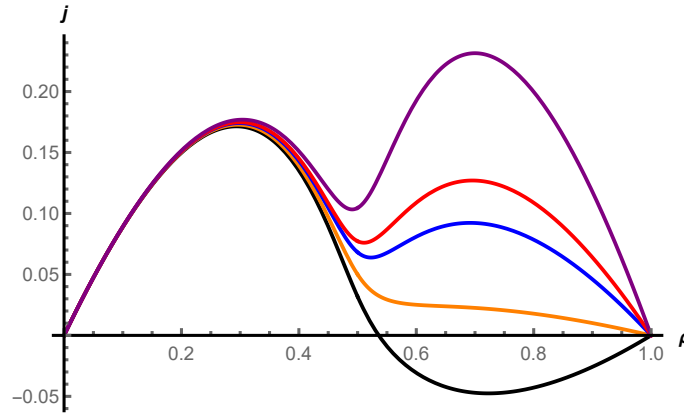
Figure 7.3: *Stationary current j with $y = 100, \omega^\star = 2, \phi^\star = 1, e^{\star 1} = 0.5$ and different values of $d^{1\star}$ as a function of the particle density ρ. Curves from the bottom to the top: $d^{1\star} = 0.1, 0.3, 0.5, 0.6, 0.9$.*
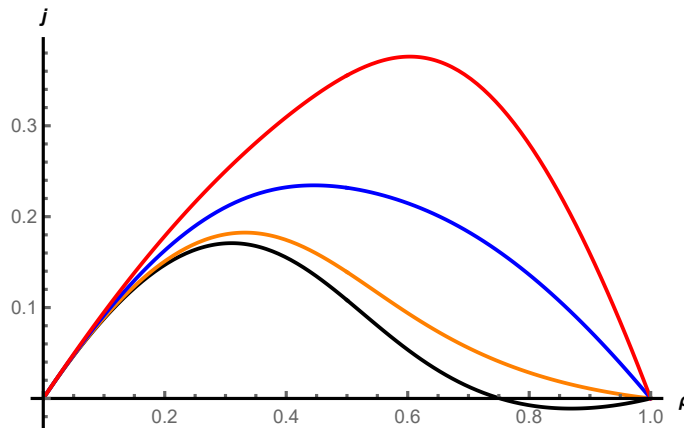
Figure 7.4: *Stationary current j with $y = 5, \omega^\star = 2, \phi^\star = 1, e^{\star 1} = 0.5$ and different values of $d^{1\star}$ as a function of the particle density ρ. Curves from the bottom to the top: $d^{1\star} = 0.1, 0.2, 0.5, 0.9$.*

Remark 7.4. *The stationary current of the KLS model can be either negative or positive at any particle density, depending on whether the value of $\omega^\star - \phi^\star$ is negative or positive, respectively. This can be shown by noting that in the KLS model, $d^{1\star} = e^{\star 1}$ and $d^{\star 01} = e^{10\star}$ are required. As a result, the stationary current (7.26) can be written as*

$$j_i = j_{i,i+1} - \frac{\phi^\star}{\omega^\star} j_{i,i+1} = \left(1 - \frac{\phi^\star}{\omega^\star}\right) j_{i,i+1}. \tag{7.48}$$

Note that since $j_{i,i+1}$ represents the current from the site i to site $i+1$, it is always positive. This leads to the desired conclusion. It should be emphasized that this is not the case for our model, as seen in Figs. 7.3 and 7.4.
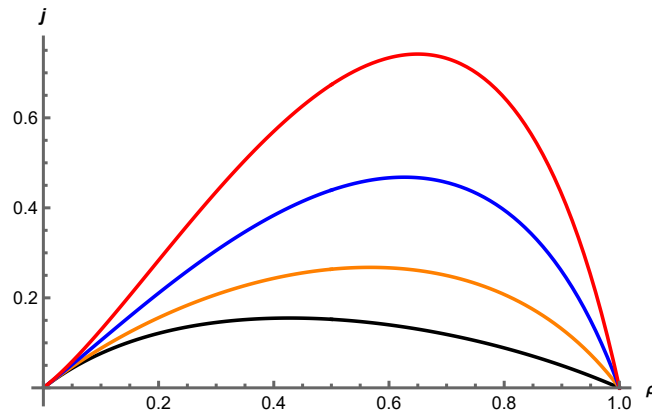
Figure 7.5: *Stationary current j with $y = 0.5$ (repulsive interaction), $\omega^\star = 2, \phi^\star = 1, e^{\star 1} = 0.5$ and different values of $d^{1\star}$ as a function of the particle density ρ. Curves from the bottom to the top: $d^{1\star} = 0.01, 0.2, 0.5, 0.9$.*

Remark 7.5. *We conjecture that the stationary current in the repulsive case ($y < 1$), depicted in Fig. 7.5, has only a single extreme point. On the other hand, the current can have two extremes in the attractive case ($y > 1$), as seen in Figs. 7.3 and 7.4. Furthermore, when the attraction is very strong, that is, when y is large, as demonstrated in Fig. 7.3, the current can exhibit either two maxima or two minima. Finally, in the attractive case, if the parameter $d^{1\star}$ is big (close to 1), the current presents one maximum and one minimum, see also in Figs. 7.3 and 7.4.*

7.3.2 Correlation length

Recall that the joint correlation $G_L(r)$ (7.38) in the thermodynamic limit is of the form (7.41). Let us rewrite it here

$$G(r) = \rho^2 + \chi^r \omega_2(1)\omega_2(2)v_2(1)v_2(2). \tag{7.49}$$

Recall that one has

$$\omega_2(1) = v_2(1) = \frac{\sqrt{x}}{\sqrt{(\lambda_1 - xy)^2 + x}}, \tag{7.50}$$

$$\omega_2(2) = v_2(2) = \frac{\sqrt{x}}{\sqrt{(\lambda_2 - xy)^2 + x}}, \tag{7.51}$$

$$\chi = \frac{1 + xy - \sqrt{(xy - 1)^2 + 4x}}{1 + xy + \sqrt{(xy - 1)^2 + 4x}}. \tag{7.52}$$

and notice that $\chi > 0$ if only if $y > 1$. Thus, in this case, the correlation function

$$C_L(r) := \langle(\eta_i - \rho_L)(\eta_{i+r} - \rho_L)\rangle_{\hat{\pi}_{gc}} = G_L(r) - \rho_L^2 \tag{7.53}$$

has the asymptotic behavior

$$C(r) = C_0 e^{-\frac{r}{\xi_1}}, \tag{7.54}$$

where the asymptotic behaviour of C_0 is

$$C_0 = \omega_2(1)\omega_2(2)v_2(1)v_2(2) \tag{7.55}$$

and the correlation length is

$$\xi_1 := -\frac{1}{\ln \chi}. \tag{7.56}$$

Thus correlations decay exponentially in the distance r along with the parameter ξ.

As for the case $\chi = 0$ corresponding to $y = 1$, one has $C(r) = 0$. This means that the two-point correlation function (7.53) vanishes in the limit $L \to \infty$ which is similar to the case of SSEP.

As for the case $\chi < 0$ corresponding to $0 < y < 1$, the correlation function (7.53) has the asymptotic behaviour

$$C(r) = \begin{cases} C_0 e^{-\frac{r}{\xi_2}}, & \text{if } r \text{ is even,} \\ -C_0 e^{-\frac{r}{\xi_2}}, & \text{if } r \text{ is odd,} \end{cases} \tag{7.57}$$

where the correlation length $\xi_2 = -\dfrac{1}{\ln(-\chi)}$ and C_0 is the same as in (7.55).

Remark 7.6. *Despite the fact that, in the non-interacting case of our model, i.e., when $y = 1$, the jump rate of a particle depends upon the occupation of the nearest-neighbor site to the left and the next-nearest site to the right, and only requires $d^{1\star} = d^{\star 01}$, the correlation still vanishes in a similar manner to that of the SSEP case.*

7.4   Summary

Our model is a generalization of the KLS model. Since the parameters that appear in the jump rates allow for wider choices as compared to the KLS model, then we were able to reveal interesting characteristic of the particle current that are not present in the KLS model. Specifically, unlike the KLS model, where the stationary current is either negative or positive at any particle density, the current in our model is a function of the particle density that can change its sign when the density is high enough.

Additionally, our model can be divided into three regimes: attractive, non-interacting, and repulsive, which correspond to $y > 1, y = 1$, and $y < 1$, respectively. At the critical point $y = 1$, the correlation vanishes in a manner similar to that in the SSEP case. In the attractive regime, the correlation is always positive, while in the repulsive regime, the sign of the correlation can change based on the distance between two particles.

Chapter 8

Generalized Ising measure with nearest and next–nearest neighbors interaction for a one–dimensional lattice gas

In order to get more information about RNA transcription model introduced in Chapter 4 such as joint density expectations and average RNAP current, we shall consider only translocation dynamics of rods whose length is 1 which is comparable to the interaction range. Because of the factorization of the generalized Ising measure (4.4) into the distance part and the part the takes into account the difference between states, one can guess that the invariant distribution of the model considered in this chapter is of the form (8.2) which is a generalized Ising measure with nearest and next–nearest neighbor interaction.

8.1 Generalized Ising measure with nearest and next–nearest neighbor interaction

Consider the Gibbs measure on the ring $\mathbb{T}_L$ that has nearest and next–nearest neighbor interaction energies as follows

$$\hat{\pi}_1(\boldsymbol{\eta}) = \frac{1}{Z_L} \exp\left\{ -\beta \sum_{i=1}^{L} \{J_1 \eta_i \eta_{i+1} + J_2 \eta_i (1 - \eta_{i+1}) \eta_{i+2} + J_3 \eta_i \eta_{i+1} \eta_{i+2}\} - \beta h \sum_{i=1}^{L} \eta_i \right\}.$$

$$(8.1)$$

Here Z_L is the partition function, the non-negative real parameter β is proportional to the inverse of experimentally strictly positive temperature T, and constant h plays the role of a chemical potential. The case $J_2 = J_3$ was studied in [12, 27, 31]. In this chapter,

we consider a generalization of the simple exclusion process which admits (8.1) as its invariant measure corresponding to the case $J_3 = 0$. Namely, the form of the Gibbs measure (8.1) for the case $J_3 = 0$ is the following

$$\hat{\pi}_2(\boldsymbol{\eta}) = \frac{1}{Z_L} \exp\left\{-\beta \sum_{i=1}^{L} \{J_1 \eta_i \eta_{i+1} + J_2 \eta_i (1 - \eta_{i+1}) \eta_{i+2}\} - \beta h \sum_{i=1}^{L} \eta_i\right\}, \qquad (8.2)$$

where Z_L is the partition function.

8.2 Exclusion processes with nearest and next-nearest neighbor interaction

In this section, we consider an exclusion process on the ring $\mathbb{T}_L$ with L sites and N particles. Denote the positions of the particles by $\mathbf{x} = (x_1, x_2, ..., x_N)$. The jump rate of ith particle at position x_i will be of the following form

$$\omega_i(\boldsymbol{\eta}) = w_i^1(\boldsymbol{\eta}) + w_i^2(\boldsymbol{\eta}), \qquad (8.3)$$

where

- $w_i^1(\boldsymbol{\eta}) := \omega_1^\star (1 + d^{1\star} \delta_{x_i, x_{i-1}+1} + d^{10\star} \delta_{x_i, x_{i-1}+2})(1 - \delta_{x_{i+1}, x_i+1}) \delta_{x_{i+1}, x_i+2}$;
- $w_i^2(\boldsymbol{\eta}) := \omega_2^\star (1 + e^{1\star} \delta_{x_i, x_{i-1}+1} + e^{10\star} \delta_{x_i, x_{i-1}+2})(1 - \delta_{x_{i+1}, x_i+1})(1 - \delta_{x_{i+1}, x_i+2})$.

In words, the microscopic dynamics is as follows. We associate with each particle a random Poissonian clock. When the clock on i^{th} particle at position x_i rings, the particle can hop to the site $x_i + 1$ provided the target site is vacant with a rate depending on the occupancy of its nearest and next-nearest neighboring sites on both sides (left and right). The parameter in the rates must be chosen to ensure the positivity of the rates. Namely, the parameter range is $\omega_1^\star, \omega_2^\star > 0, d^{1\star}, d^{10\star}, e^{1\star}, e^{10\star} \geq -1$. For pictorial representations of the rates, see Fig. 8.1.

(a) $w_i(\boldsymbol{\eta}) = \omega_1^\star(1 + d^{1\star})$

(b) $w_i(\boldsymbol{\eta}) = \omega_2^\star(1 + e^{1\star})$

(c) $w_i(\boldsymbol{\eta}) = \omega_1^\star(1 + d^{10\star})$

(d) $w_i(\boldsymbol{\eta}) = \omega_2^\star(1 + e^{10\star})$

(e) $w_i(\boldsymbol{\eta}) = \omega_2^\star$
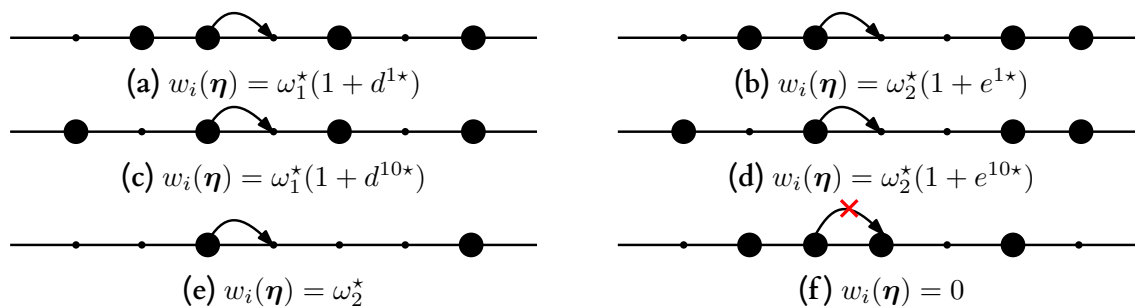
(f) $w_i(\boldsymbol{\eta}) = 0$

Figure 8.1: *Some examples of the jump rate of a particle (with arrow).*

Notice here that in the present case, the rates are different from the rates of the model studied in the case $d = 2$ of Chapter 6; in the current study, the rates depend not only

on the position of the rightmost neighboring particle but also on the leftmost neighboring one, while in in Chapter 6, the rates depend only on the position of the rightmost neighboring particle.

By applying the approach developed in Chapter 4 to the dynamics of the present model, we get the main result of this chapter which is Theorem 1.8. We will give a direct proof of the theorem.

Theorem 8.1. *If parameters $d^{1\star}, d^{\star 01}, e^{1\star}$ and $e^{10\star}$ of the model satisfy the following constraints*

$$d^{1\star} = \frac{\omega_2^\star}{\omega_1^\star}(e^{1\star} - e^{10\star}), \tag{8.4}$$

$$d^{10\star} = e^{10\star}, \tag{8.5}$$

then the process has an invariant distribution which is of the following form

$$\hat{\pi}(\boldsymbol{\eta}) = \frac{1}{Z_L}\left(\frac{\omega_2^\star}{\omega_1^\star}(1 + e^{1\star})(1 + e^{10\star})\right)^{-\sum_{i=1}^L \eta_i \eta_{i+1}}(1 + e^{10\star})^{-\sum_{i=1}^L \eta_i(1-\eta_{i+1})\eta_{i+2}} \tag{8.6}$$

where Z_L is the partition function.

Before giving proof of the theorem, let us list below some remarks.

Remark 8.1. *In the parametrization*

$$\frac{\omega_2^\star}{\omega_1^\star}(1 + e^{1\star})(1 + e^{10\star}) = e^{\beta J_1} \tag{8.7}$$

$$1 + e^{10\star} = e^{\beta J_2} \tag{8.8}$$

we see that the invariant measure (8.6) is of the (8.2) form.

Remark 8.2. *In the fully repulsive case, one requires*

$$\begin{cases} \omega_2^\star \geq \omega_1^\star, \\ d^{1\star} \geq d^{10\star}, \\ e^{1\star} \geq e^{10\star}, \\ \omega_2^\star(1 + e^{1\star}) \geq \omega_1^\star(1 + d^{1\star}). \end{cases} \tag{8.9}$$

We notices that the conditions $\omega_2^\star \geq \omega_1^\star, e^{1\star} \geq e^{10\star}$, and $\omega_2^\star(1 + e^{1\star}) \geq \omega_1^\star(1 + d^{1\star})$, imply that the condition $d^{1\star} \geq d^{10\star}$ is automatically satisfied.

Proof of Theorem 8.1. The master equation for the probability $\mathbb{P}_t(\boldsymbol{\eta})$ of finding the particles at time t in the configuration $\boldsymbol{\eta}$

$$\frac{d}{dt}\mathbb{P}(\boldsymbol{\eta}, t) = \sum_{i=1}^N \left[\omega_i(\boldsymbol{\eta}^{i-1,i})\mathbb{P}(\boldsymbol{\eta}^{i-1,i}, t) - \omega_i(\boldsymbol{\eta})\mathbb{P}(\boldsymbol{\eta}, t)\right] \tag{8.10}$$

where $\boldsymbol{\eta}^{i-1,i}$ is the configuration that leads to $\boldsymbol{\eta}$ before a forward translocation of ith particle (i.e., with coordinate $x_j^{i-1,i} = x_j - \delta_{j,i}$ for $j = 1, ..., N$). Notice here that due to periodicity, the positions x_i of the particles are counted modulo L and labels i are counted modulo N.

If a measure π is the invariant of the process then, upon dividing (8.10) by the stationary distribution $\pi(\boldsymbol{\eta})$, the stationary condition becomes

$$\sum_{i=1}^{N} \left[\omega_i(\boldsymbol{\eta}^{i-1,i}) \frac{\pi(\boldsymbol{\eta}^{i-1,i})}{\pi(\boldsymbol{\eta})} - \omega_i(\boldsymbol{\eta}) \right] = 0. \tag{8.11}$$

In order to prove the theorem, we only need to show that equation (8.11) holds for measure (8.6). For simplicity of notations, we denote by

$$\theta_i^p := \delta_{x_{i+1}, x_i+1+p} \tag{8.12}$$

the indicator functions on a headway of length p with the index i taken modulo N, i.e., $\theta_0^p \equiv \theta_N^p$.

In terms of new variable θ_i^p and

$$y_1 = \left(\frac{\omega_2^{\star}}{\omega_1^{\star}} (1 + e^{1\star})(1 + e^{10\star}) \right)^{-1}, \quad y_2 = (1 + e^{10\star})^{-1}, \tag{8.13}$$

one can rewrite measure (8.6) as follows

$$\hat{\pi}(\boldsymbol{\eta}) = \frac{1}{Z} \prod_{i=1}^{N} y_1^{\theta_i^0} y_2^{\theta_i^1}. \tag{8.14}$$

Moreover, the same new notations allow us to rewrite also the jump rates that appear in equation (8.11); the result is:

$$\begin{aligned}
\omega_i(\boldsymbol{\eta}) &= \omega_1^{\star}(1 + d^{1\star}\theta_{i-1}^0 + d^{10\star}\theta_{i-1}^1)(1 - \theta_i^0)\theta_i^1 \\
&\quad + \omega_2^{\star}(1 + e^{1\star}\theta_{i-1}^0 + e^{10\star}\theta_{i-1}^1)(1 - \theta_i^0)(1 - \theta_i^1), \tag{8.15} \\
\omega_i(\boldsymbol{\eta}^{i-1,i}) &= \omega_1^{\star}(1 + d^{1\star}\theta_{i-1}^1 + d^{10\star}\theta_{i-1}^2)(1 - \theta_{i-1}^0)\theta_i^0 \\
&\quad + \omega_2^{\star}(1 + e^{1\star}\theta_{i-1}^1 + e^{10\star}\theta_{i-1}^2)(1 - \theta_{i-1}^0)(1 - \theta_i^0). \tag{8.16}
\end{aligned}$$

One has

$$\frac{\hat{\pi}(\boldsymbol{\eta}^{i-1,i})}{\hat{\pi}(\boldsymbol{\eta})} = y_1^{-\theta_{i-1}^0 - \theta_i^0 + \theta_{i-1}^1} y_2^{\theta_{i-1}^2 - \theta_{i-1}^1 + \theta_i^0 - \theta_i^1}. \tag{8.17}$$

Let us introduce new variables as follows

$$\begin{cases} a_1 & = -\omega_2^\star(1 + e^{1\star}), \\ a_2 & = \omega_1^\star(1 + d^{1\star}) - \omega_2^\star(1 + e^{1\star}), \\ a_k & = 0, \text{ for } k \geq 3. \end{cases} \tag{8.18}$$

Under conditions (8.4) and (8.5), it is easy to check that

$$\omega_i(\boldsymbol{\eta}^{i-1,i})\frac{\hat{\pi}(\boldsymbol{\eta}^{i-1,i})}{\hat{\pi}(\boldsymbol{\eta})} - \omega_i(\boldsymbol{\eta}) = a_{m+1} - a_{n+1}, \tag{8.19}$$

where m, n are the distances between i^{th} particle and its leftmost and rightmost neighboring particle, respectively. Thus, due to periodicity of the lattice, by summing over index i from 1 to N, one gets

$$\sum_{i=1}^{N} \left[\omega_i(\boldsymbol{\eta}^{i-1,i})\frac{\hat{\pi}(\boldsymbol{\eta}^{i-1,i})}{\hat{\pi}(\boldsymbol{\eta})} - \omega_i(\boldsymbol{\eta}) \right] = 0. \tag{8.20}$$

Therefore, $\hat{\pi}$ is the invariant measure of the process. The proof is complete. $\square$

8.3   Stationary current

We consider the mean density

$$\rho_L := \langle \eta_i \rangle_{\hat{\pi}} = \frac{1}{Z_L} \sum_{\boldsymbol{\eta}} \eta_i \pi(\boldsymbol{\eta}), \tag{8.21}$$

and for $r_i \geq 1$ the joint expectations

$$\begin{aligned} G_L(r_1, ..., r_k) &:= \langle \eta_i \eta_{i+r_1} \eta_{i+r_1+r_2} ... \eta_{i+r_1+...+r_k} \rangle_{\hat{\pi}} \\ &= \frac{1}{Z_L} \sum_{\boldsymbol{\eta}} \eta_i \eta_{i+r_1} \eta_{i+r_1+r_2} \cdots \eta_{i+r_1+...+r_k} \pi(\boldsymbol{\eta}), \end{aligned} \tag{8.22}$$

with the constraint that $\sum_{i=1}^{k} r_k < L$, where π is the unnormalized invariant measure. Here $\langle \cdot \rangle_{\hat{\pi}}$ is the expectation with respect to measure $\hat{\pi}$. Because of the translation invariance the joint expectations do not depend on i.

Since the number of particles is conserved, the stationary distribution can be expressed in grand-canonical form with a fugacity z which is the following

$$\hat{\pi}_{gc}(\boldsymbol{\eta}) = \frac{1}{\hat{Z}_{gc}} y_1^{\sum_{i=1}^{L} \eta_i \eta_{i+1}} y_2^{\sum_{i=1}^{L} \eta_i(1-\eta_{i+1})\eta_{i+2}} z^{\sum_{i=1}^{L} \eta_i}. \tag{8.23}$$

Notice here that the variables y_1^{-1}, y_2^{-1} correspond, respectively, to y_1, y_2 that appear in the arguments of Chapter 6. Thus, we can make use of the same transfer matrix (B.4) in Appendix B for computations the joint expectations.

The stationary current of particles between sites $(i, i+1)$ is the following

$$
\begin{aligned}
j_i = & \langle \eta_i(1 - \eta_{i+1})[\omega_1^\star(1 + e^{10\star})\eta_{i-2}(1 - \eta_{i-1})\eta_{i+2} + \omega_1^\star(1 + d^{1\star})\eta_{i-1}\eta_{i+2} \\
& + \omega_2^\star(1 + e^{10\star})\eta_{i-2}(1 - \eta_{i-1})(1 - \eta_{i+2}) + \omega_2^\star(1 + e^{1\star})\eta_{i-1}(1 - \eta_{i+2}) \\
& + \omega_1^\star(1 - \eta_{i-2})(1 - \eta_{i-1})\eta_{i+2} + \omega_2^\star(1 - \eta_{i-2})(1 - \eta_{i-1})(1 - \eta_{i+2})]\rangle_{\hat{\pi}_{gc}} \quad (8.24) \\
= & \omega_2^\star \rho_L + \omega_2^\star(e^{1\star} - 1)G_L(1) + (\omega_2^\star e^{10\star} + \omega_1 - \omega_2)G_L(2) \\
& - (\omega_2^\star e^{10\star} + \omega_2^\star e^{1\star} + \omega_1^\star - \omega_2^\star)G_L(1,1) + (\omega_1^\star d^{1\star} - \omega_2^\star e^{1\star})G_L(1,2) - \omega_2^\star e^{10\star}G_L(2,1) \\
& + e^{10\star}(\omega_1^\star - \omega_2^\star)G_L(2,2) + (\omega_2^\star e^{10\star} - \omega_1^\star d^{1\star} + \omega_2^\star e^{1\star})G_L(1,1,1) \\
& - e^{10\star}(\omega_1^\star - \omega_2^\star)(G_L(1,1,2) + G_L(2,1,1) - G_L(1,1,1,1)) \quad (8.25)
\end{aligned}
$$

In the thermodynamic limit $L \to \infty$, one obtains

$$
\begin{aligned}
j = & \omega_2^\star \rho + \omega_2^\star(e^{1\star} - 1)G(1) + (\omega_2^\star e^{10\star} + \omega_1 - \omega_2)G(2) \\
& - (\omega_2^\star e^{10\star} + \omega_2^\star e^{1\star} + \omega_1^\star - \omega_2^\star)G(1,1) + (\omega_1^\star d^{1\star} - \omega_2^\star e^{1\star})G(1,2) - \omega_2^\star e^{10\star}G(2,1) \\
& + e^{10\star}(\omega_1^\star - \omega_2^\star)G(2,2) + (\omega_2^\star e^{10\star} - \omega_1^\star d^{1\star} + \omega_2^\star e^{1\star})G(1,1,1) \\
& - e^{10\star}(\omega_1^\star - \omega_2^\star)(G(1,1,2) + G(2,1,1) - G(1,1,1,1)), \quad (8.26)
\end{aligned}
$$

where $G(1)$, $G(2)$, $G(1,1)$, $G(1,2)$, $G(2,1)$, $G(2,2)$, $G(1,1,1)$, $G(1,1,2)$, $G(2,1,1)$, and $G(1,1,1,1)$ are the limits of $G_L(1)$, $G_L(2)$, $G_L(1,1)$, $G_L(1,2)$, $G_L(2,1)$, $G_L(2,2)$, $G_L(1,1,1)$, $G_L(1,1,2)$, $G_L(2,1,1)$, and $G_L(1,1,1,1)$ respectively as L tends to infinity.

Denote

$$
\chi_i := \frac{\lambda_i}{\lambda_1}, \text{ for } i = 1, 2, 3, 4, \quad (8.27)
$$

where $\lambda_i, i = 1, 2, 3, 4$, are the eigenvectors of the transfer matrix T_2 (B.4) (see Appendix B). To compute the mean density and the joint expectations, we use the same projectors (6.72) as follows

$$
\hat{n}_1 := \hat{n} \otimes \mathbb{1}, \qquad \hat{n}_2 := \mathbb{1} \otimes \hat{n} \quad (8.28)
$$

where $\mathbb{1}$ is the two-dimensional unit matrix and

$$
\hat{n} := \begin{pmatrix} 0 & 0 \\ 0 & 1 \end{pmatrix}. \quad (8.29)
$$

Recall from Chapter 6 that

$$
\hat{n}_1 |\eta_{2i-1}, \eta_{2i}\rangle = \eta_{2i-1} |\eta_{2i-1}, \eta_{2i}\rangle, \qquad \hat{n}_2 |\eta_{2i-1}, \eta_{2i}\rangle = \eta_{2i} |\eta_{2i-1}, \eta_{2i}\rangle, \quad (8.30)
$$

where ket-vectors $|i, j\rangle$ for $i, j \in \{0, 1\}$ are defined in (B.7). Identities in (8.30) allow one to replace the occupation variables η_i in the product $\eta_i \pi_2(\boldsymbol{\eta})$ by projectors at ap-

propriately chosen positions in the string (B.12).

The normalized left and right eigenvectors are denoted by

$$\langle \lambda_i | = (w_1(i), w_2(i), w_3(i), w_4(i)), \qquad | \lambda_i \rangle = \begin{pmatrix} v_1(i) \\ v_2(i) \\ v_3(i) \\ v_4(i) \end{pmatrix}, \text{ for } i = 1, 2, 3, 4 \qquad (8.31)$$

and we recall the completeness relation

$$\sum_{i=1}^{4} | \lambda_i \rangle \langle \lambda_i | = \mathbb{1}. \qquad (8.32)$$

The mean density (8.21) and some needed cases of joint expectations (6.53) with respect to $\hat{\pi}_2$ are the following

$$\rho_L = \frac{1}{Z_L} \mathrm{Tr} \hat{n}_2 T_2^{L/2}$$

$$= \frac{\sum_{k=1}^{4} \lambda_k^{L/2} \langle \lambda_k | \hat{n}_2 | \lambda_k \rangle}{\sum_{k=1}^{4} \lambda_k^{L/2}}, \qquad (8.33)$$

$$G_L(2m) = \frac{1}{Z_L} \mathrm{Tr} T_2^{i-1} \hat{n}_2 T_2^{m} \hat{n}_2 T_2^{L/2-i-m+1}$$

$$= \frac{\sum_{k=1}^{4} \sum_{l=1}^{4} \lambda_k^{L/2-m} \lambda_l^{m} \langle \lambda_k | \hat{n}_2 | \lambda_l \rangle \langle \lambda_l | \hat{n}_2 | \lambda_k \rangle}{\sum_{k=1}^{4} \lambda_k^{L/2}}, \qquad (8.34)$$

$$G_L(2m+1) = \frac{1}{Z_L} \mathrm{Tr} T_2^{i-1} \hat{n}_2 T_2^{m+1} \hat{n}_1 T_2^{L/2-i-m}$$

$$= \frac{\sum_{k=1}^{4} \sum_{l=1}^{4} \lambda_k^{L/2-m-1} \lambda_l^{m+1} \langle \lambda_k | \hat{n}_2 | \lambda_l \rangle \langle \lambda_l | \hat{n}_1 | \lambda_k \rangle}{\sum_{k=1}^{4} \lambda_k^{L/2}}, \qquad (8.35)$$

$$G_L(2m, 2n+1) = \frac{1}{Z_L} \mathrm{Tr} T_2^{i-1} \hat{n}_2 T_2^{m} \hat{n}_2 T_2^{n+1} \hat{n}_1 T_2^{L/2-i-m-n}$$

$$= \frac{\begin{array}{c} \sum_{j=1}^{4} \sum_{k=1}^{4} \sum_{l=1}^{4} \lambda_j^{L/2-m-n-1} \lambda_k^{m} \lambda_l^{n+1} \\ \times \langle \lambda_j | \hat{n}_2 | \lambda_k \rangle \langle \lambda_k | \hat{n}_2 | \lambda_l \rangle \langle \lambda_l | \hat{n}_1 | \lambda_j \rangle \end{array}}{\sum_{j=1}^{4} \lambda_j^{L/2}}, \qquad (8.36)$$

$$G_L(2m+1, 2n) = \frac{1}{Z_L} \mathrm{Tr} T_2^{i-1} \hat{n}_2 T_2^{m+1} \hat{n}_1 T_2^{n} \hat{n}_1 T_2^{L/2-i-m-n} \qquad (8.37)$$

$$= \frac{\begin{array}{c} \sum_{j=1}^{4} \sum_{k=1}^{4} \sum_{l=1}^{4} \lambda_j^{L/2-m-n-1} \lambda_k^{m+1} \lambda_l^{n} \\ \times \langle \lambda_j | \hat{n}_2 | \lambda_k \rangle \langle \lambda_k | \hat{n}_1 | \lambda_l \rangle \langle \lambda_l | \hat{n}_1 | \lambda_j \rangle \end{array}}{\sum_{j=1}^{4} \lambda_j^{L/2}}. \qquad (8.38)$$

We also need $G_L(1,1)$ in order to be able to compute the stationary current. One gets

$$
\begin{aligned}
G_L(1,1) &= \frac{1}{Z_L} \mathrm{Tr} T_2^{i-1} \hat{n}_2 T_2 \hat{n}_1 \hat{n}_2 T_2^{L/2-i} \\
&= \frac{\sum_{k=1}^{4} \sum_{l=1}^{4} \lambda_k^{L/2-1} \lambda_k \langle \lambda_k | \hat{n}_2 | \lambda_l \rangle \langle \lambda_l | \hat{n}_1 \hat{n}_2 | \lambda_k \rangle}{\sum_{k=1}^{4} \lambda_k^{L/2}}.
\end{aligned}
\tag{8.39}
$$

As for the case $G_L(r_1, r_2, r_3)$, in this work, we need the cases $r_1 = r_2 = r_3 = 1$, $r_1 = 2, r_2 = r_3 = 1$, and $r_1 = 1 = r_2 = 1, r_3 = 2$ only. One gets

$$
\begin{aligned}
G_L(1,1,1) &= \frac{1}{Z_L} \mathrm{Tr} T_2^{i-1} \hat{n}_2 T_2 \hat{n}_1 \hat{n}_2 T_2 \hat{n}_1 T_2^{L/2-i-1} \\
&= \frac{\begin{array}{c} \sum_{j=1}^{4} \sum_{k=1}^{4} \sum_{l=1}^{4} \lambda_j^{L/2-2} \lambda_k \lambda_l \\ \times \langle \lambda_j | \hat{n}_2 | \lambda_k \rangle \langle \lambda_k | \hat{n}_1 \hat{n}_2 | \lambda_l \rangle \langle \lambda_l | \hat{n}_1 | \lambda_j \rangle \end{array}}{\sum_{j=1}^{4} \lambda_j^{L/2}},
\end{aligned}
\tag{8.40}
$$

$$
\begin{aligned}
G_L(2,1,1) &= \frac{1}{Z_L} \mathrm{Tr} T_2^{i-1} \hat{n}_2 T_2 \hat{n}_2 T_2 \hat{n}_1 \hat{n}_2 T_2^{L/2-i-1} \\
&= \frac{\begin{array}{c} \sum_{j=1}^{4} \sum_{k=1}^{4} \sum_{l=1}^{4} \lambda_j^{L/2-2} \lambda_k \lambda_l \\ \times \langle \lambda_j | \hat{n}_2 | \lambda_k \rangle \langle \lambda_k | \hat{n}_2 | \lambda_l \rangle \langle \lambda_l | \hat{n}_1 \hat{n}_2 | \lambda_j \rangle \end{array}}{\sum_{j=1}^{4} \lambda_j^{L/2}},
\end{aligned}
\tag{8.41}
$$

$$
\begin{aligned}
G_L(1,1,2) &= \frac{1}{Z_L} \mathrm{Tr} T_2^{i-1} \hat{n}_2 T_2 \hat{n}_1 T_2 \hat{n}_1 T_2^{L/2-i-1} \\
&= \frac{\begin{array}{c} \sum_{j=1}^{4} \sum_{k=1}^{4} \sum_{l=1}^{4} \lambda_j^{L/2-2} \lambda_k \lambda_l \\ \times \langle \lambda_j | \hat{n}_2 | \lambda_k \rangle \langle \lambda_k | \hat{n}_1 | \lambda_l \rangle \langle \lambda_l | \hat{n}_1 | \lambda_j \rangle \end{array}}{\sum_{j=1}^{4} \lambda_j^{L/2}}.
\end{aligned}
\tag{8.42}
$$

As for the case $G_L(r_1, r_2, r_3, r_4)$, in this work, we only need the cases $r_1 = r_2 = r_3 = r_4 = 1$. One gets

$$
\begin{aligned}
G_L(1,1,1,1) &= \frac{1}{Z_L} \mathrm{Tr} T_2^{i-1} \hat{n}_2 T_2 \hat{n}_1 \hat{n}_2 T_2 \hat{n}_1 T_2^{L/2-i-1} \\
&= \frac{\begin{array}{c} \sum_{j=1}^{4} \sum_{k=1}^{4} \sum_{l=1}^{4} \lambda_j^{L/2-2} \lambda_k \lambda_l \\ \times \langle \lambda_j | \hat{n}_2 | \lambda_k \rangle \langle \lambda_k | \hat{n}_1 \hat{n}_2 | \lambda_l \rangle \langle \lambda_l | \hat{n}_1 | \lambda_j \rangle \end{array}}{\sum_{j=1}^{4} \lambda_j^{L/2}}.
\end{aligned}
\tag{8.43}
$$

One notices that $|\chi_i| < 1$ for $i = 2, 3, 4$ and

$$
\begin{aligned}
\langle \lambda_i | \hat{n}_1 | \lambda_j \rangle &= w_3(i) v_3(j) + w_4(i) v_4(j), \\
\langle \lambda_i | \hat{n}_2 | \lambda_j \rangle &= w_2(i) v_2(j) + w_4(i) v_4(j)
\end{aligned}
\tag{8.44}
$$

for $i, j = 1, 2, 3, 4$. Thus, in the thermodynamic limit $L \to \infty$, one gets

$$\rho = \langle \lambda_1 | \, \hat{n}_2 \, | \lambda_1 \rangle, \tag{8.45}$$

$$G(1) = \sum_{i=1}^{4} \chi_i \, \langle \lambda_1 | \, \hat{n}_2 \, | \lambda_i \rangle \langle \lambda_i | \, \hat{n}_1 \, | \lambda_1 \rangle, \tag{8.46}$$

$$G(2) = \sum_{i=1}^{4} \chi_i \, \langle \lambda_1 | \, \hat{n}_2 \, | \lambda_i \rangle \langle \lambda_i | \, \hat{n}_2 \, | \lambda_1 \rangle, \tag{8.47}$$

$$G(3) = \sum_{i=1}^{4} \chi_i^2 \, \langle \lambda_1 | \, \hat{n}_2 \, | \lambda_i \rangle \langle \lambda_i | \, \hat{n}_1 \, | \lambda_1 \rangle, \tag{8.48}$$

$$G(1,1) = \sum_{i=1}^{4} \chi_i \, \langle \lambda_1 | \, \hat{n}_2 \, | \lambda_i \rangle \langle \lambda_i | \, \hat{n}_1 \hat{n}_2 \, | \lambda_1 \rangle, \tag{8.49}$$

$$G(1,2) = \sum_{i=1}^{4} \sum_{j=1}^{4} \chi_i \chi_j \, \langle \lambda_1 | \, \hat{n}_2 \, | \lambda_i \rangle \langle \lambda_i | \, \hat{n}_1 \, | \lambda_j \rangle \langle \lambda_j | \, \hat{n}_1 \, | \lambda_1 \rangle, \tag{8.50}$$

$$G(2,1) = \sum_{i=1}^{4} \sum_{j=1}^{4} \chi_i \chi_j \, \langle \lambda_1 | \, \hat{n}_2 \, | \lambda_i \rangle \langle \lambda_i | \, \hat{n}_2 \, | \lambda_j \rangle \langle \lambda_j | \, \hat{n}_1 \, | \lambda_1 \rangle, \tag{8.51}$$

$$G(2,2) = \sum_{i=1}^{4} \sum_{j=1}^{4} \chi_i \chi_j \, \langle \lambda_1 | \, \hat{n}_2 \, | \lambda_i \rangle \langle \lambda_i | \, \hat{n}_2 \, | \lambda_j \rangle \langle \lambda_j | \, \hat{n}_2 \, | \lambda_1 \rangle, \tag{8.52}$$

$$G(1,1,1) = \sum_{i=1}^{4} \sum_{j=1}^{4} \chi_i \chi_j \, \langle \lambda_1 | \, \hat{n}_2 \, | \lambda_i \rangle \langle \lambda_i | \, \hat{n}_1 \hat{n}_2 \, | \lambda_j \rangle \langle \lambda_j | \, \hat{n}_1 \, | \lambda_1 \rangle, \tag{8.53}$$

$$G(2,1,1) = \sum_{i=1}^{4} \sum_{j=1}^{4} \chi_i \chi_j \, \langle \lambda_1 | \, \hat{n}_2 \, | \lambda_i \rangle \langle \lambda_i | \, \hat{n}_2 \, | \lambda_j \rangle \langle \lambda_j | \, \hat{n}_1 \hat{n}_2 \, | \lambda_1 \rangle, \tag{8.54}$$

$$G(1,1,2) = \sum_{i=1}^{4} \sum_{j=1}^{4} \chi_i \chi_j \, \langle \lambda_1 | \, \hat{n}_2 \, | \lambda_i \rangle \langle \lambda_i | \, \hat{n}_1 \, | \lambda_j \rangle \langle \lambda_j | \, \hat{n}_1 \, | \lambda_1 \rangle, \tag{8.55}$$

$$G(1,1,1,1) = \sum_{i=1}^{4} \sum_{j=1}^{4} \chi_i \chi_j \, \langle \lambda_1 | \, \hat{n}_2 \, | \lambda_i \rangle \langle \lambda_i | \, \hat{n}_1 \hat{n}_2 \, | \lambda_j \rangle \langle \lambda_j | \, \hat{n}_1 \, | \lambda_1 \rangle. \tag{8.56}$$

We are now in a position to plot some graphs of the stationary current corresponding to various values $\omega_1^\star, \omega_2^\star, e^{1\star}$ and $e^{10\star}$.
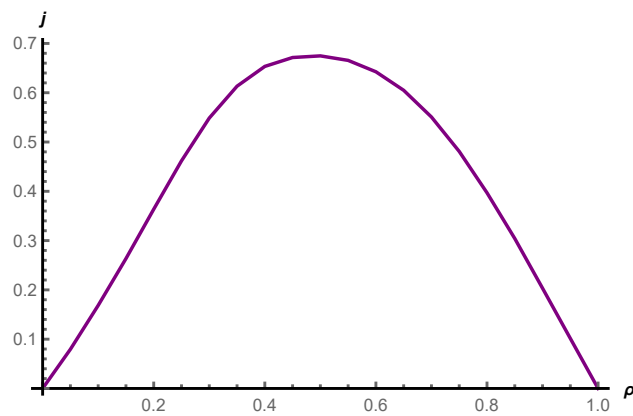
Figure 8.2: *Stationary current j as a function of the density ρ with $w_1^\star = 0.5, w_2^\star = 1.5, e^{1\star} = 2, e^{10\star} = 1$.*
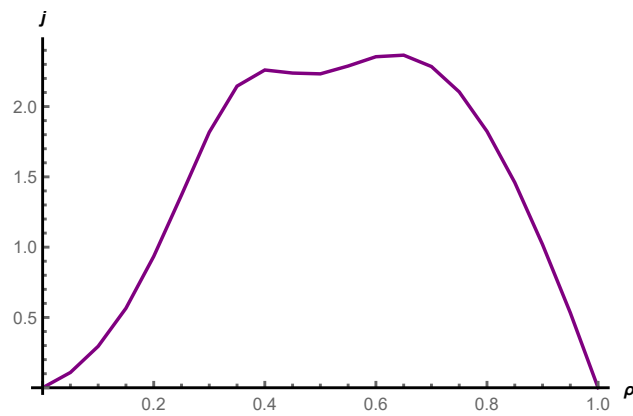
Figure 8.3: *Stationary current j as a function of the density ρ with $w_1^\star = 0.5, w_2^\star = 1.5, e^{1\star} = 9, e^{10\star} = 2$.*
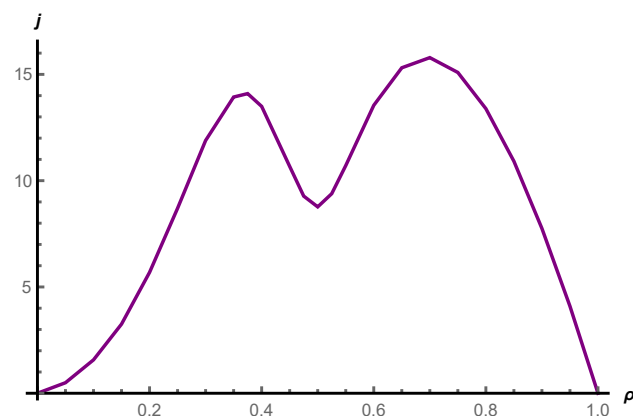
Figure 8.4: *Stationary current j as a function of the density ρ with $w_1^\star = 0.5, w_2^\star = 5, e^{1\star} = 19, e^{10\star} = 2$.*

8.4 Discussion

In Figs. 8.2, 8.4, and 8.3 above, we only consider the repulsive case, i.e., the case when $y_1^{-1} > y_2^{-1}$. The meaning of this inequality is the dependence of the rate of a particle to move away from its leftmost neighbor upon the number of the free lattice sites to the right of the moving particle. From Fig. (8.2), one can see that if y_1^{-1} and y_2^{-1} are small then the average current increases at low densities until it reaches maximum at density ρ_{max} and then decreases to 0.

The behaviour of the model of the present chapter is different from that considered in the case $d = 2$ of of Chapter 6. In that latter model, the average current only has a unique maximum. To the contrary, one of our models shows an intermediate minimum when the repulsive strengths y_1^{-1}, y_2^{-1} and blocking strength $\omega_1^\star/\omega_2^\star$ strong enough, i.e., y_1^{-1}, y_2^{-1} are large and $\omega_1^\star/\omega_2^\star$ is small, see Fig. 8.4. This conclusion has an important consequence: two models with the same invariant distribution may exhibit quite different behaviour, when one looks at their dynamic characteristics, like, for example, the particle current.

Chapter 9

Conclusions

In this thesis, the RNAP model proposed by Belitsky and Schütz [4, 5] was extended in two ways:

- We considered RNAP models previously suggested by [4] but we included into the consideration the reverse processes that may occur to the particles of the models and that were excluded from consideration in the work [4]. In this case study, we imposed the same form of invariant measure and, since the reverse processes were significantly small, the obtained results that are quite similar to the ones already reported in [4, 5]. However, the model generalization allowed us for a more deep insight at the RNAP models; this includes a better understanding of headway distribution, average excess and dwell times, and average velocity and flux of RNAP.

- We generalized the model by widening the interaction ranges both at microscopic and at macroscopic levels (Chapter 4). Namely, on the macroscopic level, the interaction range of the invariant measure was enlarged by taking into account the next-nearest interaction (added to the short-range potential as in Chapter 3). As a consequence of that, the particle interaction represented in transition rates must be extended as well; this means extension at microscopic level. The enhancements allowed us to discover novel features of the models corresponding to the following three cases: fully repulsive case, Lennard Jones potential, DLVO theory. Our conclusions show that the interactions added contribute to various phenomena and in different ways to the RNAP model. This fact motivated us to suggest further enhancement and extensions and to introduce (see Chapter 5) the interaction range in the invariant measure of an arbitrary length d.

The study of the first three chapter suggested to us to consider only translocation dynamics of the RNAP models and make the length of rods (RNAPs) be comparable to the interaction range, i.e. the length of rods becomes 1. Accordingly, the models in Chapter 6, 7 and 8 give insight into the RNAP density correlations. As a consequence, one can get information about the stationary current of the model. It worths to notice that the method used in Chapter 6 reveals how the number of speeds of particles must be related to the form of the generalized Ising measure. Moreover, the model in Chap-

ter 7 is a generalization of one-dimensional Katz–Lebowitz–Spohn model.

Finally, we would like to pose here some Open Problems.

- It would be interesting to consider RNAP models as in Chapters 4 and 5 but include the inverse processes as it has been done in Chapter 3.

- It would be interesting to study the models of Chapters 6, 7, and 8 in which particles are allowed to jump backward.

- It would be interesting to set the model as the one considered in Chapter 8 but study this model from the viewpoint of more general invariant measure mentioned like those mentioned at the beginning of that chapter.

Appendices

A Transfer matrix for Ising measure with nearest neighbor interaction

Consider the lattice gas with the nearest neighbor Bolzmann weigh

$$\pi_1(\boldsymbol{\eta}) = \exp\left\{-\beta \sum_{i=1}^{L} J_1 \eta_i \eta_{i+1} - \beta h \sum_{i=1}^{L} \eta_i\right\}. \tag{A.1}$$

Denote by

$$\omega_{1,i}(\boldsymbol{\eta}) = e^{-\beta J_1 \eta_i \eta_{i+1} - \frac{1}{2}\beta h(\eta_i + \eta_{i+1})}. \tag{A.2}$$

local Boltzmann weighs. Introduce the function $T_1 : \mathbb{S} \times \mathbb{S} \to \mathbb{R}_+$

$$T_1(\eta, \zeta) = e^{-\beta J_1 \eta \zeta - \frac{1}{2}\beta h(\eta + \zeta)}, \tag{A.3}$$

where $\mathbb{S} = \{0, 1\}$. This allows us to define the transfer matrix

$$T_1 := \begin{pmatrix} T_1(0,0) & T_1(0,1) \\ T_1(1,0) & T_1(1,1) \end{pmatrix} = \begin{pmatrix} 1 & \sqrt{x} \\ \sqrt{x} & xy \end{pmatrix}. \tag{A.4}$$

with the constants

$$x = e^{-\beta h}, \quad y = e^{-\beta J_1}. \tag{A.5}$$

Introducing the two-dimensional canonical basis vectors

$$|0\rangle = \begin{pmatrix} 1 \\ 0 \end{pmatrix}, \quad |1\rangle = \begin{pmatrix} 0 \\ 1 \end{pmatrix}. \tag{A.6}$$

with the scalar product $\langle \alpha | \beta \rangle = \delta_{\alpha,\beta}$, one finds

$$T_1(\eta, \zeta) = \langle \eta | T_1 | \zeta \rangle. \tag{A.7}$$

The invariant measure (A.1) can be written as

$$\hat{\pi}_1(\boldsymbol{\eta}) = \frac{1}{Z_{1,L}} \prod_{i=1}^{L} \omega_{1,i}(\boldsymbol{\eta}) = \frac{1}{Z_{1,L}} \prod_{i=1}^{L} T_1(\eta_i, \eta_{i+1}) = \frac{1}{Z_{1,L}} \prod_{i=1}^{L} \langle \eta_i | T_1 | \eta_{i+1} \rangle . \quad \text{(A.8)}$$

One has

$$Z_{1,L} = \sum_{\boldsymbol{\eta}} \pi_1(\boldsymbol{\eta}) \quad \text{(A.9)}$$

$$= \sum_{\eta_1=0}^{1} \sum_{\eta_2=0}^{1} \cdots \sum_{\eta_L=0}^{1} \langle \eta_1 | T_1 | \eta_2 \rangle \langle \eta_2 | T_1 | \eta_3 \rangle \cdots \langle \eta_{L-1} | T_1 | \eta_L \rangle \langle \eta_L | T_1 | \eta_1 \rangle . \quad \text{(A.10)}$$

Notice that

$$\sum_{\eta_i=0}^{1} | \eta_i \rangle \langle \eta_i | = \mathbb{1}, \quad \text{for all } i \in \{1, ..., L\}, \quad \text{(A.11)}$$

where $\mathbb{1}$ is the identity matrix. One gets

$$Z_{1,L} = \sum_{\eta_1=0}^{1} \langle \eta_1 | T_1 | \eta_1 \rangle = \text{Tr} T_1^L. \quad \text{(A.12)}$$

We denote the eigenvalues of the transfer matrix (A.4) by λ_i and assume without loss of generality that $\lambda_1 \geq \lambda_2$. The normalized left and right eigenvectors are denoted by

$$\langle \lambda_i | = (\omega_1(i), \omega_2(i)), \qquad | \lambda_i \rangle = \begin{pmatrix} v_1(i) \\ v_2(i) \end{pmatrix} \quad \text{(A.13)}$$

and one notices that

$$\sum_{i=1}^{2} | \lambda_i \rangle \langle \lambda_i | = \begin{pmatrix} w_1(1)v_1(1) + w_1(2)v_1(2) & w_2(1)v_1(1) + w_2(2)v_1(2) \\ w_1(1)v_2(1) + w_1(2)v_2(2) & w_2(1)v_2(1) + w_2(2)v_2(2) \end{pmatrix} = \mathbb{1}. \quad \text{(A.14)}$$

Namely, matrix T_1 (A.4) has eigenvalues

$$\lambda_1 = \frac{1}{2} \left(1 + xy + \sqrt{(xy-1)^2 + 4x} \right), \quad \lambda_2 = \frac{1}{2} \left(1 + xy - \sqrt{(xy-1)^2 + 4x} \right), \quad \text{(A.15)}$$

and its left and right normalized eigenvectors in (A.13) are the following

$$\langle \lambda_1 | = \left(\frac{\lambda_1 - xy}{\sqrt{(\lambda_1 - xy)^2 + x}}, \frac{\sqrt{x}}{\sqrt{(\lambda_1 - xy)^2 + x}} \right), \quad \text{(A.16)}$$

$$\langle \lambda_2 | = \left(\frac{\lambda_2 - xy}{\sqrt{(\lambda_2 - xy)^2 + x}}, \frac{\sqrt{x}}{\sqrt{(\lambda_2 - xy)^2 + x}} \right). \quad \text{(A.17)}$$

B   Transfer matrix for Ising measure with nearest and next nearest neighbor interaction

Consider the lattice gas with nearest and next–nearest neighbors Boltzmann weigh as follows

$$\pi_2(\boldsymbol{\eta}) = \exp\left\{ -\beta \sum_{i=1}^{L} \{J_1 \eta_i \eta_{i+1} + J_2 \eta_i (1 - \eta_{i+1}) \eta_{i+2} + h\eta_i\} \right\}. \tag{B.1}$$

Denote by

$$\omega_{2,i}(\boldsymbol{\eta}) := e^{-\beta[J_1(\eta_{2i-1}\eta_{2i} + \eta_{2i}\eta_{2i+1}) + J_2(\eta_{2i-1}(1-\eta_{2i})\eta_{2i+1} + \eta_{2i}(1-\eta_{2i+1})\eta_{2i+2} + h(\eta_{2i-1} + \eta_{2i}))]}. \tag{B.2}$$

the local Boltzmann weights. Introduce the function $T_2 : \mathbb{S}^2 \times \mathbb{S}^2 \to \mathbb{R}_+$

$$T_2(\eta, \eta'|\zeta, \zeta') = e^{-\beta(J_1(\eta\eta' + \eta'\zeta) + J_2(\eta(1-\eta')\zeta + \eta'(1-\zeta)\zeta') + h(\eta + \eta'))}. \tag{B.3}$$

This allows us to define the four-dimensional transfer matrix

$$T_2 := \begin{pmatrix} T_2(0,0|0,0) & T_2(0,0|0,1) & T_2(0,0|1,0) & T_2(0,0|1,1) \\ T_2(0,1|0,0) & T_2(0,1|0,1) & T_2(0,1|1,0) & T_2(0,1|1,1) \\ T_2(1,0|0,0) & T_2(1,0|0,1) & T_2(1,0|1,0) & T_2(1,0|1,1) \\ T_2(1,1|0,0) & T_2(1,1|0,1) & T_2(1,1|1,0) & T_2(1,1|1,1) \end{pmatrix} \tag{B.4}$$

$$= \begin{pmatrix} 1 & 1 & 1 & 1 \\ z & y_2 z & y_1 z & y_1 z \\ z & z & y_2 z & y_2 z \\ y_1 z^2 & y_1 y_2 z^2 & y_1^2 z^2 & y_1^2 z^2 \end{pmatrix}, \tag{B.5}$$

where

$$y_i := e^{-\beta J_i}, \qquad z := e^{-\beta h}, \ \ i = 1, 2. \tag{B.6}$$

With the bra and ket vectors

$$\langle 0, 0| = (1, 0, 0, 0), \qquad \langle 0, 1| = (0, 1, 0, 0),$$
$$\langle 1, 0| = (0, 0, 1, 0), \qquad \langle 1, 1| = (0, 0, 0, 1), \tag{B.7}$$
$$|i, j\rangle = \langle i, j|^T.$$

one gets

$$T_2(\eta, \eta'|\zeta, \zeta') = \langle \eta, \eta'| T_2 |\zeta, \zeta'\rangle. \tag{B.8}$$

Let λ_i, $i = 1, 2, 3, 4$ be four eigenvalues of the transfer matrix T_2. Since T_2 is a positive matrix meaning that all its elements greater than 0. So that without loss of generality assume that λ_1 is its dominant eigenvalue and one has $\lambda_1 > \max\{|\lambda_2|, |\lambda_3|, |\lambda_4|\}$. The

normalized left and right eigenvectors are denoted by

$$\langle \lambda_i | = (w_1(i), w_2(i), w_3(i), w_4(i)), \qquad |\lambda_i\rangle = \begin{pmatrix} v_1(i) \\ v_2(i) \\ v_3(i) \\ v_4(i) \end{pmatrix} \tag{B.9}$$

and we recall the completeness relation

$$\sum_{i=1}^{4} |\lambda_i\rangle \langle \lambda_i| = \mathbb{1}. \tag{B.10}$$

Without loss of generality, the number of sites L is assumed to be even. Observe that with $M = L/2$, one has the Boltzmann weight

$$\pi_2(\boldsymbol{\eta}) = \prod_{i=1}^{M} \omega_{2,i}(\boldsymbol{\eta}) = \prod_{i=1}^{M} T_2(\eta_{2i-1}, \eta_{2i} | \eta_{2i+1}, \eta_{2i+2}) = \prod_{i=1}^{M} \langle \eta_{2i-1}, \eta_{2i} | T_2 | \eta_{2i+1}, \eta_{2i+2} \rangle \tag{B.11}$$

which written out gives

$$\pi_d(\boldsymbol{\eta}) = \langle \eta_1, \eta_2 | T_2 | \eta_3, \eta_4 \rangle \langle \eta_3, \eta_4 | T_2 | \eta_5, \eta_6 \rangle \cdots \langle \eta_{L-3}, \eta_{L-2} | T_2 | \eta_{L-1}, \eta_L \rangle \langle \eta_{L-1}, \eta_L | T_2 | \eta_1, \eta_2 \rangle. \tag{B.12}$$

This yields the partition function

$$Z_{2,L} = \mathrm{Tr} T_2^{L/2} = \sum_{i=1}^{4} \lambda_i^{L/2}. \tag{B.13}$$

C Proof of stationarity in Chapter 3

By considering all possible cases of (3.46), one gets stationary conditions as follows

- Case 1: $\theta_{i-1}^0 = \theta_{i-1}^1 = 0$ and $\theta_i^0 = \theta_i^1 = 0$, $\Phi_{i-1} - \Phi_i = 0$:

$$s_i = 1 : -\omega^\star + x\phi^\star + x\kappa^\star - \tau^\star = 0; \tag{C.1}$$
$$s_i = 2 : x^{-1}\omega^\star - \phi^\star - \kappa^\star + x^{-1}\tau^\star = 0. \tag{C.2}$$

- Case 2: $\theta_{i-1}^0 = 1, \theta_{i-1}^1 = 0$ and $\theta_i^0 = \theta_i^1 = 0$, $\Phi_{i-1} - \Phi_i = b$

$$s_i = 1 : -\omega^\star(1 + d^{1\star}) + xy\phi^\star(1 + e^{10\star}) + x\kappa^\star(1 + f^{1\star}) - \tau^\star(1 + g^{1\star}) = b; \tag{C.3}$$
$$s_i = 2 : -\kappa^\star(1 + f^{1\star}) + x^{-1}\tau^\star(1 + g^{1\star}) = b. \tag{C.4}$$

- Case 3: $\theta_{i-1}^0 = 0, \theta_{i-1}^1 = 1$ and $\theta_i^0 = \theta_i^1 = 0$, $\Phi_{i-1} - \Phi_i = c$

$$s_i = 1 : -\omega^\star + x\phi^\star + x\kappa^\star(1 + f^{10\star}) - \tau^\star(1 + g^{10\star}) = c; \tag{C.5}$$
$$s_i = 2 : x^{-1}y^{-1}\omega^\star(1 + d^{1\star}) - \phi^\star(1 + e^{10\star}) - \kappa^\star(1 + f^{10\star}) + x^{-1}\tau^\star(1 + g^{10\star}) = c. \tag{C.6}$$

- Case 4: $\theta_{i-1}^0 = \theta_{i-1}^1 = 0$ and $\theta_i^0 = 1, \theta_i^1 = 0$, $\Phi_{i-1} - \Phi_i = -b$

$$s_i = 1 : x\kappa^\star(1 + f^{\star 1}) - \tau^\star(1 + g^{\star 1}) = -b; \tag{C.7}$$
$$s_i = 2 : x^{-1}y\omega^\star(1 + d^{\star 01}) - \phi^\star(1 + e^{\star 1}) - \kappa^\star(1 + f^{\star 1}) + x^{-1}\tau^\star(1 + g^{\star 1}) = -b. \tag{C.8}$$

- Case 5: $\theta_{i-1}^0 = \theta_{i-1}^1 = 0$ and $\theta_i^0 = 0, \theta_i^1 = 1$, $\Phi_{i-1} - \Phi_i = -c$

$$s_i = 1 : -\omega^\star(1 + d^{\star 01}) + xy^{-1}\phi^\star(1 + e^{\star 1}) + x\kappa^\star(1 + f^{\star 01}) - \tau^\star(1 + g^{\star 01}) = -c; \tag{C.9}$$
$$s_i = 2 : x^{-1}\omega^\star - \phi^\star - \kappa^\star(1 + f^{\star 01}) + x^{-1}\tau^\star(1 + g^{\star 01}) = -c. \tag{C.10}$$

- Case 6: $\theta_{i-1}^0 = 1, \theta_{i-1}^1 = 0$ and $\theta_i^0 = 1, \theta_i^1 = 0$, $\Phi_{i-1} - \Phi_i = 0$

$$s_i = 1 : x\kappa^\star(1 + f^{1\star} + f^{\star 1} + f^{1\star 1}) - \tau^\star(1 + g^{1\star} + g^{\star 1} + g^{1\star 1}) = 0; \tag{C.11}$$
$$s_i = 2 : -\kappa^\star(1 + f^{1\star} + f^{\star 1} + f^{1\star 1}) + x^{-1}\tau^\star(1 + g^{1\star} + g^{\star 1} + g^{1\star 1}) = 0. \tag{C.12}$$

- Case 7: $\theta_{i-1}^0 = 1, \theta_{i-1}^1 = 0$ and $\theta_i^0 = 0, \theta_i^1 = 1$, $\Phi_{i-1} - \Phi_i = b - c$

$$s_i = 1 : -\omega^\star(1 + d^{1\star} + d^{\star 01}) + x\phi^\star(1 + e^{10\star} + e^{\star 1}) + x\kappa^\star(1 + f^{1\star} + f^{\star 01}) - \tau^\star(1 + g^{1\star} + g^{\star 01}) = b - c; \tag{C.13}$$
$$s_i = 2 : -\kappa^\star(1 + f^{1\star} + f^{\star 01}) + x^{-1}\tau^\star(1 + g^{1\star} + g^{\star 01}) = b - c. \tag{C.14}$$

- Case 8: $\theta_{i-1}^0 = 0, \theta_{i-1}^1 = 1$ and $\theta_i^0 = 1, \theta_i^1 = 0$, $\Phi_{i-1} - \Phi_i = -b + c$

$$s_i = 1 : x\kappa^\star(1 + f^{\star 1} + f^{10\star}) - \tau^\star(1 + g^{\star 1} + g^{10\star}) = -b + c; \tag{C.15}$$
$$s_i = 2 : x^{-1}\omega^\star(1 + d^{1\star} + d^{\star 01}) - \phi^\star(1 + e^{10\star} + e^{\star 1}) - \kappa^\star(1 + f^{\star 1} + f^{10\star}) + x^{-1}\tau^\star(1 + g^{\star 1} + g^{10\star}) = -b + c. \tag{C.16}$$

- Case 9: $\theta_{i-1}^0 = 0, \theta_{i-1}^1 = 1$ and $\theta_i^0 = 0, \theta_i^1 = 1$, $\Phi_{i-1} - \Phi_i = 0$

$$s_i = 1 : -\omega^\star(1 + d^{\star 01}) + xy^{-1}\phi^\star(1 + e^{\star 1}) + x\kappa^\star(1 + f^{10\star} + f^{\star 01}) - \tau^\star(1 + g^{10\star} + g^{\star 01}) = 0; \tag{C.17}$$
$$s_i = 2 : x^{-1}y^{-1}\omega^\star(1 + d^{1\star}) - \phi^\star(1 + e^{10\star}) - \kappa^\star(1 + f^{10\star} + f^{\star 01}) + x^{-1}\kappa^\star(1 + g^{10\star} + g^{\star 01}) = 0. \tag{C.18}$$

Next, we solve the above system of equations as follows.

- Case 1 gives

$$x = \frac{\omega^\star + \tau^\star}{\phi^\star + \kappa^\star}. \tag{C.19}$$

- Case 2 gives

$$b = \frac{-\omega^\star(1 + d^{1\star}) + xy\phi^\star(1 + e^{10\star})}{1 + x}. \tag{C.20}$$

- Case 3 gives

$$c = \frac{y^{-1}\omega^\star(1 + d^{1\star}) - x\phi^\star(1 + e^{10\star}) + x\phi^\star - \omega^\star}{1 + x}. \tag{C.21}$$

- Case 4 gives

$$b = \frac{-y\omega^\star(1 + d^{\star 01}) + x\phi^\star(1 + e^{\star 1})}{1 + x}. \tag{C.22}$$

- Case 5 gives

$$c = \frac{\omega^\star(1 + d^{\star 01}) - xy^{-1}\phi^\star(1 + e^{\star 1}) + x\phi^\star - \omega^\star}{1 + x}. \tag{C.23}$$

- Case 6 gives

$$x\kappa^\star(1 + f^{1\star} + f^{\star 1} + f^{1\star 1}) - \tau^\star(1 + g^{1\star} + g^{\star 1} + g^{1\star 1}) = 0. \tag{C.24}$$

- Case 7 gives

$$b - c = \frac{-\omega^\star(1 + d^{1\star} + d^{\star 01}) + x\phi^\star(1 + e^{10\star} + e^{\star 1})}{1 + x}. \tag{C.25}$$

- Case 8 gives

$$c - b = \frac{\omega^\star(1 + d^{1\star} + d^{\star 01}) - x\phi^\star(1 + e^{10\star} + e^{\star 1})}{1 + x}. \tag{C.26}$$

- Case 9 gives

$$y = \frac{\omega^\star(1 + d^{1\star}) + x\phi^\star(1 + e^{\star 1})}{\omega^\star(1 + d^{\star 01}) + x\phi^\star(1 + e^{10\star})}. \tag{C.27}$$

From (C.1) to (C.27), one obtains stationary conditions

$$x = \frac{\omega^\star + \tau^\star}{\phi^\star + \kappa^\star} \tag{C.28}$$

$$y = \frac{\omega^\star(1 + d^{1\star}) + x\phi^\star(1 + e^{\star 1})}{\omega^\star(1 + d^{\star 01}) + x\phi^\star(1 + e^{10\star})} \tag{C.29}$$

$$b = \frac{-y\omega^\star(1 + d^{\star 01}) + x\phi^\star(1 + e^{\star 1})}{1 + x} \tag{C.30}$$

$$c = \frac{\omega^\star(1 + d^{\star 01}) - xy^{-1}\phi^\star(1 + e^{\star 1}) + x\phi^\star - \omega^\star}{1 + x} \tag{C.31}$$

$$x\kappa^\star f^{1\star} - \tau^\star g^{1\star} = -bx - x\kappa^\star + \tau^\star \tag{C.32}$$

$$x\kappa^\star f^{\star 1} - \tau^\star g^{\star 1} = -b - x\kappa^\star + \tau^\star \tag{C.33}$$

$$x\kappa^\star f^{10\star} - \tau^\star g^{10\star} = c - x\kappa^\star + \tau^\star + \omega^\star - x\phi^\star \tag{C.34}$$

$$x\kappa^\star f^{\star 01} - \tau^\star g^{\star 01} = xc + \omega^\star - x\phi^\star - x\kappa^\star + \tau^\star \tag{C.35}$$

$$x\kappa^\star f^{1\star 1} - \tau^\star g^{1\star 1} = b(1 + x) + x\kappa^\star - \tau^\star \tag{C.36}$$

Notice that $x(\phi^\star + \tau^\star) = \omega^\star + \kappa^\star$, one gets

$$x\kappa^\star f^{10\star} - \tau^\star g^{10\star} = c, \tag{C.37}$$

$$x\kappa^\star f^{\star 01} - \tau^\star g^{\star 01} = xc. \tag{C.38}$$

From (C.20), (C.21), and (C.25), one has

$$-\omega^\star(1 + d^{1\star}) + xy\phi^\star(1 + e^{10\star}) - (y^{-1}\omega^\star(1 + d^{1\star}) - x\phi^\star(1 + e^{10\star}) + x\phi^\star - \omega^\star)$$
$$= -\omega^\star(1 + d^{1\star} + d^{\star 01}) + x\phi^\star(1 + e^{10\star} + e^{\star 1}). \tag{C.39}$$

From (C.27), one gets

$$yx\phi^\star(1 + e^{10\star}) = \omega^\star(1 + d^{1\star}) + x\phi^\star(1 + e^{\star 1}) - y\omega^\star(1 + d^{\star 01}). \tag{C.40}$$

Plugging (C.27) into (C.40) gives

$$-y(1 + d^{\star 01}) - y^{-1}(1 + d^{1\star}) + (1 + d^{\star 01}) + (1 + d^{1\star}) = 0 \tag{C.41}$$

which implies

$$y = \frac{1 + d^{1\star}}{1 + d^{\star 01}}. \tag{C.42}$$

Similarly, from (C.22), (C.23), (C.26), and (C.27) one obtains

$$y = \frac{1 + e^{\star 1}}{1 + e^{10\star}}. \tag{C.43}$$

Using the new form of value y and after checking all conditions, one gets

$$x = \frac{\omega^\star + \tau^\star}{\phi^\star + \kappa^\star} \tag{C.44}$$

$$y = \frac{1 + d^{1\star}}{1 + d^{\star 01}} = \frac{1 + e^{\star 1}}{1 + e^{10\star}} \tag{C.45}$$

$$b = \frac{-\omega^\star(1 + d^{1\star}) + x\phi^\star(1 + e^{\star 1})}{1 + x} \tag{C.46}$$

$$c = \frac{\omega^\star d^{\star 01} - x\phi^\star e^{10\star}}{1 + x} \tag{C.47}$$

$$x\kappa^\star f^{1\star} - \tau^\star g^{1\star} = -bx - x\kappa^\star + \tau^\star \tag{C.48}$$

$$x\kappa^\star f^{\star 1} - \tau^\star g^{\star 1} = -b - x\kappa^\star + \tau^\star \tag{C.49}$$

$$x\kappa^\star f^{1\star 1} - \tau^\star g^{1\star 1} = -\omega^\star d^{1\star} + x\phi^\star e^{\star 1} \tag{C.50}$$

$$x\kappa^\star f^{10\star} - \tau^\star g^{10\star} = c \tag{C.51}$$

$$x\kappa^\star f^{\star 01} - \tau^\star g^{\star 01} = xc. \tag{C.52}$$

Notice that $x\phi^\star - \omega^\star = -x\kappa^\star + \tau^\star$, therefore, one gets

$$x = \frac{\omega^\star + \tau^\star}{\phi^\star + \kappa^\star} \tag{C.53}$$

$$y = \frac{1 + d^{1\star}}{1 + d^{\star 01}} = \frac{1 + e^{\star 1}}{1 + e^{10\star}} \tag{C.54}$$

$$b = \frac{-\omega^\star(1 + d^{1\star}) + x\phi^\star(1 + e^{\star 1})}{1 + x} \tag{C.55}$$

$$c = \frac{\omega^\star d^{\star 01} - x\phi^\star e^{10\star}}{1 + x} \tag{C.56}$$

$$x\kappa^\star f^{1\star} - \tau^\star g^{1\star} = \frac{1}{1 + x}(-\omega^\star + x\phi^\star) - \frac{x}{1 + x}(-\omega^\star d^{1\star} + x\phi^\star e^{\star 1}) \tag{C.57}$$

$$x\kappa^\star f^{\star 1} - \tau^\star g^{\star 1} = \frac{x}{1 + x}(-\omega^\star + x\phi^\star) - \frac{1}{1 + x}(-\omega^\star d^{1\star} + x\phi^\star e^{\star 1}) \tag{C.58}$$

$$x\kappa^\star f^{1\star 1} - \tau^\star g^{1\star 1} = -\omega^\star d^{1\star} + x\phi^\star e^{\star 1} \tag{C.59}$$

$$x\kappa^\star f^{10\star} - \tau^\star g^{10\star} = \frac{1}{1 + x}(\omega^\star d^{\star 01} - x\phi^\star e^{10\star}) \tag{C.60}$$

$$x\kappa^\star f^{\star 01} - \tau^\star g^{\star 01} = \frac{x}{1 + x}(\omega^\star d^{\star 01} - x\phi^\star e^{10\star}). \tag{C.61}$$

Bibliography

[1] Antal T. and Schütz G. M., *Asymmetric exclusion process with next–nearest–neighbor interaction: Some comments on traffic flow and a nonequilibrium reentrance transition*. Phys. Rev. E 62, 83 – Published 1 July 2000.

[2] Bai L., Santangelo T.J. , and Wang M.D. *Single-Molecule Analysis of RNA Polymerase Transcription*. Annu. Rev. Biophys. Biomol. Struct. 35, 343 (2006).

[3] Baxter R.J., *Exactly solved models in Statistical Mechanics*. Academic Press, *3rd Print ed.*, 1989.

[4] Belitsky V., Schütz G.M., *RNA Polymerase interactions and elongation rate*. Journal of Theoretical Biology 462 (2019) 370–380.

[5] Belitsky V., Schütz G.M., *Stationary RNA polymerase fluctuations during transcription elongation*. Physical Review E 99, 012405 (2019).

[6] Chowdhury D., Santen L.,Schadschneider A., *Statistical physics of vehicular traffic and some related systems*. Physics Reports, Volume 329, Issues 4–6, May 2000, Pages 199-32.

[7] Epshtein V., Nudler E., *Cooperation between RNA polymerase molecules in transcription elongation*. Science. 2003 May 2;300(5620):801-5.

[8] Epshtein V., Toulme F., Rahmouni A.R., Borukhov S., and Nudler E., *Transcription through the roadblocks: the role of RNA polymerase cooperation*. SEMBO J. 22, 4719 (2003).

[9] Evans M.R.,T. Hanney T., *Nonequilibrium Statistical Mechanics of the Zero-Range Process and Related Models*. J. Phys. A: Math. Gen. 38 (2005) R195–R240.

[10] Friedli S., Velenik Y., *Statistical Mechanics of Lattice Systems: A Concrete Mathematical Introduction*. Cambridge: Cambridge University Press, 2017.

[11] Grosskinsky S., *Phase transitions in nonequilibrium stochastic particle systems with local conservation laws*. PhD thesis.

[12] Kassan-Ogly F.A., *One-dimensional Ising model with next–nearest–neighbor interaction in magnetic field*, Phase Trans. 74(4), 353–365.

[13] Katz S., Lebowitz J. L. and Spohn H., *Nonequilibrium steady states of stochastic lattice gas models of fast ionic conductors.* Journal of Statistical Physics 34, p. 497–537(1984).

[14] Kaviani S., Jafarpour F.H., *Current fluctuations in a stochastic system of classical particles with next-nearest-neighbor interactions.* Journal of Statistical Mechanics: Theory and Experiment (2020) 013210.

[15] Kramers, H. A., Wannier, G. H., *Statistics of the Two-Dimensional Ferromagnet.* Part I. Phys. Rev. 60 (3): 252–262(1941).

[16] Kramers, H. A., Wannier, G. H., *Statistics of the Two-Dimensional Ferromagnet.* Part II. Phys. Rev. 60 (3): 263–276(1941).

[17] Kuzemsky A.L., *Thermodynamic Limit in Statistical Physics.* Int.J.Mod.Phys.B, Vol. 28, No. 09, 1430004 (2014).

[18] Liggett T.M., *Interacting Particle Systems.* Springer (1985).

[19] Liggett T.M., *Continuous Time Markov Processes: An Introduction.* American Mathematical Society (2010).

[20] MacDonald C.T., Gibbs J.H., Pipkin A.C., *Kinetics of biopolymerization on nucleic acid templates.* Biopolymers, Volume6, Issue1, Pages 1-25, January 1968.

[21] Schreckenberg M., Schadschneider A., Nagel K., and Ito N., *Discrete stochastic models for traffic flow.* SPhys. Rev. E 51, 2939 – Published 1 April 1995.

[22] Schütz G.M., *Exactly Solvable Models for Many-Body Systems Far from Equilibrium*, Phase Transitions and Critical Phenomena, Academic Press, 2001.

[23] Schütz G.M., *One-dimensional Driven Diffusive Systems*, 2016 (unpublished).

[24] Schütz G.M., *Fluctuations in Stochastic Interacting Particle Systems*, Stochastic Dynamics Out of Equilibrium, 67-134, Springer, 2017.

[25] Schütz G.M., *Kramers-Wannier transfer matrix for the 1-d Ising model*, 2021 (unpublished).

[26] Spitzer F., *Interaction of Markov processes*, Advances in Mathematics, Volume 5, Issue 2, October 1970, Pages 246-290.

[27] Stephenson J., *Two one-dimensional Ising models with disorder point*, Canadian Journal of Physics, 15 July 1970.

[28] Styer D.F., *What good is the thermodynamic limit?.* Am. J. Phys. 72, 25 (2004).

[29] Tripathi T., Chowdhury D., *Interacting RNA polymerase motors on DNA track: effects of traffic congestion and intrinsic noise on RNA synthesis.* Phys. Rev. E 77, 011921 (2008).

[30] Tripathi T., Schütz G.M., Chowdhury D., *RNA polymerase motors: dwell time distribution, velocity and dynamical phases.* J. Stat. Mech. (2009) P08018.

[31] G. Vertogen G. and Vries A.S., *The Ising Problem*, Commun. Math. Phys. 29, 131–162 (1973).

[32] Wang H.Y., Elston T.,Mogilner A., Oster G., *Force Generation in RNA Polymerase*. Biophysical Journal Volume 74 March 1998 1186–1202.

[33] Wikipedia: https://en.wikipedia.org/wiki/Ising_model